

THE WILD BIGHT GROUP, NEWFOUNDLAND APPALACHIANS:  
A COMPOSITE EARLY TO MIDDLE-ORDOVICIAN ENSIMATIC  
ARC AND CONTINENTAL MARGIN ARC-ARC RIFT BASIN

CENTRE FOR NEWFOUNDLAND STUDIES

**TOTAL OF 10 PAGES ONLY  
MAY BE XEROXED**

(Without Author's Permission)

KATE MacLACHLAN

中

卷

三

七

八

九

十

十一

十二

十三

十四

十五

十六

## **INFORMATION TO USERS**

This manuscript has been reproduced from the microfilm master. UMI films the text directly from the original or copy submitted. Thus, some thesis and dissertation copies are in typewriter face, while others may be from any type of computer printer.

**The quality of this reproduction is dependent upon the quality of the copy submitted.** Broken or indistinct print, colored or poor quality illustrations and photographs, print bleedthrough, substandard margins, and improper alignment can adversely affect reproduction.

In the unlikely event that the author did not send UMI a complete manuscript and there are missing pages, these will be noted. Also, if unauthorized copyright material had to be removed, a note will indicate the deletion.

Oversize materials (e.g., maps, drawings, charts) are reproduced by sectioning the original, beginning at the upper left-hand corner and continuing from left to right in equal sections with small overlaps. Each original is also photographed in one exposure and is included in reduced form at the back of the book.

Photographs included in the original manuscript have been reproduced xerographically in this copy. Higher quality 6" x 9" black and white photographic prints are available for any photographs or illustrations appearing in this copy for an additional charge. Contact UMI directly to order.

# **UMI**

A Bell & Howell Information Company  
300 North Zeeb Road, Ann Arbor MI 48106-1346 USA  
313/761-4700 800/521-0600



**The Wild Bight Group, Newfoundland Appalachians: A Composite  
Early to Middle-Ordovician Ensimatic Arc and  
Continental Margin Arc-Arc Rift Basin**

By

**©Kate MacLachlan, B.Sc. (Hons.), M.Sc.**

A thesis submitted to the School of Graduate Studies  
in partial fulfillment of the requirements  
for the degree of  
Doctor of Philosophy

Department of Earth Sciences  
Memorial University of Newfoundland  
St. John's, Newfoundland  
January, 1998



**National Library  
of Canada**

**Acquisitions and  
Bibliographic Services**

**395 Wellington Street  
Ottawa ON K1A 0N4  
Canada**

**Bibliothèque nationale  
du Canada**

**Acquisitions et  
services bibliographiques**

**395, rue Wellington  
Ottawa ON K1A 0N4  
Canada**

*Your file Votre référence*

*Our file Notre référence*

**The author has granted a non-exclusive licence allowing the National Library of Canada to reproduce, loan, distribute or sell copies of this thesis in microform, paper or electronic formats.**

**The author retains ownership of the copyright in this thesis. Neither the thesis nor substantial extracts from it may be printed or otherwise reproduced without the author's permission.**

**L'auteur a accordé une licence non exclusive permettant à la Bibliothèque nationale du Canada de reproduire, prêter, distribuer ou vendre des copies de cette thèse sous la forme de microfiche/film, de reproduction sur papier ou sur format électronique.**

**L'auteur conserve la propriété du droit d'auteur qui protège cette thèse. Ni la thèse ni des extraits substantiels de celle-ci ne doivent être imprimés ou autrement reproduits sans son autorisation.**

**0-612-36208-6**



Lagging  
Trickles, NF  
KM '98

## **Abstract**

The Wild Bight Group (WBG) and South Lake Igneous Complex (SLIC) represent a peri-Gondwanan Ordovician accreted oceanic terrane of the central Newfoundland Appalachians. The Wild Bight Group is a sequence of volcanic and volcanoclastic rocks, and the South Lake igneous complex is comprised of layered gabbro and sheeted dykes intruded by hornblende diorite and tonalite plutons.

This study involves detailed mapping (~ 1:12,500) in the South Lake igneous complex and adjacent rocks of the eastern Wild Bight Group, combined with petrography, geochemical, and Sm-Nd isotopic studies, and U-Pb geochronology. It shows that there are two temporally and genetically distinct sequences of volcanic, volcanoclastic and sedimentary rocks in the WBG, separated by up to 10 Ma. The older sequence is genetically related to plutonic rocks of the South Lake igneous complex, and these older rock packages have been structurally interleaved with the younger sequence during subsequent deformation. The younger sequence has also been structurally imbricated and does not represent a simple conformable sequence in its present configuration.

Magmatic rocks related to the older sequence of the WBG formed predominantly between 486  $\pm$  4 and 489  $\pm$  3 Ma (Tremadoc to early Arenig), and range in composition from normal island arc tholeiitic basalt (IATs), to incompatible element-depleted low-Ti, high-Mg IATs and boninites, and high-Si, low-K rhyolite/tonalite. They are interpreted to represent the initiation and stabilization of a primitive ensimatic oceanic arc. Sm-Nd isotope systematics in the depleted IATs and boninites, show an apparent decoupling of isotopic and geochemical characteristics, which require a complex source or melt generation process for these rocks. The geochemical, isotopic and field relationships in the older volcanic sequence and SLIC provide some insight into tectonomagmatic processes in volcanic arcs in general.

The younger sequence of the Wild Bight Group comprises two volcanic successions which are stratigraphically separated. The lower one has a calc-alkalic geochemical affinity, and its age is confined to  $472 \pm 3$  Ma (late Arenig), by felsic tuffs within the succession. The upper volcanic succession has enriched tholeiitic to alkalic within-plate geochemical signatures, and geochemically related gabbro sills are dated at  $470 \pm 5$  and  $471 \pm 4$  Ma. Geochemical and isotopic characteristics suggest that these two volcanic sequences were produced from a similar mantle source. Sm-Nd isotope systematics indicate that the calc-alkaline rocks were contaminated by an old continentally-derived component. The younger sequence of the Wild Bight Group is interpreted to represent a volcanic arc that formed on or immediately adjacent to thinned continental crust of the Gondwanan margin, and was subsequently rifted.

Blocks in melanges and debris flows within the younger succession have geochemical signatures which indicate that they were derived from both the older and younger volcanic sequences of the WBG. This suggests that the older arc formed part of the substrate on which the younger sequence developed. Intrabasinal uplifts exposed the older substrate which then provided a source of detritus for the younger basin. The occurrence of a Precambrian detrital zircon in a volcanoclastic unit of the younger sequence suggests that there was an even older component to the uplifted substrate. The uplifts are interpreted to result from horsts and grabens formed in an extensional back arc and subsequent arc rift setting. In most places the contact between the older and younger sequences is structurally modified, although locally a stratigraphic contact may be preserved.

The tectonomagmatic evolution of the WBG and SLIC has four main stages: firstly, formation of a primitive ensimatic arc outboard of the Gondwanan margin, by westward (present coordinates) subduction; secondly arc/continental margin "collision", which involved attempted subduction of the thinned continental margin,

and resulted in the termination of westward subduction; thirdly, initiation of a second subduction zone outboard of the continental margin, but with the opposite polarity, such that the subsequent arc developed on the composite margin; and finally, arc rifting which formed an extensive marginal basin.

The Wild Bight Group has traditionally been correlated with the Exploits Group to the east. These groups are interpreted to represent different parts of the same late Arenig to Llanvirn, arc/back-arc/arc-rift system, and were probably also contiguous during generation of the older ensimatic arc. The eastern WBG is interpreted to represent the remnant arc following arc rifting, and the western WBG is interpreted to represent the main rift basin. The Exploits Group probably formed in the pre-rift back arc basin in close proximity to the continental margin.

There are lithological, structural and stratigraphic differences between ophiolites and volcanic rock packages in the Exploits Subzone interpreted to be correlative with the older sequence of the WBG, and late Arenig to Llanvirn volcanic/volcaniclastic and epiclastic sequences which are interpreted to be correlative with the younger sequence of the WBG. These differences are interpreted to be related to the presence of a promontory on the Gondwanan margin, as suggested by previous workers. The Exploits Subzone can be divided into two Ordovician tectonic zones, one in the east and south which underwent an important compressional event during the middle to late Arenig (Penobscot Orogeny), but only minor late Arenig to Llanvirn/Llandeilo extension, and the other in the north and west with the opposite characteristics. The boundaries of these zones are likely transitional, but roughly coincide with Silurian structures such as Noel Pauls Line and Dog Bay Line, which have been used to subdivide the Dunnage zone in the past.

## **Acknowledgments**

Firstly I would like thank my supervisor, Dr. Greg Dunning for all his support, both technical and moral. I am also grateful to Greg for his understanding and encouragement of my extracurricular activities, in particular my artistic endeavours. The Newfoundland landscape has been a great inspiration to me, and I'm sure it will lure me back again and again.

I have really enjoyed my experience at Memorial, in a large part because of a great working relationship with my supervisor and colleagues in the Earth Sciences Department, and at the Newfoundland Department of Mines and Energy. In particular I am greatly indebted to Dr. Brian O'Brien for suggesting the area of study; providing an introduction to the geology and people of Notre Dame Bay; and continued guidance in the field. Brian's broad range of knowledge of Newfoundland geology has been invaluable to me during our many discussions; and his easy going nature and generous accessibility are much appreciated. I have also been privileged to attend several of his dinner parties, and sample his gourmet cooking. The Newfoundland Department of Mines and Energy has also been very generous in providing field equipment, and I would like to thank Steve Colman-Sadd in particular for facilitating this.

Several other people have contributed their knowledge and expertise to my educational experience. I would like to thank Dr. Scott Swinden for his guided tours of the Wild Bight Group, and discussions on geochemistry of Ordovician volcanic rocks in Newfoundland. I was fortunate to have Scott's Ph.D. thesis on the Wild Bight Group as a starting point for my thesis, and Scott has been very helpful in providing additional information on and insight into these rocks, that he has gained since the completion of his thesis. I would also like to thank Dr. George Jenner for discussions regarding assessment of my geochemical data, and basalt geochemistry in general.

I have been fortunate to share my office with John Ketchum, who has provided valuable expertise and assistance during my introduction to U-Pb geochronology. He has been an understanding and easy going office co-habitant, and has also become a good friend. I would also like to thank Caroline Petibon, my housemate, for her understanding of my moods and ways, and for encouraging me to get out and have some fun once in a while. I look forward to having her correcting my French when I visit France, instead of me correcting her English. It has been fun getting to know numerous other graduate students in Earth Sciences, and I will not attempt to name them all. I would also like to thank Mark Wilson for his encouragement in various directions, and numerous interesting discussions on a wide variety of subjects, not least of which was isotope geochemistry. I also really enjoyed his course on Chemical Fluxes in the Earth System, it broadened my outlook on geochemistry and geology in general.

It is not possible to complete a Ph.D. without the technical expertise of numerous other people. In particular I would like to thank Pat Horan and Robbie Hicks for their technical work/assistance in the Sm-Nd and U-Pb laboratories, respectively. I would also like to acknowledge all the work done by Pam King, Mike Tubrett and Lakmali Hewà in providing the reams of XRF and ICP-MS data that comprise a significant part of this thesis.

A large part of this thesis is based on extensive field work in central Notre Dame Bay. I spent three fabulous, sunny summers in the small fishing community of Leading Tickles. The people of Leading Tickles were very friendly, welcoming and helpful (as is typical of Newfoundlanders in general), and I am greatly indebted to them for this. I consider myself very fortunate to have had the chance to live in a small Newfoundland community, and experience a different side of Newfoundland than city life in St. John's. I developed a great appreciation for the way of life in small fishing communities, despite the cod fish moratorium, and I hope that it will not

become obsolete in the future. I know that "fish" equals "cod", and that "going fishing" means "going to get some cod". Not only were people very generous with the small amount of cod that turned up in their nets, but we were also provided with numerous meals of mussels, crab and lobster. In particular I would like to thank Lyndon and Jeanette Martin who became very special friends, and welcomed me and my various assistants into their home regularly. I also spent several lovely relaxing days picnicing with them and other friends in the small coves and bays around Leading Tickles, and these are experiences I will never forget. Lyndon is also thanked for his considerable expertise, and trustworthy boatmanship during our mapping forays out around the headlands and larger unprotected bays. I would also like to thank my field assistants Rob Taylor, Alan Cull and Steve Israel for their good natured companionship and assistance, particularly on geochron sampling days.

I have made numerous other friends in St. John's who have enriched my time in Newfoundland and they are all thanked. In particular I would like to thank Di Dabinett for all her direction and encouragement of my attempts to convey my love of Newfoundland scenery through watercolour painting.

## **Table of Contents**

Title Page	i
Abstract	ii
Acknowledgments	v
Table of Contents	vi
List of Maps	xiii
List of Figures	xiv
List of Tables	xvii
List of Plates	xviii

### **Chapter 1**

#### **Introduction**

1.1 Subject and scope	1
1.2 Location and access	4
1.3 Regional geology	5
1.4 Previous work in the area	7
1.5 Rational for thesis presentation	10

### **Chapter 2**

#### **Age, Origin and Tectonomagmatic Evolution of the Older Sequence of the Wild Bight Group and the South Lake Igneous Complex**

2.1 Introduction	12
2.2 Geology	14
2.2.1 South Lake Igneous Complex	14
2.2.2 Older sequence of the Wild Bight Group	16
2.3 Linking the Wild Bight Group and South Lake Igneous Complex	18

2.4 U-Pb geochronology	19
2.4.1 U-Pb samples	19
2.4.2 Interpretation	22
2.5 Geochemistry	22
2.5.1 Alteration and metamorphism	23
2.5.2 Purpose	24
2.5.3 Geochemical characteristics of mafic rocks	24
2.5.4 Geochemical characteristics of felsic rocks	30
2.6 Sm-Nd isotope systematics	32
2.7 Discussion	35
2.7.1 Tectonic setting	36
2.7.2 Subduction zone processes	41
2.8 Conclusions	45

### **Chapter 3**

#### **Age, Origin and Tectonomagmatic Evolution of the Younger Sequence of the Wild Bight Group**

3.1 Introduction	47
3.2 Geology	48
3.3 U-Pb geochronology	50
3.3.1 U-Pb samples	51
3.3.2 Interpretation	54
3.4 Geochemistry	55
3.4.1 Alteration and metamorphism	55
3.4.2 Geochemical characteristics of the lower volcanic succession	56
3.4.3 Geochemical characteristics of the upper volcanic succession	57
3.4.4 Interpretation	59

3.5 Sm-Nd isotope systematics and mantle source components	61
3.5.1 Sm-Nd isotopic signatures of the upper volcanic succession	61
3.5.2 Sm-Nd isotopic signatures of the lower volcanic succession	62
3.5.3 Interpretation	62
3.6 Discussion	63
3.6.1 Tectonic setting	63
3.7 Conclusions	65

## **Chapter 4**

### **Regional Structural and Stratigraphic Relationships in the Wild Bight Group**

4.1 Introduction	66
4.2 Regional relationships in the Wild Bight Group	67
4.2.1 Stratigraphic relationships	67
4.2.2 Early fault imbrication	70
4.2.3 Deformation events	75
4.3 Detrital components in volcanoclastic rocks of the Wild Bight Group	76
4.3.1 Older sequence	76
4.3.2 Younger sequence	77
4.3.3 Interpretation	78
4.4 Tectonomagmatic evolution of the Wild Bight Group	79
4.5 Correlation with the Exploits Group	81
4.6 Paleogeography of the Late Arenig to Llanvirn Wild Bight/Exploits Arc	86
4.7 Conclusions	89

**Chapter 5**  
**Regional Correlations, and Implications for**  
**Evolution of the Gondwanan Margin**

5.1 Introduction	91
5.2 Correlation with other parts of the Exploits Subzone	91
5.2.1 Ophiolites of the Exploits Subzone	91
5.2.2 Volcanic/volcaniclastic sequences of Notre Dame Bay	94
5.2.3 Volcanic/volcaniclastic sequences of Central Newfoundland	97
5.3 Comparison with rocks in northern New Brunswick	103
5.4 Along-strike variation on the Gondwanan margin	106
5.5 Compression versus extension in the Exploits Subzone	109
5.5.1 Mid-Arenig (Penobscot) compression	109
5.5.2 Late Arenig to Llanvirn extension	110
5.5.3 Summary	110
5.6 Significance of post-Ordovician structural breaks	112
5.6.1 Red Indian Line	113
5.6.2 Dog Bay Line	114
5.6.3 Noel Pauls Line	116
5.7 Conclusions	116

**Chapter 6**  
**Summary and Directions for Future Work**

6.1 Summary	120
6.2 Regional implications	123
6.3 Significance of this work	124
6.4 Directions for future studies	125
6.4.1 Wild Bight Group	125
6.4.2 Dunnage Zone	126

References	128
Figures	148
Tables	176
Plates	190
Appendix 1: Sample Lists	215
Appendix 2: Sample Locations	224
Appendix 3: Geochemical Data	228
Appendix 4: Analysis of Precision and Accuracy of Geochemical Data	244
Appendix 5: Analytical Techniques	278
Appendix 6: Thin Section Petrography	282

## **List of Maps**

(all in pocket, inside back cover)

**Map A1:** Detailed map of the eastern Wild Bight Group showing structural measurements and location of geochronology samples.

**Map A2:** Detailed map of the eastern Wild Bight Group showing all sample locations.

**Map B:** Detailed map of the South Lake Igneous Complex showing structural measurements and sample locations.

**Map C1:** Regional compilation of the entire Wild Bight Group and adjacent units.

**Map C1b:** Cross-sections for map C1.

## List of Figures

<b>Figure 1.1</b> Tectonostratigraphic zones of the Newfoundland Appalachians.	148
<b>Figure 1.2</b> Simplified regional geology of the Wild Bight Group (WBG).	149
<b>Figure 2.1</b> Extended-rare earth element (E-REE) plots comparing similar rocks types of the Wild Bight Group and South Lake Igneous Complex (SLIC).	150
<b>Figure 2.2</b> U-Pb concordia plots for samples from the SLIC and the older sequence of the WBG.	151
<b>Figure 2.3</b> E-REE plots which characterize the different mafic suites of the older sequence of the WBG and the SLIC.	152
<b>Figure 2.4</b> Tectonic discrimination diagrams for all samples from the older sequence of the WBG and the SLIC.	153
<b>Figure 2.5</b> A plot of $^{147}\text{Sm}/^{144}\text{Nd}$ vs $\epsilon \text{ Nd}$ showing isotopic components involved in generating magmatic rocks of the older sequence of the WBG and related plutonic rocks of the SLIC.	154
<b>Figure 2.6</b> Qualitative model showing the effect on trace element patterns, of mixing mantle and subduction components.	155
<b>Figure 2.7</b> Model for the tectonomagmatic evolution of the older sequence of the WBG and the SLIC.	156
<b>Figure 3.1</b> U-Pb concordia plots for felsic tuffs and gabbro sills from the younger volcanic sequence of the WBG.	158
<b>Figure 3.2</b> E-REE plots of representative samples from the various geochemical groups in the younger sequence of the WBG.	160
<b>Figure 3.3</b> Tectonic discrimination plots of all samples from the lower volcanic succession of the younger WBG sequence.	161
<b>Figure 3.4</b> Tectonic discrimination plots of all samples from the upper volcanic succession of the younger WBG sequence.	162

<b>Figure 3.5</b> Qualitative model for the effect on trace element patterns, of mixing mantle and subduction components.	163
<b>Figure 3.6</b> A plot of $^{147}\text{Sm}/^{144}\text{Nd}$ versus $\epsilon\text{Nd}$ showing the various isotopic components involved in generating the mafic volcanic rocks of the younger WBG sequence.	164
<b>Figure 3.7</b> Model for the tectonomagmatic evolution of the younger sequence of the WBG.	165
<b>Figure 4.1</b> E-REE plot comparing the composition of detrital volcanic blocks in sedimentary units of the younger WBG sequence with the composition of volcanic and plutonic rocks of the older WBG sequence and the SLIC.	166
<b>Figure 4.2</b> E-REE plot comparing the composition of rhyolite blocks in a debris flow of the younger WBG sequence with the composition of felsic to intermediate volcanic rocks of the younger and older sequences of the WBG.	167
<b>Figure 4.3</b> U-Pb concordia plot and E-REE pattern of a quartz diorite cobble from a polyolithic conglomerate in the younger sequence of the WBG.	168
<b>Figure 4.4</b> Model for the paleogeography of the late Arenig to Llanvirn Wild Bight/Exploits arc.	169
<b>Figure 5.1</b> Tectonostratigraphic zones of the Newfoundland Appalachians with subdivisions of the Gander Zone and Exploits Subzone.	170
<b>Figure 5.2</b> Compilation diagram of the ages and geochemical affinities of all the main volcanic/volcaniclastic groups of the Exploits Subzone, and volcanic rocks of northern New Brunswick, and proposed correlation with the Wild Bight and Exploits groups.	171

- Figure 5.3** Model for along-strike variation in the evolution of the Gondwanan margin during the early to middle-Ordovician. 173
- Figure 5.4** Model showing proposed Ordovician tectonic divisions dominated by mid-Arenig compression, versus late Arenig to Llanvirn extension. 174

## **List Tables**

<b>Table 2.1</b> U-Pb data for samples from the older sequence of the WBG and the SLIC.	176
<b>Table 2.2</b> Geochemical data for samples used to define the geochemical suites in the older sequence of the WBG and the SLIC.	178
<b>Table 2.3</b> Sm-Nd isotopic data for samples from the older sequence of the WBG and the SLIC.	181
<b>Table 2.4</b> Element ratios which characterise the volcanic suites of the older sequence of the WBG and the SLIC.	182
<b>Table 3.1</b> U-Pb data for samples from the younger sequence of the WBG.	183
<b>Table 3.2</b> Geochemical data for samples plotted on E-REE plots.	185
<b>Table 3.3</b> Sm-Nd data for samples from the younger sequence of the WBG.	188
<b>Table 4.1</b> U-Pb data for detrital blocks from sedimentary rock units within the younger sequence of the WBG.	189

## **List of Plates**

<b>Plate 2.1</b>	Field relationships in the South Lake Igneous Complex	190
<b>Plate 2.2</b>	Field relationships and rocks types in the older volcanic sequence of the WBG	194
<b>Plate 2.3</b>	Photomicrographs of gabbro and hornblende diorite from the SLIC	196
<b>Plate 3.1</b>	Field relationships and rocks types in the younger sequence of the WBG	198
<b>Plate 3.2</b>	Field photos and photomicrographs of dated felsic tuffs from the younger sequence of the WBG	201
<b>Plate 4.1</b>	Field photos showing detrital components within sedimentary units of the younger WBG sequence	204
<b>Plate A6-1</b>	Photomicrographs of various plutonic rocks in the SLIC	206
<b>Plate A6-2</b>	Photomicrographs of various plutonic rocks in the SLIC	208
<b>Plate A6-3</b>	Photomicrographs of various volcanic rocks in the WBG	210
<b>Plate A6-4</b>	Photomicrographs of various volcanic rocks in the WBG	212

## **Chapter 1**

### **Introduction**

#### **1.1 Subject and Scope**

The objective of this research was to undertake an integrated tectonomagmatic study of plutonic rocks of the South Lake Igneous Complex (SLIC) and possible volcano-sedimentary equivalents in the early to middle Ordovician Wild Bight Group (WBG), of the central Newfoundland Appalachians. This was accomplished through a comparison of the timing and nature of magmatic and deformational events within these two rock packages, by combining detailed mapping, with whole rock geochemical and Sm/Nd isotopic studies of magmatic rocks, and by determining precise age constraints using U/Pb geochronology.

These rocks represent an early to middle-Ordovician accreted oceanic terrane of the Exploits Subzone of the Dunnage Zone in central Newfoundland (Fig.1.1). By developing a detailed tectonomagmatic history for these well exposed rock packages, this study sheds light on the origin of less well-exposed and studied, correlative sequences within the Exploits Subzone, and elsewhere in the northern Appalachians.

A previous interpretation of the tectonomagmatic history of the Wild Bight Group, based on a regional geochemical study, suggested that it represents an early to middle-Ordovician arc/arc rift/back arc transition (Swinden et al. 1990). A previous geochemical study of the plutonic rocks of the SLIC, suggested that they were also formed in a subduction zone environment (Lorenz and Fountain, 1982). Various workers (Lorenz and Fountain 1982, O'Brien 1992, and Dean 1977) interpreted the SLIC to be

Ordovician in age, although no data was published to support this interpretation. The present study was designed to investigate the possibility that these two packages represent different levels of the same Ordovician arc. Any evidence bearing on the relationships between the WBG and SLIC should provide insight into the early Ordovician evolution of this part of the Iapetus Ocean. Furthermore, if the South Lake Igneous Complex does represent a deeper crustal level of the Wild Bight arc, it might provide insights into processes in volcanic arcs in general.

The first objective of this research was to develop a tectonomagmatic history for the South Lake Igneous Complex, which could be compared to that of the Wild Bight Group (Swinden et al. 1990). This included detailed mapping of the complex to determine the relationships between magmatism and deformation; geochemical characterization of magmatic suites using modern trace-element and Nd-isotopic techniques similar to those used in the Wild Bight Group (Swinden et al. 1990); and U/Pb dating of critical units.

A similarly detailed study of the adjacent sequence of the Wild Bight Group was also carried out. Based on a regional compilation map (Dean and Strong 1976), and a regional geochemical study (Swinden 1988), the area between Seal Bay and Western Arm was thought to be underlain by a representative stratigraphic sequence, and occurrences of all the different volcanic rock types (Fig. 1.2). Thus it should not only provide a link with regional tectonomagmatic interpretations, but also provide new constraints on them.

Although the structural history and variations in magmatic rock types of the WBG were known on a regional scale, prior to this study there were no controls on the

absolute age of different magmatic events. Furthermore, the possible occurrence of bedding parallel faults made determining even the relative ages of some sequences difficult. The second objective of this work was to refine stratigraphic units and their distributions, provide absolute time constraints on the stratigraphic succession, and determine the relationship of different volcanic rock types to the stratigraphic sequence. This is particularly important because mineral deposits in the WBG have been shown by previous work (Swinden 1988) to be associated with a group of geochemically distinct rocks which have been linked with a specific stage of arc development (Swinden et al. 1990). However, these rocks seemed to occur at various stratigraphic levels, and their relationship to the rest of the stratigraphic sequence was previously unclear.

The age of the Wild Bight Group is loosely constrained between Tremadoc/Arenig to Llandeilo/earliest Caradoc, which spans approximately 40 m.y. The third primary objective of this work is to assess the possibility of a significant break within the sequence. The presence of a stratigraphic and/or structural break in the Wild Bight Group could have important implications for correlative rocks in the Exploits Group which span a similar age range (O'Brien et al. 1997).

Conglomerates and debris flows in the central part of the stratigraphic sequence of the Wild Bight Group were also examined as they might represent the expression of early Arenig to mid-Llanvirn tectonic uplift which has been suggested in the Exploits Group (O'Brien et al. 1997). Furthermore, these deposits contain granitoid fragments which could be from the South Lake Igneous Complex (B.H. O'Brien pers. comm. 1994), and

volcanic fragments which are likely from within the arc, and could constrain the timing of uplift and unroofing of various elements within the sequence.

By gaining a better understanding of the detailed magmatic and structural relationships between the South Lake Igneous Complex and the Wild Bight Group, it should be possible to interpret in more detail the Ordovician/Silurian evolution of the Gondwanan margin in the northern Exploits Subzone, and perhaps extrapolate events in this part of the Appalachians to rocks with similar characteristics elsewhere in the orogen.

## **1.2 Location and Access**

The Wild Bight Group is the northwestern-most, accreted, Ordovician, oceanic terrane of the Exploits Subzone of the Dunnage Zone (Fig. 1.1). It is centered at approximately 49° 20' N and 55° 30' W, and covers parts of the NTS 1:50,000 map sheets 2E/3 (Botwood), 2E/4 (Hodges Hill), 2E/5 (Robert's Arm) and 2E/6 (Point Leamington). It outcrops over a large area from just north of Botwood in the southeast, to Sops Arm in the northwest, and is well exposed along the coast of central Notre Dame Bay (Fig. 1.2). The area of detailed study for this project is located in the eastern part of the Wild Bight Group, where most of the volcanic rocks of the Wild Bight Group, and the SLIC occur (Fig. 1.2). The study area extends from just southwest of Point Leamington in the south, to Leading Ticks in the north. Highway 350, which joins the Trans Canada highway just south of Botwood, provides easy access to the area, and field operations were based out of the small fishing community of Leading Ticks, where the highway terminates.

Inland mapping was done by a combination of traverses from the highway and lake and river access with a canoe. However, the best outcrop and most geological control

was provided by the extensive coastal exposure along the deeply indented shoreline of Notre Dame Bay. In protected bays and tickles, these exposures were accessed with a small 4 person Zodiac, based in Glovers Harbour. The larger unprotected bays and headlands were accessed with the aid of an experienced local fisherman and his boat.

### **1.3 Regional Geology**

The Newfoundland Appalachians are commonly divided into 4 tectonostratigraphic zones based on their different lower Paleozoic and older rocks; from west to east they are the Humber, Dunnage, Gander, and Avalon zones (Williams, 1978 ) (Fig. 1). The Humber Zone represents the Paleozoic Laurentian margin of Iapetus; the Dunnage Zone is a composite of oceanic terranes that are remnants of the crust and mantle of the Iapetus Ocean; and the Gander and Avalon zones are suspect terranes which originated on the Gondwanan side of the Iapetus ocean (Williams 1979).

The Dunnage Zone is characterized by ophiolites and thick sequences of Cambro-Ordovician arc-related, volcanic, sub-volcanic and epiclastic sequences. The latter were previously thought to represent island arc volcanism and sedimentation during the closure of the Iapetus Ocean (e.g., Bird and Dewey 1970, Williams et al. 1974 and Dewey et al. 1983). However, more recent geochemical (e.g., Swinden et al. 1990 , and references therein) and geochronological (e.g., Dunning et al. 1986 and 1987) studies show that volcanic rocks with non-arc geochemical signatures are also present and that volcanism spans more than 50 Ma. Ophiolites of the Exploits Subzone are thought to represent the transition from arc to back arc volcanism (e.g., Swinden et al. 1990, Jenner and Swinden 1993), during an extended period in the early Ordovician.

Williams et al. (1988) divided the Dunnage Zone into the northwestern Notre Dame and southeastern Exploits subzones, separated by the Red Indian Line, a post-Ordovician, regional, structural feature (Williams et al. 1988) (Fig. 1.1). The pre-mid-Ordovician volcano-sedimentary sequences of the Exploits Subzone have Gondwanan faunal affinities and were emplaced onto the Gander Zone during the late early Ordovician Penobscot orogeny (Colman-Sadd et al. 1992), prior to amalgamation of the Notre Dame and Exploits subzones of the Dunnage Zone (Neuman 1988). A minimum age of emplacement of the Exploits Subzone onto the Gander Zone in central Newfoundland, is provided by the late Arenig U-Pb age on the Partridgeberry Hills Granite (474 Ma, Colman-Sadd et al. 1992), the oldest dated pluton which intrudes both the Gander Zone and the Exploits Subzone.

The northern Exploits Subzone can be separated into two broad lithostratigraphic divisions, an older Cambrian to mid-Ordovician volcano-sedimentary succession (e.g., Wild Bight Group), and a younger mid-Ordovician to early Silurian shale-turbidite sequence (e.g., Shoal Arm Formation and Point Leamington greywacke of the Badger Group) (Dean 1977). Silurian rocks which overlap both the Gander Zone and the Exploits Subzone (Williams et al. 1988, Williams 1972 and Dunning et al. 1990) are both conformable and unconformable on the Ordovician volcano-sedimentary sequences of the Exploits Subzone (Colman-Sadd 1980, and references therein).

Dunning et al. (1990) presented abundant evidence from the Hermitage Flexure for Silurian orogeny in the Newfoundland Appalachians. Elsewhere in the Exploits Subzone, Silurian strata were involved in thrusting and 3 phases of folding (Karlstrom et

al. 1982) prior to intrusion of the early Devonian (408  $\pm$  2 Ma) Loon Bay Granite (Elliot et al. 1991), providing evidence that this event was widespread.

#### **1.4 Previous Work in the Area**

The term Wild Bight Volcanics was first introduced by Espenshade (1937), for volcanic and interbedded sedimentary rocks at the bottom of Badger Bay (Wild Bight). His work demonstrated a linkage between this area and the Bay of Exploits-New Bay region to the east (Heyl 1936). Systematic mapping in the western WBG was also carried out by Hayes (1951) of the Geological Survey of Canada. Hayes and Espenshade both included the Roberts Arm Volcanics and Crescent Lake Formation in the Exploits Group (or other equivalents of the Exploits Subzone), and did not recognize the Red Indian Line structure. However most subsequent workers have considered these rock packages to be part of the Notre Dame Subzone (Williams et al. 1988) of the Dunnage Zone. The first regional map of the NTS 2E district (which includes the entire WBG), was produced by Williams (1964), as part of a synthesis of the Notre Dame Bay area (see Williams 1962 and 1972). Williams (1964) redefined stratigraphic relationships in the western part of NTS 2E/5 (i.e., western WBG) such that rocks west of Badger Bay were included in a redefined Exploits Group. Thus the Exploits Group included middle and upper Ordovician strata contained in the Gull Island- Shoal Arm succession which were positioned stratigraphically above the middle Ordovician and older Wild Bight Formation, which he elevated to group status (Williams 1963). Williams also reassigned the Roberts Arm Volcanics and Crescent Lake Formation to the Roberts Arm Group, and recognized that their contact with the redefined Exploits Group was a fault. Regional

mapping in the central Notre Dame Bay area was continued by Dean (1977, 1978), Horne and Helwig (1978), O'Brien (1991, 1992 and 1993), and O'Brien and MacDonald (1997), and included the South Lake Igneous Complex, parts of the Wild Bight Group, Shoal Arm Formation and the Point Leamington Greywacke succession (Badger Group) (Fig.1.2). These studies produced various refinements of the WBG stratigraphy. Dean and Strong (1976) produced a regional compilation map, and along with reports by Dean (1977, 1978) they formally defined a number of formations within the Wild Bight Group. The stratigraphic divisions defined by Dean (1977, 1978) and Dean and Strong (1976) have provided the framework for most subsequent work in the WBG, including this study.

The South Lake Igneous Complex (Dean 1977) is comprised of cumulate layered gabbro and sheeted dykes, originally termed the South Lake Ophiolite (Dean 1977) intruded by hornblende diorite to tonalite plutons with an island arc affinity (Lorenz and Fountain 1982). O'Brien (1992) recognized that the SLIC occupies the core of a regional structural culmination in the eastern Wild Bight Group and is structurally juxtaposed against the WBG and younger, upper Ordovician rocks of the Point Leamington Greywacke to the east. O'Brien (1992) interpreted contacts on all sides of the SLIC to be high angle reverse faults, possibly as young as Silurian. The layering and gneissic foliation in the gabbro strike N-S, dip sub-vertically, and are cut by E-W striking, sub-vertical, meta-diorite dyke swarms (Lorenz and Fountain 1982). Based on the deformed nature of late leucogabbro veins, O'Brien (1992) suggested that deformation and intrusion were roughly synchronous. Foliation within and parallel to the dyke swarms led O'Brien

(1992) to suggest that they were emplaced, synkinematically into shear zones. A set of mafic to intermediate dykes cross-cuts all other units and structures (Lorenz and Fountain, 1982 and O'Brien, 1992). The various shear zones and associated fabrics within the complex are oblique to the generally N-S trending external contacts (O'Brien, 1992). O'Brien (1992) envisaged the development of the South Lake Igneous Complex in terms of an episodically active, long-lived shear zone with associated dynamothermal metamorphism, which was coeval with plutonism.

A geochemical study of the South Lake Igneous Complex (Lorenz and Fountain, 1982), showed that the dykes and gabbroic rocks of the layered gabbro tract have the geochemical characteristics of tholeiitic basalt, are strongly depleted in incompatible elements, but are unusual in that Zr and  $P_2O_5$  are depleted relative to other elements such as Ti and Y. These rocks were interpreted to have formed in a back arc basin environment (Lorenz and Fountain 1982). The hornblende diorite and tonalite were also found to be depleted in incompatible and light rare earth elements (LREEs). Lorenz and Fountain (1982) interpreted them to be genetically related, and to have formed in an island arc environment. Furthermore, they found that the late dykes which cross-cut all other rock units in the complex, were mildly alkalic and incompatible element- and LREE-enriched, and suggested that a subducted oceanic ridge could have generated such magmas.

A regional geochemical study of the volcanic rocks in the Wild Bight Group (Swinden et al. 1990) recognized 4 types of arc-related volcanic rocks, 3 mafic and 1 felsic, and 3 types of non-arc-related mafic volcanic and intrusive rocks. The arc-related mafic rocks range from strongly incompatible element-depleted, LREE-depleted

tholeiites to LREE-enriched basalts and andesites possibly with calc-alkalic affinities (Swinden et al. 1990). The arc-related felsic rocks are high-Si, low-K rhyolites with flat heavy REE's (HREEs) and slight LREE depletion. The non-arc mafic rocks range from slightly LREE-enriched tholeiitic basalt to strongly LREE-enriched alkalic basalt.

Swinden et al. (1990) interpreted the entire sequence to represent formation of an intra-oceanic arc, and its subsequent rifting, followed by back arc basin development.

Regional structural studies in the Notre Dame Bay area (e.g., van der Pluijm et al. 1987, Blewett and Pickering 1988, Blewett 1991, Elliot and Williams 1988, Elliot et al. 1989, O'Brien 1993, and O'Brien and MacDonald 1997) have documented superposed, polyphase, folding and thrusting of Ordovician and Silurian strata at low metamorphic grade. Structures formed during the main phase of deformation (D<sub>2</sub>) recognized in these studies have predominantly northwest-vergence; however, earlier southeast-directed tectonic transport (D<sub>1</sub>) has been proposed based on large scale regional tectonic and stratigraphic considerations (Lafrance and Williams 1992, and O'Brien 1993). O'Brien (1993) proposed 4 phases of deformation which are distinctly domainal, with D<sub>1</sub> and D<sub>4</sub> structures trending predominantly NW and D<sub>2</sub> and D<sub>3</sub> structures trending NE. The regional, thrust-bounded, domes and basins proposed by O'Brien (1993), were interpreted to be a result of D<sub>1</sub> thrusts being folded by large scale D<sub>2</sub> folds, with second order domes and basins being produced by locally intense D<sub>3</sub> deformation (O'Brien, 1993). D<sub>4</sub> caused tightening of earlier folds and produced transcurrent faults (O'Brien, 1993).

### **1.5 Rational For Thesis Presentation**

The nature of the results of this study have dictated the format in which this thesis is presented. The South Lake Igneous Complex has been shown to be genetically related to a discrete package of volcanic rocks within the Wild Bight Group. These rocks are up to 10 Ma older than volcanic rocks in the younger sequence of the Wild Bight Group with which they have been structurally interleaved during later deformation. Furthermore, the older and younger sequences formed in distinct tectonic settings. For these reasons, the ages, geochemical characteristics, and origins of the two packages are discussed in separate chapters (2 and 3).

Although the older sequence has a magmatic history distinct from the younger sequence, they do share a common history prior to final juxtaposition during Silurian deformation. The nature of these relationships, and their significance for regional interpretations of Wild Bight Group structure and stratigraphy are discussed in Chapter 4. The implications of this work for the origin of correlative sequences in the Exploits Subzone and evolution of the Gondwanan margin in the northern Appalachians are presented in Chapter 5.

## **Chapter 2**

### **Age, Origin and Tectonomagmatic Evolution of the Older Volcanic Sequence of the Wild Bight Group and the South Lake Igneous Complex**

#### **2.1 Introduction**

The South Lake Igneous Complex (SLIC) and adjacent arc-related volcanic and volcanoclastic rocks of the Wild Bight Group (WBG) comprise one of the many accreted Ordovician oceanic terranes of the Exploits Subzone of the central Newfoundland Appalachians (Fig. 1.1). The SLIC has been interpreted by previous workers (Dean 1977, Lorenz and Fountain 1982, and O'Brien 1992) to be Ordovician in age, and predominantly in fault contact with surrounding rocks of the WBG and the Point Leamington Greywacke of the Badger Group, although no geochronological data has been published to support this interpretation. Dean (1977) interpreted the youngest phase of the SLIC to locally be intrusive into the WBG.

Detailed mapping for this study has shown that part of the WBG has a similar structural setting to the SLIC (Map A). U/Pb ages and trace element and Nd-isotopic data suggest that these two packages are also temporally and genetically related. Furthermore, they are geochemically distinct from volcanic rocks in the rest of the WBG, and are up to 10 Ma older. The older sequence of rocks (map units 1-3, Map A) occurs predominantly as fault-bounded packages within the younger Wild Bight Group sequence (map units 4-8, Map A), although locally at the stratigraphic base of the younger sequence, the original stratigraphic contact may be preserved.

The South Lake Igneous Complex (SLIC) consists of two parts, a layered gabbro-sheeted dyke complex, which also contains minor massive gabbro and gabbro pegmatite, previously interpreted to represent part of an ophiolite suite (Dean 1977, and Lorenz and Fountain 1982); and hornblende diorite and tonalite plutons which intrude it, thought to represent the base of a volcanic arc (Lorenz and Fountain 1982). There is a close relationship between deformation and magmatism in these units which indicates a very dynamic setting for their origin. Late, mafic to intermediate dykes which cross-cut all other rock types are an integral part of the magmatic history of the complex.

The older sequence of the WBG comprises pillowed basalts and pillow breccias interbedded with quartz- and plagioclase-phyric rhyolite flows and domes, minor felsic to intermediate tuffs/lapilli tuffs and tuffaceous sandstone and minor red chert and argillite. Stratigraphic relationships in this sequence are difficult to determine because of the possible occurrence of bedding parallel structures and poor outcrop away from the coast. However, by developing a genetic link between these rocks and the SLIC, some inferences can be made.

These rocks are interpreted to represent the initiation and stabilization of a primitive ensimatic arc that formed outboard of the Gondwanan margin in the early Ordovician. The South Lake Igneous Complex is interpreted to represent a deeper crustal level of the volcanic rocks of the older sequence of the WBG.

## 2.2 Geology

### 2.2.1 *South Lake Igneous Complex*

The layered gabbro-sheeted dyke complex also contains small amounts of massive gabbro and gabbro pegmatite. The gabbroic rocks dominate in the north, whereas the central part of the complex consists of a mixture of tonalite and diorite, and the southern part is comprised entirely of tonalite (Map A). This distribution of rock types suggests that an oblique section through the base of the arc is exposed. The regional change in direction of plunge of the domal structure in the WBG (Map A) exposes the deepest levels of the WBG at approximately the same location as the layered gabbro tract. Based on this interpretation the oldest rocks (layered gabbro tract), which have the strongest penetrative deformation, occur in what would represent the lowest levels of the arc. In the central part of the complex, hornblende diorite and tonalite are intermingled on all scales, and impart a structural grain which strikes NNW and generally dips steeply (Map B). In the southernmost part of the complex where diorite and gabbro are absent, the tonalite does not have any structural grain. A set of late mafic to intermediate dykes with no penetrative deformation cross-cuts all other units and structures (Plate 2.1a).

The proportion of dykes in the layered gabbro tract varies from 10% to about 80%, but no systematic variation was observed. The dykes locally have a sheeted aspect (Plate 2.1b), but more commonly individual dykes are separated by screens of layered gabbro (Plate 2.1c). Several sets of dykes were recognized, including: fine-grained to aphanitic dark grey dykes; fine-grained, speckled, light grey diabase dykes; and aphanitic, dark green, variably phyrlic dykes. Some light grey dykes cross-cut the dark grey ones, but

no other temporal relationships could be recognized, because of metamorphism and deformation. A dyke-parallel fabric ranging from a well-developed foliation to mylonitic (Plate 2.1d) occurs in many of the dykes and rarely in gabbro screens between dykes. Fracture sets in the dykes, originally oblique to dyke orientation are commonly rotated into the fabric along dyke margins (Plate 2.1e) suggesting that dyke-parallel movement may have occurred. These relationships are compatible with O'Brien's (1992) interpretation that the dykes were emplaced synkinematically into shear zones. The dykes and dyke-parallel fabrics are offset along numerous small N-NE striking and less commonly N-NW striking (Map B), steeply dipping faults with both sinistral and dextral offset. The entire layered gabbro tract is divided into panels by several N-NE striking, sub-vertical faults (Lorenz and Fountain 1982) which are confined to the layered gabbro tract (Map B), and pre-date the younger plutonic suite. However, the orientation of hornblende diorite and tonalite sheet-like intrusions (Map B) is similar to these shear zones suggesting the same principal stress orientations at the time of intrusion. In some places, tonalite and diorite actually intrude along these early deformation zones (Map B).

The hornblende diorite may contain visible quartz, and varies considerably from leucocratic to melanocratic. The tonalite is typically coarse-grained, quartz-rich and multiphase. All phases contain the large (3-8mm) bluish quartz blebs which distinguish the more melanocratic phases from those of the hornblende diorite, in which quartz is a late interstitial phase. In places, both the diorite and layered gabbro are brecciated and cemented by tonalite/trondjemite net veins (Plate 2.1f).

In the central part of the SLIC, the hornblende diorite and tonalite are intermingled on all scales, and impart a structural grain to the complex (Map B). The tonalite commonly contains abundant inclusions which are elongated parallel to the trains in which they occur. These mixed units are commonly separated, and probably cross-cut by parallel tonalite sheets without inclusions (Plate 2.1g). In some places the tonalite has a noticeable foliation defined by flattened quartz eyes, which generally parallels the tonalite sheets (Map B).

Fragments of both hornblende diorite and sheeted dykes (plate 2.1h) occur in the tonalite. Irregular altered and deformed intrusions with similar compositions also occur within the diorite and gabbro adjacent to large tonalite bodies, and as irregular deformed and altered bodies within the tonalite. These probably represent either: inclusions that have resided in the tonalite for extended periods of time, and have lost their coherence; or the product of magma mixing.

### *2.2.2 Older sequence of the Wild Bight Group*

The fault-bounded package of the older sequence north of the SLIC is dominated by pillowed basalts (Plate 2.2a) and pillow breccias (Plate 2.2b) with numerous syn-volcanic dykes and sills. Inter-pillow red chert and argillite locally form thick lenses. The basalts are predominantly aphyric, commonly strongly vesicular and locally strongly hematized. The most intense hematization occurs along the western bounding fault which is exposed on the shore (Plate 2.2c), and may have been enhanced at this locality as a result of the fault. The mafic volcanic rocks are interbedded with felsic to intermediate tuffs, lapilli tuffs (Plate.2.2d) and minor fine- to medium-grained volcanoclastic rocks. Pillows in this

sequence of rocks face and dip steeply toward the northwest on the northwestern side, whereas on the southeast side they face to the southeast. No evidence of a fold was observed, and thus this sequence is interpreted to be fault-imbricated. This interpretation is supported by the occurrence of numerous high strain zones both on surface and in drill core. Within the mafic volcanic rocks is a small sulphide deposit which Swinden (1988) interpreted as the stockwork alteration zone of a volcanogenic massive sulphide deposit.

The western bounding fault juxtaposes thinly bedded red and green argillite and tuffaceous sandstone at the base of the younger WBG sequence (unit 4), against strongly sheared and hematized pillowed volcanic rocks of the fault-bounded older sequence (Plate 2.2c). The bedding and foliation in the argillite are sub-vertical and parallel to the fault, as is the foliation in the sheared volcanic rocks. Minor folds in the argillite that are truncated by the fault indicate that there is a dextral component to the youngest movement on this fault. Overturned bedding in the footwall elsewhere (Map A1) suggests that this was originally an east-dipping, west-verging thrust fault. The location of the eastern bounding fault is inferred from the nature of volcanoclastic units, basalt geochemistry and intensity of deformation.

The part of the older sequence which is the south of the SLIC (Map A) is also dominated by pillowed basalts, with a thin package of rhyolite flows and crystal-rich tuffs at the northern end, and a massive quartz- and plagioclase-phyric rhyolite unit in the south. There is a small sulphide showing associated with the rhyolites at the north end. In this area, because of poor exposure, the styles of structural and stratigraphic relationships inferred are based on those mapped in the northern area. To the east, the older sequence

is in contact with the middle part of the younger sequence, which faces toward it, and thus, the contact is interpreted to be a D<sub>1</sub> fault. As the contact is between two different sequences of mafic volcanic rocks, the location is interpolated based on differences in basalt geochemistry. On the western side of the older package, north of the D<sub>2</sub> Long Pond Fault (Map A1), depleted-rhyolite of the older sequence is stratigraphically overlain by unit 4 sedimentary rocks at the base of the younger sequence. The rocks of unit 4 face west and overlie the older sequence, compatible with an original stratigraphic contact; although there is no clear cut bedding in the rhyolite and thus the nature of the stratigraphic contact is equivocal. South of the Long Pond fault the older WBG sequence is in contact with rocks in the middle part of the younger sequence which face east, toward the older sequence, and thus the contact is interpreted to be a D<sub>1</sub> fault. The location of this fault is interpolated based on differences in lithology, and basalt geochemistry.

### **2.3 Linking the WBG and SLIC**

Detailed mapping has shown that parts of the Wild Bight Group occur in a similar structural setting to rocks of the South Lake Igneous Complex, suggesting that they might be related. Spatial continuity is strengthened by the fact that they have similar geochemical characteristics. Primitive mantle-normalized, extended rare earth element (extended-REE) patterns for a typical sheeted dyke and a gabbro pegmatite from the SLIC and a typical pillowed basalt from the northern fault-bounded package of the older WBG sequence are very similar (Fig. 2.1a) and they have the geochemical characteristics of low-Ti, high-Mg tholeiitic basalt. There is also very good agreement between the

extended-REE patterns of tonalites from the SLIC and rhyolites from the older sequence of the WBG (Fig. 2.1b), which are unusual in that they have very low levels of incompatible elements, and relatively flat extended-REE patterns. Furthermore, the late, less-depleted, tholeiitic, mafic to intermediate dykes which cross-cut the SLIC have extended-REE patterns similar to the tholeiitic basalts in the southern part of the older sequence (Fig. 2.1c). Although geochemical similarity does not prove a genetic relationship, it suggests that these two packages are related, particularly as the composition of most of the rocks in both packages are so distinctive in their degree of incompatible element depletion. Thus, U/Pb geochronology was undertaken to determine if these two packages of rocks have similar ages. The geochemical characteristics will be discussed in more detail below.

## 2.4 U-Pb Geochronology

A tonalite, quartz hornblende diorite, and gabbro pegmatite from the South Lake Igneous Complex were dated. Mafic dykes which cross-cut the complex did not yield any datable minerals. An alkalic gabbro dyke which intrudes the volcanic rocks in the older sequence on the west side of Glovers Harbour, provides a minimum age for this sequence. The analytical technique is described in Appendix 5.

### 2.4.1 U-Pb Samples

*The tonalite age is determined from the combined data of two samples (GD91-6 and D47-10, Map B) which are different phases of the same pluton. In sample GD91-6, most of the zircon occurs as brown fragments, which show some prism faces, although few entire prismatic crystals were observed. The brown colour is indicative of high U content,*

and all fractions were taken from the magnetic at 3° franz split. The high U content also indicates the potential for more significant Pb loss, and all fractions, except one, were strongly abraded. Sample D47-10 had a similar zircon population, although there were also abundant rounded prisms. All fractions from this sample were from the 1.7A franz fraction, and were strongly abraded, except for the most discordant point. Separately, these two samples give ages of  $484 \pm 7/-5$  and  $487 \pm 7/-4$  Ma, respectively, but together they define a 10 point discordia line with a 45 % probability of fit and an upper intercept age of  $486 \pm 3$  Ma (Fig. 2.2a, Table 2.1), excluding point AZ5.

*A gabbro pegmatite (95GC03)* from the southern part of the SLIC (Map B) was also dated. It is comprised predominantly of coarse-grained (1-4cm) cumulate Ca-rich plagioclase, clinopyroxene and orthopyroxene, with interstitial more Na-rich plagioclase, orthopyroxene, hornblende and minor quartz. The hornblende in places rims and replaces the clinopyroxene (Plate 2.3a), and the orthopyroxene is mostly altered to bastite (Plate 2.3b). This sample is geochemically very similar to sheeted dykes from the SLIC and pillow lavas from the northern fault-bounded package of the older volcanic sequence of the WBG (Glovers Harbour west unit, Map C) (Fig. 2.1a). Small, euhedral, gem quality, zircon prisms were abundant in the 0° nm fraction. Six fractions of like morphology grains were analysed: 2 fractions were strongly abraded elongate prisms; two were strongly abraded stubby multi-faceted prisms; and two were unabraded needles and prisms, respectively. The abraded fractions were all less than 1 % discordant, and the unabraded fractions were 1 - 2 % discordant. All fractions together define a discordia line

with 84 % probability of fit and an upper intercept age of  $489 \pm 3$  Ma (Fig. 2.2b, Table 2.1).

The dated *hornblende diorite* (95GC04) comes from a roadcut on highway 350 (Map A). It comprises a small component of cumulate plagioclase crystals (up to 5 mm), but is dominated by finer-grained plagioclase laths surrounded by ophitic to sub-ophitic hornblende, with interstitial quartz (Plate 2.3c). This sample yielded a small quantity of tiny, euhedral, gem quality zircon prisms, and slightly larger irregular fragments in the 0° nm fraction. Five fractions of abraded zircon were analysed, three were prisms and two were the larger fragments. They range from 0.5 to 2.4 % discordant, and define a discordia line with 28% probability of fit, that gives an upper intercept age of  $489 \pm 2$  Ma (Fig. 2.2c, Table 2.1).

Numerous unsuccessful attempts were made (and more than 250 kg of rock processed in total) both in this and a previous study, to date rhyolite flows/domes and felsic tuffs within the older fault-bounded volcanic sequences of the WBG. However, an *alkalic gabbro dyke* (GHG, Map A) which intrudes the mafic volcanic sequence in the northern fault-bounded package of the older volcanic sequence of the WBG (Glovers Harbour west unit of map C), yielded sufficient baddeleyite to obtain a minimum age for this sequence. This gabbro dyke is medium-grained and massive, but locally contains coarser pegmatitic patches, one of which was sampled for dating. This sample yielded a small amount of tiny baddeleyite blades and flakes in the 3° nm fraction. Many of these grains were too small and delicate to withstand abrasion, although three fractions of equant grains were weakly abraded. The five fractions of baddeleyite analysed range from

4 to 12 % discordant. This high degree of discordance is probably a result of the small grain size. A discordia line through all 5 fractions has a 32% probability of fit, with an upper intercept age of  $486 \pm 4$  Ma (Fig. 2.2d, Table 2.1).

#### *2.4.2 Interpretation*

Although all U-Pb ages within the SLIC overlap within uncertainties, the ages are consistent with field relationships which show that the tonalite is younger than the mafic rocks. Thus, the relative U-Pb ages are interpreted to be meaningful. This has significant implications for the timing of deformation. Although the gabbro pegmatite is not deformed, geochemically related dykes from the sheeted dyke complex and the layered gabbro are deformed, and these fabrics are crosscut by the hornblende diorite, which overlaps in age with the gabbro pegmatite. Thus the deformation of the mafic dykes and layered gabbro occurred synchronously with magmatism. The mafic magmatism was followed very shortly by voluminous tonalitic magmatism which also occurred in a dynamic setting creating the NNE fabric within the central part of the complex. Furthermore, the alkalic mafic dyke which crosscuts the mafic volcanic rocks within the northern part of the older WBG sequence (GHW unit), provides a minimum age of  $486 \pm 4$  Ma (late Tremadoc, time scale of Tucker and McKerrow 1995) for that sequence.

#### **2.5 Geochemistry**

All geochemical samples were analysed for major oxides and a suite of trace elements (Sc, V, Cr, Ni, Rb, Sr, Y, Zr, Nb, Ba, Ce, and Th ) by standard X-ray fluorescence (XRF), on fused glass beads and pressed pellets, respectively. A subset of samples was also analysed for a comprehensive suite of trace elements (Y, Zr, Nb, Ba, rare earth elements

(REEs), Hf and Th) by inductively coupled plasma mass spectrometry (ICP-MS), using a Na-sinter dissolution technique. A representative suite of samples was also analysed for Sm/Nd isotopic composition by thermal ionization mass spectrometry (TIMS), using isotope dilution. These techniques and the precision and accuracy of all geochemical data are described in detail in appendices 5 and 4, respectively. All analytical work was done at Memorial University of Newfoundland.

### *2.51 Alteration and metamorphism*

All samples have been metamorphosed to lower greenschist facies during regional metamorphism, and many of the volcanic rocks have spilitic mineral assemblages typical of sea-floor alteration. Many major (e.g., Si, Na, K, Ca) and trace (e.g., Cs, Rb, Ba, Sr) elements may be mobile under these metamorphic conditions; however, the rare earth elements (REEs), as well as Y, Zr and Ti (Saunders et al. 1979, and Ludden et al. 1982), Nb (Bienvenu et al. 1990), V, Cr and Ni (Canil 1987) and Th (Wood 1980, and Merriman et al. 1986) have been shown to be relatively immobile under a wide range of metamorphic conditions, including sea-floor alteration. On Hughes' (1973) plot of  $K_2O + Na_2O$  vs  $K_2O/(K_2O + Na_2O)$ , which screens samples for spilitization and K-metasomatism, the plutonic rocks plot in or near the igneous spectrum suggesting that even these easily mobilized elements have not been significantly changed by regional metamorphism, although most of the volcanic rocks plot in the spilitized field. On primitive mantle-normalized, extended-rare earth element plots (see below), patterns of related plutonic and volcanic rocks show little variation. Thus the above immobile trace elements, as well as some major element ratios (e.g.,  $MgO/FeO^*$  Alt and Emmerman

1985 and Humphries and Thompson 1978) can be used as indicators of the sources and processes involved in generating these rocks.

### *2.5.2 Purpose*

In the previous section, structural, stratigraphic and geochronological data were presented to show that the SLIC and the fault-bounded packages of the older WBG sequence are likely genetically related. In the following section the geochemistry is discussed in detail, for both packages together, based on this interpretation. The geochemical groups are distinguished based exclusively on geochemical characteristics and include samples from both packages. The purpose of this section is to distinguish different geochemical groups and interpret the tectonic setting in which they formed; and secondly to determine if the geochemical relationships between the SLIC and the WBG are internally consistent and consistent with other relationships. Linking volcanic rocks from the older WBG sequence with geochemically similar rocks in the SLIC also provides some constraints on the stratigraphic sequence. Geochemical data are presented in Table 2.2 for samples plotted on extended-REE diagrams used to define the various geochemical groups are, and all other geochemical data is presented in Appendix 3.

### *2.5.3 Geochemical characteristics of mafic rocks*

Layered gabbros were not analysed as their compositions are strongly controlled by the cumulate phases. Cumulate minerals occur of the massive gabbros and thus, they do not represent liquid compositions. The mafic dykes and basalts provide the best estimates of liquid compositions, but the massive gabbros have very similar trace element

characteristics suggesting that the accumulated minerals have preserved the unique trace element signature of the magma from which they were derived.

Based on the major element cation classification diagram (Fe+Ti vs Al vs Mg) of Jensen (1976) the partially cumulate mafic rocks of the SLIC range from komatiitic basalt (ultramafic xenolith in tonalite) to high-Fe tholeiitic basalt (large amount of cumulate Fe/Ti-oxide). These end-member compositions are clearly caused by mineral accumulation. The compositional variation in the sheeted dykes and the mafic volcanic rocks is more limited and most samples are classified as tholeiitic basaltic komatiite or high-Mg tholeiitic basalt. The hornblende diorite is also classified as high-Mg tholeiitic basalt. The dark green dykes from the layered gabbro tract of the SLIC are the least fractionated rocks ( $Mg\#$  ( $MgO/MgO+FeO+Fe_2O_3$ )  $\sim 65$ ,  $SiO_2 \sim 49$ wt%), while the majority of sheeted dykes, hornblende diorite, and volcanic rocks appear to be more fractionated ( $Mg\# \sim 25$  to  $50$ ,  $SiO_2$  from  $48$  to  $56$  wt%). The late basaltic dykes and most of the mafic volcanic rocks of the older sequence south of the SLIC are classified as high-Fe tholeiitic basalt and are the most fractionated ( $Mg\# \sim 21$  to  $33$ ,  $SiO_2$   $49$  to  $56$  wt%).

With the exception of the late dykes and geochemically similar volcanic rocks, all the mafic rocks are strongly depleted in incompatible elements. This, combined with the significant cumulate component in some, prohibits unequivocal interpretation using many popular tectonic discrimination diagrams. Primitive mantle-normalized, extended rare earth element (extended-REE) diagrams provide a useful way of comparing the trace element composition of these rocks amongst themselves, and with other similar rock

types, and have been used in combination with certain element ratios, to characterize different geochemical groups. Furthermore, extended-REE patterns can be interpreted in terms of source compositions and magma generation processes.

The least fractionated samples have been used to define each group and are plotted on primitive mantle-normalized extended-REE diagrams (Fig. 2.3). Element ratios of which help to distinguish the different groups are summarized in Table 2.4. The critical aspects of the extended-REE patterns are reflected in the normalized trace element ratios, and the Mg# and the  $\text{CaO}/\text{Al}_2\text{O}_3$  and  $\text{TiO}_2$  values give a qualitative reflection of the degree of fractionation and source depletion, respectively. Source depletion is also reflected in the absolute abundance of the heavy REEs (HREEs) and Y and the high-field strength elements (HFSEs) (Zr, Hf, Nb, Ti) which Pearce and Peate (1995) interpreted to be conservative with respect to the mantle source, and thus reflect its composition prior to the influence of subduction. The following five groups of mafic rocks have been recognized.

Group 1, normal island arc tholeiites (IATs). This group is represented by the late mafic to intermediate dykes which cross-cut the SLIC and by mafic volcanic rocks of the older WBG sequence south of the SLIC. They have high-Fe tholeiitic basalt compositions and are quite fractionated (Mg# typically from 38 to 48). The extended-REE patterns (Fig. 2.3a), are very similar to modern IATs (Fig. 2.3f) and at similar absolute abundances (HREEs 5 to 8 x primitive mantle), although these rocks are more strongly fractionated than the IAT example shown in Figure 2.3f. Thus they may have had somewhat lower abundances prior to fractionation, suggesting greater degrees of partial melting. They

have slightly light REE (LREE)-depleted to slightly LREE-enriched patterns, strong negative Nb and positive Th anomalies, slight negative or positive Zr and Hf anomalies ( $(\text{Zr/Sm})_N = 0.97\text{--}1.10$ ) and relatively flat HREEs. The  $\epsilon_{\text{Nd}}$  values range from +3 to +6 (Table 2.3), which suggests a source dominated by depleted mantle, although the strong negative Nb anomaly is indicative of a subduction-related component.

Group 2, low-Ti Island Arc Tholeiites (Low-Ti IATs). This group is represented by the grey dykes in the layered gabbro tract and the hornblende diorite of the SLIC, and by mafic volcanic rocks in the northern part of the older WBG sequence. They have the composition of high-Mg tholeiitic basalt and are somewhat less fractionated ( $\text{Mg\#}$  typically from 32 to 69) than group 1 IATs. The extended-REE patterns (Fig. 2.3b) are very similar to group 1 IATs, but the absolute abundances are somewhat lower (HREEs 2–3 x primitive mantle), and the negative Zr and Hf anomalies are slightly greater ( $(\text{Zr/Sm})_N = 0.91$ ). The  $\text{TiO}_2$  content is also considerably lower (0.3 to 0.9, as opposed to 1.1 to 1.7) than that of group 1 IATs. The  $\epsilon_{\text{Nd}}$  values range from +3 to +6 (Table 2.3), compatible with a source dominated by depleted mantle, although the negative Nb anomaly is again indicative of a subduction-related component. The lower  $\text{TiO}_2$  and HREE contents suggest that the mantle source for these rocks was more incompatible element depleted than for group 1, but they were probably produced by similar processes.

Group 3, low-Ti, LREE-depleted Island Arc Tholeiites (low-Ti, LREE-depleted IATs). This group is represented by the green mafic dykes and massive gabbro/gabbro pegmatites of the SLIC and the majority of mafic volcanic rocks in the northern part of the older WBG sequence. These rocks have the composition of high-Mg tholeiitic basalt

and basaltic komatiite, and are the least fractionated of all the rocks sampled (Mg# typically 33 to 79). The extended-REE patterns of this group (Fig. 2.3c) show much stronger LREE depletion ( $(\text{La/Yb})_N = 0.3$ ) and much larger negative Zr and Hf anomalies ( $(\text{Zr/Sm})_N = 0.6$ ). The Nb anomaly is difficult to assess because at these very low levels (less than 0.5 x primitive mantle) Nb is very close to the detection limit and the uncertainties are relatively large (see error bars Fig. 2.3c, and Appendix 4). The  $\text{TiO}_2$  content of this group is similar to that of group 2, although the absolute abundance of the HREEs is somewhat lower ( $\sim 2$  x primitive mantle). This group is unusual in that it has a very wide range in  $\epsilon_{\text{Nd}}$  values from -1 to +8 (Table 2.3). The strong LREE depletion, and the low  $\text{TiO}_2$  and HREE levels suggest a very depleted mantle source. The presence of a subduction component is not clear based on the Nb anomalies in the least fractionated samples, although more evolved samples with slightly higher incompatible element concentrations do typically have negative Nb anomalies indicative of a subduction-related component. The Nd isotopic data clearly indicates a more complicated source or process of formation for this group compared to groups 1 and 2.

Group 4, low- $\text{CaO/Al}_2\text{O}_3$ , LREE-depleted, low-Ti Island Arc Tholeiites (Low- $\text{CaO/Al}_2\text{O}_3$ , low-Ti IATs). This group is only represented by 2 volcanic rocks in the northern part of the older WBG sequence. These rocks have the composition of high-Mg tholeiitic basalt (Jensen 1976), and are somewhat more fractionated than group 3 (Mg# 45 and 47), but have very similar extended-REE patterns (Fig. 2.3d) at similar absolute abundances (HREEs 1-2 x primitive mantle). The  $\text{TiO}_2$  content is slightly lower, but the main difference is the  $\text{CaO/Al}_2\text{O}_3$  ratio, which is considerably lower. This could partially

be a result of fractionation or alteration, but may also be a primary feature related to the clinopyroxene content of the source. Prior to fractionation, the REE abundances might also have been somewhat lower. The strong LREE-depletion, low  $\text{TiO}_2$  content and low  $\text{CaO}/\text{Al}_2\text{O}_3$  ratio point to a strongly depleted harzburgite mantle source. As with group 3, the Nb anomaly is unclear and thus a subduction component in the source is uncertain. The  $\epsilon \text{Nd}$  values range from +5 to +7 (Table 2.3), compatible with a source dominated by depleted mantle.

Group 5, low  $\text{CaO}/\text{Al}_2\text{O}_3$ , LREE-enriched, boninites (Low- $\text{CaO}/\text{Al}_2\text{O}_3$  boninites). This group is only represented by 3 volcanic rocks in the northern part of the older WBG sequence. The least fractionated boninite has lower  $\text{CaO}/\text{Al}_2\text{O}_3$ ,  $\text{TiO}_2$  and HREE abundances ( $\sim 1 \times$  primitive mantle, Fig. 2.3e) than samples in group 4, which is compatible with its lower degree of fractionation ( $\text{Mg\#}$  35-65). The boninites have flat to slightly LREE-enriched patterns ( $(\text{La}/\text{Yb})_{\text{N}} \sim 1$ ) and strong positive Zr and Hf anomalies ( $(\text{Zr}/\text{Sm})_{\text{N}} = 1.3$ ). This pattern is characteristic of modern day boninites, and these rocks are geochemically similar to group 3 low-Ca boninites (Crawford 1989). The  $\epsilon \text{Nd}$  values of the boninites are both around +5 (Table 2.3) indicative of a depleted mantle source. The low  $\text{CaO}/\text{Al}_2\text{O}_3$ ,  $\text{TiO}_2$  and HREE abundances and positive  $\epsilon \text{Nd}$  values are compatible with a source dominated by strongly depleted mantle harzburgite; however, the slight LREE-enrichment and strong positive Zr and Hf anomalies indicate that the source region and/or processes which generated these rocks were complicated.

Because of the very trace element-depleted composition of many of these rocks, they plot outside all fields on many common tectonic discrimination diagrams. However, some of these diagrams are useful for comparing the more fractionated members of each group, and samples for which REE data are not available. On the Ti vs V plot of Shervais (1982) (Fig. 2.4a), all of these samples plot in the IAT field, as expected, but it effectively discriminates between the depleted (i.e., low-Ti) and the normal IATs. The depleted rocks define a trend with chondritic Ti/V ratios ( $\sim 10$ ), with the more depleted samples plotting at lower absolute abundances. The normal IATs have Ti/V ratios between 15 and 20, and higher absolute abundances. The low  $\text{CaO}/\text{Al}_2\text{O}_3$  rocks have the lowest Ti/V ratios ( $\sim 5$ ), which are well below chondritic values. On Wood's (1980) Nb-Hf-Th ternary plot (Fig. 2.4b), the samples all plot in the destructive plate margin field; however, the low-Ti samples plot predominantly in the calc-alkaline as opposed to tholeiitic field. Major element compositions and extended-REE plots show that these rocks are clearly not calc-alkaline, and this misclassification can be attributed to their relative depletion in Hf (and Zr). A similar argument can be made for Meschede's (1986) Nb-Y-Zr ternary plot (Fig. 2.4c), where the more depleted samples plot outside the IAT field, away from the Zr apex, and the boninites plot outside the IAT field in the opposite direction because of their positive Zr (and Hf) anomalies. The normal IATs plot in the appropriate field, as on other diagrams.

#### *2.5.4 Geochemical Characteristics of Felsic Rocks (Group 6)*

Based on Jensen's major element cation plot (Jensen 1976) the tonalites and rhyolites are classified as calc-alkaline andesite to rhyolite, although they plot very close to the

tholeiitic field. The intermediate compositions of tonalite are dominated by cumulate Ca-rich plagioclase and quartz in thin section (Plate A6-2a), and have higher  $\text{CaO}/(\text{CaO}+\text{Na}_2\text{O})$  and  $\text{Mg\#}$ . The more felsic compositions of tonalite are dominated by granophyric intergrowth of Na-rich plagioclase and quartz (Plate A6-2b) and have lower  $\text{CaO}/(\text{CaO}+\text{Na}_2\text{O})$  and  $\text{Mg\#}$ . The rhyolites are comprised of a very fine-grained quartzofeldspathic matrix with quartz and plagioclase phenocrysts. All the felsic rocks are very low in  $\text{K}_2\text{O}$  (most  $<0.75$  wt%) and high in  $\text{SiO}_2$  (most  $>70$  wt%). There is also a range in Zr and  $\text{P}_2\text{O}_5$  from lowest Zr and highest  $\text{P}_2\text{O}_5$  in the intermediate compositions to higher Zr and lower  $\text{P}_2\text{O}_5$  in the most felsic samples. However, all of these rocks are low in  $\text{P}_2\text{O}_5$  and Zr relative to typical calc-alkaline felsic rocks.

Most of the tonalites have flat to slightly LREE-depleted extended-REE patterns with strongly negative Ti and slightly negative Eu anomalies, and a negative Nb anomaly characteristic of arc-related rocks (Fig. 2.1b). This is in contrast to typical calc-alkaline felsic rocks which have moderate to strong LREE enrichment. The HREE abundances range from 8 to 11 x primitive mantle and the LREE from 4 to 10 x primitive mantle. This pattern is very similar to the hornblende diorite, but at slightly greater absolute abundances. The  $\epsilon_{\text{Nd}}$  values range from +3.5 to +8.5 which is indicative of a depleted source.

These kinds of low-K, high- $\text{SiO}_2$  felsic rocks are generally interpreted as the products of partial melting of mafic rocks (e.g., Barker 1976, Drummond and Defant 1990 and Jenner and Swinden 1993), as opposed to being the result of fractionation of the mafic rocks. This is compatible with the high proportion of tonalite to mafic rocks in the

SLIC (Map B) which makes generation by crystal fractionation from the mafic rocks unlikely. It also explains why the extended-REE patterns of the felsic rocks mimic those of the mafic rocks observed, but at slightly higher absolute abundances.

## 2.6 Sm/Nd Isotope Systematics

Most of the mafic rocks have high positive  $\epsilon$  Nd values, compatible with a source dominated by depleted mantle. However, negative Nb anomalies on primitive mantle-normalized, extended-REE diagrams indicate a contribution to their chemistry from a subduction-related component. The effect of mixing these two components is depicted on a plot of  $^{147}\text{Sm}/^{144}\text{Nd}$  vs  $\epsilon$  Nd (Fig. 2.5).

The isotopic signatures of the normal island arc tholeiites (IATs, group 1) can be explained by mixing normal MORB-like depleted mantle (DM), or slightly more depleted mantle, with a subduction-related component dominated by juvenile material (i.e., only a small component of pelagic sediment), which could be either melts from, or fluids that were in equilibrium with, subducted material. Some of the low-Ti and LREE-depleted, low-Ti tholeiites can also be explained by a similar mixing process of VDM and a subduction-related component. Other of the LREE-depleted, low-Ti tholeiites from this study, a previous study of the WBG and Western Tasmania, and IATs from an ophiolitic terrane in SW Norway have  $^{147}\text{Sm}/^{144}\text{Nd}$  ratios significantly higher ( $>0.3$ - $0.45$ ) than compositions proposed for early Ordovician very depleted mantle ( $\sim 0.26$ - $0.28$ , Swinden et al. 1990) (Fig. 2.5, Table 2.3). Together, all of these samples define a roughly triangular zone with  $\epsilon$  Nd values less than very depleted mantle, but with higher

$^{147}\text{Sm}/^{144}\text{Nd}$  ratios. The samples which plot at lower  $\epsilon \text{ Nd}$  and  $^{147}\text{Sm}/^{144}\text{Nd}$  values can be explained by mixing a subduction component that has continental crust isotopic characteristics with a component which has higher  $\epsilon \text{ Nd}$  and extreme  $^{147}\text{Sm}/^{144}\text{Nd}$  ratios ( $> 0.35$ ). However, these extreme  $^{147}\text{Sm}/^{144}\text{Nd}$  ratios would require a significantly more depleted mantle than the VDM used here (DM minus MORB melt, Swinden et al. 1990).

Rocks with low  $\text{CaO}/\text{Al}_2\text{O}_3$  (groups 4 and 5), both low-Ti tholeiites and boninites, plot in the same location as many of the other low-Ti tholeiites on the  $\epsilon \text{ Nd}$  vs  $^{147}\text{Sm}/^{144}\text{Nd}$  plot (Fig. 2.5). This suggests that the LREE-enrichment in the boninites could not be a long-lived characteristic of the source region, but developed, only slightly before or during their generation. That boninites from elsewhere have significantly lower  $\epsilon \text{ Nd}$  and  $^{147}\text{Sm}/^{144}\text{Nd}$  values suggests that the component which generates the LREE-enrichment and positive Zr and Hf anomalies typical of boninites could also affect their isotopic signature.

Mixing of subduction-related components with variably depleted mantle melt (e.g., Pearce and Peate, 1995 and references therein) can create the various geochemical and isotopic characteristics of samples which define mixing trends with positive slopes on  $\epsilon \text{ Nd}$  vs  $^{147}\text{Sm}/^{144}\text{Nd}$  plots (Fig. 2.5). This is illustrated qualitatively in Figure 2.6. From a) to c) the mantle source is progressively more depleted, which results in stronger LREE-depletion and greater negative Zr and Hf anomalies, and lower  $\text{CaO}/\text{Al}_2\text{O}_3$  ratios in the magma produced. This mantle component is overprinted in all cases, by a

subduction component which is most enriched in LREE, slightly enriched in middle REEs (MREEs) and has virtually no HREEs or HFSEs (high field strength elements). This component is interpreted to be hydrous fluids that were in equilibrium with the subducting slab (as per Pearce and Peate 1995), which may or may not have included some component of continentally-derived pelagic sediment cover. To produce the boninitic rocks a third component is necessary to create stronger LREE-enrichment and positive Zr and Hf anomalies. This third component could be a siliceous melt (as per Pearce and Peate 1995); and in the case of samples with low  $\epsilon_{Nd}$  values, either this component or the hydrous fluid must have a more significant contribution from pelagic sediments. In these very depleted rocks, the Sm and Nd contents are extremely low, so that even very small amounts of pelagic sediment with  $\epsilon_{Nd}$  values similar to continental crust ( $\sim -10$  for early Ordovician, see Fig. 2.5) and much higher Sm and Nd contents, could significantly shift the isotopic compositions.

The samples which plot below and to the right of VDM on the  $\epsilon_{Nd}$  vs  $^{147}\text{Sm}/^{144}\text{Nd}$  plot (Fig. 2.5) have some of the most depleted REE patterns suggesting a source as refractory as the boninites and other low  $\text{CaO}/\text{Al}_2\text{O}_3$  rocks. However, they have somewhat higher  $\text{CaO}/\text{Al}_2\text{O}_3$  values indicative of a source with some clinopyroxene. The very high  $^{147}\text{Sm}/^{144}\text{Nd}$  values can not be created by fractionation during partial melting of even very depleted mantle (Jenner and Swinden 1993), and it is difficult to imagine a process that can impart a negative  $\epsilon_{Nd}$  value, without also creating a lower  $^{147}\text{Sm}/^{144}\text{Nd}$  ratio. If this is the case, the  $^{147}\text{Sm}/^{144}\text{Nd}$  ratios may have been even

higher prior to the process which lowered the  $\epsilon$  Nd values, and perhaps also increased the CaO/Al<sub>2</sub>O<sub>3</sub> ratio.

The felsic rocks have  $\epsilon$  Nd values which range from +3 to +9, with a very narrow range of <sup>147</sup>Sm/<sup>144</sup>Nd values from 0.20 to 0.24 (Table 2.3). The variation in  $\epsilon$  Nd values reflects that of the mafic rocks from which they were derived. The small range in <sup>147</sup>Sm/<sup>144</sup>Nd reflects the limited degree of fractionation of these two elements during partial melting.

## 2.7 Discussion

The geochemical characteristics of mafic volcanic rocks are key to understanding the development of ancient orogens. This is particularly true in the Newfoundland Appalachians where so many different mafic sequences, including several well-preserved ophiolites, are well exposed. In orogenic belts, where numerous phases of deformation overprint original relationships, geochronological control is essential to gaining a proper understanding of the stratigraphy. Without correct age relationships, it is difficult to accurately assess the sequence of tectonic events. The deformation and unroofing of orogenic belts also provides an opportunity to see rocks not exposed in equivalent modern tectonic settings. Thus, by combining careful detailed mapping with geochronology and geochemical analysis, these older sequences can add to our understanding of processes in recent analogues.

### *2.7.1 Tectonic setting*

Although previous geochemical studies have been undertaken in both the Wild Bight Group (WBG) and the South Lake Igneous Complex (SLIC), and interpretations of tectonic setting made, a link between these two packages of rocks was not recognized. The new interpretation of the tectonic setting presented here, is the result of geochronological control linked with detailed mapping in the WBG, and modern geochemical data combined with Sm/Nd isotopic analyses and U-Pb geochronology in the SLIC.

Swinden et al. (1990), interpreted the very depleted mafic rocks (groups 2 and 3 of this study) and associated rhyolites of the Wild Bight Group (group 6 of this study) to have formed during the rifting of an oceanic arc represented by adjacent LREE-enriched volcanic rocks. However, data presented here show that the depleted volcanic rocks of the fault-bounded packages of the older WBG sequence are up to 10 Ma older than adjacent LREE-enriched volcanic rocks in the younger WBG sequence. In fact, the depleted rocks are part of the oldest package of rocks in the WBG.

Relationships in the contemporaneous South Lake Igneous Complex (SLIC) provide critical information related to the tectonic evolution of the WBG. With the exception of boninitic compositions, all the geochemical groups within the older sequence of the WBG are represented in the SLIC where unambiguous crosscutting relationships can be observed, and absolute age constraints are provided by U-Pb zircon ages. The earliest phase of magmatism is represented by the layered gabbro and sheeted dyke complex. The sheeted dykes are interpreted to have been emplaced synkinematically

into an extensional shear. Geochemically, these rocks are low-Ti, high-Mg, island arc tholeiitic basalts (groups 2 and 3) which formed from a very depleted mantle source. Abundant magmatic amphibole indicates that these magmas were also hydrous. Sm/Nd isotopic signatures for most samples indicate a source dominated by a very depleted mantle, although their extended-REE patterns indicate the presence of a subduction component. The hydrous and subduction components are interpreted to be one and the same, and to be related to dehydration of the down-going slab. Taken together, the evidence suggests an extensional, suprasubduction zone setting during the earliest stages of arc development.

Stern and Bloomer (1992) proposed a model for subduction zone infancy in the Izu-Bonin-Mariana (IBM) arc whereby subduction was initiated at a transform boundary. They suggested that older crust on one side eventually became unstable and began to subside (sinking vertically, with no horizontal component). The initiation of subsidence of the older crust was thought to have caused extension in the upper oceanic plate, upwelling of particularly depleted mantle, and catastrophic melting of this mantle as a result of decompression and an influx of hydrous material from the subsiding plate. In the case of the IBM arc, this process is suggested to have produced voluminous boninitic magmas over an area much wider than the present magmatic front. This magmatism would have rapidly built up a thick mafic crust upon which the later arc is built. However, the boninitic rocks are now observed only in the fore arc region where they are not buried by younger arc rocks. In their model, Stern and Bloomer (1992) proposed that eventually subsidence of the slab is replaced by subduction (with a horizontal component to slab

movement) and that upwelling of very depleted mantle was then prohibited. This idea explains why the degree of depletion decreases to produce normal IATs. They also suggested that subduction was accompanied by stabilization of a discrete magmatic front, a marked decrease in the degree of extension and migration of the locus of extension to a back arc position (Stern and Bloomer 1992, and references therein). Following stabilization of the magmatic front, normal island arc volcanism developed.

The model of Stern and Bloomer (1992) provides a good starting point for the tectonic evolution of the Wild Bight Group and the South Lake Igneous Complex (Fig. 2.7). The change from a normal transform boundary (Fig. 2.7a) to one with significant extension and finally subduction, provides a possible explanation for the style of emplacement of the sheeted dykes and the continued dynamic relationship between plutonism and deformation in the SLIC, which O'Brien (1992) envisaged as a long lived, episodically active shear zone. This model also provides an explanation for the very depleted nature of the least fractionated and earliest magmatic rocks of the SLIC and WBG. Although this setting is characterized by boninitic rocks in the IBM Arc, isotopic and geochemical characteristics of depleted magmatic rocks of the WBG and SLIC suggest that boninites and high-Mg, low-Ti island arc tholeiites are temporally and spatially, if not genetically related.

In the model proposed by Stern and Bloomer (1992), it is not clear exactly where in the mantle the very depleted source resides, or how it became very depleted. Contrary to their model of more strongly depleted mantle at depth, it is commonly believed that the deeper part of the mantle is more fertile than the upper mantle from which MORB is

derived (e.g., Zindler and Hart 1986). The relationships in the WBG and related rocks of the Exploits Group suggest a possible origin for the very depleted mantle source. In the WBG, the very depleted rocks are intimately associated with somewhat less depleted IATs, and it is not clear which are older. In the correlative sequence in the Exploits Group, the earliest volcanic rocks of the older sequence are island arc tholeiites (O'Brien et al. 1997) with a MORB-like degree of depletion ( $\text{TiO}_2 = 1 \text{ wt\%}$  at  $\text{Mg\# } 42$ ), but with much lower overall abundances of trace elements ( $0.6$  to  $1 \times \text{PM}$ ) than in typical IATs. The trace element composition of these rocks is compatible with high degrees of melting of MORB-like mantle (depleted MORB mantle (DMM) of Zindler and Hart, 1986), which could have caused the degree of depletion necessary to form the low-Ti IATs and boninites which comprise much of the older sequence (Fig. 2.7b and c). Thus progressive depletion of DMM by high degrees of melting, through a combination of decompression and hydrous fluxing, eliminates the necessity for a special, very depleted mantle source.

The style of intrusion of mafic rocks in the SLIC changed from sheeted dykes to more massive plutons (hornblende diorite) with time, indicating less significant extension (Fig. 2.7d). This was accompanied by a change in geochemical character, toward less depleted compositions. This is interpreted to result from an addition of DMM to the source area. Normal DMM can be incorporated into the source region by moving laterally into the area of extension (Fig. 2.7d) once the subducting slab prohibits significant upwelling. In this case the new DMM would undergo a normal, MORB-like degree of partial melting ( $10$ - $15\%$ ), without the added effect of decompression, thus generating normal IATs.

The rapid rate of crust formation proposed for subduction zone infancy (Stern and Bloomer 1992) provides an explanation for the formation of tonalites (and rhyolites) within several million years of the depleted mafic sequence. The very low levels of high field strength elements (HFSEs), flat to LREE-depleted extended-REE patterns and the low-K<sub>2</sub>O contents in the felsic rocks are compatible with an origin by melting of the depleted rocks at the base of the thickened crust.

The late mafic to intermediate dykes which cross-cut all other phases of the SLIC, and are relatively undeformed, have the geochemical characteristics of normal island arc tholeiites (group 1), and are interpreted to represent the development of normal island arc volcanism, after stabilization of the volcanic front (Fig. 2.7e). Volcanic rocks with normal IAT geochemical signatures are the predominant lithology within older Wild Bight Group sequence south of the South Lake Igneous Complex. This package also contains rhyolites, produced by continued melting of depleted rocks at the base of the crust.

To summarize, the South Lake Igneous Complex and related rocks of the Wild Bight Group are interpreted to represent the initiation of a subduction zone along what may have originally been a transform boundary. As the subduction zone evolved, the degree of extension and depletion of the source decreased. At some point the crust thickened enough to allow melting at the base and the production of tonalites and rhyolites. Further evolution lead to true subduction and the establishment of a stable magmatic arc where normal island arc tholeiites were produced.

The applicability of the subduction zone infancy model (Stern and Bloomer 1992) to this area is significant because field relationships and U-Pb ages link extension with the production of high-Mg, low-Ti island arc tholeiites and boninites, and show that tonalitic magmatism is closely linked in time and space with this extensional phase. Field relationships are unknown in the IBM arc, where the majority of samples are obtained from dredging.

### *2.7.2 Subduction zone processes*

Numerous recent papers (e.g., Pearce and Peate 1995, and references therein) have pointed out the complexities of subduction zone processes, although the level of understanding of some of these processes is still qualitative. For example, the extent of chromatographic effects (Navon and Stolper 1987) on both magmatic and fluid phases as they migrate through the mantle is relatively unknown. A better understanding of the effects of residual minerals on the geochemistry of hydrous fluids is being developed through experimental work (e.g., Brenan et al. 1994, 1995), although extrapolating these results to such a complex environment is still problematic. The role of mantle source depletion or enrichment prior to subduction influences has also been recognized in many volcanic arcs (e.g., Pearce and Peate 1995 and references therein). The effect of some of these processes may be seen qualitatively in the geochemical variations observed amongst the very depleted rocks of the Wild Bight Group and South Lake Igneous Complex.

A recent summary of the state of understanding of the relationships between tectonic processes and the composition of volcanic arc magmas (Pearce and Peate 1995) suggests that the trace elements Zr, Hf, Ti, HREEs Y, Sc, Ga, Ni, Cr, Co and major or

minor elements except K, Na and P are conservative with respect to the mantle source (i.e., not affected by the subduction component), and thus best reflect the mantle source composition. Bivariant plots of ratios of conservative elements in volcanic arc basalts plot within the MORB array (Pearce and Peate 1995 and references therein). The important implication of this observation is that it is inconsistent with the idea of minor residual phases controlling the HFSE content of arc magmas. Thus, Pearce and Peate (1995) conclude that the characteristic LIL enrichment relative to the HFSEs must be explained by the fact that the LIL are non-conservative whereas the HFSE are conservative with respect to the mantle source. Thus trends of conservative elements can be used to examine source characteristics, and to extrapolate to pre-subduction component abundances of non-conservative elements (e.g., the mantle melt patterns shown in Fig. 2.6).

A method similar to that of Pearce and Parkinson (1993) is used here to qualitatively characterize the mantle and subduction components on primitive mantle-normalized, extended-REE diagrams (Fig. 2.6). The lines labeled mantle melt are based on the trends of conservative elements in the least fractionated samples, but have been extrapolated to show the hypothetical pre-subduction-component level of non-conservative elements. Experimental studies of partition coefficients between hydrous fluids and mantle mineral assemblages (e.g., Brenan et al. 1994 and 1995), and the relationship between bulk partition coefficients and ionic radius (summarized by Pearce and Peate 1995) suggest that only the MREE, LREE and LILE can be mobilized by aqueous fluids and that the degree of enrichment in the fluids increases from MREE

through LREE to large ion lithophile elements (LILE). Thus the lines labeled hydrous fluid in Figure 2.6 have these characteristics. The mantle melt and hydrous fluid components are combined to produce the observed rock compositions of the normal and depleted island arc tholeiites (Fig. 2.6a and b). Aqueous fluids do not have the appropriate composition to create the extended-REE patterns characteristic of boninites (Fig. 2.6c); therefore, there must be a third component or process involved in their genesis. Pearce et al. (1992) suggest that the enrichment in Zr and Hf relative to Nb in boninites is the result of melting of the slab in amphibolite facies. This interpretation is compatible with the greater degree of enrichment of the LREE and the non-conservative behavior of Nb. A comparison of the distribution coefficients for these elements between mantle/melt and mantle/aqueous fluid (e.g., Pearce and Parkinson 1993, and Brenan et al. 1994, 1995) show that melts are much more effective at extracting the LREE and other incompatible elements (including Zr, Hf, Nb and Ta) from the mantle. Residual amphibole present during melting would reverse the usual order of incompatibility of Zr (and Hf) and Nb (and Ta) resulting in the positive Zr and Hf anomalies characteristic of boninites (Pearce et al. 1992).

This provides a possible explanation for the relationships observed between the depleted IATs and boninites in the WBG, whereby both are produced by high degrees of melting by fluxing of a very depleted mantle with subduction-related hydrous fluid, but the boninites have an additional component generated by melting of the subducted slab with amphibole in the residue. This interpretation is compatible with the Sm/Nd isotopic data which shows that the different trace element patterns are not caused by long-lived

characteristics of the source. Some boninites have much lower  $\epsilon$  Nd and Sm/Nd values (e.g., boninites from elsewhere in Newfoundland, Fig. 2.5) which suggest that crustally derived sediment must have contributed to the subduction component in such cases.

The processes outlined above have been used to explain arc geochemical signatures previously (e.g., Pearce and Peate 1995 and references therein), and work well for explaining samples which plot on mixing lines between DM or VDM and subduction zone fluids on a  $^{147}\text{Sm}/^{144}\text{Nd}$  vs  $\epsilon$  Nd plot (Fig. 2.5). However, many of the samples in this and other studies of similar rocks types, have  $^{147}\text{Sm}/^{144}\text{Nd}$  ratios significantly higher than VDM. Removal of a 10% partial melt from VDM, could increase the Sm/Nd ratio of the residue  $\sim$  50% (DePaolo 1988) to about 0.40. Thus, theoretically these extreme  $^{147}\text{Sm}/^{144}\text{Nd}$  ratios could be produced by multi-stage depletion of the same mantle source. However, this would result in an extremely refractory and depleted mantle source. Such a source would likely have no clinopyroxene remaining and would undoubtedly require hydrous conditions to facilitate melting. The magmas generated would be extremely depleted in incompatible elements and would have low  $\text{CaO}/\text{Al}_2\text{O}_3$ . These characteristics are qualitatively compatible with the compositions of the most depleted samples observed in this study. However, such a multiply depleted source could not generate the normal IAT compositions observed in the ophiolite terrane of SW Norway (Pedersen and Hertogen 1990 and Pedersen and Dunning 1997), which also have extremely high  $^{147}\text{Sm}/^{144}\text{Nd}$  ratios. Therefore, although a multiply depleted source could explain the high  $^{147}\text{Sm}/^{144}\text{Nd}$  ratios of strongly incompatible element depleted,

LREE-depleted rocks, it may not be a reasonable explanation for the production of the similarly high  $^{147}\text{Sm}/^{144}\text{Nd}$  ratios in non-LREE-depleted.

This apparent decoupling of  $^{147}\text{Sm}/^{144}\text{Nd}$  geochemical and isotopic characteristics could be reflecting chromatographic effects of the mantle wedge, or other poorly quantified subduction-related processes. These unusual  $^{147}\text{Sm}/^{144}\text{Nd}$  isotopic characteristics are observed in depleted Ordovician oceanic sequences throughout the Appalachian/Caledonian orogen and also in Tasmania which suggests that this effect is related to some process which occurs consistently during the generation of magma in extensional suprasubduction zone settings. Alternatively, it may be a process that occurs in all stages of subduction, but its effect is not as readily seen in less depleted rock types where isotopic compositions are buffered by the higher Sm and Nd compositions of the original melt. The Sm/Nd isotopic composition of very depleted rocks can be shifted easily as Sm and Nd are present in such small amounts (Sm < 0.6 ppm and Nd < 1 ppm). Thus very depleted basalt compositions may offer the best opportunity to investigate the possible chromatographic effects of the mantle wedge. Unfortunately in most modern arcs only the most recent volcanic rocks are easily observed and sampled, and evidence suggests that these very depleted rocks typically form during subduction initiation.

## 2.8 Conclusions

The South Lake Igneous Complex (SLIC) was previously interpreted to be Ordovician in age, and this has now been conclusively demonstrated by U/Pb geochronology, which shows that most of the SLIC formed between 489  $\pm$  3 and 486  $\pm$  3 Ma (latest Tremadoc to earliest Arenig). Furthermore, the SLIC can be convincingly linked to a discrete

sequence of volcanic rocks in the Wild Bight Group (WBG), which is at least in part older than  $486 \pm 4$  Ma. These volcanic rocks are up to 10 Ma older than volcanic rocks of the younger sequence of the WBG, and are typically separated from them by faults.

The very depleted mafic rocks and tonalite/rhyolite represent the earliest magmatic event in the Wild Bight Group and formed in an extensional suprasubduction zone setting. The demonstrated link between extension and the production of high-Mg, low-Ti tholeiites and boninites lends support to a model for their genesis, similar to that proposed for subduction zone initiation in the IBM arc. Furthermore, the generation of normal IATs with low levels of incompatible trace elements, prior to the more depleted IATs and boninites, provides a mechanism for producing the very depleted mantle source of these rocks. The youngest magmatic event in this sequence is represented by normal island arc tholeiites likely formed during typical island arc volcanism.

The mantle source for most of the older volcanic rocks in the WBG and related plutonic rocks of the SLIC, was variably depleted mantle overprinted by a subduction zone component. There is clearly a close spatial and temporal relationship between boninites and low-Ti, high-Mg island arc tholeiites formed during subduction zone initiation. In this case, the unique trace element signature of the boninites is interpreted to have been generated at their time of formation. Some of the most depleted basalts exhibit an apparent decoupling of Sm/Nd geochemical and isotopic characteristics which requires a complex melt generation process for their formation.

## **Chapter 3**

### **Age, Origin and Tectonomagmatic Evolution of the Younger Volcanic/volcaniclastic Sequence of the Wild Bight Group**

#### **3.1 Introduction**

The lower- to middle-Ordovician Wild Bight Group is well-exposed on the shore of Notre Dame Bay in central Newfoundland (Fig. 1.1) (O'Brien, 1992). This study has shown that fault-bounded slivers of volcanic and related plutonic rocks (South Lake Igneous Complex) that are mostly pre 486  $\pm$  3 Ma (chapter 2), are structurally interleaved within the younger stratigraphic sequence of the WBG (Map A). Volcanic rocks in the older sequence are genetically unrelated to the younger sequence and have been described in the previous chapter.

Regionally, the younger WBG sequence (map units 4-8, Map A) grades conformably up into black shale of the Caradocian Shoal Arm Formation (Dean, 1977, 1978) which provides a minimum age for the WBG, although there were previously no constraints on the distribution of ages within it. This chapter documents the ages and chemical characteristics of volcanic rocks that are conformable within the younger stratigraphic sequence. This sequence comprises pillowed mafic volcanic rocks interbedded with volcaniclastic sedimentary rocks, rare felsic tuffs, minor chert and argillite, intruded by diabase/gabbro sills and dykes. The volcanic rocks occur at two stratigraphic levels which represent distinct tectonomagmatic settings. Felsic tuffs at three stratigraphic levels provide constraints on the age of lower calc-alkaline volcanic succession (map unit 5, Map A) and related sedimentary rocks and show that much of the

sequence developed in several million years at about 470 Ma. Two gabbro sills with geochemical characteristics similar to enriched tholeiitic to alkaline basalts of the upper volcanic succession (map unit 8, Map A), were also dated and confirm the ~ 470 Ma age for most of the volcanic rocks in the younger sequence of the WBG.

Geochemical and isotopic characteristics of the volcanic rocks suggest the development of a volcanic arc in proximity to thinned continental crust of the Gondwanan margin. The transition to within plate, non-arc volcanic rocks is interpreted to represent the formation of an intra-arc rift basin.

### **3.2 Geology**

The best stratigraphic and structural control on relationships in the younger WBG sequence is in the area between Locks Harbour, Leading Ticks and Osmonton Arm (Map A), where there is almost 100% exposure along the coast. Although the regional stratigraphic divisions of the WBG (Dean and Strong 1976) vaguely match those defined for this detailed area, Dean and Strong (1976) included most rocks of what has now been identified as the older sequence, within their youngest Pennys Brook Formation. Thus the stratigraphic nomenclature for formations within the WBG has been abandoned in favour of numbered units (Map A). Where numbered units concur with specific formations, this will be noted.

The stratigraphic base of the younger succession (unit 4, Map A) comprises thinly bedded to laminated red and green argillite and tuffaceous sandstone, massive green tuffaceous sandstone and greywacke and minor black shale (Plate 3.1a, Omega Point Formation of Dean and Strong 1976). This grades up into thickly bedded coarse-grained

volcaniclastic rocks and poly lithic conglomerates (Plate 3.1b) with minor greywacke and thinly bedded to laminated red and green argillite and chert (unit 6, broadly concurrent with Seal Bay Brook Formation of Dean and Strong 1976). This unit is conformably overlain by and grades up into finer grained volcaniclastic rocks with a greater proportion of greywacke and thinly bedded to laminated argillite and chert (unit 7). Conformably within the lower, dominantly volcaniclastic, succession (unit 6) is a thick sequence of plagioclase-phyric mafic to intermediate pillowed volcanic flows (Plate 3.1c,d) and intermediate to felsic sub-volcanic sills and dykes (unit 5, lower volcanic succession). The finer grained volcaniclastic succession grades up into a unit dominated by thinly bedded to laminated red, green and grey argillite and chert (unit 7a), (Plate 3.1e), with minor thinly bedded, fine-grained greywacke, and minor dark grey to black argillite near the top (unit 7 + 7a is broadly equivalent to the volcaniclastic member of the Penny's Brook Formation of Dean and Strong 1976). Interbedded with the chert and argillite at the top of the younger sequence of the Wild Bight Group (unit 7a) are thin lenses of pillowed mafic volcanic rocks (unit 8, upper volcanic succession). Throughout the entire stratigraphic succession are diabase and gabbro dykes and sills (unit 8a) related to the upper pillowed volcanic rocks, many of which are vesicular suggesting that they intruded at shallow levels. Regionally, the WBG grades upward into Caradocian black shale of the Shoal Arm Formation (and biostratigraphic/lithostratigraphic equivalents), although in this area the contact between them is a fault.

Two phases of faulting and folding were recognized in the study area. The earliest structures recognized are  $D_1$  thrust faults which trend approximately NNW-SSE and

juxtapose the older and younger sequences of the Wild Bight Group and the SLIC.

Associated  $F_1$  folds of the entire Wild Bight Group (Map A) are mappable on a regional scale.  $F_2$  faults trend NE-SW and have small, open, asymmetric folds associated with them. Both  $D_1$  and  $D_2$  faults are sub-vertical at the surface, but based on overturned bedding in the footwall of some faults, and regional fold patterns, are interpreted to be dominantly west-directed, east-dipping thrust faults. However, east-directed  $D_1$  thrust faults also occur. In the northeastern part of the map area,  $D_1$  structures are transposed into the  $D_2$  orientation making it difficult to distinguish them. However, further south where  $D_1$  structures are predominately NNW-SSE the effect of  $D_2$  deformation is easier to recognize. The  $D_2$  faults and folds cause only minor offsets and undulation of the stratigraphy, whereas the  $D_1$  deformation produced the observed regional distribution of units. Both major and minor  $F_1$  and  $F_2$  folds are doubly plunging which could indicate another phase of folding. NE-striking brittle transcurrent faults previously recognized, transect the area and represent  $D_4$  deformation. The deformational events described here are compatible with the 4 phases of regional deformation recognized by other workers (e.g., van der Pluijm et al. 1987, Blewett 1991, Blewett and Pickering 1988, Elliot and Williams 1988, and O'Brien, 1993).

### **3.3 U-Pb Geochronology**

Three felsic tuffs from different stratigraphic levels within the younger WBG succession were dated by U-Pb analysis of igneous zircons, and bracket the age of the lower volcanic succession (unit 5). Two diabase/gabbro sills, geochemically similar to the volcanic rocks in the upper volcanic succession (unit 8), were dated by U-Pb analysis of zircon and/or

baddeleyite, and are interpreted to be the age of at least some of the volcanic rocks. The analytical technique is described in detail in Appendix 5.

### 3.3.1 U-Pb samples

*Pig Island Tuff (95GC09)*. This sample is from just below the lower volcanic succession, and occurs on Pig Island in Glovers Harbour (Map A). It is interbedded with numerous thin felsic and mafic tuffs and lapilli tuffs, and red and green argillite. It is very fine-grained, siliceous and deformed, and no primary textures can be recognized (Plate 3.2a). However, the abundance and predominance of tiny, gem quality, euhedral zircon prisms that were separated from this sample, indicate that this tuff did not undergo significant reworking during submarine deposition. Four fractions of high quality zircons were picked from the NM 0° franz split. All fractions were strongly abraded and overlap on concordia to give an age of 471  $\pm$  2 Ma, with emphasis placed on the most concordant data (Z1 and Z2, Fig. 3.1a, Table 3.1).

*Duck Island Tuff (95057)*. The second tuff comes from within the coarse volcanoclastic sequence (unit 6), probably above the lower volcanic succession, and occurs on Duck Island in Thimble Ticks (Map A). It is interbedded with thickly bedded volcanoclastic rocks, conglomerates and debris flows, and occurs at the top of a thick, graded, poly lithic, volcanoclastic bed (Plate 3.2b). It is quite siliceous and has recognizable, tiny quartz phenocrysts and rock fragments in thin section, as well as more rounded, probably detrital quartz grains which are distinct from the rest of the quartzofeldspathic groundmass (Plate 3.2c). This sample clearly has a detrital component; however, by carefully selecting only small, euhedral zircons it was possible to avoid

detrital grains. Two fractions (Z2 and Z3) of abraded, euhedral, clear zircon prisms are less than 1.5% discordant and have  $^{207}\text{Pb}/^{206}\text{Pb}$  ages of 472. A third fraction, with a significantly larger error, is concordant at 470 Ma. This sample also contained large irregular grains of turbid, hydrothermally altered zircon. A strongly abraded fraction of these zircons (Z4) is 8% discordant, with a  $^{207}\text{Pb}/^{206}\text{Pb}$  age of 466 Ma. A discordia line through all 4 points has a 93% probability of fit and an upper intercept age of  $472 \pm 3$  Ma (Fig. 3.1b, Table 3.1), which is interpreted as the age of the tuff. An abraded, single, large, zircon prism tip (Z5, not shown in Fig. 3.1) is highly discordant, with a  $^{207}\text{Pb}/^{206}\text{Pb}$  age of 1419 Ma (Table 3.1), indicating the presence of a Proterozoic detrital component.

*Locks Harbour Tuff (95092).* The third tuff is from within the argillite and chert unit (unit 7a) at the top of the younger WBG sequence. It occurs on a small point at the north end of Locks Harbour in Seal Bay. Unfortunately there are no volcanic lenses in this part of the sequence, and the pervasive isoclinal folding makes estimating stratigraphic thicknesses impossible. Thus, the position of this tuff in relation to the younger volcanic lenses in the stratigraphy, or in relation to the top of the stratigraphic sequence is unknown. However, it is significantly higher in the stratigraphy than either of the other two dated tuffs, and is definitely above the lower volcanic succession. This tuff is interbedded with other thinly bedded mafic and felsic tuffs within the argillite sequence (Plate 3.2d). Flattened cusate fragments, probably originally glass shards, and lapilli size rock fragments occur locally in a fine-grained, siliceous, matrix (Plate 3.2e). Subrounded grains observed in thin section (Plate 3.2e) may indicate a small detrital component;

however, the presence of probable glass shards suggests that there was only minor reworking of this unit. This is confirmed by the fact that abundant high quality euhedral igneous zircon, and only a small component of sub-rounded detrital grains were recovered after mineral separation. Two fractions of small, clear, euhedral, zircon prisms were strongly abraded and overlap concordia, with  $^{207}\text{Pb}/^{206}\text{Pb}$  ages of 470 Ma and 473 Ma (Fig. 3.1c, Table 3.1). With more weight given to the more precise analysis (Z1), an age of  $472 \pm 3$  Ma has been assigned to this sample, which encompasses the age of both analyses, but is more precise than fraction Z2.

*Gabbro Sill (95GC10).* This sample comes from a roadside outcrop on highway 350, just north of the turnoff to Glovers Harbour. This gabbro sill is within the coarse volcanoclastic sequence (unit 6), but has a chemical composition similar to enriched-tholeiitic basalts (Fig. 3.2c), suggesting a genetic link with the volcanic rocks of the upper succession (unit 8). This sill is predominantly medium-grained massive gabbro, but locally has coarser-grained pegmatitic patches, one of which was sampled for U-Pb dating. It is comprised of cumulate, plagioclase, clinopyroxene and subhedral skeletal oxides with interstitial fibrous chlorite which has replaced the original minerals. Mineral separation revealed abundant apatite, a small amount of tiny plates of baddeleyite, rare, sub-rounded, multi-faceted zircon and irregular, thin fragments of zircon. Two fractions of unabraded baddeleyite are 1% and 2% discordant with  $^{207}\text{Pb}/^{206}\text{Pb}$  ages of 470 and 469 Ma, respectively (Table 3.1). The irregular fragments of zircon, interpreted to be pieces of larger skeletal igneous zircons, are 9% discordant. A discordia line through all 3 points has a 93% probability of fit and an upper intercept age of  $472 \pm 22/-12$  Ma (Fig.

3.1d, Table 3.1). However, this sill intruded a sequence that is more precisely dated at 472  $\pm$  3 Ma, which provides a maximum age for this sample. The more concordant of the two baddeleyite analyses has a minimum age given by the  $^{206}\text{Pb}/^{238}\text{U}$  age, of 466  $\pm$  3 Ma (Table. 3.1). Therefore, we assign an age of 470  $\pm$  5 Ma to this sample. A fraction of multifaceted zircons (Z2, not shown in Fig. 3.1) is 25% discordant and has a  $^{207}\text{Pb}/^{206}\text{Pb}$  age of 689 Ma, demonstrating the presence of an inherited zircon component in this sample.

*Gabbro Sill (95GC03).* This sample comes from the south end of the eastern-most island in Thimble Tickles. This gabbro sill is within the coarse volcanoclastic sequence (map unit 6), and is medium grained and massive, with some coarser pegmatite patches, one of which was sampled for U-Pb dating. This sample has a composition similar to volcanic rocks in the upper volcanic succession (map unit 8), which are transitional between enriched tholeiitic and alkalic basalt (Fig. 3.2d). The mineralogy and textures observed in thin section are the same as those in sample D. However, this sample contains only baddeleyite, no zircons were recovered after mineral separation. Five fractions of unabraded baddeleyite range from < 1% to 4.5% discordant. A discordia line through all 5 points, and pinned at 25  $\pm$  25 Ma has a 27% probability of fit and an upper intercept of 471  $\pm$  4 Ma (Fig. 3.1e, Table 3.1).

### 3.3.2 Interpretation

The three tuffs from throughout the sequence bracket the lower volcanic succession and confine its age to 472  $\pm$  3 Ma (late Arenig, time scale of Tucker and McKerrow 1995). Furthermore, much of the volcanoclastic sequence was deposited rapidly within no more

than 6 Ma. Although the stratigraphic relationship of the youngest tuff to the lenses of volcanic rocks in the argillite-chert unit (unit 7a) is equivocal, the age of geochemically similar gabbro sills overlaps, within error, the age of all the tuffs. Thus, although there is some stratigraphic separation between the volcanic packages, it does not represent a significant time gap. However, the fact that the dated sills related to the upper volcanic lenses intrude the sequence at the approximate stratigraphic level of the older volcanic pile, means that the former must be slightly younger than the latter.

### **3.4 Geochemistry**

All samples were analysed for major oxides and a suite of trace elements by XRF, and a subset of samples were also analysed for other trace elements by ICP-MS, as per chapter 2. A representative suite of samples were also analysed for Sm/Nd isotopes.

#### *3.4.1 Alteration and metamorphism*

All samples have been metamorphosed to lower greenschist facies during regional metamorphism, and some of the volcanic rocks have spilitic mineral assemblages typical of sea-floor alteration. Apparently fresh clinopyroxene is preserved in many samples suggesting that there was less pervasive seafloor alteration in these rocks than in the older succession. On Hughes' (1973) plot of  $K_2O + Na_2O$  vs  $K_2O/(K_2O + Na_2O)$ , which screens samples for spilitization and K-metasomatism, diabase/gabbro sills and dykes plot predominantly within the igneous spectrum suggesting that even these easily mobilized elements have not been significantly changed by regional metamorphism, although some of the volcanic rocks plot in the spilitized field. On extended-rare earth element plots (see below), intrusive and volcanic rocks from related suites show little

variation in their patterns indicating that the elements used in these plots have not been significantly affected by alteration and metamorphism.

#### *3.4.2 Geochemical characteristics of the lower volcanic succession*

The lower volcanic succession of the younger sequence of the WBG (unit 5) consists predominantly of plagioclase phyric mafic-intermediate pillowed volcanic rocks and minor intermediate to felsic sub-volcanic sills, which are classified as calc-alkaline to tholeiitic basalt to rhyolite (geochemical group 7) based on major element classification diagrams (e.g., AFM diagram of Irvine and Baragar 1971, and the Fe+Ti-Al-Mg cation plot of Jensen 1976). Plots of Mg# versus  $\text{Fe}_2\text{O}_3\text{T}$  (total Fe as  $\text{Fe}_2\text{O}_3$ ) and  $\text{TiO}_2$  show a slight increase in these elements in the least fractionated compositions, although throughout most of the range of Mg# (20-55),  $\text{Fe}_2\text{O}_3$  and  $\text{TiO}_2$  decrease with Mg#. The least fractionated samples have some characteristics of tholeiitic rocks, but the majority, which are more evolved, have clear calc-alkaline affinities. Part of the ambiguity of major element classification could be a result of element mobility during seafloor alteration. Based on trace element classification schemes (e.g., Nb/Y-Zr/ $\text{TiO}_2$  Winchester and Floyd 1977) these rocks are subalkaline basalt/andesite to rhyolite, which is compatible with their major element compositions.

Trace element patterns of representative mafic to intermediate samples on primitive mantle-normalized, extended-rare earth element (extended-REE) plots (Fig. 3.2a), show moderate to strong light rare earth element (LREE) enrichment, strong negative Nb and positive Th anomalies and flat heavy rare earth elements (HREEs). This pattern is compatible with the calc-alkaline affinity suggested by major element

compositions. The least fractionated basalts generally have lower trace element concentrations and the more fractionated samples have higher concentrations, which is compatible with crystal fractionation of plagioclase. However, variable trace element contents of samples with similar Mg#s indicate that there must have been several different magma batches involved in generating these rocks, but the differentiation processes and mantle sources were likely similar. Although there is minor overlap between tholeiitic and calc-alkaline fields on major element plots, all samples have trace element characteristics of calc-alkaline rocks.

Extended-REE diagrams are useful for examining the relative behavior of various elements, and the processes they represent, but tectonic discrimination diagrams can be used to classify and compare rocks within a particular suite for which REE data are not available. All samples from the calc-alkaline suite have been plotted on several of these diagrams (Fig. 3.3), all of which effectively classify most samples as calc-alkaline and/or destructive plate margin rocks, although several samples are transitional to within plate or ocean floor tholeiite fields.

#### *3.4.3 Geochemical characteristics of the upper volcanic succession*

Volcanic rocks in the upper part of the succession (unit 8), are rare in this study area, although they occur at several other localities within the upper Wild Bight Group (Swinden et al. 1990). The entire compositional spectrum is represented by diabase/gabbro sills and dykes in the study area; however, to encompass the entire range of volcanic compositions, samples from other localities have been included (from Swinden et al. 1990). Based on major element classification schemes these rocks straddle

the subalkaline/alkaline boundary and range from high-Fe and high-Mg tholeiitic basalt (Fe+Ti-Al-Mg cation plot, Jensen 1976) to alkaline basalt. Bivariant plots show that Fe<sub>2</sub>O<sub>3</sub> and TiO<sub>2</sub> increase, whereas Cr decreases, with decreasing Mg#, characteristic of tholeiitic fractionation trends. Part of the ambiguity of major element classification could reflect element mobility during seafloor alteration; however, trace element classification schemes (Nb/Y vs Zr/TiO<sub>2</sub>, Winchester and Floyd 1977) also suggest that these rocks range from subalkaline to mildly alkaline.

Based on primitive mantle-normalized, extended-REE patterns, volcanic rocks of the upper sequence, and intrusive equivalents, can be divided into 4 geochemical groups. Group 11 samples, have steep extended-REE patterns, with strong LREE-enrichment, HREE-depletion, positive Nb and negative Th anomalies characteristic of alkaline rocks (Fig. 3.2b). Group 8 samples have moderate LREE enrichment, flat HREEs, and slight positive or negative Nb anomalies (Fig. 3.2c). This pattern is similar to E-MORB and within plate tholeiites and suggests that a fertile component in the mantle source contributed to the production of these enriched tholeiites. Group 9 samples are transitional between groups 1 and 2; they have slight HREE depletion, but less than group 1 rocks, and larger positive Nb anomalies than group 2 rocks (Fig. 3.2d). Group 10 samples have unusual patterns (Fig. 3.2e) with LREE enrichment, flat HREEs and positive Th (relative to La) similar to the calc-alkaline rocks; however, they have positive Nb and Zr (and Hf) anomalies similar to boninites. The positive Nb and Zr (and Hf) anomalies could be interpreted in the same way as those anomalies in boninites elsewhere in the WBG (chapter 2), as the effect of siliceous melts from the subducting slab

combined with mantle melt (Fig. 3.5b). However, in this case the mantle melt was LREE-enriched as opposed to depleted in the case of boninites. Volcanic rocks from all of these groups can be found together in certain volcanic packages in the younger WBG sequence, and as dykes and sills throughout the entire WBG succession.

To compare samples for which REE data are not available, all samples have been plotted on a number of tectonic discrimination diagrams (Fig. 3.4), which all classify them as within plate tholeiitic/E-MORB to within plate alkalic rocks, compatible with the extended-REE patterns. The Zr-Nb-Th diagram of Wood (1980) (Fig. 3.4b) and the Ti-V diagram of Shervais (1982) (Fig. 3.4c) do not distinguish well between E-MORB and within plate tholeiites, but do effectively discriminate between the non-arc tholeiitic and alkaline suites and subduction-related rocks. The Nb-Zr-Y diagram of Meschede (1986) suggests a within plate as opposed to E-MORB origin for the tholeiitic as well as the alkalic rocks. All these diagrams suggest that there is a continuum of compositions from enriched tholeiitic to alkalic compositions, which is interpreted as evidence for a similar mantle source. However, in the case of group 10, there appears to be an additional component, which might be related to subduction.

#### *3.4.4 Interpretation*

Based on the present understanding of subduction zone processes, most arc-related magmas have a mantle component and a subduction component, variably modeled as hydrous fluids from dehydration, or siliceous melts from partial melting, of the subducting slab (+/- subducted sediments) (e.g. Pearce and Peate 1995). Furthermore, the occurrence of both trace element depleted and enriched mantle components (prior to the

influence of subduction) have been recognized (Pearce and Peate 1995 and references therein).

The mantle source composition is best reflected by the heavy rare earth elements (HREEs) and Y, and the high field strength elements (HFSE, Zr, Hf, Nb, Ta, Ti) which Pearce and Peate (1995) interpret to be conservative with respect to the mantle source, and therefore reflect its composition prior to the influence of subduction. Thus the trends of conservative elements can be extrapolated to estimate the pre-subduction abundances of non-conservative elements (e.g., Pearce and Parkinson 1993), and give some indication of the composition of the mantle source. This is shown schematically in figure 3.5, and suggests a mantle melt with slight LREE enrichment. The increase in the middle and light REEs above that interpolated for the mantle melt is attributed to the subduction component. This component has virtually no HREEs or HFSE, some MREEs, and is most enriched in LREE, which is qualitatively compatible with the composition expected for slab-derived hydrous fluids (see discussion in chapter 2). Thus the calc-alkaline rocks can be produced by a combination of a fertile mantle (like an E-MORB source as opposed to a typical N-MORB source which is depleted), and a hydrous fluid from the subducting slab.

The calc-alkaline trace element patterns characteristic of the lower volcanic succession, and the group 10 rocks of the upper succession can be created by overprinting an enriched tholeiite composition with a subduction derived component (Fig. 3.5). In the case of the calc-alkaline rocks, this subduction component is modeled as a hydrous fluid, and for the group 10 volcanic rocks is modeled as a siliceous melt. The

extended-REE patterns used in this figure are real patterns from rocks in the WBG, including the hypothetical mantle melt component, which is the least fractionated (Mg # 66) enriched tholeiitic basalt from group 8 (for which REE data are available). Thus, the enriched tholeiitic basalts and calc-alkaline basalts are interpreted to have a similar, incompatible element-enriched mantle source, but the latter also have a component derived from the subducting slab.

The more alkaline rocks (groups 11 and 9) could be generated from the same slightly enriched source, but at greater depths (i.e., garnet in the residue causing the HREE-depletion) and smaller degrees of partial melting (producing greater LREE and incompatible element enrichment).

### **3.5 Sm/Nd Isotope Systematics and Mantle Source Components**

#### *3.5.1 Sm-Nd isotopic signature of the upper volcanic succession (groups 8-11)*

The volcanic rocks from the upper succession, and related intrusive rocks, have  $\epsilon$  Nd values between +4 and +7, which indicates a source dominated by depleted mantle. However, trace element compositions indicate a more fertile component in the mantle source. The fact that the  $\epsilon$  Nd values for most samples are not significantly lower than those expected for primary melts of normal depleted mantle ( $\sim +7$  for early Ordovician, Jenner and Swinden 1993) suggests that the more fertile component is either fairly recent, or only very slightly LREE-enriched, and that much of the LREE-enrichment and HREE-depletion in the alkaline and transitional groups is the result of melt generation processes and/or residual phases.

### *3.5.2 Sm-Nd isotopic of the lower volcanic succession*

The calc-alkaline suite has  $\epsilon$  Nd values mostly between +1 and +3.5, which suggests a component of long-term source depletion, but indicates a more significant contribution of material with long-term LREE-enrichment. Geochemical characteristics, as outlined above are compatible with a similar mantle source for the calc-alkaline and enriched tholeiitic to alkalic rocks. Thus, the lower  $\epsilon$  Nd values of the calc-alkaline rocks are attributed to either the subduction component, or contamination by older crust (with an  $\epsilon$  Nd of  $\sim -10$ , Fig. 3.6), during emplacement.

### *3.5.3 Interpretation*

The effect of mixing different isotopic components is shown on a plot of  $^{147}\text{Sm}/^{144}\text{Nd}$  vs  $\epsilon$  Nd (Fig. 3.6). The enriched tholeiitic to alkalic rocks of the upper volcanic sequence define an array with a positive slope between the depleted mantle (DM) end-member and a hypothetical fertile mantle (FM) end-member, which has slightly lower  $\epsilon$  Nd values, but a significantly lower  $^{147}\text{Sm}/^{144}\text{Nd}$  ratio. The lower  $^{147}\text{Sm}/^{144}\text{Nd}$  ratio indicates LREE-enrichment (i.e.,  $\text{Nd}_n/\text{Sm}_n > 1$ ), but the positive  $\epsilon$  Nd value suggests that this material was derived from a depleted source and has not had time to evolve to lower  $\epsilon$  Nd values.

The calc-alkaline rocks and group 10 rocks of the upper volcanic succession define an array between the enriched tholeiitic and alkalic rocks of the upper volcanic succession (unit 8, 9 and 11), and continental crust (Fig. 3.6). It is not possible to

distinguish whether the crustal signature comes from the subduction component or from crustal contamination during magma emplacement.

### ***3.6 Discussion***

#### ***3.6.1 Tectonic setting***

In a previous study of volcanic rocks in the Wild Bight Group (Swinden et. al 1990), the calc-alkaline rocks of the younger WBG sequence were interpreted to represent an intra-oceanic arc, and the upper volcanic succession to represent subsequent rifting of that arc and formation of a back arc basin. The data presented here support the idea of arc-rifting, but suggest that the arc was influenced by continental material, indicating proximity to a continent, as opposed to an intra-oceanic setting.

Geochemical arguments presented above do not indicate a significantly different mantle source for the upper and lower volcanic successions of the younger WBG sequence. Thus, the processes by which they formed and by inference the tectonic setting, must account for their different geochemical signatures. The lower volcanic succession is clearly generated by subduction and probably represents the magmatic front of a volcanic arc. Some rocks in the upper sequence may also have been affected by subduction (group 10), but the majority have within plate signatures (Fig. 3.4a). The within-plate/E-MORB and alkalic composition of the upper succession basalts suggests rifting. The overlap in age with calc-alkaline volcanism suggests arc-rifting.

The lower  $\epsilon$  Nd values of the subduction-influenced rocks suggest that either the subduction component has been influenced by material from an old crustal source, and/or that the magma was contaminated by continental crust during emplacement. This implies

proximity of continental crust, and suggests that the entire younger sequence of the WBG formed adjacent to, or possibly on, thinned continental crust of the Gondwanan margin.

Relationships elsewhere in the Exploits Subzone of central Newfoundland (Colman-Sadd et al. 1992) indicate that early Ordovician volcanic rocks correlative with the older sequence of the WBG were structurally emplaced onto the Gondwanan margin of Iapetus by ~474 Ma. The older WBG volcanic sequence is interpreted to have formed over a west-dipping (present coordinates) subduction zone (chapter 2), and is believed to have been partially emplaced onto the Gondwanan margin prior to the formation of the 470 Ma sequence (Fig. 3.7). The arrival of Gondwana at the subduction zone, and attempted subduction of the thinned continental margin is interpreted to have resulted in the termination of westward subduction. The subsequent subduction zone, which produced the calc-alkaline rocks, is interpreted to have been eastward-dipping beneath the composite continental margin (Fig. 3.7). Thus, the younger calc-alkaline arc is not interpreted to be a truly continental arc, but to have formed on a composite substrate of thinned continental crust/ and/or sediment derived therefrom and ensimatic, arc-related rocks.

The model of subduction polarity reversal for the northern Appalachians has been proposed by van Staal (1994) based on similar rocks in New Brunswick. However, the data presented here provide absolute constraints on the timing of different events proposed in this model. The interpretation proposed herein is different from traditional ideas on the origin of early to middle Ordovician arcs of the Exploits Subzone as being completely intra-oceanic (e.g., Swinden et al. 1990, and O'Brien et al. 1997).

### 3.7 Conclusions

The younger sequence of the WBG comprises volcanic and sedimentary rocks that represent two distinct tectonic settings. The lower volcanic succession is comprised of calc-alkaline basalts and andesites which represent the volcanic front of an arc built on or near the composite Gondwanan continental margin. The age of this sequence ( $\sim 472 \pm 3$  Ma) is constrained by three felsic tuffs which occur both stratigraphically above and below it. The upper volcanic succession has been indirectly dated by U-Pb analysis of baddeleyite from geochemically-related gabbro sills, and overlaps in age with the main volcanic sequence. These enriched tholeiitic and alkalic basalts have within plate affinities and represent arc rifting. The interpretation that the entire sequence formed in close proximity to the Gondwanan margin is different from previous interpretations of arcs in the northern Exploits Subzone as being intra-oceanic, and has significant implications for the evolution of the Gondwanan margin in the Northern Appalachians during closure of the Iapetus Ocean. In particular, the rocks of the northern Exploits Subzone show evidence of the same magmatic and tectonic events as the rest of the Exploits Subzone, although they are manifested in different ways.

## **Chapter 4**

### **Regional structural and stratigraphic relationships in the Wild Bight Group**

#### **4.1 Introduction**

Volcanic rocks of the older sequence of the WBG and related plutonic rocks (South Lake Igneous Complex) that are largely pre 486  $\pm$  3 Ma, are structurally interleaved with and locally stratigraphically overlain by the younger WBG sequence which includes volcanic rocks which are dominantly post 472  $\pm$  3 Ma. Volcanic rocks in these two sequences are not genetically related, and are interpreted to have formed in different tectonic settings. The older sequence represents a late Tremadoc to early Arenig ensimatic arc, and the younger sequence, represents a different volcanic arc which formed in close proximity to the Gondwanan margin. Detritus within the sedimentary rocks of the younger sequence indicates that the older and younger volcanic arcs were juxtaposed by about 475 Ma, and do have a common history prior to final structural imbrication. The youngest volcanic rocks of the WBG represent rifting of the younger calc-alkaline arc and formation of a marginal basin.

Regionally, the younger WBG sequence grades conformably up into Caradocian black shale (Dean 1977, 1978) which is a wide-spread stratigraphic marker within the northern Exploits Subzone. Because of similarities in the compositional variation and ages of volcanic rocks, and in the stratigraphic sequences, previous workers (e.g., O'Brien 1997) have correlated the WBG with the Exploits Group to the east. The Wild Bight and Exploits groups are interpreted to represent different parts of the same late Arenig to

Llanvirn arc system. The eastern WBG represents a more proximal position relative to the main arc, the Exploits Group represents the pre-arc rift, back arc basin and the western WBG is interpreted as the main rift basin (fig. 4.4). The Wild Bight and Exploits Groups were probably also contiguous during development of the older ensimatic arc.

#### **4.2 Regional relationships in the Wild Bight Group**

By combining the regional geochemistry (Swinden et al. 1990), and compilation map (Dean and Strong 1976) with new geochronological data and stratigraphic and petrogenetic relationships in the northeastern WBG, a new interpretation of the regional structure and stratigraphy has been developed (Map C). Because some of the formations defined by Dean and Strong (1976) combined volcanic rocks of both the older and younger sequences, they have been abandoned in favour of numbered units, but the geographic names of volcanic units (Swinden et al. 1990) are retained.

##### ***4.2.1 Stratigraphic relationships***

The stratigraphic succession within the older fault-bounded packages is not well known, but crosscutting relationships in the SLIC suggest that the incompatible element-depleted island arc tholeiitic basalts (IAT's) and boninites are the oldest, followed by rhyolite and then normal IATs. However, in the volcanic successions, rhyolite is interbedded with both depleted and normal IATs, suggesting that there may have been a second period of felsic magmatism not recorded in the SLIC. Thus the only stratigraphic relationship that is unequivocal is that the mafic and felsic volcanic and volcanoclastic rocks are interbedded.

The lowermost stratigraphic unit of the younger WBG sequence (unit 4), coincides with the Omega Point Formation of Dean and Strong (1976), which outcrops in the core of the Seal Bay anticline (Map C1). This unit comprises thinly bedded to laminated red and green argillite and tuffaceous sandstone, minor massive green tuffaceous sandstone and black shale, which locally forms the matrix of an olistostrome. At the bottom of Seal Bay, this unit is overlain by a thin package of pillowed basalt with calc-alkalic affinities (unit 5). This sequence is correlated with the thicker succession of pillowed calc-alkaline volcanic rocks of the Glovers Harbour East unit (b on Map C), which occurs at approximately the same stratigraphic level, and with geochemically similar rocks toward the south end of the SLIC. In the northern part of the map area, where there is good outcrop, and stratigraphic relationships can be seen, the calc-alkaline volcanic rocks are interbedded with and are conformably overlain by a fining upward sequence of thickly bedded coarse-grained volcanoclastic rocks and polyolithic conglomerates (unit 6). This package is similar to the Seal Bay Brook Formation of Dean and Strong (1976), although its distribution is somewhat different. It grades up into finer-grained, more thinly bedded volcanoclastic rocks and greywackes interbedded with red, green and grey argillite and chert (unit 7, Map C1, which is broadly coincident with the volcanoclastic member of the Penny's Brook Formation of Dean and Strong 1976). The proportion of chert and argillite increases up section and comprises greater than 80% at the top. At various levels within this unit are successions of LREE-enriched, within-plate tholeiitic to alkalic pillowed basalts (unit 8).

In the Kerry Lake calc-alkaline volcanic unit (m on Map C), the volcanic rocks are underlain by red tuffaceous sandstone and argillite typical of the basal unit (unit 4) of the younger WBG sequence, and have been re-assigned to this unit (as opposed to the Pennys Brook Formation (= unit 7 on Map C) as proposed by Dean and Strong 1976). At the north end of this calc-alkaline sequence, north of the D<sub>2</sub> Long Pond fault, rocks of unit 4 appear to be in stratigraphic contact with, and overlying depleted rhyolite of the older sequence (Map A). Bedding is not well defined in the massive rhyolites, and thus the nature of the contact is equivocal. This package faces to the west; therefore there must be a syncline between it and the Seal Bay anticline, analogous to the one which occurs to the north between the Seal Bay anticline and the Winter House Cove Fault (WHCF, Map C). South of the D<sub>2</sub> Long Pond Fault (LPF), this package faces in the opposite direction (east) and underlies the calc-alkaline volcanic rocks compatible with the stratigraphic sequence defined in the northeastern WBG. The sedimentary rocks which occur interbedded with the Northern Arm calc-alkaline rocks on the southeast side of the SLIC are assigned to unit 6, based on the relationships observed in the NE.

Dean and Strong (1976) showed only two occurrences of volcanic rocks west of Seal Bay (j and l, Map C1), both of which have LREE-enriched, within-plate geochemical signatures (Swinden et al. 1990). However, recent mapping (O'Brien and MacDonald, 1997 and O'Brien 1998) has delimited numerous other volcanic horizons in this package. All of these volcanic units occur within a sedimentary succession similar to unit 7, compatible with the stratigraphic relationships defined herein. In parts of the western

WBG the original conformable relationship with the Caradocian shale is preserved (O'Brien and MacDonald 1997).

#### *4.2.2 Early Fault Imbrication*

In the northeastern WBG, the older sequence of the WBG and related plutonic rocks (SLIC) were shown to be up to 10 Ma older than the younger sequence of the WBG, and were interpreted to occur as fault-bounded slivers within the younger sequence. The Winter House Cove Fault (WHCF) bounds the east side of the Glovers Harbour west volcanic unit of the older sequence (a on Map C1), and exposed in several places along the shore. Strong deformation along the eastern margin of the GHW unit is compatible with an eastern faulted boundary. However, elsewhere contacts cannot be directly observed and thus, faults are only inferred.

Rocks geochemically and lithologically similar to the older sequence documented in the northeastern WBG (chapter 2), occur at three other localities within the WBG (Swinden et al. 1990) (Map C1). These sequences are also interpreted to be predominantly fault-bounded. Kusky (1985) showed that the Frozen Ocean Group (Dean 1978, k on Map C) is structurally emplaced over the Shoal Arm Formation and Point Leamington Greywacke to the east, by a pre-folding thrust fault (Map C1 and cross-sections C2). Swinden and Jenner (1992) showed that the geochemical affinities of rocks in the Frozen Ocean Group are similar to the WBG, and proposed that they be included in the WBG and renamed the New Bay Pond sequence (NBPS). This nomenclature will be followed henceforth. Based on geophysical data, Swinden and Jenner (1992) traced the Western Arm Brook Thrust (WABT, Kusky 1985) to the north where they interpreted it

to juxtapose incompatible element-depleted mafic rocks in the footwall of the Point Leamington Deposit (PLD), with light rare earth element (LREE)-enriched tholeiitic to alkalic basalts of the Big Lewis Lake volcanic unit (g on Map C1) of the younger WBG sequence. Furthermore, they suggested that this fault may constitute the western limit of the Side Harbour unit (f on Map C1). Because the Shoal Arm Formation and Point Leamington Greywacke cut across stratigraphy and pinch out just east of the PLD, a second fault bounding these units on the east side is proposed. These faults are interpreted to coalesce just east of the PLD. The inference of these proposed faults is continuity of the incompatible element-depleted rocks which host the Point Leamington deposit, and the New Bay Pond unit of the older WBG sequence, and the Side Harbour and Big Lewis Lake volcanic units of the younger WBG sequence. As pointed out by Swinden and Jenner (1992), such an interpretation removes the necessity of extreme displacement of the D<sub>2</sub> fault which separates the Big Lewis Lake and Side Harbour units (as per Dean and Strong 1976). The easternmost unit of the NBP sequence comprises incompatible element-depleted mafic volcanic and minor silicic volcanic and volcanoclastic rocks (Swinden and Jenner 1992) (Map C1), consistent with this interpretation; however, the adjacent part of the sequence to the west faces toward this package and has geochemical and lithological characteristics of the younger WBG succession (Swinden and Jenner 1992). Thus, as suggested by Swinden and Jenner (1992), there must be another structural break within this package. This break is interpreted to link up with an as yet unobserved fault which must exist above the Point Leamington deposit, as it is overlain by rocks that occur in the upper part of the younger WBG sequence. This fault is interpreted to

coalesce with those which bound the Point Leamington Greywacke and Shoal Arm Formation package, and one of these three faults probably continues along the western side of the Side Harbour unit. We have interpreted the westernmost, west-dipping fault to occupy this position, which is compatible with the dip of bedding to the west of the fault (see Map C1 and cross-sections Map C1b).

The Indian Cove volcanic unit on the west side of Seal Bay comprises a bimodal mafic and felsic volcanic sequence which has incompatible element-depleted geochemical characteristics (Swinden et al. 1990), and is correlated with the older sequence of the WBG. Where rocks of the older sequence and the oldest units of the younger sequence are adjacent to the Side Harbour unit, there is an interpreted fault within the sequence (Map C1). Detailed mapping by Rubicon Minerals Corporation has recognized structural and stratigraphic relationships compatible with early faulting, possibly of fold and thrust style, on the southwest side of the dome cored by the Indian Cove unit (Tom Calon, pers comm). Based on the compilation map of Dean and Strong (1976), faults have been interpreted to run on either side of unit 4, as there is a structural discordance between it and the bedding in the older volcanic sequence to the east; and the calc-alkaline volcanic unit is missing on the western side. These faults do not continue very far to the south, as the complete stratigraphic succession of the younger sequence is preserved. On the eastern edge of the Indian Cove dome, Noranda Inc. property maps (Butler and Stewart 1993) show a stratigraphic contact between the older rhyolite and a volcanoclastic unit what might be unit 4 or 6 sedimentary rocks, but could also be part of the older sequence. The marked increase in thickness of unit 6 south of the older

volcanic sequence is probably dominantly original stratigraphic variation, but may have been enhanced by subsequent structural imbrication.

Based on mapping and geochemical sampling south of the SLIC, several new divisions of the volcanic rocks have been defined (Map C1). There is a unit of calc-alkaline mafic volcanic rocks on either side of the IAT basalts and rhyolites (older sequence) of the Nanny Bag Lake unit (h on Map C1). As the age of calc-alkaline rocks in the northeast has been confined to  $472 \pm 3$  Ma, and geochemically similar volcanic packages bordering the Nanny Bag Lake unit face toward the older sequence, the two packages are interpreted to be separated from each other by faults, except north of the Long Pond Fault as previously noted. Farther south, the western side of unit 4 is a fault (Dean and Strong 1976) that juxtaposes this unit with rocks in the upper part of the younger WBG sequence (unit 7) which face toward the older sequence. This fault is interpreted as an east-dipping, west-verging D<sub>1</sub> thrust, and is interpolated all the way along the western margin of this package. The D<sub>2</sub> Long Pond Fault separates the fault-bounded, east-facing package of units 4 and 5 to the south, from the west facing package to the north where the original stratigraphic contact at the base of unit 4 may be preserved (Map C1 and cross-sections Map C1b). At the north end of the Northern Arm calc-alkaline volcanic unit (i on Map C1), is a package of unit 7 rocks which face in the opposite direction, and is interpreted as another thrust slice.

There are no exposures of the older WBG sequence west of the Side Harbour Fault (Map C1). In fact the western part of the WBG comprises only the upper stratigraphic units (7 and 8) of the younger WBG sequence. There is some early fault

imbrication which repeats volcanic horizons and has created several large scale folds (O'Brien and MacDonald 1997, O'Brien 1998) (Map C1 and cross-sections Map C1b).  $D_1$  thrust faults have also emplaced the WBG over Caradocian shale, melange tracts of the Sops Head Complex, and volcanic rocks of the Roberts Arm Group (O'Brien and MacDonald 1997) which bound the WBG on its western edge (Map C1 and cross-sections C2). Although during  $D_2$  deformation, these other units have been thrust back over the WBG in places (O'Brien and MacDonald 1997) (Map C1 and cross-sections Map C1b).

Along its eastern side, various stratigraphic levels of the Wild Bight Group are juxtaposed against Caradocian shale which young both into and away from the WBG. As the younger Wild Bight Group sequence is regionally conformably overlain by Caradocian shale, this contact is interpreted as a thrust fault which has emplaced the WBG over the younger sedimentary succession. Coarse pebble/cobble conglomerates with abundant tonalite clasts occur at the base of the Point Leamington Greywacke (PLG) of the Badger Group along the contact with the South Lake Igneous Complex, and in this area the Shoal Arm Formation (SAF) is conspicuously absent (O'Brien 1992). The absence of the SAF could be a result of fault excision; however, the presence of conglomerates at the base of the PLG suggests a second possibility (O'Brien 1992). Relationships presented herein indicate that rocks of the SLIC and older volcanic sequence probably existed as an uplifted block (horst) in this area during development of the younger WBG sequence. It is probable that this structural high persisted during

development of the Point Leamington basin (O'Brien 1992), locally providing a source for conglomeratic units and resulting in non-deposition of the Shoal Arm Formation.

The Exploits Group shows a similar style of early fault imbrication (O'Brien et al. 1997), and is thrust westward over the Shoal Arm Formation and Point Leamington greywacke creating a triangle zone geometry (Williams and O'Brien 1994) (Map C1 and cross-sections Map C1b). A similar geometry occurs in the New Bay Pond area where these younger units are overridden by different parts of the WBG (cross-section J-K).

#### *4.2.3 Deformational Events*

There are two predominant phases of deformation recognized in the area of detailed study, which can be extrapolated to the rest of the WBG and correlated with regional phases of deformation recognized in previous studies. The first phase of deformation is correlative with  $D_1$  recognized regionally (e.g., O'Brien 1993), which created NW-SE-striking, folds and thrusts which are responsible for disposing the WBG into the regional fault-bounded dome and basin pattern proposed by O'Brien (1993). Minor folding of  $D_1$  thrusts is a result of subsequent  $D_2$  deformation (Map C1 and cross-sections C1b).  $D_1$  thrusting was approximately bedding parallel and interleaved rocks of the older and younger sequences of the Wild Bight Group, creating imbricate thrust stacks previously mistaken for a conformable stratigraphic succession. Much of the thrust imbrication during this event is nucleated around the older volcanic/plutonic packages, suggesting that perhaps these successions were the locus of pre- $D_1$  structures.  $D_2$  deformation of the thrust imbricated sequence created regional and mesoscopic asymmetric folds which locally reorient  $D_1$  structures into parallelism with  $D_2$ , as in the northeastern WBG.

Thrusting during  $D_1$  is interpreted to be both east and west vergent, exposing the older rocks in the cores of modified flower structures (see cross-sections Map C1b), similar to those within the Exploits Group (e.g., O'Brien et al. 1997). Fabrics in rocks adjacent to proposed faults are dominantly sub-vertical, and the faults have undoubtedly been steepened and reoriented during later deformation. Thus, these interpretations are based primarily on regional fold patterns, and the presence of stratigraphic breaks, and while they are internally consistent, they do not represent a unique solution.

The  $D_2$  event recognized in this study corresponds to the regional, main phase, northwest-directed  $D_2$  thrusting defined in previous studies. This event resulted in northeast striking/trending thrusts and folds which cause minor offsetting and undulation of units (Map C1 and cross-sections Map C1b), and a regional slaty/spaced cleavage. The northwest vergence of these structures in the area of detailed study is confirmed by overturned bedding in the footwall of Winter House Cove Fault (Map A), and by the easterly dip of bedding in the hanging wall unit at depth (Swinden 1988). However, in the western part of the WBG, O'Brien and MacDonald (1997) have mapped  $D_2$  SE-directed thrusts. These structures cross-cut the NW-directed ones indicating that they are slightly younger. Some of the  $D_2$  faults are overprinted and accentuated by younger, brittle, transcurrent structures (Kusky 1985), which are not shown.

### **4.3 Detrital Components in Volcaniclastic Rocks of the WBG**

#### ***4.3.1 Older volcanic sequence***

Within the older sequence of the WBG, volcaniclastic rocks are rare and most contain only one type of volcanic clasts (Plate 2.2c). This is interpreted to indicate a pyroclastic

origin with little reworking or mixing during submarine deposition. This contrasts with the younger sequence of the Wild Bight Group which contains numerous polyolithic conglomerates, debris flows and rare olistostromes which contain detritus from a number of sources.

#### *4.3.2 Younger volcanic sequence*

A shale olistostrome in unit 4, just north of the Winter House Cove Fault contains blocks of pillowed volcanic rocks (Plate 4.1a) up to several metres in diameter, polyolithic pebble conglomerate boulders and crystal rich laminations which have chaotic fold patterns suggestive of soft sediment deformation. At least some of the volcanic blocks have boninitic geochemical compositions (Fig. 4.1) and are interpreted to have been derived from the older volcanic sequence. This implies that the older succession forms part of the substrate to the younger arc and that this substrate was exposed in intra-basinal uplifts during development of the younger sequence.

Debris flows in the central part of the younger stratigraphic succession contain large (> 2m) and small blocks of altered rhyolite (Plate 4.1b) similar to that found in association with the Lockport deposit in the Glovers Harbour west unit (H.S. Swinden pers comm). Geochemical analyses confirm that three of these blocks have the same composition as the LREE-depleted, high-Si, low-K rhyolites of the older succession (Fig. 4.1). An attempt was made to date one of these blocks, and a tiny amount of sub-rounded, multifaceted zircon prisms were recovered after mineral separation. Four single, abraded, multifaceted grains that are < 2% discordant have  $^{207}\text{Pb}/^{206}\text{Pb}$  ages ranging from 1.9 to 2.8 Ga (Table 4.1), and are all inherited. This inheritance shows that there must have been

some contamination by an older crustal component in at least some rocks of the older sequence, as suggested by Sm-Nd isotope systematics (chapter 2).

The younger volcanoclastic sequence also contains blocks and boulders derived from within the succession. One of the debris flows (Plate 4.1c) containing older LREE-depleted rhyolite blocks (96GC10) also contains fragments of rhyolite with LREE-enriched calc-alkalic compositions (96GC08) interpreted to come from the younger succession (Fig. 4.2). A quartz diorite cobble (96GC07) from a polyolithic conglomerate (Plate 4.1d) below the calc-alkaline volcanic rocks of the Glovers Harbour East unit (b on Map C1), has a LREE-enriched geochemical signature similar to felsic to intermediate calc-alkaline volcanic rocks in the younger succession (Fig. 4.3). Although the abundance of trace elements in this sample are somewhat lower than the volcanic rocks, the primitive mantle-normalized extended-REE plot has the same slope and pattern. This cobble was dated by U-Pb zircon geochronology. Four fractions ranging from 11 to 1 % discordant, define a discordia line with a 14% probability of fit, and an upper intercept of age of  $473 \pm 3$  Ma (Fig. 4.2, Table 4.1). Although no plutonic rocks associated with the calc-alkaline sequence have been observed in the WBG, this is the same age, within error, as arc-related stitching plutons in central Newfoundland which intrude the composite Gondwanan margin (Colman-Sadd et al. 1992 and Tucker et al. 1994). This age also overlaps within error the age of the calc-alkaline volcanic rocks in the younger WBG sequence ( $472 \pm 3$  Ma).

There is also evidence of an old continentally derived detrital component within the younger sequence. A single large zircon prism tip from one of the dated tuffs (Duck

Island Tuff) is highly discordant (70%) and has a  $^{207}\text{Pb}/^{206}\text{Pb}$  age of 1419 Ma (Table 3.1).

#### *4.3.3 Interpretation*

Detrital components in the younger succession are derived both from within the sequence and from its older substrate, which is comprised of primitive island arc material, old continental crust, and/or sedimentary rocks derived therefrom (e.g., Gander Zone siliciclastic sedimentary rocks) and plutonic rocks probably related to volcanism in the younger sequence. This indicates that structural uplift occurred prior to and during development of the younger succession. These structural highs are interpreted to have been related to horsts and grabens, and probably existed throughout the evolution of the younger arc, and subsequently provided a locus for faulting during regional deformation. This idea is supported by the predominance of fault imbrication around the predominant exposure of older substrate in the eastern WBG (Map C1). These structural highs also influenced the thickness and distribution of sedimentary facies within the surrounding basins.

#### **4.4 Tectonomagmatic Evolution of the Wild Bight Group**

The distinctive geochemical composition of incompatible element-depleted, refractory island arc tholeiites and high-Si, low-K rhyolites in certain parts of the Wild Bight Group was recognized by Swinden et al. (1990), who interpreted these rocks to be related to rifting of an island arc represented by the adjacent calc-alkaline sequence. However, age constraints provided by U-Pb dating show that the calc-alkaline sequence is significantly younger than the depleted tholeiitic sequence and thus, it could not be related to arc rifting.

The older sequence of refractory island arc tholeiites, boninites and rhyolites certainly formed in an extensional suprasubduction zone setting, but there is no evidence of an earlier arc preserved in the WBG. Thus this sequence is re-interpreted to record the initiation and stabilization of a primitive intra-oceanic arc (Fig. 2.7).

Samarium-Nd isotopic characteristics of the incompatible element-depleted igneous rocks of the older succession indicate a source dominated by very depleted mantle. However, the isotopic systematics are somewhat unusual and indicate that minor contamination by an older crustal component may have occurred, possibly as a result of material transfer from the down-going slab and its sedimentary cover. This idea is supported by the presence of inherited Proterozoic and Archean zircons in a rhyolite block interpreted to have been derived from this sequence. Thus, this ensimatic arc was close enough to older continental crust to receive at least minor sediment input from such a source. The short amount of time between the youngest volcanism (post ~485 Ma) and obduction (pre ~475 Ma) of this primitive arc is compatible with an origin close to the continental margin onto which it was partially emplaced.

There is a hiatus of up to 10 Ma (~485 to 475 Ma), in the volcanic activity of the WBG. This could be a result of imperfect preservation, although in the correlative Exploits Group a complete sedimentary record from lower to middle Ordovician age rocks is preserved across this same gap. This hiatus corresponds well with the period of Penobscot deformation and ophiolite obduction in central and southern Newfoundland (Colman-Sadd et al. 1992, Tucker et al. 1994), and is interpreted to record this event within the Wild Bight Group (Fig. 3.7). The continuous record of marine sedimentation in

the Exploits Group, and the submarine nature of the younger WBG sequence, suggest submergence during partial emplacement of the primitive arc, and that the arc remained in an extensional rather than compressional setting. This could be accounted for if the primitive ensimatic arc was partially emplaced onto the continent by subducting the thinned continental margin beneath the primitive arc. During this arc-continent "collision", only the fore-arc accretionary prism was likely to have undergone compression. Attempted subduction of continental crust is interpreted to have caused termination of westward (present coordinates) subduction and cessation of ensimatic volcanism.

Renewed arc-related volcanism at about 473–472 Ma suggests that continued convergence resulted in the initiation of an east-dipping (present coordinates) subduction zone beneath the composite Gondwanan margin (Fig.3.7). The geochemical and Sm-Nd isotopic characteristics of the volcanic rocks in this younger arc indicate, respectively an enriched mantle source and significant contamination by an old crustal component. Subsequent within-plate tholeiitic to alkaline volcanism is interpreted to represent arc rifting and formation of a marginal basin (Fig. 3.7).

#### **4.5 Correlation with the Exploits Group**

The Wild Bight Group can be directly correlated with the Exploits Group immediately to the east, which spans a similar age range from late Tremadoc to early Caradoc (O'Brien et al. 1997). A well developed geochemical stratigraphy has been defined for the Exploits Group (O'Brien et al. 1997). The earliest volcanic rocks in the sequence are substantially fractionated tholeiitic basalts with trace element patterns similar to normal island arc

tholeiites (IATs), but at much lower abundances. These rocks do not have an analogue in the WBG. They are overlain by trace element depleted, high-Si, low-K, slightly LREE-enriched felsic to intermediate volcanic rocks which have been dated at  $486 \pm 3$  Ma (O'Brien et al. 1997), and incompatible element-depleted refractory mafic rocks which are mostly LREE-depleted island arc tholeiites. One sample with a LREE-enriched signature (O'Brien et al. 1997, group TA-5) is transitional in composition to boninite-like volcanic rocks of similar age in the WBG. The unusual IATs at the base of this succession have very low levels of incompatible elements suggesting that they may represent large degrees of partial melting. The flat to slightly LREE-enriched primitive mantle-normalized extended-REE patterns of these IATs (O'Brien et al. 1997) suggest a normal MORB-like source. Thus their compositions are compatible with those expected of high degree, initial, partial melts formed by hydrous and decompression induced catastrophic melting during subduction initiation (e.g., Stern and Bloomer 1992). This phase of volcanism could have generated the degree of mantle depletion necessary to form the more refractory tholeiitic basalts that overlie them. The age and compositional variation of rocks in this sequence are analogous to the older succession of the WBG, and are compatible with formation in a primitive ensimatic oceanic arc.

The central stratigraphic part of the Exploits Group consists of the New Bay Formation which does not contain any volcanic rocks, although gabbroic sills are abundant. The basal Charles Brook Member contains thickly bedded pyroclastic lapillistones, epiclastic pebble conglomerates and mixed source wackes (O'Brien et al. 1997) similar to, but finer-grained than the coarse volcanoclastic rocks in the central part

of the younger sequence of the WBG (unit 6). The Charles Brook Member is overlain by finer-grained, thinly bedded sedimentary rocks of the Brooks Harbour Member, which is dominated by massive dark shales, with minor siltstone and greywacke (O'Brien et al. 1997). The uppermost Saltwater Pond Member comprises a muddy olistostromal sequence at the base which gives way to a fining upward succession of volcanoclastic wackes and porcellanites with abundant poorly bedded conglomeratic units (O'Brien et al. 1997).

The New Bay Formation is overlain by the Lawrence Head volcanics which are interbedded with ferruginous chert that grades conformably up into Caradocian shale. Most of the volcanic rocks in this succession have incompatible element enriched-tholeiitic to alkalic compositions, although one group (LH-3, O'Brien et al. 1997) has trace element compositions transitional to calc-alkalic. Graptolitic shales interbedded with these volcanic rocks indicate a late Arenig to early Llanvirn age for this package (O'Brien et al. 1997). The geochemical compositions, stratigraphic position and lithologic associations of the Lawrence Head volcanics are similar to the upper volcanic unit of the younger succession of the Wild Bight Group, and thus, are interpreted to be correlative with it.

A notable difference in the upper Exploits Group is the presence of a thin discontinuous limestone unit (Hummock Island Limestone) which O'Brien et al. (1997) interpreted to be the partial lateral equivalent of the Lawrence Head Volcanics. However, the youngest bioclastic carbonates are appreciably younger than the youngest volcanic rocks (O'Brien et al. 1997).

There is not a correlative unit in the Exploits Group for the calc-alkaline volcanic rocks in the lower part of the younger WBG sequence. This is likely the result of the position of the Exploits Group relative to the main volcanic arc. Rocks of the Charles Brook member at the base of the New Bay Formation were interpreted as proximal turbidites deposited on the middle portion of a deep sea submarine fan (O'Brien et al. 1997). Helwig (1967) demonstrated that graded turbiditic sandstones were derived from a volcanic landmass to the southwest. The Brooks Harbour Member of the New Bay Formation was interpreted to represent distal turbidites and basin plain mudstones formed on the outer part of a submarine fan or on the oceanic abyssal plain (Helwig, 1967 and Dec et al. 1993). Sedimentary structures in this package are also consistent with a source in the WBG to the southwest (Helwig, 1967 and Dec et al. 1993). The progression of sedimentary rocks in the basal two members of the New Bay Formation suggest a deepening of the basin with time. This is compatible with the fining upward nature of the volcanoclastic rocks in the younger WBG sequence, which are clearly more proximal to the main volcanic arc, as they are interbedded calc-alkaline volcanic rocks.

Conglomeratic rocks interbedded with porcellanites in the uppermost Saltwater Pond member of the New Bay Formation represent a change in source and depositional environment. These rocks were interpreted to represent a supra-fan deposit on the lower-slope apron of a submarine fan (Hughes and O'Brien 1994). Paleocurrent measurements indicate a new direction of flow was initiated from a landmass to the south east (Helwig 1967) during deposition of this unit. At and above this horizon in the New Bay Formation large magmatic clasts and slump folds are prominent (O'Brien et al. 1997), and suggest

that already lithified sedimentary and volcanic rocks were mixed with unconsolidated intra-basinal sediment and redeposited within the Saltwater Pond member of the New Bay Formation (O'Brien et al. 1997).

One possible interpretation for the origin of the lower New Bay Formation is that it represents the more distal parts of the back arc basin prior to arc-rifting. The change in source and depositional environment represented by the Saltwater Pond Member at the top of the New Bay Formation may herald the initiation of arc rifting. The New Bay Formation is overlain by volcanic rocks of the Lawrence Head Formation which, based on correlation with the WBG, represent rift-related volcanism. This idea is supported by the fact that in some places Lawrence Head volcanics occur isolated in small horsts structurally separated from older Exploits Group rocks, as well as within conformable successions above the New Bay Formation (O'Brien et al. 1997). The more distal back arc position of the Exploits Group relative to the eastern WBG is supported by the greater thickness and more distal facies of sedimentary rocks, and the lack of calc-alkaline arc-related volcanic rocks.

Based on the similarities outlined above, the Wild Bight and Exploits groups are interpreted to represent different parts of the same late Arenig to Llanvirn arc, and were probably also contiguous during early Ordovician development of the older ensimatic arc which underlies both sequences.

#### **4.6 Paleogeography of the late Arenig to Llanvirn Wild Bight/Exploits Arc**

In this section, a model for the paleogeography of the Wild Bight/Exploits Arc, which accounts for variations in stratigraphic relationships within these two closely related groups, will be discussed.

This model (Fig. 4.4) comprises five main spatial components, from west to east they are: the active arc; the intra-arc rift basin; the ensimatic spreading centre; the remnant arc; and the pre-arc-rift back arc basin. Both the active and remnant parts of the main arc contain horsts of uplifted older substrate which possibly included continental crust and/or siliciclastic sedimentary rocks derived therefrom, "obducted" slivers of the older primitive ensimatic arc, and plutonic rocks related to arc-volcanism. This substrate is assumed to underlie the entire "arc", perhaps discontinuously, with the exception of the ensimatic part of the rift basin.

The eastern part of the WBG is interpreted to represent part of the remnant arc (Fig. 4.4) comprising a large uplifted block of older substrate, arc-related mafic volcanic rocks, a thick sequence of proximal volcanogenic sedimentary rocks, and a thin sequence of finer-grained volcanoclastic rocks, chert and argillite with rare lenses of rift-related volcanic rocks at the top. This intra-basinal high resulted in variable thicknesses of certain stratigraphic units. Just northwest of the Winter House Cove Fault (Map A1), the lower part of the younger sequence, units 4 and 6, are missing to the SW, and are overlain by a continuous sequence of the finer-grained volcanoclastic rocks of unit 7. Toward the NE, away from the older rocks, unit 6 becomes much thicker and is exposed on all the islands south of Leading Tickles. This is interpreted to be largely original

stratigraphic thinning, although it may be accentuated by the fault. A similar relationship occurs adjacent to a fault-bounded part of the Tea Arm Formation (older sequence) near Strong Island in the Exploits Group (O'Brien 1997). Fault imbrication around the southern end of the old sequence makes it difficult to recognize a similar relationship there.

The central part of the Wild Bight Group (Seal Bay area) is interpreted to have been on the margin of the remnant arc, toward the main rift basin. It doesn't contain such large uplifted blocks, but the older substrate does occur below the base of the younger succession in the core of the Seal Bay anticline at Indian Cove. Abrupt changes in the thickness of unit 6 on the west side of the dome suggest that this package may have been a smaller uplifted region. Unit 6 is overlain by a continuous basalt unit (Side Harbour) which extends to the southern end of the WBG where it is underlain by a thick succession of unit 7 (and presumably unit 6 beneath it). On the margin of the dome there are also interpreted thrust faults, but most of the thinning of units 6 and 7 is probably a primary stratigraphic feature, because farther south the stratigraphic separation on the fault is much less significant. The central WBG (Seal Bay area) also contains mafic calc-alkaline volcanic rocks, but only a very thin sequence; a moderately thick sequence of coarse-grained volcanoclastic rocks, a thin sequence of finer-grained volcanoclastic rocks, argillite and chert, and numerous sills with rift-related geochemical characteristics.

A transition to more central parts of the rift basin occurs towards the west. The calc-alkaline sequence is thin in the central part of the group (Seal Bay), and completely absent in the western WBG, which is interpreted to represent the main rift basin (Fig.

4.4). It does not contain uplifted blocks of older substrate, and comprises predominantly fine-grained volcanoclastic rocks and rift-related volcanic rocks. Abundant hydrothermal alteration in this sequence (O'Brien 1997) suggests that there was high heat flow, and is compatible with this sequence representing the main rift basin.

Based on this model, somewhere to the west of the main rift basin, the active part of the rifted arc should exist, and the older sequence should underlie the western margin of the rift basin. This idea is supported by the work of Clarke (1992) on the Sops Head Melange. He suggested that many of the volcanic blocks in the Sops Head Melange have geochemical characteristics which are more like tholeiitic arc-related volcanic rocks of the eastern WBG, although some could come from calc-alkaline volcanic rocks of the adjacent Roberts Arm Group. Based on previous models, it was difficult to explain how rocks that only occur on the eastern side of the WBG could be present as blocks in a melange on the western side.

The Exploits Group comprises, within various thrust slices, a complete stratigraphic sequence from late Tremadoc to Caradoc and is interpreted to represent the pre-rift back arc basin. In this relatively volcanically inactive area, pelagic material and volcanoclastic sediments derived from the younger arc were deposited more or less continuously on top of the older ensimatic arc. There are numerous gabbro sills in this sequence, but they may be related to the younger volcanic sequence, as in the WBG. Thus, although there is a marked hiatus in volcanic activity, sedimentation may have been essentially continuous in the deeper basins of the Wild Bight/Exploits arc from late Arenig to Caradoc time. The occurrence of minor rifting in the back arc basin is

suggested by the presence of the Lawrence Head volcanics near the top of the sequence. The onset of rifting was preceded by a change in source of the underlying volcanoclastic rocks (O'Brien et al. 1997 and references therein) suggesting that uplift occurred continentward of the back arc basin at this time. This uplift could account for the carbonate which is locally present at higher stratigraphic levels.

Although there is no evidence of ensimatic, N-MORB-like volcanism in the WBG which would represent the spreading centre, there is evidence in other parts of the Exploits Subzone and New Brunswick (see chapter 5) that some oceanic crust was produced at this time. This tectonic setting is shown in Figure 4.4 only to indicate how it could be incorporated into the model.

#### **4.7 Conclusions**

The younger late Arenig to Llanvirn arc/arc rift/back arc succession is interpreted to have formed on the thinned edge of the composite Gondwanan margin, which was comprised of crustally derived siliciclastic sedimentary rocks (and or thinned continental crust), and rocks of a partially obducted primitive ensimatic arc. The ensimatic arc provides the immediate substrate upon which the younger rocks were deposited. Structural horsts within the younger arc exposed the older underlying rocks, which provided detritus to the younger sequence.

The late Arenig to Llanvirn parts of Wild Bight and Exploits groups represent different parts of the same arc system. They were probably also contiguous during development of the Tremadocian to early Arenig ensimatic arc which formed part of the composite substrate on which they were formed. The eastern Wild Bight Group is

interpreted to represent the late Arenig remnant arc following arc rifting, and progressively farther west the central and western WBG represent the margin of the remnant arc and the main rift basin, respectively. The Exploits group is interpreted to represent the pre-rift back arc basin, which experienced only minor rifting late in its evolution.

## **Chapter 5**

### **Regional Correlations and Implications for Evolution of the Gondwanan Margin**

#### **5.1 Introduction**

In addition to the Wild Bight and Exploits groups which have been interpreted as part of the same arc system, there are other fragments of Ordovician ophiolitic crust and volcanic arcs within the Exploits Subzone in Newfoundland (Fig.5.1) and in New Brunswick which have similar rocks types and geochemical characteristics (Fig. 5.2). Precise age constraints, petrogenetic and stratigraphic relationships within many of these sequences are not well-defined, but some insights into their origin can be gained by analogy with similar well-constrained rock packages in the WB/Exploits arc.

Although there are broad similarities between various volcanic belts in the Exploits Subzone, there are also significant differences, which suggest that there were along strike variations in the degree to which the late Arenig to Llanvirn arcs interacted with the Gondwanan margin. A model is proposed which accounts for the similarities and differences in the early to middle Ordovician volcanic/epiclastic sequences of the Exploits Subzone in Newfoundland, and is compared with the model proposed by others for analogous rocks in the Miramichi Highlands of northern New Brunswick.

#### **5.2 Correlation with Other parts of the Exploits Subzone**

##### **5.2.1 *Ophiolites***

Most of the ophiolites preserved in the Newfoundland Appalachians occur in the Notre Dame Subzone, and are associated with the Laurentian margin of Iapetus. However, there

are several small, partially preserved ophiolites within the Exploits Subzone. The *Pipestone Pond*, *Coy Pond* and *Great Bend complexes* in the central Exploits Subzone, consist of ultramafic cumulates, layered and massive gabbros and pillowed volcanic rocks, and are completely fault-bounded. These complexes rim the Mount Cormack Subzone, which Colman-Sadd and Swinden (1984) suggested is a structural window of the Gander Zone (Fig. 5.1). These ophiolites were interpreted as erosional remnants of a once continuous allocthonous thrust sheet, emplaced onto the Gander Zone (Colman-Sadd and Swinden 1984). In a detailed study of Gander-Exploits relationships, Colman-Sadd et al. (1992) showed that emplacement of these ophiolites occurred prior to intrusion of the Partridgeberry Hills Granite at  $474 \pm 3$  Ma. Constraints on the ages of the Coy Pond and Pipestone Pond complexes are provided by a trondhjemite pod within the gabbro portion of each sequence. The age of the Pipestone Pond complex is precisely determined at  $494 \pm 2$  Ma, and a minimum age of 489 for the Coy Pond complex is provided by one fairly discordant zircon fraction (Dunning and Krogh 1985).

A geochemical study of the Pipestone Pond complex shows that there are two geochemically distinct suites (Jenner and Swinden 1992). The mafic and ultramafic plutonic rocks and dyke swarms are refractory, incompatible element-depleted, LREE-depleted IATs. Related plagiogranite/trondhjemite pods have similar geochemical characteristics. These rocks have  $\epsilon_{Nd}$  values which range from -1 to +4. In contrast, the pillowed volcanic rocks have MORB-like geochemical and isotopic compositions ( $\epsilon_{Nd} +7$ ). Because this ophiolite is structurally disrupted, the relationship between the plutonic and volcanic rocks is unclear. However, it is clear that they are not petrogenetically

related. No geochemical data is available for the Coy Pond or Great Bend ophiolites, but they are assumed to be related to the Pipestone Pond complex (Jenner and Swinden 1992). Sedimentary rocks interbedded with the volcanic rocks of the Pipestone Pond Complex (Williams et al. 1992), are similar to and interpreted to be correlative with Unit 7 (Colman-Sadd 1985) sedimentary rocks of the Coy Pond complex (Williams et al, 1992). A late Arenig faunal occurs within Unit 7 at one locality (Williams et al. 1992) and provides a minimum age for the underlying volcanic rocks. This suggests that the volcanic rocks are younger than the plutonic part of the ophiolite (Fig. 5.2).

Middle Ordovician limestones unconformably overlie the Coy Pond Complex and adjacent rocks of the Mount Cormack Subzone of the Gander Zone (Colman-Sadd et al. 1992). They are interpreted as part of an overlap sequence which links early Ordovician ophiolites of the Exploits Subzone and clastic sedimentary rocks of the Gander Zone (Colman-Sadd et al. 1992).

The age, geochemical and isotopic signatures of the plutonic part of the Pipestone Pond Complex are similar to the older sequence of the Wild Bight Group (Fig. 5.2), and their structural setting and age of emplacement are compatible with the model proposed for the tectonic evolution of the Wild Bight Group. In fact these ophiolites provide evidence to support the model for a hiatus in volcanism in the WBG, and are interpreted to represent oceanic crust of a primitive ensimatic arc. Jenner and Swinden (1992) also suggested that these ophiolites could have formed during subduction initiation. Fossil control suggests that the volcanic rocks of the ophiolite are younger than the plutonic part (late Arenig), but their original relationship to the plutonic rocks is equivocal.

### 5.2.2 *Volcanic/volcaniclastic sequences of Notre Dame Bay*

In addition to the large package of early to middle Ordovician volcanic and volcaniclastic sedimentary rocks of the combined Wild Bight and Exploits groups in Notre Dame Bay, there are two smaller packages of similar rocks: the Noggin Cove Formation in Gander Bay; and the Summerford Group on New World Island (NWI, Fig. 5.1).

The *Summerford Group* is comprised of pillowed mafic flows, coarse volcaniclastic agglomerates, tuffs, sandstones with variable amounts of calcareous matrix, and several lenses of limestone (Elliot et al. 1989). On eastern NWI, calcareous rocks form a continuous late Llandeilo unit, the Cobbs Arm Limestone (Bergstrom et al. 1974), which overlies the volcanogenic rocks. The Cobbs Arm Limestone is conformably overlain by Caradocian black shale of the Rogers Cove Formation (Elliot et al. 1989), but at Back Cove of Toogood Arm on NWI, volcanic rocks of the Summerford Group are unconformably overlain by red conglomeratic turbidites of the lower Silurian Goldson Formation (Arnott 1983). The geochemical signature of the volcanic rocks in the Summerford Formation range from within plate tholeiitic to alkalic, and were previously interpreted to represent an oceanic island (Jacobi and Wasowski 1985). The stratigraphic position of these rocks immediately below Caradocian black shale, and Llandeilian limestone, and their within-plate geochemical signatures, are very similar to the Lawrence Head Volcanics of the Exploits Group. Thus, at least part of the Summerford Formation is interpreted to be correlative with the youngest volcanic rocks of the Exploits Group (Fig. 5.2).

Volcanic rocks associated with Tremadocian limestone occur locally in the Summerford Formation and are likely in fault contact with Caradocian black shale. These rocks probably represent a different tectonic setting, although the composition of the volcanic rocks is not known and thus provides no constraints on the possibilities. Their age suggests that they could be correlative with the older volcanic sequence of the WBG. This suggests that the Summerford Formation could represent another uplift within the marginal rift basin. Perhaps this is the uplift which provided detritus to the uppermost member of the New Bay Formation of the Exploits Group.

The *Noggin Cove Formation* occurs on the southeast side of the Dog Bay line, a structural feature which separates distinctive Silurian sequences (Williams et al. 1993). The Noggin Cove Formation is comprised of volcanoclastic conglomerate and sandstone, minor mafic lavas and dykes, bedded tuffs, lapilli breccia and minor black shale (Johnston et al. 1994). It is overlain by siltstone, shale, olistostromes and coticule beds of the Woody Island formation, which is in turn overlain by the Carmanville Melange (Johnston et al. 1994, Currie 1992, 1993). Together these three units make up the Hamilton Sound Group (Currie 1992, 1993, Williams, 1993 and Williams et al. 1993), which is unfossiliferous, but which is similar to other middle Ordovician groups and melange tracts of the Exploits Subzone (Williams 1992). The presence of coticule horizons in the Woody Island Formation indicates that this was a restricted basin, whereas other time-equivalent basins were non-restricted and lack coticule units. The Hamilton Sound sequence is overlain apparently conformably by fossiliferous Llandovery limestone breccia, limestone and shale of the basal Indian Islands Group (Williams et al.

1993). However, the abrupt lithic contrast was interpreted to indicate a major erosional break (Williams et al. 1993).

The volcanic rocks of the Hamilton Sound Group have geochemical compositions which range from MORB to island arc tholeiite to within plate alkalic, which lead to the interpretation that these rocks formed in a back arc basin (Johnston et al. 1994). The Noggin Cove Formation is interpreted to be correlative with the youngest volcanic rocks of the Wild Bight and Exploits groups (Fig. 5.2) and to have formed in an extensional marginal basin. The presence of volcanic rocks with N-MORB-like chemistry in this succession, suggests that: either the late Arenig arc/back arc system was still slightly outboard of the Gondwanan margin and thus was always above depleted oceanic mantle; or the rift-basin progressed to a small oceanic spreading centre with normal depleted mantle as opposed to enriched mantle which produced the rift-related rocks.

Although the contact now is everywhere a fault (Johnson et al. 1994), Williams (1995) suggested that the original relationship of the Carmanville Melange to the Noggin Cove Formation is analogous to the relationship of the Dunnage Melange to the Exploits Group (Hibbard and Williams 1979, and Williams 1995). The Dunnage Melange may have originally overlain and interfingered with the New Bay Formation in the southwest, and may also have been contiguous with the Lawrence Head Volcanics in the northwest (Williams 1995). The Duder Group and the Garden Point Melange on the other side (NW) of the Dog Bay Line (Williams et al. 1993) are interpreted to be correlative with and analogous to the Noggin Cove Formation and Carmanville Melange.

### 5.2.3 *Volcanic/volcaniclastic sequences of central Newfoundland*

There are several large belts of Cambro-Ordovician volcanic/volcaniclastic/epiclastic rocks in the Exploits Subzone in central and southern Newfoundland: the Bay du Nord Group in the southern Hermitage Flexure, the Victoria Lake Group adjacent to the Red Indian Line in central Newfoundland; and the Bay d'Espoir and Davidsville groups in the eastern Dunnage Zone (Fig. 5.1).

The *Victoria Lake Group* (VLG) hosts numerous volcanogenic sulphide and gold showings. Thus, although most parts are not well exposed, drill core has facilitated preliminary geochemical and geochronological studies of the belt (e.g., Evans et al. 1990, Kean and Evans 1988, Swinden et al. 1989, and Dunning et al. 1991). These studies have shown that the Victoria Lake Group is a composite belt comprised of volcanic rocks of at least three different ages, and spanning a large range of geochemical compositions. The Lake Ambrose volcanic belt along the southeast side of the VLG is the oldest package, dated by U/Pb zircon geochronology at  $513 \pm 2$  Ma (Dunning et al. 1991). It comprises variably LREE-enriched island arc tholeiitic basalt, and minor rhyolite which was interpreted to be the result of secondary melting of amphibolite facies rocks at the base of the arc (Dunning et al. 1991). A small package of volcanic rocks along strike comprises mafic volcanic rocks previously interpreted as boninitic (Swinden et al. 1989), although they are perhaps more similar to refractory low-Ti, island arc tholeiites. The stratigraphic relationship of these rocks to the dated sequence is unknown. Based on relationships in modern arcs (e.g., Stern and Bloomer 1992), and in the Wild Bight Group, these kinds of refractory rocks can form during subduction zone initiation, or island arc rifting as in the

Betts Cove ophiolite (Coish et al. 1982, Bedard et al. in press). The Lake Ambrose volcanic rocks are the oldest of the Exploits Subzone, and represent an island arc which predates the ophiolites and other arcs of the Exploits Subzone (Fig. 5.2). These rocks apparently do not have a correlative sequence in the Wild Bight Group or elsewhere in the Exploits Subzone.

The Diversion Lake Group, along strike to the northeast from the Lake Ambrose volcanics, is a fault-bounded package of basalts with LREE-enriched tholeiitic, non-arc geochemical compositions. The stratigraphic position of these rocks is not known, but they are compositionally similar to the youngest basalts of the WBG, and are interpreted to be correlative with them (Fig. 5.2), and to represent rift-related volcanism.

The Tulks Hill belt on the northwestern side of the VLG, is comprised of sequences which include volcanic rocks of two distinct ages,  $498 \pm 6/-4$  and  $462 \pm 4/-2$  Ma (Evans et al. 1990). Mafic volcanic rocks associated with the dated felsic units of the 498 Ma sequence are strongly incompatible element- and LREE-depleted island arc tholeiites (Evans et al. 1990, and Swinden et al. 1989). Structurally (and stratigraphically ?) below this package is a sequence of slightly incompatible element-depleted, weakly LREE-enriched island arc tholeiites of the Harmsworth Steady volcanics (Evans et al. 1990). Some of the rocks in this package are more strongly LREE-enriched (Evans et al. 1990, and Swinden et al. 1989), but have somewhat irregular trace element patterns which might reflect alteration. The degree of incompatible element depletion in these rocks is similar to that of low-Ti island arc tholeiites of the older sequence of the WBG, although the Harmsworth Steady IATs are slightly more LREE-enriched. Evans et

al.(1990) interpreted the Harmsworth Steady volcanics to stratigraphically underlie the dated 498 Ma sequence. However, the presence of topographically and geophysically defined linears surrounding this package (Evans et al. 1990, and Kean and Evans 1988) suggest an alternate interpretation; that this sequence is fault bounded, and not necessarily in the correct stratigraphic position.

Although the age of the strongly incompatible element depleted sequence is slightly older than that of geochemically similar volcanic rocks in the WBG, they are interpreted to be correlative (Fig. 5.2), and suggest that perhaps subduction began slightly earlier in this area. Based on similarity in geochemical composition to low-Ti IATs of the older WBG succession, the Harmsworth Steady volcanics are interpreted to be part of the 498 Ma sequence, although their stratigraphic position is not certain.

The upper basalts of the Tulks Hill volcanic belt are separated from the main volcanic sequence by faults, and have LREE-enriched, non-arc tholeiitic compositions. Lenses of volcanic rocks with similar compositions occur near the top of the volcanoclastic package in the central part of the Victoria Lake Group, which is interpreted to be conformably overlain by Caradocian shale (Evans et al. 1990). The composition and stratigraphic position of these volcanic rocks suggests that they are correlative with the youngest volcanic rocks of the WBG (Fig. 5.2), and represent arc rifting.

The Victoria Mine sequence is the youngest dated package of volcanic rocks in the Victoria Lake Group (462  $\pm$  4/-2 Ma, Evans et al. 1990), and occurs along the eastern margin of the belt. It is separated from the Tulks Hill volcanics by what Evans et al. (1990) interpreted to be a northwest-dipping, thrust fault. This sequence comprises calc-

alkaline basalts, rhyolite porphyry (dated sample) and abundant felsic pyroclastic rocks, and although slightly younger, is correlated with calc-alkaline rocks of the younger WBG sequence (Fig. 5.2).

The *Bay du Nord Group* occurs along the northern edge of the Hermitage Flexure in southern Newfoundland (Fig. 5.1). At the western end of the flexure, Tucker et al. (1994) divided the Bay du Nord Group into 3 belts, from NW to SE: the North Bay; Rattling Brook; and Dolman Cove belts. The North Bay belt comprises graphitic, pelitic and semi-pelitic rocks locally intercalated with volcanic flows and pyroclastic rocks of felsic composition, and youngs to the southeast. The Rattling Brook belt is a wide shear belt composed largely of mylonite, but also locally includes recognizable sedimentary and volcanic rocks, and shear-bounded meta-gabbro pods. Both of these belts are intruded, post tectonically, by the Bagg's Hill granite, dated at  $478 \pm 2$  Ma (Tucker et al. 1994), and must therefore be older than this. A felsic volcanic rock from the North Bay belt was dated at  $485 \pm 2$  Ma (Dunning unpublished data), confirming its older age. Based on the age of the North Bay belt, both of these packages are interpreted to be correlative with the older sequence of the Wild Bight Group (Fig. 5.2). There is no data available on the geochemical composition of the magmatic rocks in either belt.

The Dolman Cove belt is comprised predominantly of amphibolite grade felsic tuffs, with minor psammite and pelite units, and rare conglomerates (Tucker et al. 1994). The conglomerates contain clasts of foliated Bagg's Hill Granite which led Tucker et al. (1994) to distinguish it as a separate and younger belt. An age of  $419 \pm 3$  Ma for a tuff

from this unit (Dunning and O'Brien unpublished data) shows that this belt is much younger and is actually Silurian in age.

The Bay du Nord Group in the eastern Hermitage Flexure comprises submarine flows and volcanoclastic/pyroclastic rocks of dominantly felsic composition, interbedded with pelitic and psammitic metasedimentary rocks. A felsic tuff from within the Bay du Nord Group in this area was dated at  $466 \pm 3$  Ma (Dunning et al. 1990), indicating that there are at least two phases of Ordovician volcanic activity within this Group. The age of this younger volcanism overlaps with the age of calc-alkalic and within-plate volcanism in the WBG, and is thus correlated with that succession of the WBG.

The *Baie d'Espoir* and *Davidsville* groups cover a large area in the eastern Exploits Subzone, and comprise predominantly volcanoclastic rocks, shale and sandstone, with only minor volcanic rocks (Williams 1995 and references therein). In the Davidsville Group to the north, the volcanic rocks are dominantly mafic, whereas in the southern Bay d'Espoir Group volcanic rocks are dominantly felsic (Williams 1995 and references therein). Based on fossil evidence, these two groups are believed to range from late Arenig to Caradoc in age (Boyce et al. 1988, and Colman-Sadd 1976). The Twillick Brook member is a quartz-plagioclase porphyry unit which is predominantly enclosed within the Bay d'Espoir Group, and is interpreted to be interbedded with these Ordovician rocks (Blackwood 1983). It is spatially associated with Llandeilo-Caradoc black shale along its southeast margin. To the northeast, the Twillick Brook Member extends into the outcrop area of the Gander Lake Subzone, and Blackwood (1983) interpreted it to be conformable on top of the Gander Group. A U-Pb zircon age of  $468 \pm 2$  Ma (Colman-

Sadd et al. 1992, suggests that the Twillick Brook member is correlative with the younger sequence of the WBG.

Late Llanvirn to early Llandeilo limestone of the Davidsville Group directly overlies ultramafic rocks of the Gander River Complex at Weirs pond , and contains detrital components indicating a mixed provenance (ultramafic and Gander Group) (Stouge 1979, and O'Neill 1987). Elsewhere distinctive conglomerates with abundant ultramafic clasts, overlie the Gander River Complex (Williams 1995, and references therein). These relationships suggests that these mid-Ordovician sequences of the Bay d'Espoir and Davidsville groups, which are interpreted to be correlative with the younger volcanic sequence of the WBG, are part of an overlap sequence which unconformably overlies the composite Gondwanan margin (as suggested by Williams and Piasecki 1990, and Colman-Sadd et al. 1992). This idea is compatible with the interpretation of Williams (1995) who suggested that the mid- to upper-Ordovician sequences represent a cover sequence to obducted and already deformed ophiolite sequences; and supports the interpretation of a continental margin setting for the younger WBG sequence.

The Llanvirn to Llandeilo age for the base of the overlap sequence in the Davidsville Group at Weirs Pond, is younger than to the late Arenig to Llanvirn age elsewhere on the GRUB, such as at Gander Lake. This suggests that this area was exposed and being eroded while other areas were already experiencing submarine deposition. Perhaps the Weirs Pond area was continentward of the submarine basin in late Arenig time, and only later did rifting occur this far east (present coordinates).

### **5.3 Comparison with rocks of northern New Brunswick**

Ordovician rocks of the northern Miramichi Highlands of New Brunswick have been extensively studied, as they contain the numerous VMS deposits of the Bathurst camp. These volcanic rocks are divided into the older Tetagouche and younger Fournier Groups, the former of which unconformably overlies siliciclastic rocks of the Miramichi Group (van Staal and Fyffe 1991 and Rice and van Staal 1992). The Miramichi Group comprises lower Ordovician quartz-rich sandstone and shale and has generally been correlated with the Gander Group in Newfoundland (e.g., Rast et al. 1976 and Williams 1979).

Although these rocks have been extensively structurally imbricated (van Staal 1994), U-Pb geochronology and fossil occurrences have helped to define stratigraphic relationships. Calcareous rocks of the Vallee Lourdes Formation at the base of the Tetagouche Group contain middle Arenig to early Llanvirn conodonts and late Arenig brachiopods (Nowlan 1981 and Neuman 1984) which provide a maximum late Arenig age limit on overlying volcanic rocks. The calcareous rocks are overlain by dark shales and siltstones of the Patrick Brook Formation (van Staal 1994). The oldest volcanic rocks of the succession conformably overlie the Patrick Brook Formation, and comprise predominantly porphyritic felsic volcanic and pyroclastic rocks of the correlative, but structurally separated, Spruce Lake, and Nepisiguit Falls formations and mafic volcanic rocks of the Canoe Landing Lake Formation (van Staal 1994, Sullivan and van Staal 1996). Mafic volcanic rocks of the Canoe Landing Lake Formation and those interlayered with the porphyritic felsic rocks have within plate tholeiitic to alkalic compositions (van Staal et al. 1991). The felsic rocks have variable compositions ranging

from within plate granite to calc-alkaline (van Staal et al. 1991 and Rogers 1994, 1995). Two felsic tuffs from the Nepisiguit Falls Formation were dated at  $471 \pm 3$  and  $469 \pm 2$  Ma (Sullivan and van Staal 1996), and a syn-volcanic dacite porphyry sill of the Spruce Lake Formation was dated at  $470 \pm 5$  Ma. A rhyolite intercalated with the basalts of the Canoe Landing Lake Formation gives an age of  $470 \pm 2$  Ma for this sequence (Sullivan and van Staal 1993). The Flat Landing Brook Formation is interpreted to stratigraphically overlie the Nepisiguit Falls Formation and comprises interbedded felsic porphyritic volcanic and volcanoclastic rocks, within-plate tholeiitic basalts and minor shales (Sullivan and van Staal 1996). A rhyolite from this unit yielded a date of  $466 \pm 5$  Ma (Sullivan and van Staal 1993), which is slightly younger than, but overlapping with the age of underlying volcanic rocks. Thus all of these sequences are roughly synchronous and overlap in age with the arc/arc-rift-related rocks of the younger WBG sequence. Furthermore, mafic rocks in both successions have within plate tholeiitic to alkalic geochemical signatures, and are thus interpreted to be correlative and to have formed in an arc rifting environment as suggested by van Staal et al. (1991).

The Boucher Brook Formation of the Tetagouche Group comprises dark siltstone and shale interbedded with chert and alkali basalts, and stratigraphically overlies the volcanic sequences of the Flat Landing Lake, Spruce Lake and Canoe Landing Lake Formations (Sullivan and van Staal 1996). The Boucher Brook Formation conformably overlies different but correlative older volcanic packages within different thrust slices. It is interpreted as a regional capping sequence to the older volcanic dominated successions of the lower Tetagouche Group (Sullivan and van Staal 1996). A composite dyke ranging

from comendite to alkali basalt, which is interpreted as a feeder to geochemically similar volcanic rocks in the upper Boucher Brook Formation was dated at  $459 \pm 3$  Ma (Sullivan and van Staal 1996). This is compatible with the age of a trachyandesite flow in the upper part of the sequence which was dated at  $457 \pm 3$  Ma. These U-Pb ages are compatible with Caradocian ages previously determined by fossil occurrences in interbedded shale (van Staal et al. 1991). The composition of these rocks is somewhat more alkaline than older alkali basalts of the Canoe Landing Lake Formation which are transitional to enriched tholeiitic rocks with which they are interbedded. There are no volcanic rocks of this age in the Wild Bight Group, although geochemically similar intermediate to felsic dykes do occur in the WBG (Appendix 3) and have been observed within Caradocian shale of the Shoal Arm Formation (Appendix 1). The dykes generally lack a penetrative fabric, but the shale has a very strong slaty cleavage. It is difficult to assess whether these dykes pre-date or post date deformation, as the competency difference could account for variable degrees of deformation; however some clearly postdate the folding of the WBG and overlying middle to upper Ordovician sedimentary rocks and must be Silurian or younger.

The Fournier Group is best exposed in the Belledune-Elmtree inlier where it comprises ophiolitic rocks of the Devereaux Formation, which structurally overlie volcanic rocks, lithic wackes and shales of the Pointe Verde Formation (van Staal 1994). Van Staal (1994) interpreted these rocks to be correlative with volcanic and sedimentary rocks of the Sormany, and Mill Stream formations in the northern Miramichi Highlands. The mafic volcanic rocks of the Sormany Formation have geochemical characteristics

ranging from N-MORB to E-MORB/within-plate tholeiite to alkalic basalt (van Staal et al. 1991). A date of  $464 \pm 1$  Ma for a gabbro unit in the Devereaux Formation, and  $460 \pm 1$  Ma age for a plagiogranite dyke that cuts it (van Staal et al. 1988), show that these ophiolitic rocks are slightly younger than the predominantly felsic volcanic rocks of the Tetagouche Group. Van Staal et al. (1991) interpreted the Fournier Group as the ensimatic part of a back arc basin. There are no correlative rocks in the WBG, where arc rifting apparently did not progress to the point of ensimatic volcanism, although rocks of the Noggin Cove Formation in Gander Bay have similar geochemical characteristics, and could have formed in an analogous setting.

#### **5.4 Along Strike Variations on the Gondwanan Margin**

In contrast to the calc-alkaline WBG succession, the late Arenig to Llanvirn calc-alkaline volcanic sequences of the southern Exploits Subzone have a significant component of felsic volcanic/pyroclastic rocks (Fig. 5.2). In addition, at least one of these sequences extends to a slightly younger age (Victoria Mine Sequence  $462 \pm 2$  Ma). One possible explanation for this is that these groups represent the active part of the arc after rifting, and that the active arc continued to evolve to younger ages and more felsic compositions (Fig. 5.3 b). This concurs with the model proposed by van Staal (1994), for the arc-related andesites and picrites of the Balmoral Group in the Popelogan Inlier of northern New Brunswick. Van Staal (1994) proposed that back arc spreading combined with slab roll back translated the active arc toward the Laurentian margin where it was obducted, prior to closing of the back arc basin and final collision of the Laurentian and Gondwanan margins. The ophiolitic Devereaux Formation ( $\sim 460$  Ma, van Staal et al. 1988) of the

Fournier Group in northern New Brunswick is the youngest ophiolite presently recognized in the Appalachians. It is interpreted as evidence of the back arc spreading which is purported to have translated the active arc toward the Laurentian margin. Within plate basalts and felsic volcanics of the structurally underlying Tetagouche Group represent the rifting stage of the intra-arc basin (van Staal 1994).

An alternative explanation is that there was a more extensive continental substrate to the felsic-dominated arcs, perhaps as a result of a more significant Penobscot collision (Fig. 5.3a). It is probable that the late Arenig to Llanvirn peri-Gondwanan arc (or arcs) interacted to varying degrees with the continent, such that in the south (e.g., Victoria Mine sequence, Bay du Nord Group) the arc was truly continental; whereas farther north (present coordinates) it was on thinned crust of the composite continental margin (WB/Exploits groups) and perhaps in places still partially intra-oceanic (e.g., Fig. 5.3c). Such a situation could occur if there was a promontory on the Gondwanan margin south of the Hermitage Flexure (e.g., Williams 1979, and Lin et al. 1994), producing a more significant collision and obduction of the primitive ensimatic Penobscot arc in this area (Fig. 5.3a), and "softer" less complete collision progressively farther north. Thus, the subsequent east-dipping (present coordinates) subduction zone would have formed on a composite margin varying from dominantly continental to dominantly oceanic.

Evidence of obduction of the primitive arc in the central Exploits Subzone is provided by remnants of a probably once continuous thrust slice of ophiolitic rocks which sit structurally above continental margin siliciclastic sedimentary rocks of the Gander Zone (Colman-Sadd and Swinden 1984). These ophiolites, which include the Pipestone

Pond, Coy Pond and Great Bend complexes, are interpreted to be correlative with the older ensimatic part of the WBG (Fig. 5.2). There are several large tectonic windows of Gander Zone rocks within the southern Exploits Subzone (Fig. 5.1), suggesting that much of Exploits Subzone in this area is allocthonous and sits above a continentally-derived substrate. The Patridgeberry Hills pluton which cuts both the Gander Zone and Exploits Subzone in this area (Colman-Sadd et al. 1992) indicates that this relationship existed at the time the younger arc was active. There is no evidence for such a relationship in the northern Exploits Subzone, although the hiatus in volcanism during this period suggests that this area was affected by related tectonic events.

Differences in the extent of the continental component of the composite substrate of the late-Arenig to Llanvirn Gondwanan arc may also have exerted some control on subsequent rifting, such that less significant rifting occurred where there was thick continental crust and increased toward the north where the continental crust was thinned (Fig. 5.3d). In places where the arc was still largely intra-oceanic, rifting may have progressed to a marginal basin spreading centre (Fig. 5.3d). Evidence of this in the most northeastern part of the Exploits Subzone is provided by the Noggin Cove Formation which comprises volcanic rocks with IAT, N-MORB and within-plate tholeiite compositions (Johnston et al. 1994).

The Lake Ambrose Belt of the Victoria Lake Group does not fit this model as it is significantly older (513  $\pm$  2 Ma). This belt indicates that there was subduction related volcanism within Iapetus prior to the dominant phase which produced most of the other volcanic belts and ophiolites. The volcanic sequences and ophiolites herein interpreted to

represent a primitive ensimatic arc, were previously interpreted to represent rifting of a volcanic arc. The Lake Ambrose Belt is the only evidence for an older arc in the Exploits Subzone, which could have been rifted. Thus, arc rifting is still a possible explanation for the older refractory volcanic rocks and ophiolites; however, if this were the case, one might expect to see more evidence for this older arc throughout the Exploits Subzone. Perhaps as additional geochronology is done, evidence of a more extensive older arc will emerge to support the arc rifting model.

### **5.5 Compression versus extension in the Exploits Subzone**

It is clear that there are significant differences in the relationships between early and middle Ordovician arc-related sequences in different parts of the Exploits Subzone. Based on the model proposed herein, these variations are interpreted to be related to extensional versus compressional tectonic settings and the extent of continental substrate.

The Tremadoc to early Arenig ensimatic arc seems to comprise relatively consistent components, including normal and depleted IATs, boninites and depleted tonalite/trondhjemite/high-Si, low-K rhyolite, throughout the Exploits Subzone. However its structural and stratigraphic relationships to underlying rocks of the Gander Zone and overlying rocks of the late Arenig to Llanvirn calc-alkaline arcs and correlative volcanoclastic-epiclastic sequences are quite variable.

#### ***5.5.1 Mid-Arenig (Penobscot) Compression***

In central and southern Newfoundland, where there is clearly a structural contact at the base of the suprasubduction zone ophiolites related to the primitive ensimatic arc (e.g., where the Pipestone Pond Complex and related ophiolite sequences rim the Mount

Cormack Subzone, Colman-Sadd et al. 1992), there is strong evidence for obduction and early (pre 474 Ma) thrust emplacement of these rocks onto the Gondwanan margin. A similar relationship has been interpreted to occur between the Gander River Complex and the Gander Group along the eastern margin of the Exploits Subzone (Williams 1995 and references therein). Pre-478 Ma deformation of the Bay du Nord Group in southern Newfoundland suggests early tectonism there also. In both the Mount Cormack area and the Weirs Pond area of the Gander River Complex, there is interpreted to be an erosional surface between the tectonically juxtaposed older sequences and the overlying onlap sequences represented by the Indian Bay Big Pond Formation (Colman-Sadd et al. 1992) and the lower Davidsville Group (Stouge 1979, and O'Neill 1987), respectively. The presence of a significant carbonate component in the basal parts of both of these predominantly siliciclastic packages is compatible with a continental margin setting for the onlap sequence. Thus the southwestern, central and northeastern parts of the Exploits Subzone are interpreted to have undergone a significant compressional event in the late early Ordovician (Penobscot Orogeny of Colman-Sadd et al 1992); however, they show evidence of only minor late Arenig to Llanvirn extension which is ubiquitous in the northwestern Exploits Subzone. Thus this area is interpreted to define an Ordovician tectonic domain characterised by early-mid Arenig compression, and limited subsequent Ordovician extension (Fig 5.4).

#### *5.5.2 Late Arenig-Llanvirn Extension*

In the northern Exploits Subzone, evidence from the Exploits Group (O'Brien et al. 1997) and the Wild Bight Group suggests that there was continuous deposition of marine rocks

on top of the primitive arc/ophiolite sequence. Furthermore, the occurrence of late Arenig to Llanvirn debris flows and melanges, ubiquitous volcanic rocks with rift-like compositions, and abrupt variations in the thickness of some stratigraphic units suggests an environment dominated by extension and significant intra-basinal relief. The relationship of the primitive arc to the continental margin sequence has not been observed in either the WBG or the Exploits Group, but if/where it occurs is assumed to be structural (e.g., Fig 4.4). The composite substrate of the late Arenig to Llanvirn sequence of the WB-Exploits arc should occur at least discontinuously beneath all the melange tracts and submarine volcanic sequences of northeastern Notre Dame Bay. Such an interpretation is supported by the presence of volcanic blocks in the Carmanville and Teakettle melanges which have the composition of low-Ti tholeiitic basalt (Lee 1986), and other blocks, both igneous and sedimentary, which show significant deformation and metamorphism prior to incorporation into the melanges. The clasts with low-Ti tholeiitic basalt composition are interpreted to come from uplifted blocks of the older primitive arc sequence; and the deformed rocks could represent rocks of the older volcanic/plutonic sequence and Gander Zone which were on the compressional side of the forearc sliver, closer to the Penobscot subduction complex. The northern Exploits Subzone is interpreted to define an Ordovician tectonic domain which might have undergone a minor late early-Ordovician compression in the easternmost part, but which was dominated by an extensional setting throughout most of the Ordovician (Fig. 5.4)

### 5.5.3 *Summary*

In the northern Exploits Subzone, the Penobscot ophiolite obduction event is documented by a hiatus in volcanism between approximately 485 and 475 Ma. During this time the primitive ensimatic arc began to interact with the continental margin. In the south where there was a promontory, collision resulted in a significant compressional event. In the north, thinned crust of the continental margin is interpreted to have been partially subducted, resulting in the termination of subduction, but no significant compressional event. The leading edge of the accretionary wedge might have undergone compression, whereas the rest of the arc remained under extension, and in a deep submarine setting. Continued convergence related to closing of the Iapetus resulted in the development of another subduction zone outboard of the continental margin, and with the opposite polarity. Thus subsequent subduction was to the east (present coordinates), beneath the composite Gondwanan margin (Fig. 5.3)

The late Arenig to Llanvirn calc-alkaline, continental margin arc of the Exploits Subzone shows significant compositional and lithological variation. In the southwest there are more felsic relative to mafic volcanic rocks, compared to the northern area where mafic rocks predominate. Furthermore, in the south most of the volcanic rocks have calc-alkaline signatures, as opposed to the north where volcanic rocks with tholeiitic within plate to alkalic compositions dominate. The increase in the felsic component of calc-alkaline volcanism in the south has been interpreted to be the result of a more significant continental substrate. This is compatible with evidence for an early

compressional event which exists over a large area in the southwest, and a much narrower belt in the northeast (Figure 5.4).

The increase in the amount of enriched, within-plate tholeiitic to alkaline volcanism in the late Arenig to Llanvirn sequence toward the north, is accompanied by a concomitant increase in olistostromal melanges. These features are interpreted to represent a major extensional event which resulted in rifting of the calc-alkaline arc and continental margin and production of a marginal basin. This marginal basin had significant topography resulting from horsts and grabens and locally producing coticule rich, restricted or starved basins. The main intrabasinal high was the remnant, inactive part of the arc, represented by the eastern Wild Bight Group. The extent of the rift basin is very minor in the southwest in the Victoria Lake Group, where volcanic rocks with rift-related compositions occur as small fault-bounded packages adjacent to older sequences, and as small lenses in the volcanoclastic/argillite sequence just below the Caradocian shale. However, in the north, this basin extended from the east side of Gander Bay in the east, to Sops Arm in the west. Thus in the north the remnant arc and the active arc were separated by tens to hundreds of kilometers by a deep rift basin, whereas in the south they were virtually coincident and sitting on the continental margin, possibly partially in a subaerial setting (as per Fig. 5.3 and 5.4).

### **5.6 Significance of Post-Ordovician Structural Breaks to Ordovician Tectonics**

Major structural breaks within the Dunnage Zone are mostly Silurian and younger, but roughly coincide with certain differences in the Ordovician sequences. Thus they are interpreted to be partially controlled by earlier Ordovician structures, or at least to have

some significance for Ordovician tectonics. The most significant of these breaks is the Red Indian Line, which subdivides the Dunnage Zone into the Notre Dame and Exploits subzones (Fig. 5.4). Early Ordovician rocks of the Notre Dame Subzone are interpreted to be peri-Laurentian in origin based on faunal provinciality, as opposed to similar aged rocks in the Exploits Subzone which have Gondwanan faunal affinities. However in the middle Ordovician, the faunal distinctions break down, as the extent of the Iapetus Ocean is interpreted to have been much more limited. Noel Paul's line in the central Exploits Subzone is at least locally a mylonite zone (probably Silurian in age, B.H. O'Brien, pers comm, 1997), but which is defined as the Gander/Dunnage boundary along the western side of the Meelpaeg Subzone (Colman-Sadd 1988) (Fig. 5.4). The Dog Bay Line in the northeastern Exploits Subzone is a Silurian fault zone (Fig. 5.4), which separates very different Silurian sequences, but which has similar Ordovician rocks on either side (Williams et al. 1993). All of these lines coalesce in southwestern Newfoundland where all the zones and subzones become obscured by significant Siluro-Devonian deformation, metamorphism and plutonism.

#### *5.6.1 The Red Indian Line (RIL)*

In Notre Dame Bay, where the RIL is exposed, it coincides with the Sops Head and Boones Point melanges which have a late Arenig to Llanvirn olistostromal component (e.g., Clarke 1992 and Dec et al. 1997), but are overprinted by and incorporated into Silurian tectonic melange belts; unbroken formations of uncertain affinity; or tectonically interleaved packages of Notre Dame and Exploits subzone rocks. The RIL locally separates the Roberts Arm Group from the Wild Bight Group. Late Arenig to Llanvirn-

Llandeilo volcanic rocks (with inferred or documented enriched tholeiitic compositions) occur both in place in volcano-sedimentary units of the WBG (O'Brien and MacDonald 1997) and Roberts Arm Group (and or correlative sequences) (Dec et al. 1997, Clarke 1992). Geochemically similar volcanic rocks also occur as blocks in olistostromal melanges (Clarke 1992), on either side of the RIL. This suggests that the RIL in the Ordovician coincided with a tectonically active late Arenig to Llanvirn-Llandeilo marine basin. This basin is interpreted to be analogous to, and possibly contiguous with the main rift basin of the northern Exploits Subzone (proposed herein).

Evidence from clasts within the Sops Head melange (Clarke 1992) suggests that this area may have been adjacent to an intrabasinal high on the western margin of the rift basin. The presence of limestones interbedded with the rift-related, enriched tholeiites also suggests an intrabasinal high, or basin margin similar to that represented by the Summerford Group in the eastern Exploits Subzone. The relationship of the Roberts Arm Group and correlative sequences to this basin is uncertain. It may be a different, but age-equivalent arc that was separated from the Exploits active arc (assumed to have originally existed on the western side of the rift basin), by another marine basin. Alternatively, perhaps the RAG could be the active part of the Exploits arc, as proposed by van der Pluijm et al (1995). Thus, although there are significant differences between the Notre Dame and Exploits subzones in the early Ordovician, perhaps these differences do not extend into Llanvirn-Llandeilo.

### *5.6.2 The Dog Bay Line*

The Dog Bay Line is another post Ordovician structure which is used to define belts of Silurian rocks. It is a Silurian fault zone which separates distinct Silurian volcano sedimentary sequences (Williams et al. 1993). West of the line, Silurian terrestrial sandstone and volcanic rocks (Botwood Group) conformably overlie a thick sequence of upper Ordovician marine greywackes and conglomerates (Badger Group) (Williams et al. 1993). East of the line, red sandstones overlie a sequence of lower Silurian marine shales and limestones of the Indian Islands Group (Williams et al. 1993). The Dog Bay line coincides with the transition from the area affected by significant Penobscot compression to the east an area to the west with the opposite characteristics (Fig. 5.4). However, early to middle Ordovician sequences with olistostromal melanges, overlain by Caradoc shale and marine shales and greywackes correlative with the Badger group, occur on both sides of the structure, and thus it lies within the zone dominated by the younger extensional setting. Thus, the Dog Bay line approximately corresponds to the margin of the Ordovician rift basin. The Ordovician transition from continental margin to marginal rift basin, probably also exerted significant control on Silurian deposition, but extension did not progress to the point of producing a Silurian ophiolite (Williams et al. 1993).

The Ashgill and younger marine shales and greywackes of the Badger Group which predominantly occur west of the Dog Bay line, conformably overlie the early to middle Ordovician rocks of the extensional basin and could represent infilling of the basin once “significant extension” ended. Terrestrial sandstones and volcanic rocks of the Botwood Group are regionally conformable on the Badger Group, suggesting that the

basin was completely infilled without significant tectonic disruption. On the continental margin (i.e., east of the extensional domain (Fig. 5.4) and approximately east of the Dog Bay Line), during this time, initially Silurian shallow marine carbonates and carbonaceous siliciclastic rocks were deposited, followed conformably by terrestrial sedimentary rocks of the Indian Islands Group. Williams (1995) suggested that these terrestrial rocks may be correlative with the youngest rocks of the Botwood Group, and may represent a coextensive overlap sequence which transgressed the Dog Bay line (i.e., continental margin in this model). This interpretation is compatible with the ideas presented herein; however, there is no evidence for the existence of the Dog Bay structure in the Ordovician. Rather it is the presence of the continental margin in this vicinity which is of importance to the Ordovician tectonics, and probably also affected subsequent Silurian sedimentation.

### *5.6.3 Noel Pauls Line*

Noel Pauls Line, as defined by Colman-Sadd (1987) coincides with the western edge of the Meelpaeg Subzone of the Gander Zone, and merges with the location of the Red Indian Line south of Victoria Lake. As such, it also roughly coincides with the division between the extensional and compressional Ordovician zones defined herein, and is thus analogous with the Dog Bay line in terms of its relationship to Ordovician tectonics. This is compatible with the interpretation of Williams et al. (1993) who suggested that the Dog Bay Line might be continuous with Noel Pauls Line beneath younger cover sequences.

## 5.7 Conclusions

Differences in the lithological characteristics of other volcanic sequences in the Exploits Subzone, which are correlative with the late Arenig to Llanvirn WB/Exploits arc system, and pre-late Arenig belts, suggest that there were significant differences in the degree to which the arcs interacted with the Gondwanan margin. There was probably more significant interaction with continental crust in the southern and central Exploits Subzone, and less toward the NE. The degree of subsequent extension and rifting of the arc also varied along the Gondwanan margin, with more extensive rifting in the northwest where the continental substrate is interpreted to have been thinner.

The post Ordovician Dog Bay Line-Noel Pauls Line approximately coincides with the eastern margin of the late Arenig to Llanvirn extensional basin, which was probably the Gondwanan continental margin. The extensional zone is delineated by the extent of Ordovician olistostromal melanges and rift-related volcanic rocks. The division between the Ordovician extensional rift basin and the continental margin was important in controlling the different Ordovician and Silurian sequences east and west of the approximate location of the Dog Bay Line. In Notre Dame Bay, The Red Indian Line corresponds with the Sops Head and other melanges interpreted to represent a deep marine basin on the western side of the rift basin, and may have been adjacent to the active arc, although it is not clear where the active arc is now. It is possible that late Arenig to Llanvirn calc-alkaline volcanic sequences on either side of the Red Indian Line represent active and remnant parts of the same arc, that were separated by an intra arc rift basin. This idea is contentious, as a previous study shows that the Pb isotope signatures in

massive sulphide deposits in the two belts are different (Swinden 1988). However, the deposits on either side are now known to be related to volcanic sequences of different ages and possibly also different tectonic settings, which could explain the different isotopic characteristics of associated massive sulphide deposits. More work needs to be done to examine these possibilities, but the model proposed herein suggests that the significance attributed to the Red Indian Line may be obscuring important late Arenig to Llanvirn relationships between rocks on either side.

## Chapter 6

### Summary and Directions for Future Work

#### 6.1 Summary

Detailed mapping (~ 1:15,000) in the South Lake Igneous Complex and adjacent rocks of the eastern Wild Bight Group, combined with major and trace element geochemical, and Sm-Nd isotopic analyses of magmatic rocks, and U-Pb geochronology have proved a powerful tools for: determining volcanic stratigraphy; linking volcanic and plutonic events; and providing absolute time constraints on the tectonomagmatic history of these rocks. An understanding of the absolute age of oceanic sequences is critical to understanding the evolution of the Iapetus Ocean as it closed, prior to the final collision of Gondwana and Laurentia.

This work has shown that the Wild Bight Group is composite in nature, and that there are two temporally and genetically distinct periods of arc volcanism separated by up to 10 Ma. The older sequence is genetically related to plutonic rocks of the South Lake Igneous Complex, and these older rocks have been structurally interleaved with the younger volcanic/volcaniclastic sequence during subsequent deformation. The younger sequence has also been structurally imbricated and does not represent a simple conformable sequence in its present configuration.

The older magmatic rocks formed predominantly between 489  $\pm$  3 and 486  $\pm$  4 Ma (Tremadoc to early Arenig). These rocks compositionally range from normal island arc tholeiitic basalt (IATs), to incompatible element-depleted low-Ti, high-Mg IATs and boninites, and high-Si, low-K rhyolite/tonalite. They are interpreted to represent the

initiation and stabilization of a primitive ensimatic oceanic arc. The incompatible element- depleted, low-Ti, high-Mg IATs and boninites were produced in a broad, strongly extensional suprasubduction zone setting during the earliest stages of arc formation. Subsequent mafic magmatism was less depleted, and represents a decrease in the degree of extension, as the arc evolved. The felsic rocks were formed by melting of depleted mafic rocks at the base of the newly formed arc crust, once it attained a sufficient thickness. Following stabilization of the magmatic front and migration of the locus of extension to a back arc position, normal IATs were produced. Samarium-Nd isotope systematics in the depleted IATs and boninites show an apparent decoupling of isotopic and geochemical characteristics, which require a complex source or melt generation process for these rocks. Isotopic systematics also suggest that there must have been a component with long-term incompatible element enrichment (continental crust ?). Furthermore, the LREE-enriched signature which is diagnostic of boninites was produced during their generation and was not a long-lived characteristic of the mantle source from which they were generated. The geochemical, isotopic and field relationships in the older volcanic sequence and SLIC provide important insight into tectonomagmatic process in volcanic arcs in general.

The younger sequence of the Wild Bight Group comprises two volcanic successions which are stratigraphically separated but which, based on U-Pb data, are roughly synchronous. The lower volcanic succession has a calc-alkalic geochemical affinity and its age is confined to  $472 \pm 3$  Ma (late Arenig), by felsic tuffs within the succession. The upper volcanic succession has enriched tholeiitic to alkalic within-plate

geochemical signatures, and related gabbro sills were dated at 471  $\pm$  4 and 470  $\pm$  5 Ma. Geochemical and isotopic characteristics suggest that these two volcanic sequences were produced from a similar mantle source which had both a depleted and fertile component, but the calc-alkaline rocks have an added component related to subduction. The Sm-Nd isotope systematics indicate that the calc-alkaline rocks also have significant contamination by an old crustal component, which suggests the proximity of continental crust. The fact that inherited zircon was found in a non-arc gabbro suggests that there was an older continental component in the substrate to this sequence. Thus the younger succession of the Wild Bight Group is interpreted to represent a volcanic arc that formed on the composite Gondwanan margin, and was subsequently rifted.

A study of detrital components in sedimentary units of the younger package of the Wild Bight Group indicates that older and younger sequences do have a common history prior to final structural juxtaposition. Blocks in melanges and debris flows within the younger sequence have geochemical characteristics which indicate that they were derived from the older sequence. This suggests that the older arc formed part of the substrate on which the younger one developed. Intrabasinal uplifts must have exposed the older substrate which then provided detritus to the younger basin. The occurrence of Precambrian detrital zircon in a volcanoclastic unit of the younger sequence suggests that there was an even older component to the substrate of the younger arc. This component could either have been continental crust or sediments derived therefrom. Structural and stratigraphic relationships within the WBG support the presence of intrabasinal uplifts of the older substrate: firstly much of the structural imbrication within the WBG is localized

around the fault-bounded older sequences, suggesting the existence of previous structures; and secondly, there are marked variations in the thickness of the younger stratigraphic units adjacent to the older packages. In most places the contact between the older and younger sequences is structurally modified but locally, at the stratigraphic base of the younger sequence, there may be an original stratigraphic contact preserved, although the nature of the contact is equivocal.

The tectonomagmatic evolution of the WBG and SLIC has four main stages: firstly, formation of a primitive ensimatic arc outboard of the Gondwanan margin by westward (present coordinates) subduction; secondly arc/continental margin "collision", which involved attempted subduction of the thinned continental margin, and resulted in the termination of westward subduction; thirdly, stepping out, and polarity reversal of subduction, such that the subsequent arc developed on the composite Gondwanan margin; and finally, arc rifting which produced a large extensional marginal basin.

## **6.2 Regional Implications**

The Wild Bight Group has traditionally been correlated with the adjacent Exploits Group to the east. This correlation still holds and relationships in each group provide additional constraints on the evolution of the other. In fact, they are interpreted to represent different parts of the same late Arenig to Llanvirn, continental margin arc/back-arc/arc-rift system. They were probably also contiguous during generation of the older ensimatic arc. The eastern WBG is interpreted to represent the remnant arc following arc rifting, and the western WBG is interpreted to represent the main rift basin. The Exploits Group probably formed in the pre-rift back arc basin in proximity to the continental margin.

There are numerous other fragments of ophiolite and arc-related volcanic/volcaniclastic/epiclastic sequences in the Exploits Subzone of Newfoundland and in northern New Brunswick, although the ages and petrogenetic relationships in many of them are not well known. However, by correlating them with well-constrained sequences in the Wild Bight and Exploits groups, some inferences can be made. Such correlations show that although there are general similarities in the ages and geochemical affinities of certain sequences, there are also significant differences. These differences suggest that the degree to which both the Tremadoc to early Arenig ensimatic arc, and the younger late Arenig to Llanvirn arc interacted with the Gondwanan margin, varied considerably along strike. This variation is interpreted to be related to the presence of a promontory on the Gondwanan margin, as suggested by previous workers. The degree of arc rifting is interpreted to be related to the extent of continental substrate in the late Arenig arc.

One problem with the arc rifting model is that the active part of the arc seems to be missing in the Exploits Subzone. However, the Buchans-Roberts arm belt in the Notre Dame Subzone is a possible candidate. Based on the model proposed herein for the evolution of the northern Exploits Subzone, it is speculated that Ordovician significance attributed to the Red Indian Line may be obscuring some important relationships between rocks on either side.

### **6.3 Significance of This Work**

This work has significant implications for mineral exploration in the WBG, as it is now clear that all the major massive sulphide showings and deposits are part of the oldest

sequence of the Wild Bight Group. Furthermore, the older package is most commonly structurally isolated from the younger sequence. By combining new interpretations of structural and stratigraphic relationships in the eastern Wild Bight Group, with regional geochemical data and compilation maps, a new interpretation of the regional geology of the entire WBG has been developed. Four composite, interpretive cross-sections through the WBG and SLIC, attempt to show the nature of these relationships in the third dimension. Together these regional interpretations should help to focus exploration, and provide models for interpreting structural and stratigraphic relationships on a more detailed scale.

#### **6.4 Directions for Future Study**

##### ***6.4.1 Wild Bight Group***

There is still considerable uncertainty about the nature of the original stratigraphic relationship between the older and younger sequences. In most places the contact is structurally modified, but locally at the base of the younger sequence, an original stratigraphic contact may be preserved. The nature of this relationship is important, as all the known massive sulphide deposits in the WBG are associated with the older volcanic sequence. Based on the present U-Pb ages most of the older sequence is pre 486  $\pm$  4 Ma, however if the normal island arc tholeiites of the Nanny Bag Lake unit are related to the late dykes which cross-cut the SLIC, then some of the magmatism related to the older arc is younger than 486 Ma, and the hiatus in volcanism could be somewhat less than 10 Ma. Furthermore the base of the younger sequence could be somewhat older than 472  $\pm$  3 Ma, as the position of the stratigraphically lowest tuff is not at the very base of the

succession. Thus, although there is certainly a hiatus in volcanism, it may be somewhat less than 10 Ma, and sedimentation could have been more or less continuous in deeper parts of the basin. It is necessary to understand the original stratigraphic relationship in order to understand how subsequent deformation has affected it.

The age constraints on, and understanding of genetic and stratigraphic relationships of volcanic rocks in the WBG provided by this study, are based on only the eastern WBG and have been extrapolated to include the rest. The stratigraphic sequence in the western WBG is quite different, and there is no data available on the composition of volcanic rocks west of Badger Bay. Detailed studies in this area could provide new insight into, and constraints on, the rifting episode. In general, more U-Pb ages in other areas are needed to determine whether the model proposed for the eastern WBG, can be generally accepted for the entire sequence.

#### *6.4.1 Dunnage Zone*

Speculations that have been generated by this study suggest that one place to look for the active arc on the other side of the rift basin is in the Roberts Arm Group and correlative sequences. However, even if the RAG represents a different, but age-equivalent arc, there may be important clues in the late Arenig to Llanvin basins on either side of the RIL which will shed light on the relationships of the younger calc-alkaline sequences on either side, and the time at which they began to interact. Detailed studies which examine the age, paleontological and lithological/geochemical affinities of blocks in melanges, and their relationships to intact, adjacent stratigraphic sequences can provide important clues

to the origin of the melanges and their tectonic setting, and to the timing of interaction between opposing basin margins.

### References

- Alt, J.C. and Emmerman, R. 1985. Geochemistry of hydrothermally altered basalts: Deep Sea Drilling Project Hole 504B, Leg 83. Initial Report DSDP 83, pp. 249-262.
- Arnott, R.J. 1983. Sedimentology of Upper Ordovician-Silurian sequences on New World Island, Newfoundland: separate fault-controlled basins? *Canadian Journal of Earth Sciences*, **20**: 345-354.
- Barker, F., Arth, F.G., Peterman, Z.E. and Freidman, I. 1976. The 1.7 to 1.8 b.y. old trondhjemites of southwestern Colorado and northern New Mexico: geochemistry and depths of genesis. *Geological Society of America Bulletin*, **87**: 189-198.
- Bedard, J.L., Lauziere, K., Sangster, A., Boisvert, E., Tellier, M., Tremblay, A. and Dec, T. 1998. Evidence for forearc seafloor spreading from the Betts Cove ophiolite; oceanic crust of boninitic affinity. *Tectonophysics*, **284**: 233-245.
- Bergstrom, S.M., Riva, J. and Kay, M. 1974. Significance of conodonts from the Ordovician of western and north-central Newfoundland. *Canadian Journal of Earth Sciences*, **11**: 1625-1660.
- Bienvenu, P., Bougault, H., Joron, J.L., Treuil, M. and Demitriev, L. 1990. Rare-earth element/non rare-earth element hygromagmaphile element fractionation. *Chemical Geology*, **82**: 1-14.
- Bird, J.M. and Dewey, J.F. 1970. Lithosphere plate-continental margin tectonics and the evolution of the Appalachian orogen. *Geological Society of America Bulletin*, **81**: 1031-1060.

- Blackwood, R.F. 1983. Notes on the geology of the Great Gull Lake area (2D/6) Newfoundland (to accompany Map 82-71). Newfoundland Department of Mines and Energy, Mineral Development Division, 10 p.
- Blewett, R.S. 1991. Slump folds and early structures, northeastern Newfoundland Appalachians: re-examined. *Journal of Geology*, **99**: 547-557.
- Blewett, R.S., and Pickering, K.T. 1988. Sinistral shear during the Acadian deformation in north-central Newfoundland, based on transecting cleavage. *Journal of Structural Geology*, **10**: 125-127.
- Boyce, W.D. Ash, J.S., O'Niell, P. and Knight, I. 1988. Ordovician biostratigraphic zones in the Central Mobile Belt and their implications for Newfoundland tectonics. Newfoundland Department of Mines and Energy, Mineral Development Division, Report 88-1, pp. 177-182.
- Brenan, J.M., Shaw, H.F., Phinney, D.L. and Ryerson, F.J. 1994. Rutile-aqueous fluid partitioning of Nb, Ta, Hf, Zr, U and Th: implications for high field strength element depletions in island-arc basalts. *Earth and Planetary Science Letters*, **128**: 327-339.
- Brenan, J.M., Shaw, H.F., Ryerson, F.J. and Phinney, D. 1995. Mineral-aqueous fluid partitioning of trace elements at 900 C and 2.0 GPa: Constraints on the trace element chemistry of mantle and deep crustal fluids. *Geochimica et Cosmochimica Acta*, **59**: 3331-3350.

- Brown, A.V. and Jenner, G.A. 1989. Geologic setting, petrology and chemistry of Cambrian boninite and low-Ti lavas in western Tasmania. *In* Boninites and Related Rocks. *Edited By* A.J. Crawford. Unwin Hyman, London, pp. 233-263.
- Butler, D.J. and Stewart, R.D. 1993. The Indian Cove prospect, Notre Dame Bay, Newfoundland. *In* Ore Horizons Volume 2. *Edited By* A.S. Hogan and H.S. Swinden Department of Mines and Energy, Geological Survey, pp. 61-75.
- Canil, D. 1987. The geochemistry of komatiites and basalts from Deadman Hill area, Munro Township, Ontario Canada. *Canadian Journal of Earth Sciences*, 24: 998-1008.
- Clarke, E.J. 1992. Tectonostratigraphic development and economic geology of the Sops Head Complex, western Notre Dame Bay, Newfoundland. B.Sc. (Honours), Memorial University of Newfoundland. 102 p.
- Coish, R.A. Hickey, R. and Frey, F. 1982. Rare earth element geochemistry of the Betts Cove ophiolite, Newfoundland: complexities in ophiolite genesis. *Geochimica et Cosmochimica Acta*, 46: 2117-2134.
- Colman-Sadd, S.P. 1980. Geology of south-central Newfoundland and evolution of the eastern margin of Iapetus. *American Journal of Science*, 292: 317-355.
- Colman-Sadd, S.P. and Swinden, H.S. 1984. A tectonic window in central Newfoundland? Geological evidence that the Appalachian Dunnage Zone is allochthonous. *Canadian Journal of Earth Sciences*, 21: 1349-1367.

- Colman-Sadd, S.P., Dunning, G.R. and Dec, T. 1992. Dunnage-Gander relationships and Ordovician orogeny in central Newfoundland: A sediment provenance and U/Pb age study. *American Journal of Science*, **292**: 317-355.
- Crawford, A.J. Falloon, T.J. and Green, D.H. 1989. Classification, petrogenesis and tectonic setting of boninites. *In* *Boninites and Related Rocks. Edited By A.J. Crawford.* Unwin Hyman, London, 1-49.
- Currie, K.L. 1992. Carmanville map area (2E/8): A new look at Gander-Dunnage relations in Newfoundland. *In* *Current Research part D. Geological Survey of Canada, Paper 93-1A*, pp. 27-33.
- Currie, K.L. 1993. Ordovician-Silurian stratigraphy between Gander Bay and Birchy Bay, Newfoundland. *In* *Current Research part D. Geological Survey of Canada, Paper 93-1A*, pp. 11-18.
- Davis, D.W. 1982. Optimum linear regression and error estimation applied to U-Pb data. *Canadian Journal of Earth Sciences*, **19**: 2141-2149.
- Dean, P.L. 1977. A report on the geology and metallogeny of the Notre Dame Bay area, to accompany metallogenic maps 12/H/1,8,9 and 2E/3,4,5,6,7,9,10,11,12. Newfoundland Department of Mines and Energy, Report 77-10.
- Dean, P.L. 1978. The volcanogenic stratigraphy and metallogeny of Notre Dame Bay, Newfoundland. Memorial University of Newfoundland, Geology Report 7.
- Dean, P.L. and Strong, D.F. 1976. Compilation Geological Maps for north-central Newfoundland. Geological Survey of Canada, Open File Maps.

- Dec, T., O'Brien, B.H., Dickson, W.L. and Evans, D.T.W. 1993. Fortune Harbour Peninsula, Notre Dame Bay: Geological Association of Canada-Newfoundland and Labrador section field trip guide book series.
- Dec, T. Swinden, H.S. and Dunning, G.R. 1997. Lithostratigraphy and geochemistry of the Cottrells Cove Group, Buchans-Roberts Arm Belt: New constraints for the paleotectonic setting of the Notre Dame Subzone, Newfoundland Appalachians. *Canadian Journal of Earth Sciences*, **34**: 86-103.
- DePaolo, D.J. 1988. Neodymium Isotope Geochemistry. New York, Springer-Verlag. 187 p.
- Dewey, J.F., Kennedy, M.J. and Kidd, W.F.S. 1983. A geotraverse through the Appalachians of northern Newfoundland. *In Profiles of Orogenic Belts. Edited by N. Delany and F.M. Rast. American Geophysics Union/Geological Society of America (Geodynamics Series 10).*
- Drummond, M.S. and Defant, D.M.J. 1990. A model for trondhjemite-tonalite-dacite genesis and crustal growth by slab melting: Archean to modern comparisons. *Journal of Geophysical Research*, **95**: 503-521.
- Dunning, G.R. and Krogh, T.E. 1985. Geochronology of ophiolites of the Newfoundland Appalachians. *Canadian Journal of Earth Sciences*, **22**: 1659-1670.
- Dunning, G.R., Krogh, T.E., Kean, B.F., O'Brien, S.J. and Swinden, H.S. 1986. U/Pb zircon ages of volcanic groups from the central mobile belt, Newfoundland. *Geological Association of Canada Program with Abstracts*, **11**: A66.

- Dunning, G.R., Kean, B.F., Thurlow, J.G. and Swinden, H.S. 1987. Geochronology of the Buchans, Roberts Arm and Victoria Lake Groups and the Mansfield Cove Complex Newfoundland. *Canadian Journal of Earth Sciences*, **24**: 1175-1184.
- Dunning, G.R., O'Brien, S.J., Colman-Sadd, S.P., Blackwood, R.F., Dickson, W.L., O'Neill, P.P. and Krogh, T.E. 1990. Silurian orogeny in the Newfoundland Appalachians. *Journal of Geology*, **98**: 895-931.
- Dunning, G.R., Swinden, H.S., Kean, B.F., Evans, D.T.W. and Jenner, G.A. 1991. A Cambrian island arc in Iapetus: geochronolgy and geochemistry of the Lake Ambrose volcanic belt, Newfoundland Appalachians. *Geological Magazine*, **128**: 1-17.
- Elliot, C.G. and Williams, P.F. 1988. Sediment slump structures: a review of diagnostic criteria and application to an example from Newfoundland. *Journal of Structural Geology*, **10**: 171-182.
- Elliot, C.G. Barnes, C.R., and Williams, P.F. 1989. Southwest New World Island stratigraphy: new fossil data, new implications for the history of the Central Mobile Belt, Newfoundland. *Canadian Journal of Earth Sciences*, **26**: 2062-2074.
- Elliot, C.G., Dunning, G.R., and Williams, P.F. 1991. New U/Pb zircon age constraints on the timing of deformation in north-central Newfoundland and implications for early Paleozoic Appalachian orogenesis. *Geological Society of America Bulletin*, **103**: 125-135.

- Espenshade, G.H. 1937. Geology and mineral deposits of the Pilley's Island area. Newfoundland Department of Natural Resources, Geology Division, Bulletin 9, 36 p.
- Evans, D.T.W., Kean, B. F. and Dunning, G. R. 1990. Geological Studies, Victoria Lake Group, Central Newfoundland. Newfoundland Department of Mines and Energy, Geological Survey Branch, Report 90-1, pp.131-144.
- Hayes, J.J. 1951. Marks Lake Newfoundland. Geological Survey of Canada, Paper 95-2, 1:50,000 map and marginal notes.
- Helwig, J.A. 1967. Stratigraphy and structural history of the New Bay area, north central Newfoundland. Ph.D., Columbia University
- Heyl, G.R. 1938. Geology and mineral deposits of the New Bay area, Notre Dame Bay, Newfoundland. Geological Survey of Newfoundland, Bulletin 3.
- Hibbard, J.P. and Williams, H. 1979. The regional setting of the Dunnage Melange in the Newfoundland Appalachians. *American Journal of Science*, 279: 993-1021.
- Horne, G.S. and Helwig, J.A. 1978. Ordovician stratigraphy of Notre Dame Bay, Newfoundland. *In* North Atlantic geology and continental drift. *Edited by* M. Kay. American Association of Petroleum Geology, pp. 308-407.
- Hughes, C.J. 1973. Spilites, keratophyres and the igneous spectrum. *Geological Magazine*, 109: 513-527.

- Hughes, R.A. and O'Brien, B.H. 1994. Syndepositional transport on a deep-marine slope and soft-sediment reworking of detritus from an exhumed Iapetan arc: Evidence from the upper New Bay Formation of the Exploits Group. Newfoundland Department of Mines and Energy, Geological Survey, Report 94-1, pp. 135- 145.
- Humphries, S.E. and Thompson, G. 1978. Hydrothermal alteration of oceanic basalts by seawater. *Geochimica et Cosmochimica Acta*, **42**: 107-125.
- Irvine, T.N. and Baragar, W.R.A. 1971. A guide to the classification of common volcanic rocks. *Canadian Journal of Earth Sciences*, **8**: 523-548.
- Jacobi, R.D. and Wasowski, J. J. 1985. Geochemistry and plate tectonic significance of the volcanic rocks of the Summerford Group, north-central Newfoundland. *Geology*, **13**: 126-130.
- Jaffey, A.H., Flynn, K.F., Glendenin, L.E., Bentley, W.C. and Essling, A.M. 1971. Precision measurements of half-lives of  $^{235}\text{U}$  and  $^{238}\text{U}$ . *Physics Review C*, **4**: 1889-1906.
- Jenner, G.A. and Swinden, H.S. 1993. The Pipestone Pond Complex, central Newfoundland: Complex magmatism in an eastern Dunnage Zone ophiolite. *Canadian Journal of Earth Sciences*, **30**: 434-448.
- Jenner, G.A., Longerich, H.P., Jackson, S.E. and Fryer, B.J. 1990. ICP-MS-A powerful tool for high-precision trace element analysis in earth sciences: evidence from analysis of selected USGS reference samples. *Chemical Geology*, **83**: 133-148.

- Jensen, L.S. 1976. A new cation plot for classifying subalkalic volcanic rocks. Ontario Division of Mines, Miscellaneous Paper 6.
- Johnston, D.H. Williams, H. and Currie, K. L. 1994. The Noggin Cove Formation: A middle Ordovician back-arc basin deposit in northeastern Newfoundland. *Atlantic Geology*, **30**: 183-194.
- Karlstrom, K.E., van der Pluijm, B.A. and Williams, P.F. 1982. Structural interpretation of the eastern Notre Dame Bay area. Newfoundland: regional post-middle Silurian thrusting and asymmetric folding. *Canadian Journal of Earth Sciences*, **19**: 2325-2341.
- Kean, B.F. and Evans, D.T.W. 1988 Regional Metallogeny of the Victoria Lake Group. Newfoundland Department of Mines and Energy, Geological Survey Branch, Report 88-1, pp. 319-330.
- Krogh, T.E. 1973. A low-contamination method for hydrothermal decomposition of zircon and extraction of U and Pb for isotopic age determinations. *Geochimica et Cosmochimica Acta*, **37**: 485-494.
- Krogh, T.E. 1982. Improved accuracy of U-Pb zircon ages by the creation of more concordant systems using an air abrasion technique. *Geochimica et Cosmochimica Acta*, **46**: 637-649.
- Kusky, T.M. 1985. Geology of the Frozen Ocean Lake-New Bay Pond area, north central Newfoundland. M.Sc., State University of New York (Albany)
- Lafrance, B. and Williams, P.F. 1992. Silurian Deformation in eastern Notre Dame Bay, Newfoundland. *Canadian Journal of Earth Sciences*, **29**: 1899-1914.

- Lee, C.B. 1996. Polykinematic evolution of the Teakettle and Carmanville Melanges in the Exploits Subzone, northeast Newfoundland. M.Sc., Memorial University of Newfoundland, 153 p.
- Lin, S., van Staal, C.R. and Dube, B. 1994, Promontory-Promontory collision in the Canadian Appalachians, *Geology*, **22**: 897-900.
- Longerich, H.P., Jenner, G.A., Fryer, B.J. and Jackson, S.E. 1990. Inductively coupled plasma mass spectrometric analysis of geological samples: case studies. *Chemical Geology*, **83**: 105-118.
- Lorenz, B.E. and Fountain, J.C. 1982. The South Lake Igneous Complex, Newfoundland: a marginal basin-island arc association. *Canadian Journal of Earth Sciences*, **19**: 490-503.
- Ludden, J., Gelinas, L. and Trudel, P. 1982. Archean metavolcanics from the Rouyn-Noranda district, Abitibi greenstone belt, Quebec. 2. Mobility of trace elements and petrogenetic constraints. *Canadian Journal of Earth Sciences*, **19**: 2276-2287.
- Merriman, R.J., Bevins, R.E. and Ball, T.K. 1986. Petrological and geological variations within the Taly Fan intrusion: a study of trace element mobility during low grade metamorphism with implications for petrogenetic modelling. *Journal of Petrology*, **27**: 1409-1436.
- Meschede, M. 1986. A method of discrimination between different types of mid-ocean basalts and continental tholeiites with the Nb-Zr-Y diagram. *Chemical Geology*, **56**: 207-218.

- Navon, O. and Stolper, E.M. 1987. Geochemical consequences of melt percolation: the upper mantle as a chromatographic column. *Journal of Geology*, **95**: 285-307.
- Newman, R.B. 1967. Bedrock geology of the Shin Pond and Staceyville Quadrangles, Penobscot County, Maine. U.S. Geological Survey, Professional Paper 524-I.
- Neuman, R.B. 1984. Geology and paleobiology of islands in the Ordovician Iapetus Ocean: Review and implications. *Geological Society of America Bulletin*, **94**: 1188- 1201.
- Neuman, R.B. 1988. Paleontological evidence bearing on the Arenig-Caradocian development of the Iapetus Ocean basin. *In The Caledonian-Appalachian Orogen. Edited By A.L. Harris and D.J. Fettes. Geological Society of London Special Publication No. 38, pp. 269-274.*
- Nowlan, G.S. 1981. Some Ordovician conodont faunules from the Miramichi Anticlinorium, New Brunswick. *Geological Survey of Canada, Bulletin 345*: 35 p.
- O'Brien, B.H. 1991. Geological development of the Exploits and Notre Dame subzones in the New Bay area (parts of NTS 2E/6 and 2E/11), map area, Notre Dame Bay, Newfoundland. Newfoundland Department of Mines and Energy, Geological Survey Branch, Report 93-1, pp. 155-166.
- O'Brien, B.H. 1992. Internal and external relationships of the South Lake igneous complex, north-central Newfoundland (NTS 2E/5,6): Ordovician and later tectonism in the Exploits Subzone? Newfoundland Department of Mines and Energy, Geological Survey Branch, Report 92-1, pp. 159-169.

- O'Brien, B.H. 1993. A mapper's guide to Notre Dame Bay's folded thrust faults: Evolution and regional development. Newfoundland Department of Mines and Energy, Geological Survey Branch, Report 93-1, pp. 279-291.
- O'Brien, B.H. 1998. How deeply buried are prospective arc volcanic rocks in the western Wild Bight Group. Newfoundland Department of Mines and Energy, Geological Survey Branch, Report 98-1, pp.85-92.
- O'Brien, B.H. and MacDonald, D.L. 1997. Stratigraphy and structure of the Tommy's Arm River-Shoal Arm Brook area (NTS 2E/5) with reference to the stratabound alteration zones of the upper Wild Bight Group, North-Central Newfoundland. Newfoundland Department of Mines and Energy, Geological Survey Branch, Report 97-1, pp. 237-255.
- O'Brien, B.H., Swinden, H.S., Dunning, G.R., Williams, S.H. and O'Brien, F.H.C. 1997. A Peri-Gondwanan arc-back arc complex in the Iapetus: Early-mid Ordovician evolution of the Exploits Group, Newfoundland. *American Journal of Science*, 297: 220-272.
- O'Neill, P.P. 1987. Geology of the west half of the Weirs Pond (2E/1) map area and its regional significance. Department of Mines and Energy, Mineral Development Division, Report 87-1, pp. 271-281.

- Pearce, J.A. and Parkinson, I.J. 1993. Trace element models for mantle melting: application to volcanic arc petrogenesis. *In* Magmatic Processes and Plate tectonics. *Edited by* H.M. Pritchard, T. Alabaster, N.B.W. Harris and C.R. Neary. Geological Society of London Special Publication No. 76. pp. 373-403.
- Pearce, J.A. and Peate, D.W. 1995. Tectonic implications of the composition of volcanic arc magmas. *Earth and Planetary Science Annual Review*, 23: 251-285.
- Pearce, J.A., van der Laan, S.R., Arculus, R.J., Murray, B.J. and Ishii, T. 1992. Boninite and harzburgite from Leg 125 (Bonin-Mariana forearc): a case study of magma genesis during the initial stages of subduction. *In* Proceedings of Ocean Drilling Project Scientific Results. *Edited By* P. Fryer, J.A. Pearce, and L.B. Stokking, College Station TX: Ocean Drilling Project, 623-659.
- Pedersen, R.B. and Dunning, G. R. 1997. Evolution of arc crust and relations between contrasting sources: U-Pb (age), Nd and Sr isotope systematics of the ophiolite terrain of SW Norway. *Contributions to Mineralogy and Petrology*, 128: 1-15.
- Pederson, R.B. and Hertogen, J. 1990. Magmatic evolution of the Karmoy Ophiolite complex, SW Norway: Relationships between MORB-IAT-boninite-calc-alkaline and alkaline magmatism. *Contributions to Mineralogy and Petrology*, 1990: 277-293.
- Rast, N., Kennedy, M.J. and Blackwood, R.F. 1976. Comparison of some tectonostratigraphic zones in the Appalachians of Newfoundland and New Brunswick. *Canadian Journal of Earth Sciences*, 13: 868-875.

- Rice, R.J. and van Staal, C.R. 1992. Sedimentological studies in the Miramichi, Tetagouche and Fournier Groups, Bathurst Camp, Belledune-Elmtree inlier, Northern New Brunswick. *In* Current Research part B. Geological Survey of Canada, Paper 92-1D, pp. 257-264.
- Rogers, N. 1994. The geology and geochemistry of felsic volcanic rocks of the Acadians Range Complex, Tetagouche Group, New Brunswick. Ph.D., Keele University, U.K.
- Rogers, N. 1995. Petrological variations of the Ordovician felsic volcanic rocks of the Tetagouche Group, New Brunswick. *In* Current Research part E. Geological Survey of Canada, Paper 95-1E, pp. 279-286.
- Saunders, A. and Tarney, J. 1991. Back-Arc Basins. *In* Oceanic Basalts. *Edited By* P.A. Floyd. Van Nostrand Reinhold, New York, pp. 219-262.
- Saunders, A.D., Tarney, J., Marsh, N.G., and Wood, D.A. 1979. Ophiolites as ocean crust or marginal basin crust: a geochemical approach. *In* Ophiolites, Proceedings from the International Ophiolite Symposium. *Edited by* A. Panayiotou. Ministry of Agriculture and Natural Resources, Geological Survey Department, Nicosia, Cyprus, pp. 193-204.
- Shervais, J.W. 1982. Ti-V plots and the petrogenesis of modern and ophiolitic lavas. *Earth and Planetary Science Letters*, **59**: 101-118.
- Stacey, J.S. and Kramers, J.D. 1975. Approximation of terrestrial lead isotope evolution by a two-stage model. *Earth and Planetary Science Letters*, **26**: 207-221.

- Stern, R.J. and Bloomer, S.H. 1992. Subduction zone infancy: Examples from the Eocene Izu-Bonin-Mariana and Jurassic California arc. *Geological Society of America Bulletin*, **104**: 1621-1636.
- Stouge, S. 1979. Conodonts from Davidsville Group of Botwood Zone, Newfoundland. Newfoundland Department of Mines and Energy, Mineral Development Division, Report 79-1, pp. 43-44
- Sullivan, R.W. and van Staal, C.R. 1993. U-Pb age of the Canoe Landing Lake Formations Tetagouche Group, New Brunswick. *In Radiogenic Age and Isotope Studies: Report 7*. Geological Survey of Canada, Paper 93-2, pp. 39-43.
- Sullivan, R.W. and van Staal, C.R. 1996. Preliminary chronostratigraphy of the Tetagouche and Fournier Groups in Northern New Brunswick. Geological Survey of Canada, Special Report 9: pp. 43-56.
- Sullivan, R.W. van Staal, C.R. and Langton, J.P. 1990. U-Pb zircon ages of plagiogranite and gabbro from the ophiolitic Devereux Formation, Fournier Group, northeastern New Brunswick. *In Radiogenic Age and Isotopic Studies: Report 3*, Geological Survey of Canada, Paper 89-2, pp. 119-122.
- Sun, S-S. and McDonough, W.F. 1989. Chemical and isotopic systematics of oceanic basalts: implications for mantle composition and processes. *In Magmatism in the Ocean Basins. Edited By A.D. Saunders and M.J. Norry*. pp. 313-345.
- Swinden, H.S. 1988. Ordovician volcanism and mineralization in the Wild Bight Group, central Newfoundland: A geological, petrological, geochemical and isotopic study. Ph.D., Memorial University of Newfoundland. 452 p.

- Swinden, H.S. and Jenner, G.A. 1992. Volcanic stratigraphy northwest of New Bay Pond, Central Newfoundland, and the strike-extent of the Point Leamington massive sulphide horizon. *In* Report 92-1. Newfoundland Department of Mines and Energy, Geological Survey Branch 267-279.
- Swinden, H.S. Kean, B.F. and Dunning, G.R. 1988 Geological and paleotectonic setting of volcanogenic sulphide mineralization in central Newfoundland. *In* The volcanogenic sulphide districts of central Newfoundland. *Edited By* H.S. Swinden B.F. Kean. Geological Association of Canada, Mineral Deposits Division, St. John's, Newfoundland, pp.5-26.
- Swinden, S.H. Jenner, G.A., Kean, B. F. and Evans, D.T.W. 1989. Volcanic rock geochemistry as a guide for massive sulphide exploration in central Newfoundland. Newfoundland Department of Mines and Energy, Geological Survey Branch, Report 89-1, pp. 201-219.
- Swinden, H.S., Jenner, G.A., Fryer, B.J., Hertogen, J. and Roddick, J.C. 1990. Petrogenesis and paleotectonic history of the Wild Bight Group, an Ordovician rifted island arc in central Newfoundland. *Contributions to Mineralogy and Petrology*, **105**: 219-241.
- Taylor, R.N., Nesbitt, R.W., Vidal, P., Harmon, R.S., Auvray, B. and Croudace, I.W. 1994. Mineralogy, chemistry and genesis of the boninite series volcanics, Chichijima , Bonin Islands, Japan. *Journal of Petrology*, **35**: 577-617.

- Tucker, R.D. and McKerrow, W.S. 1995. Early Paleozoic chronology: a review in light of new U-Pb zircon ages from Newfoundland and Britain. *Canadian Journal of Earth Sciences*, **32**: 368-379.
- Tucker, R.D., O'Brien, S.J. and O'Brien, B.H. 1994. Age and implications of Early Ordovician (Arenig) plutonism in the type area of the Bay du Nord Group, Dunnage Zone, southern Newfoundland Appalachians. *Canadian Journal of Earth Sciences*, **31**: 351-357.
- van der Pluijm, B.A., van der Voo, R. and Torsvik, T.H. 1995. Convergence and subduction at the Ordovician margin of Laurentia. *In* *New Perspectives in the Appalachian-Caledonian Orogen. Edited By* J.P. Hibbard, C R. van Staal and P.A. Cawood. Geological Association of Canada Special Paper 41, pp. 127-136.
- van der Pluijm, B.A. Karlstrom, K.E. and Williams, P.F. 1987. Fossil evidence for fault-derived stratigraphic repetition in the northeastern Newfoundland Appalachians. *Canadian Journal of Earth Sciences*, **24**: 2337-2350.
- van Staal, C.R. 1994. Brunswick Subduction Complex in the Canadian Appalachians: Record of the late Ordovician to Silurian collision between Laurentia and the Gander margin of Avalon. *Tectonics*, **13**: 946-962.
- van Staal, C.R. and Fyffe, L.R. 1991. Dunnage and Gander Zones New Brunswick: Canadian Appalachian Region. New Brunswick Natural Resources and Energy, Geoscience Report 91-2 39 p.

- van Staal, C.R., Langton, J.P. and Sullivan, R.W. 1988. A U-Pb age for the ophiolitic Devereaux Formation, Elmtree Terrane, northeastern New Brunswick. Geological Association of Canada, Paper 88-2: 37-40
- van Staal, C.R., Winchester, J.A. and Bedard, J.H. 1991. Geochemical variations in middle Ordovician rocks of the northern Miramichi Highlands and their tectonic significance. Canadian Journal of Earth Sciences, **28**: 1031-1049.
- Williams, H. 1962. Botwood (west half) map area, Newfoundland, Geological Survey of Canada, Paper 62-9, 16 p.
- Williams, H. 1963. Botwood map area. Geological Survey of Canada Open File Map 60-1963.
- Williams, H. 1964. The Appalachians in northeastern Newfoundland-A two-sided symmetrical system. American Journal of Science, **262**: 1137-1158.
- Williams, H. 1972. Stratigraphy of Botwood map area, northeastern Newfoundland. Geological Survey of Canada, Open File 113.
- Williams, H. 1978. Tectonic lithofacies map of the Appalachian Orogen. Memorial University of Newfoundland, Map 1.
- Williams, H. 1979. Appalachian Orogen in Canada. Canadian Journal of Earth Sciences, **16**: 702-807.
- Williams, H. 1992. Melanges and coticule occurrences in the northeast Exploits Subzone, Newfoundland. *In* Current Research part D. Geological Survey of Canada, Paper 92-1D, pp. 121-127.

- Williams, H. 1993. Stratigraphy and structure of the Botwood Belt and definition of the Dog Bay Line in northeastern Newfoundland. *In* Current Research part D. Geological Survey of Canada, Paper 93-1D, pp. 19-27.
- Williams, H. 1995. Dunnage Zone-Newfoundland. *In* Chapter 3 Geology of the Appalachian-Caledonian Orogen in Canada and Greenland. *Edited By* H. Williams. Geological Survey of Canada, No.6, pp. 142-166.
- Williams, H. and Piasecki, M.A.J. The Cold Spring Melange and a possible model for Dunnage-Gander zone interaction in central Newfoundland. *Canadian Journal of Earth Sciences*, 27: 1126-1134.
- Williams, H., Colman-Sadd, S.P. and Swinden, H.S. 1988. Tectonic-stratigraphic subdivisions of central Newfoundland. *In* Current Research Part B. Geological Survey of Canada, Paper 88-1B, pp. 91-98.
- Williams, H. Currie, K.L. and Piasecki, M.A.J. 1993. The Dog Bay Line: a major Silurian tectonic boundary in northeast Newfoundland. *Canadian Journal of Earth Sciences*, 30: 2481-2494.
- Williams, S.H., Boyce, W.D. and Colman-Sadd, S.P. 1992. A new Lower Ordovician (Arenig) faunule from the Coy Pond Complex, central Newfoundland, and a refined understanding of the closure of the Iapetus Ocean. *Canadian Journal of Earth Sciences*, 29: 2046-2057.

- Williams, H., Kennedy, M.J.. and Neale, E.W. 1974. The northeastern termination of the Appalachian orogen. *In* The ocean basins and margins, the North Atlantic. *Edited by* A.E. Nairn, and F.G. Stehli. Plenum Publishing Corporation, New York, pp. 79-123.
- Williams, S.H. and O'Brien, B. H. 1994. Graptolite biostratigraphy within a fault-imbricated black shale and chert sequence: Implications for a triangle zone in the Shoal Arm Formation of the Exploits Subzone. Newfoundland Department of Mines and Energy, Geological Survey Branch, Report 94-1, pp. 201-209.
- Winchester, J.A. and Floyd, P.A. 1977. Geochemical discrimination of different magma series and their differentiation products using immobile elements. *Chemical Geology*, **20**: 325-343.
- Wood, D.A. 1980. The application of the Th-Hf-Ta diagram to problems of tectonomagmatic classification and to establishing the nature of crustal contamination of basaltic lavas of the British Tertiary volcanic province. *Earth and Planetary Science Letters*, **50**: 11-30.
- Zindler, A. and Hart, S. 1986. Chemical Geodynamics. *Earth and Planetary Science Letters, Annual Review*, **14**: 493-571.

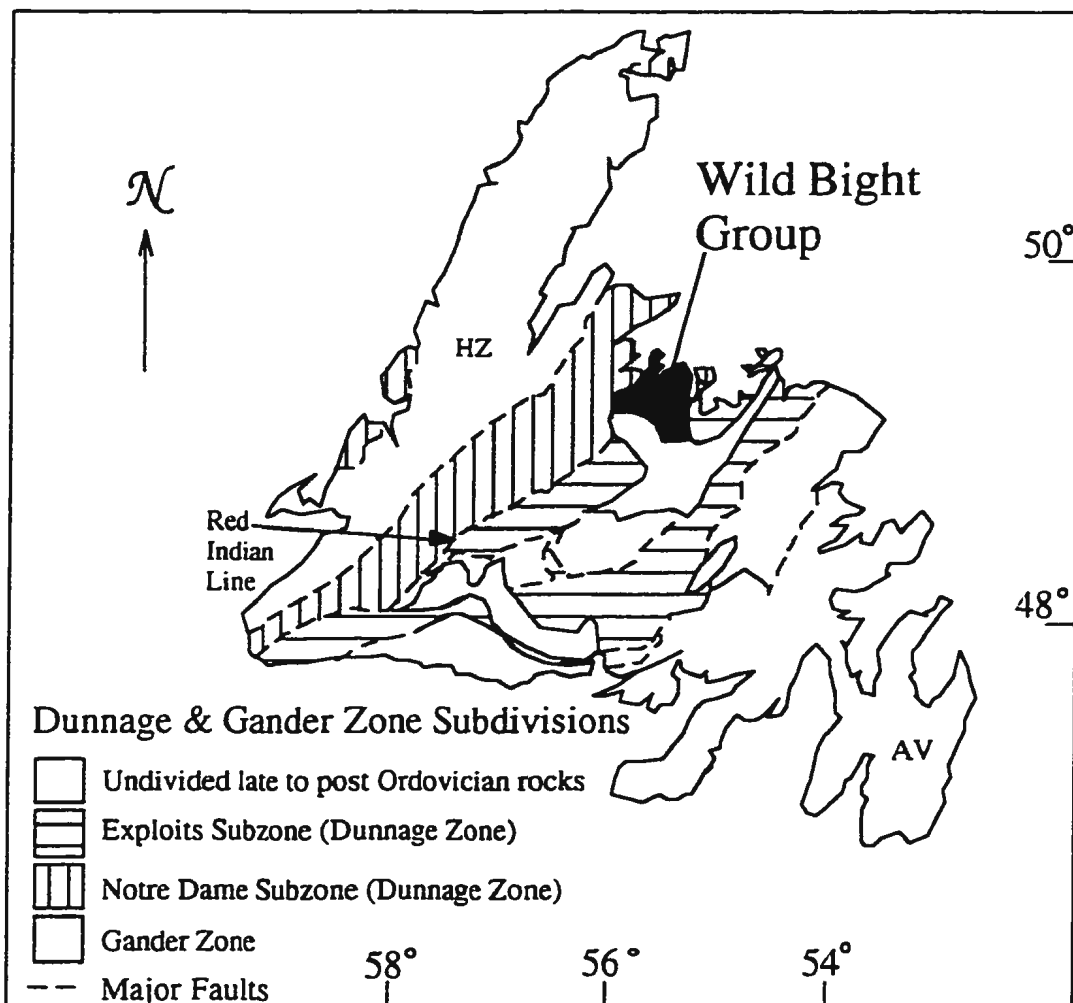


**Figure 1.1.** Tectonostratigraphic zones of the Newfoundland Appalachians. Units within the Avalon Zone (AV) and Humber Zone (HZ) are not differentiated. Simplified from Colman-Sadd et al. 1992.

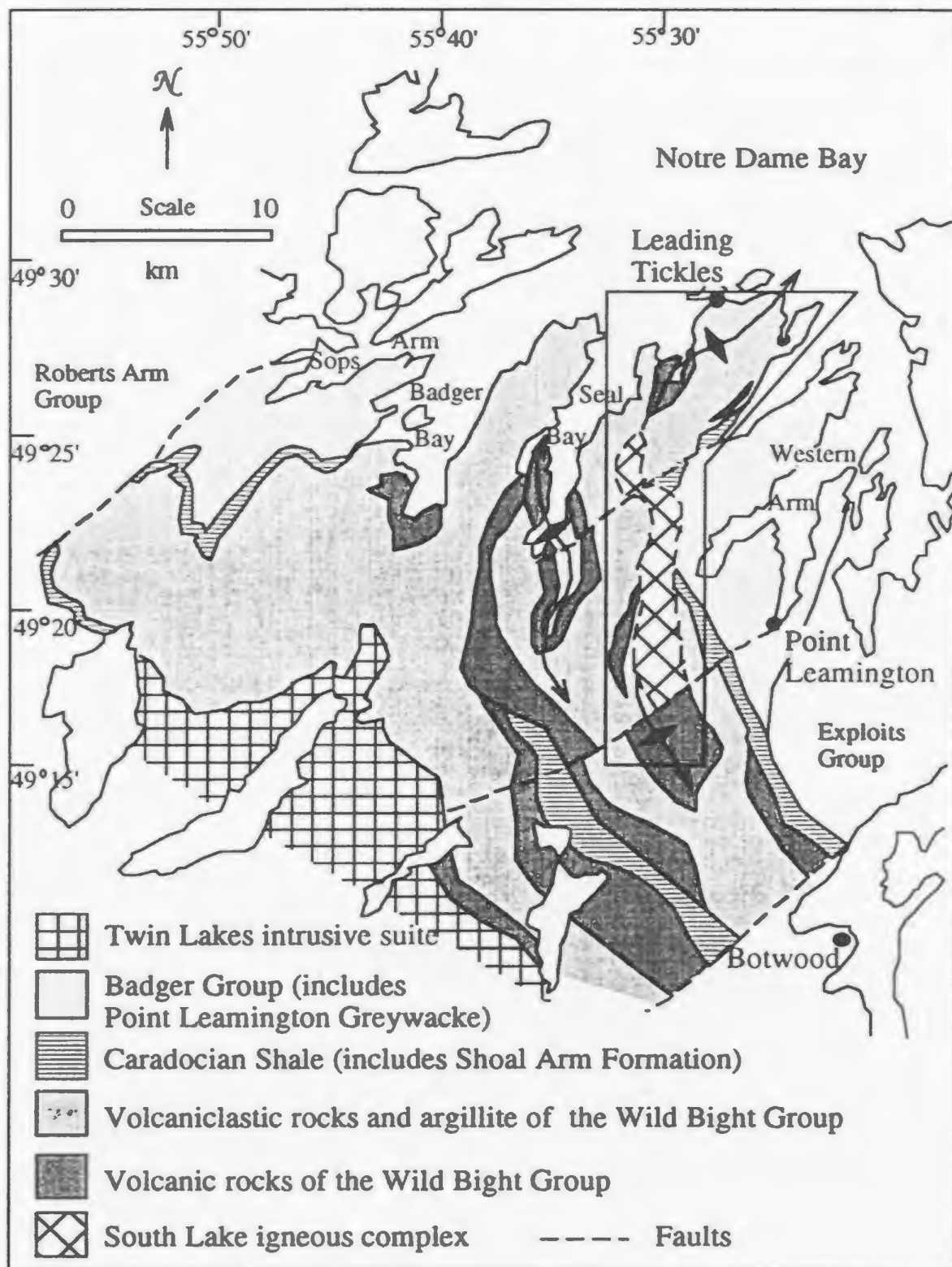


**Figure 1.2.** Simplified regional geology of the Wild Bight Group and adjacent rocks. Modified from Swinden et al. 1990. The approximate area of this detailed study is outlined by the box.

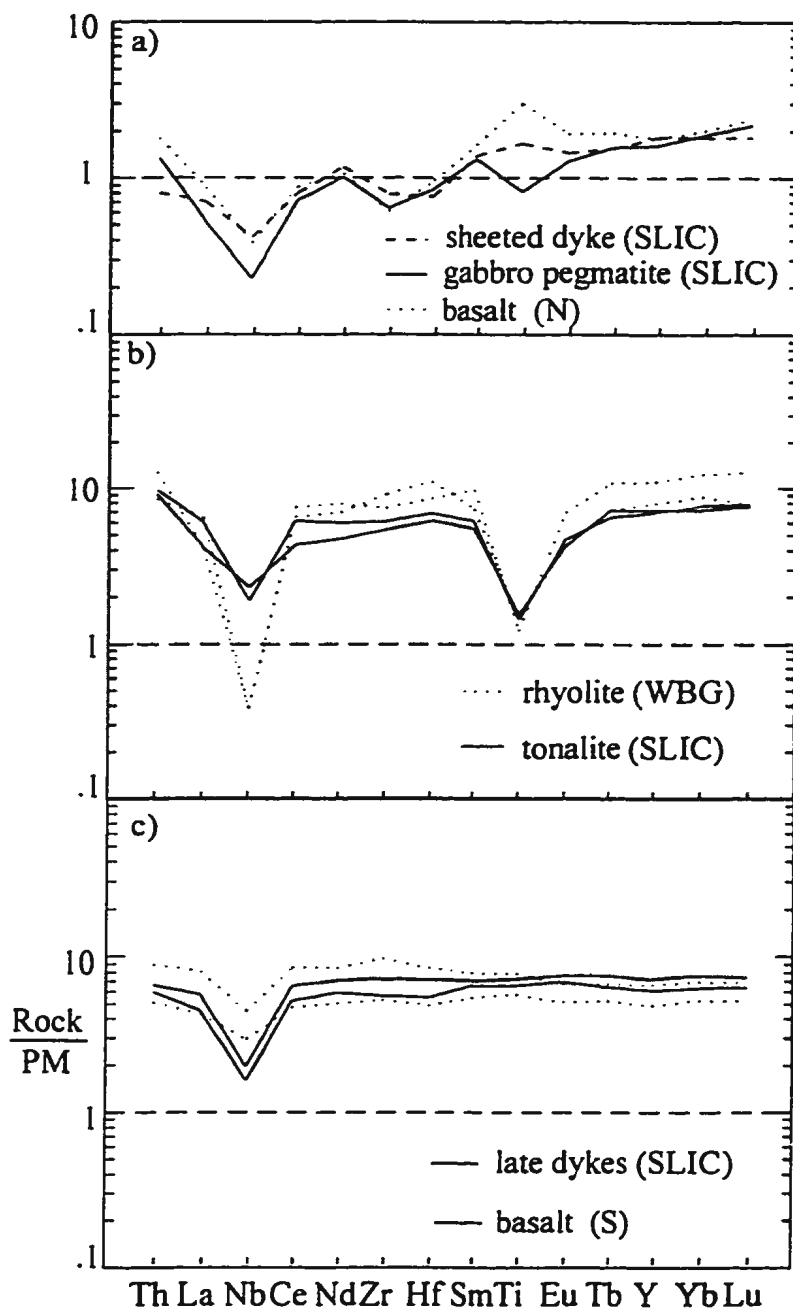


**Figure 2.1** Primitive mantle-normalized, extended-REE plots showing similar patterns for samples from the South Lake igneous complex (SLIC) and the older volcanic packages of the Wild Bight Group (WBG): a) low-Ti tholeiites; b) felsic rocks; c) island arc tholeiites. Basalts are from both the northern (N) and southern (S) fault-bounded packages of the older WBG sequence. Normalizing values from Swinden et al. 1990.

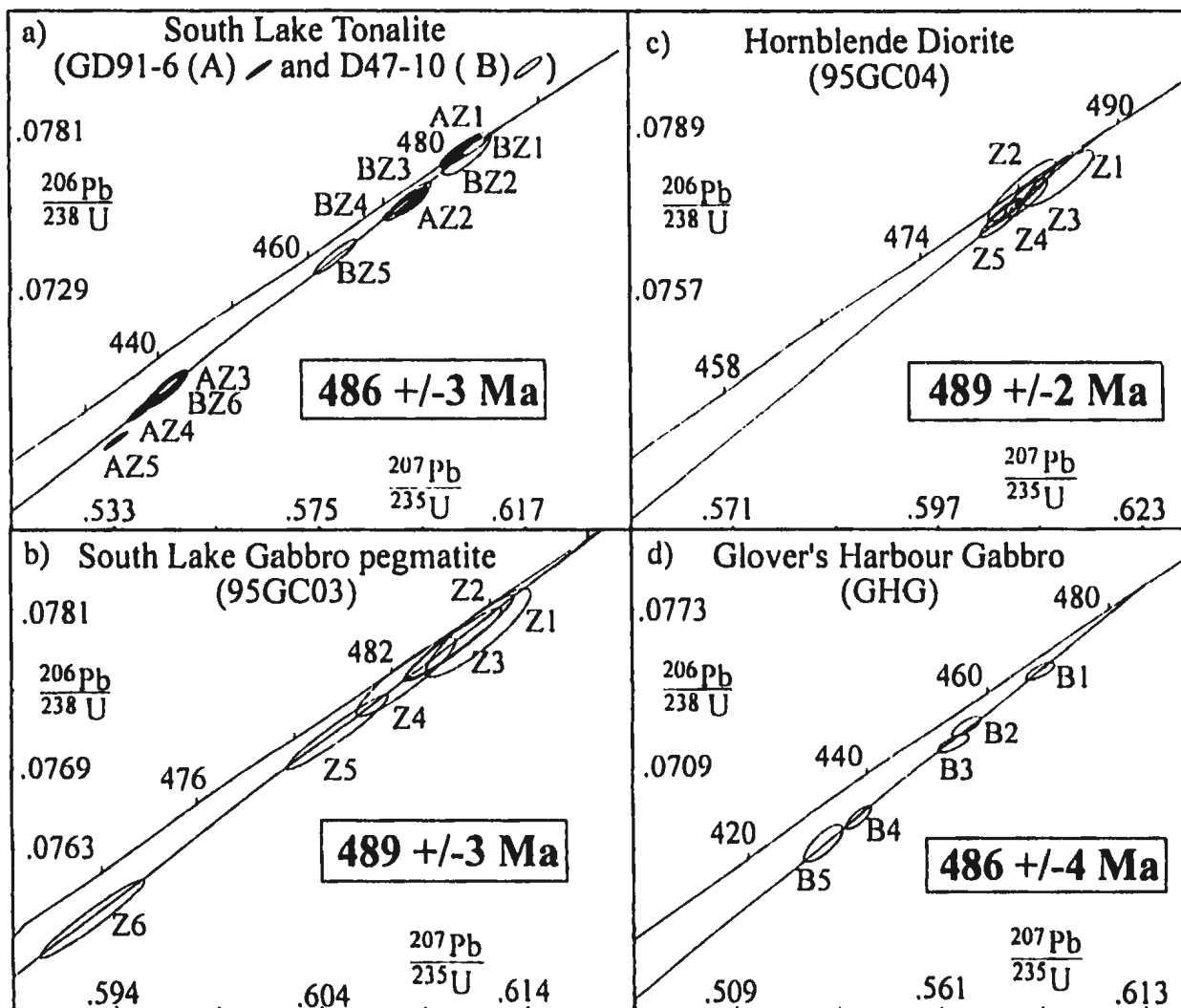


**Figure 2.2** U-Pb concordia plots for dated samples from the South Lake igneous complex and older volcanic sequence of the Wild Bight Group (Glover's Harbour west unit).

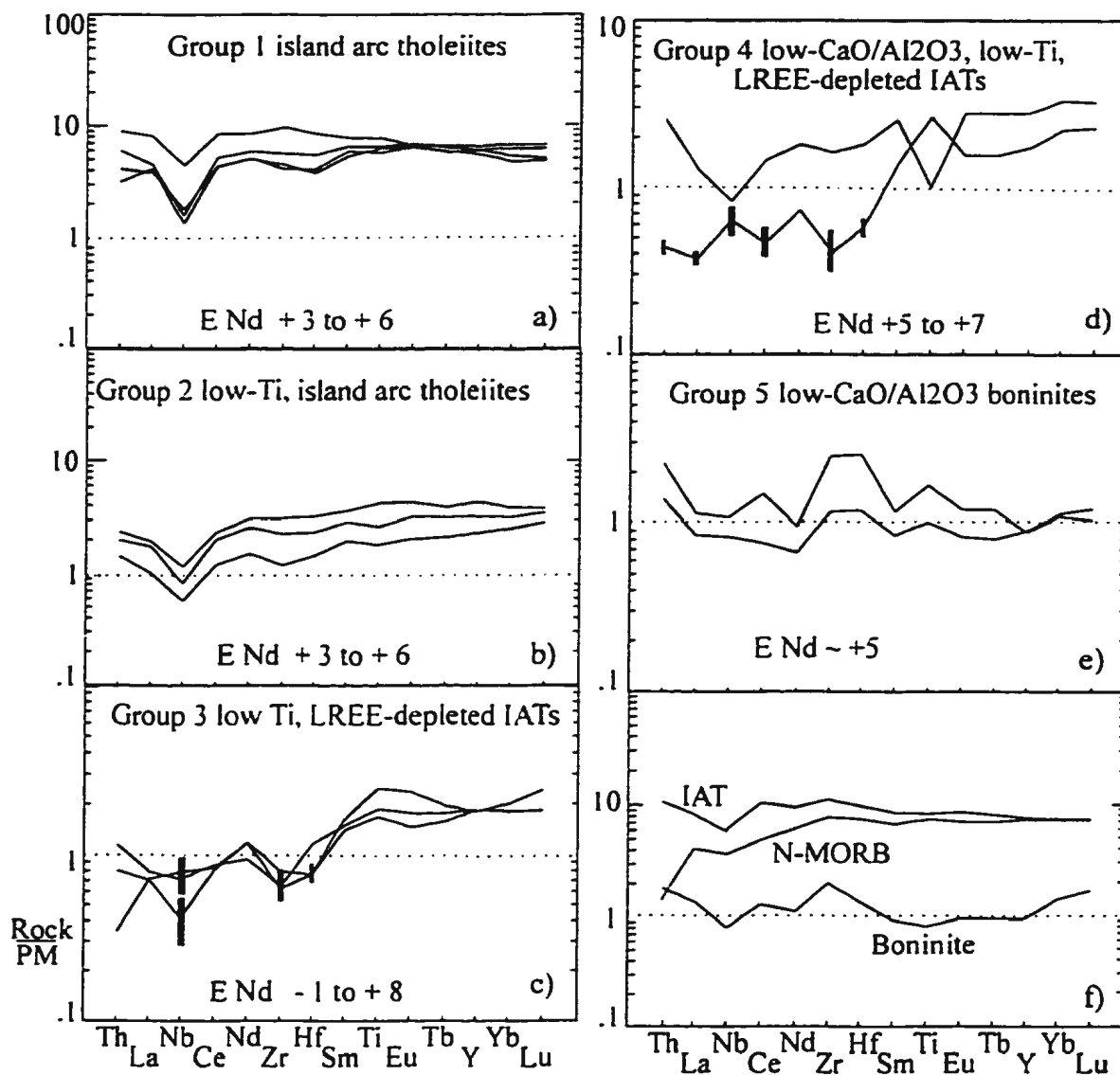


**Figure 2.3** Primitive mantle-normalized, extended-REE plots of the most primitive samples used to define the various geochemical groups: a) group 1 island arc tholeiites; b) low-Ti island arc tholeiites; c) LREE-depleted low-Ti island arc tholeiites; d) low CaO/Al<sub>2</sub>O<sub>3</sub> low-Ti island arc tholeiites; and e) low CaO/Al<sub>2</sub>O<sub>3</sub> boninites. Part f) shows patterns for modern equivalents taken from the literature. See table 2.2 for references and data. Normalizing values from Swinden et al 1990.

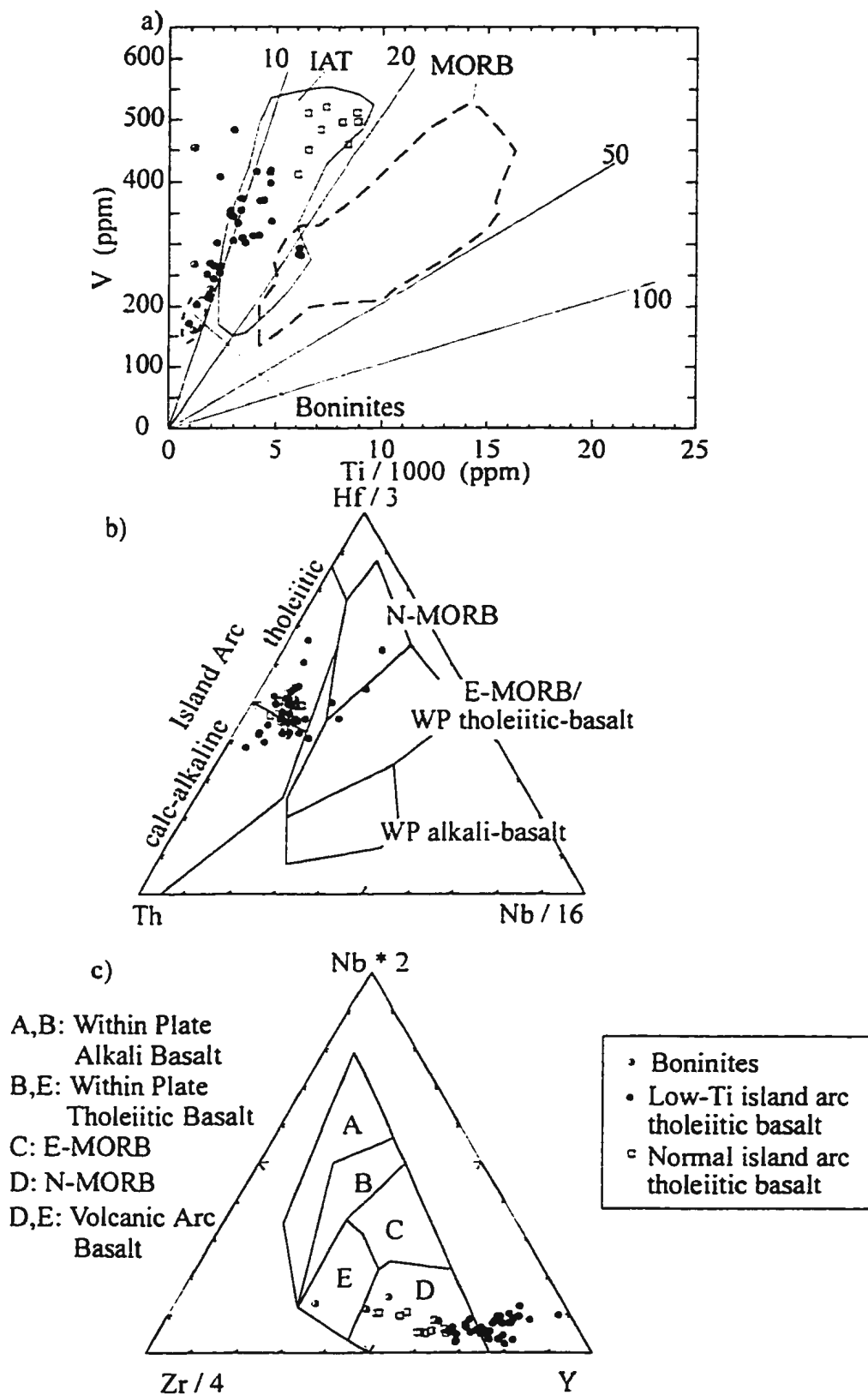
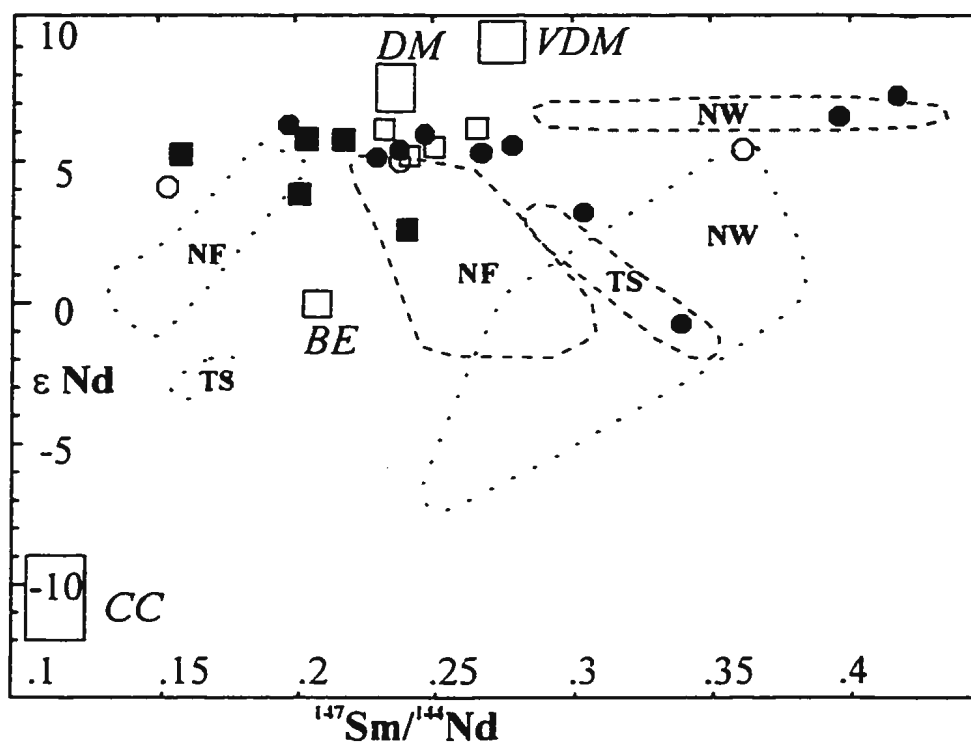
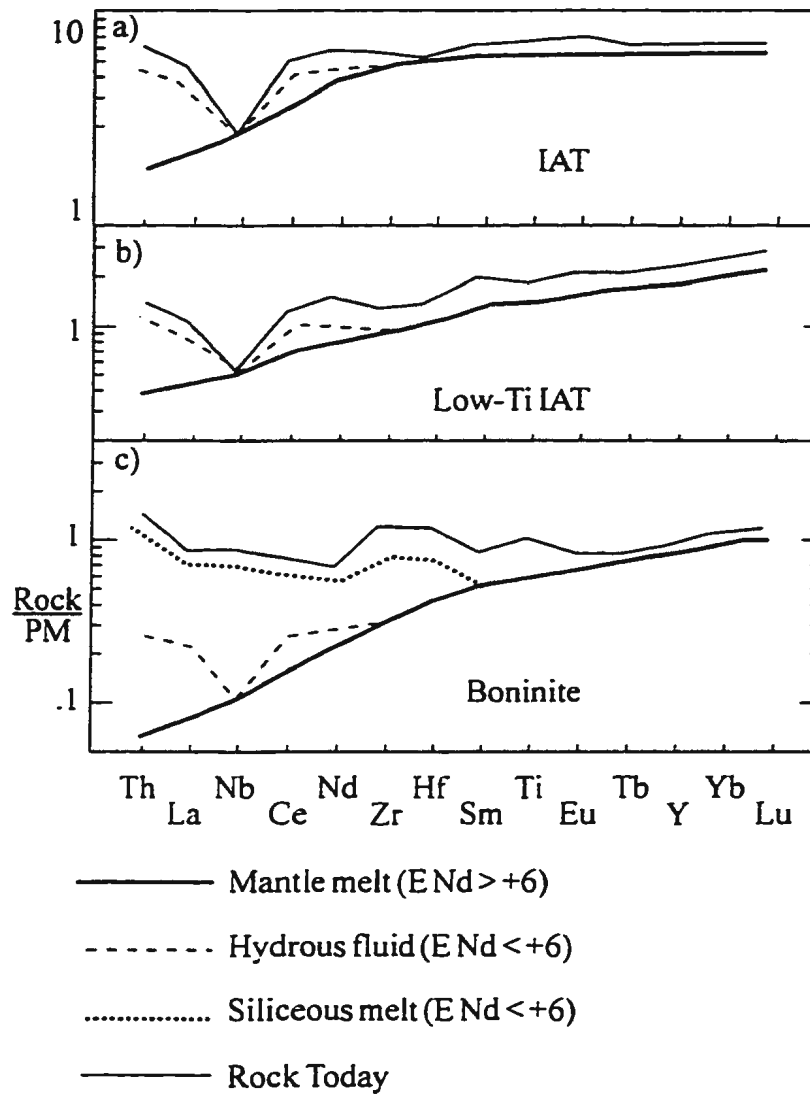


**Figure 2.4** Tectonic discrimination diagrams for all samples from the geochemical groups defined in figure 2.3: a) fields defined by Shervais (1982); b) fields defined by Wood (1980); and c) fields defined by Meschede (1986)

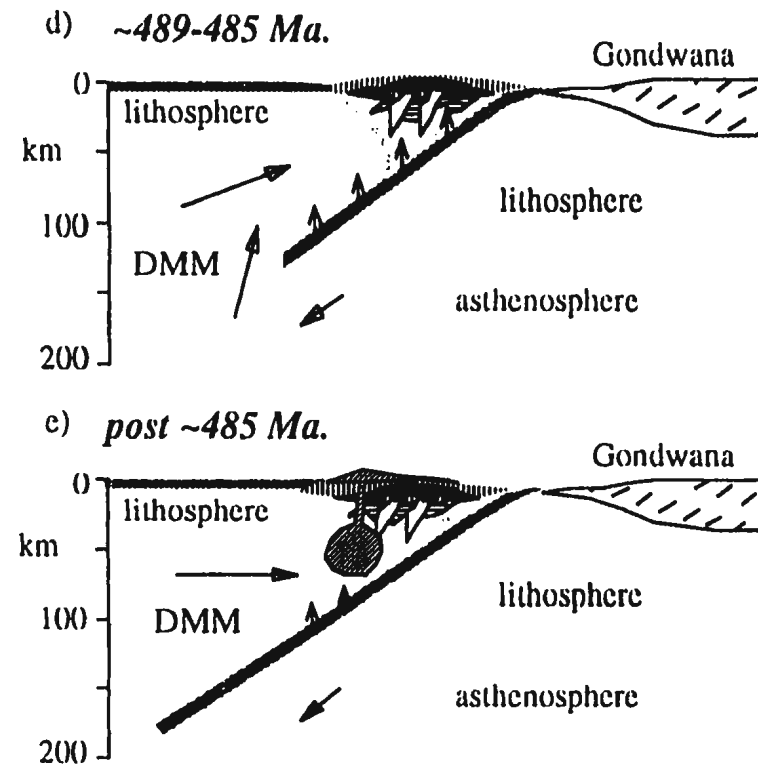
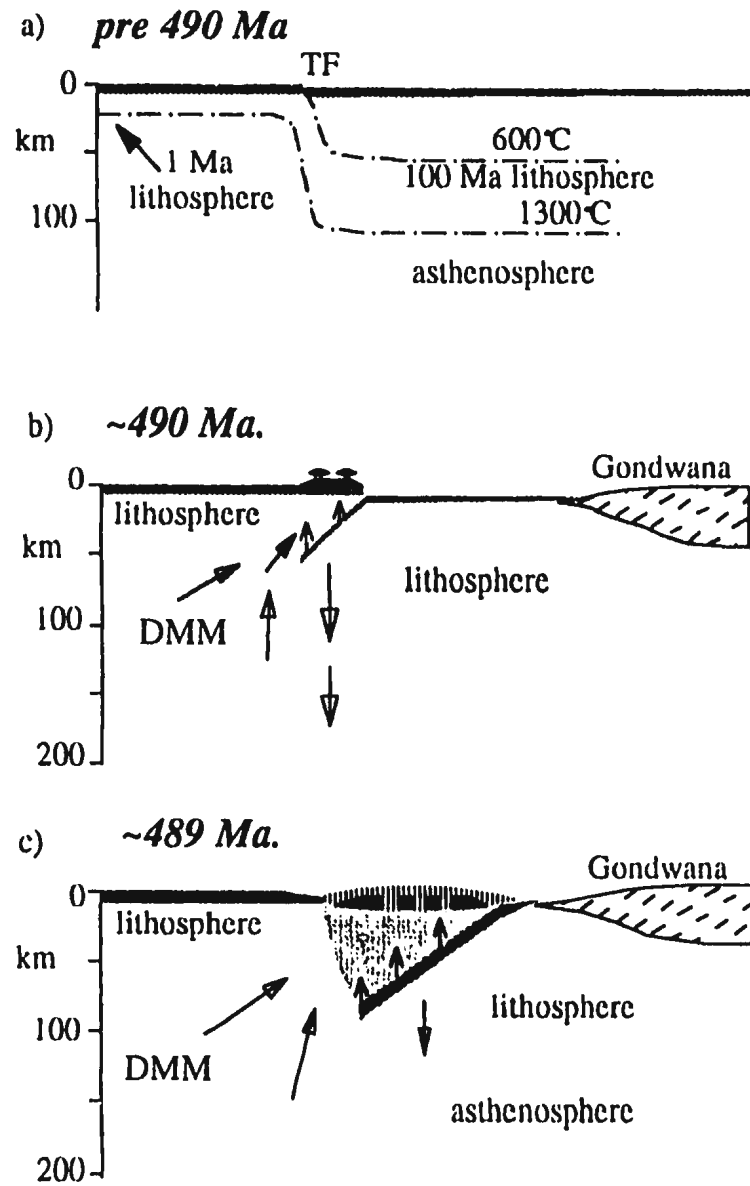


○ boninite; ● low-Ti, LREE-depleted IAT; □ low-Ti, IAT;  
 ■ IAT; --- other IATs; ··· other boninites

**Figure 2.5** Plot of  $\epsilon \text{Nd}$  vs  $^{147}\text{Sm}/^{144}\text{Nd}$  for samples from the geochemical groups defined for the South Lake igneous complex and the older volcanic sequence of the Wild Bight Group, and fields for similar Ordovician rocks elsewhere in Newfoundland (NF), Tasmania (TS) and SW Norway (NW). Fields are based on: for Newfoundland, unpublished data from George Jenner for the Pacquet Harbour Group and Betts Cove ophiolite (boninites), and a previous study of the WBG by Swinden et al. 1990 (low-Ti tholeiites); for Tasmania, data from Brown and Jenner 1989; and for SW Norway, data from Pedersen and Dunning 1997. The fields labelled DM, VDM, CC and BE are depleted mantle (MORB source), very depleted mantle, continental crust and bulk earth, respectively, calculated for the early Ordovician (Swinden et al. 1990).



**Figure 2.6** A qualitative model showing the effects on trace element patterns, of mixing variably depleted mantle melts with different subduction components. See text for further explanation.



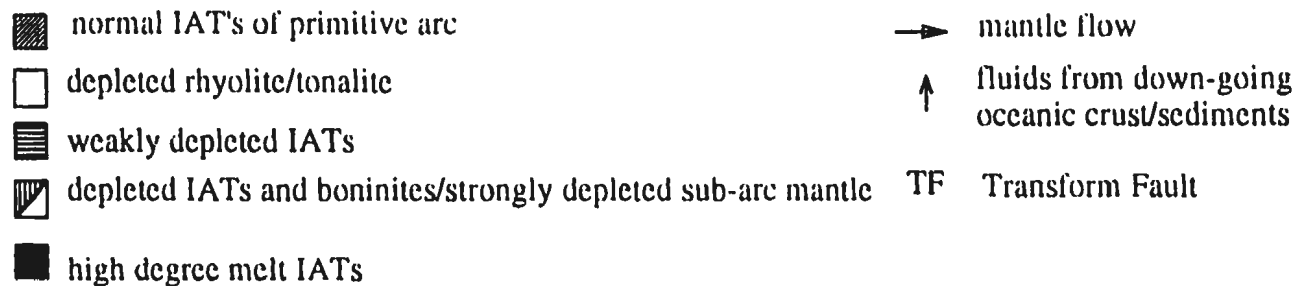


**Figure 2.7.** Tectonic model for formation of the older volcanic rocks of the Wild Bight Group and the South Lake igneous complex. a) Pre-subduction initiation configuration along hypothetical transform boundary; b) initiation of subsidence of older crust, and extensional suprasubduction zone magmatism in upper oceanic plate, producing IATs with low levels of trace elements by high degrees of melting of normal MORB-like mantle; c) continued high degree of melting creates a strongly depleted mantle wedge leading to the production of low-Ti IATs and boninites; d) subsidence changes to subduction and mantle upwelling is prohibited. New MORB-like mantle is injected laterally into the mantle wedge and mixes with depleted mantle to produce less depleted IATs. Crust is sufficiently thickened to produce tonalite/rhyolite by secondary melting at the base of the crust; and e) Extension moves to a back arc position and a stable magmatic front develops producing normal IATs. Based on the model of Stern and Bloomer (1992), for subduction initiation in the Izu-Bonin-Mariana Arc.

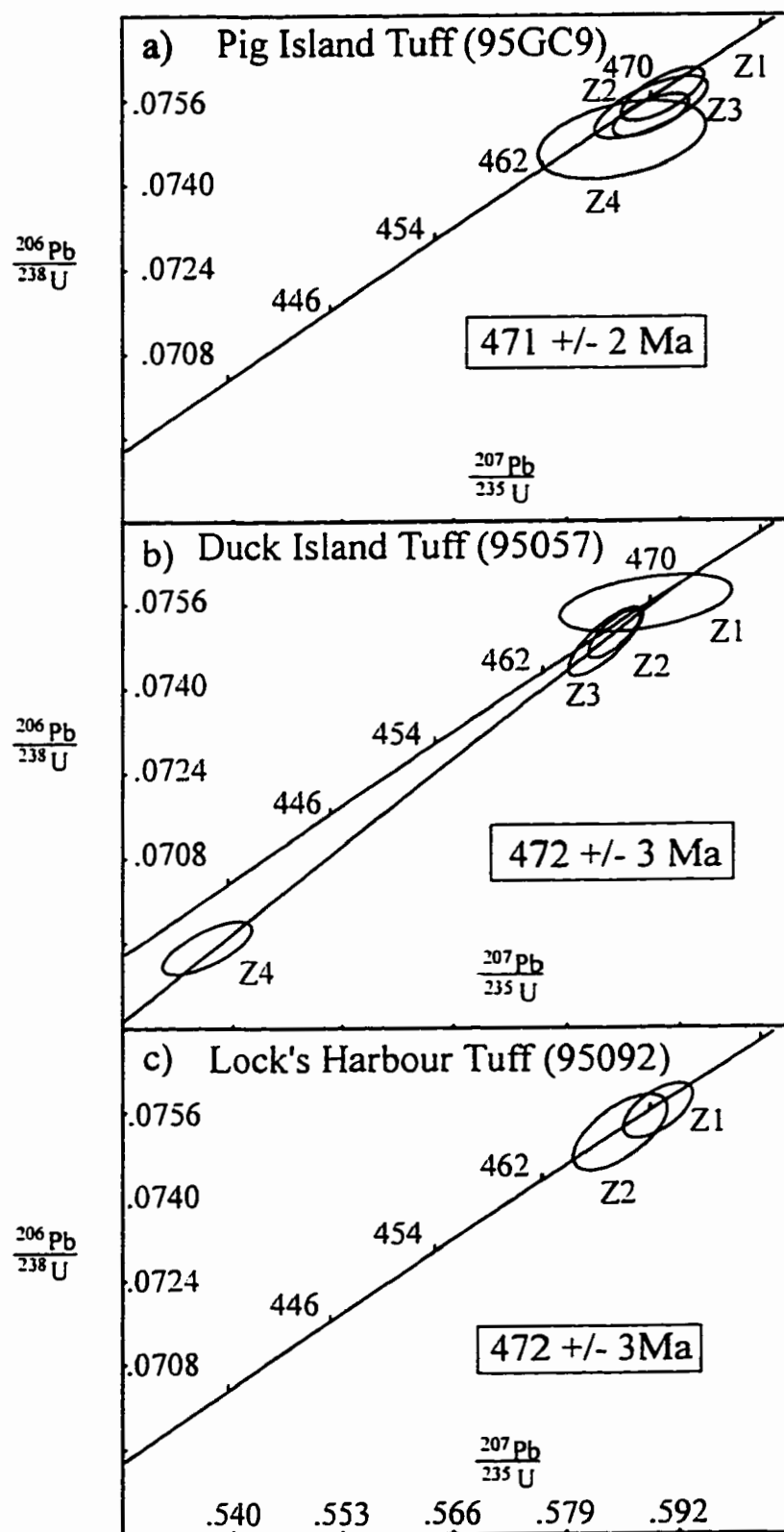


**Figure 3.1** U-Pb concordia plots of dated tuffs and gabbro sills from the younger volcanic succession of the Wild Bight Group.

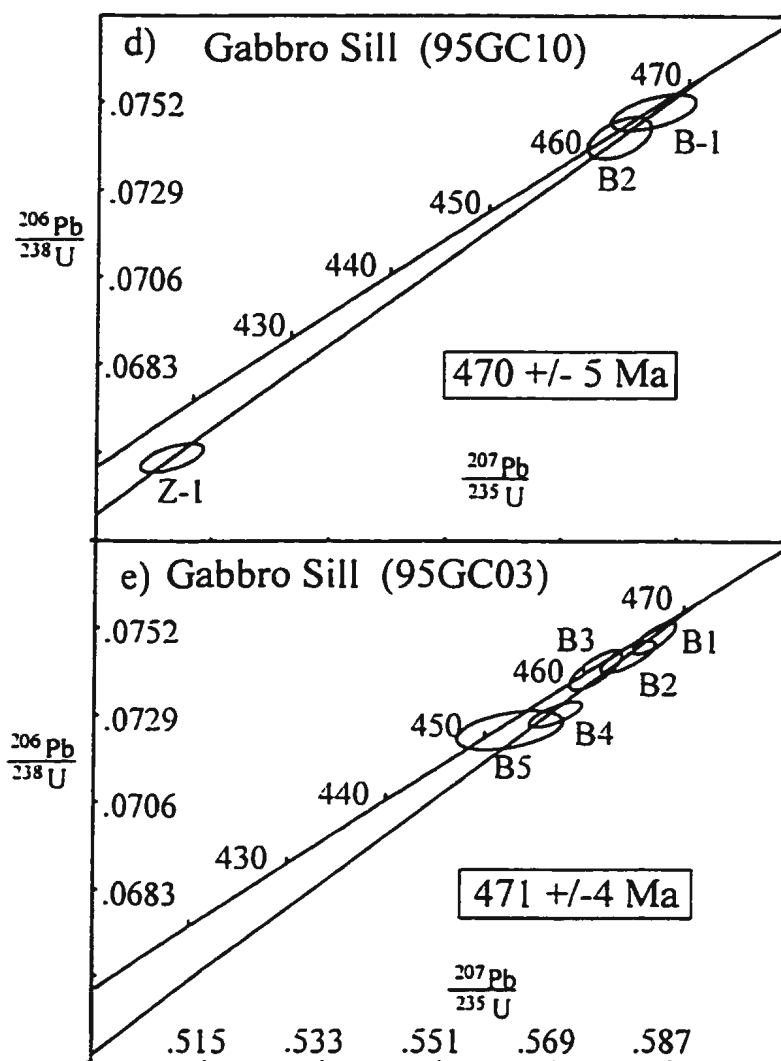


Figure 3.1 Continued.

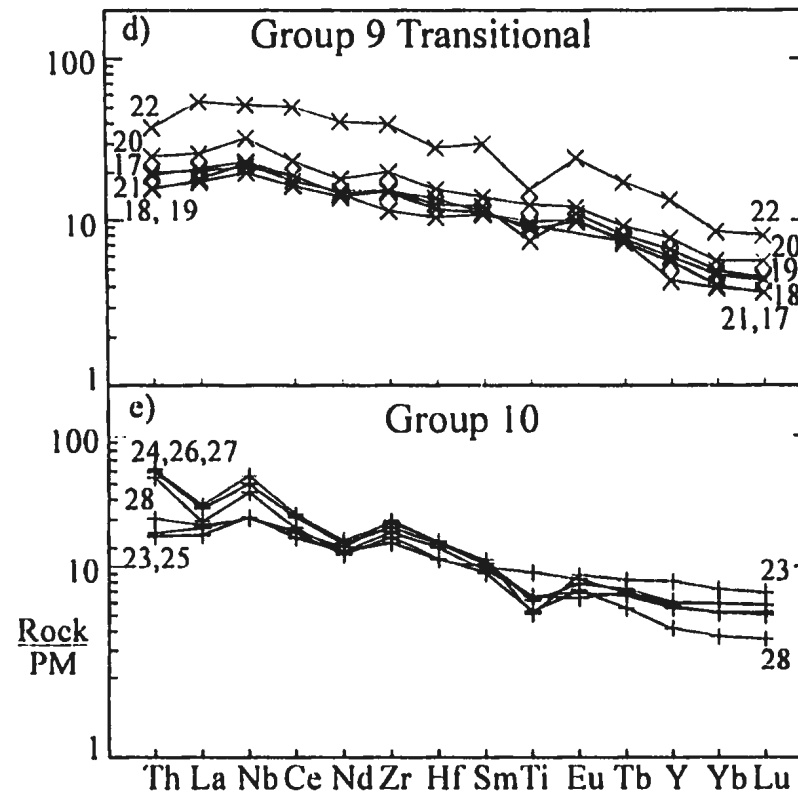
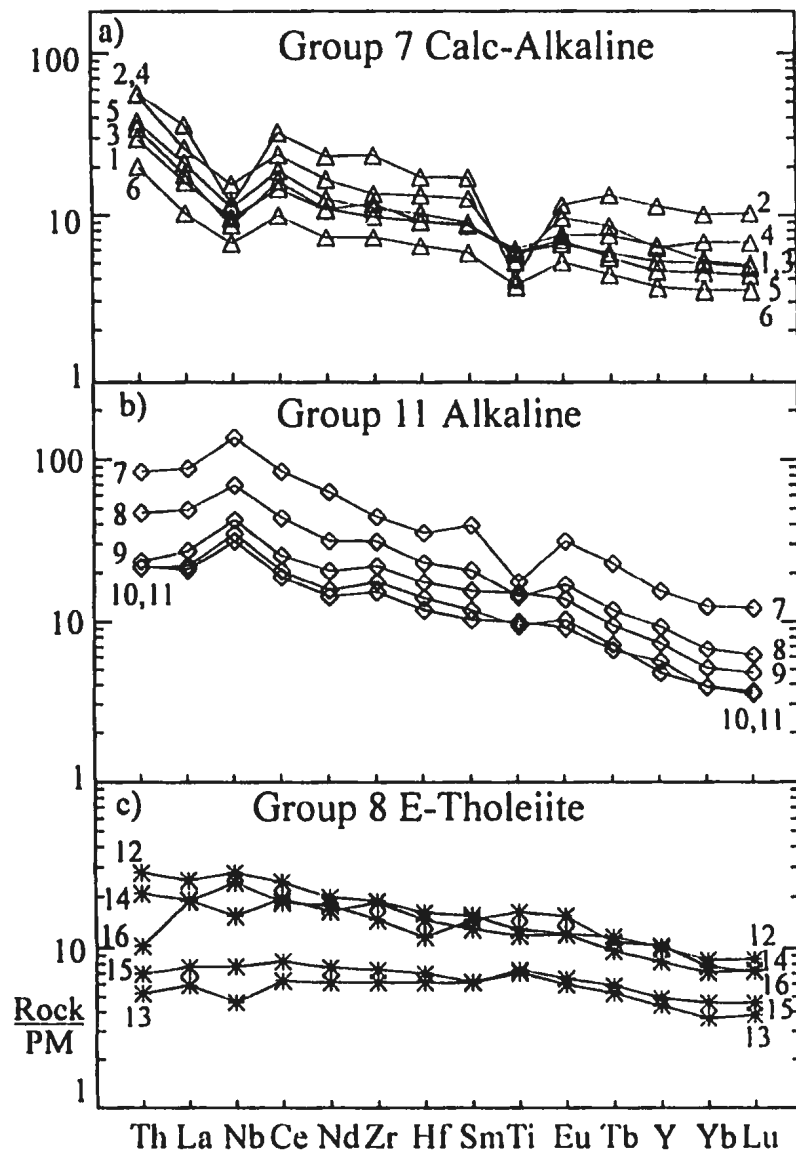
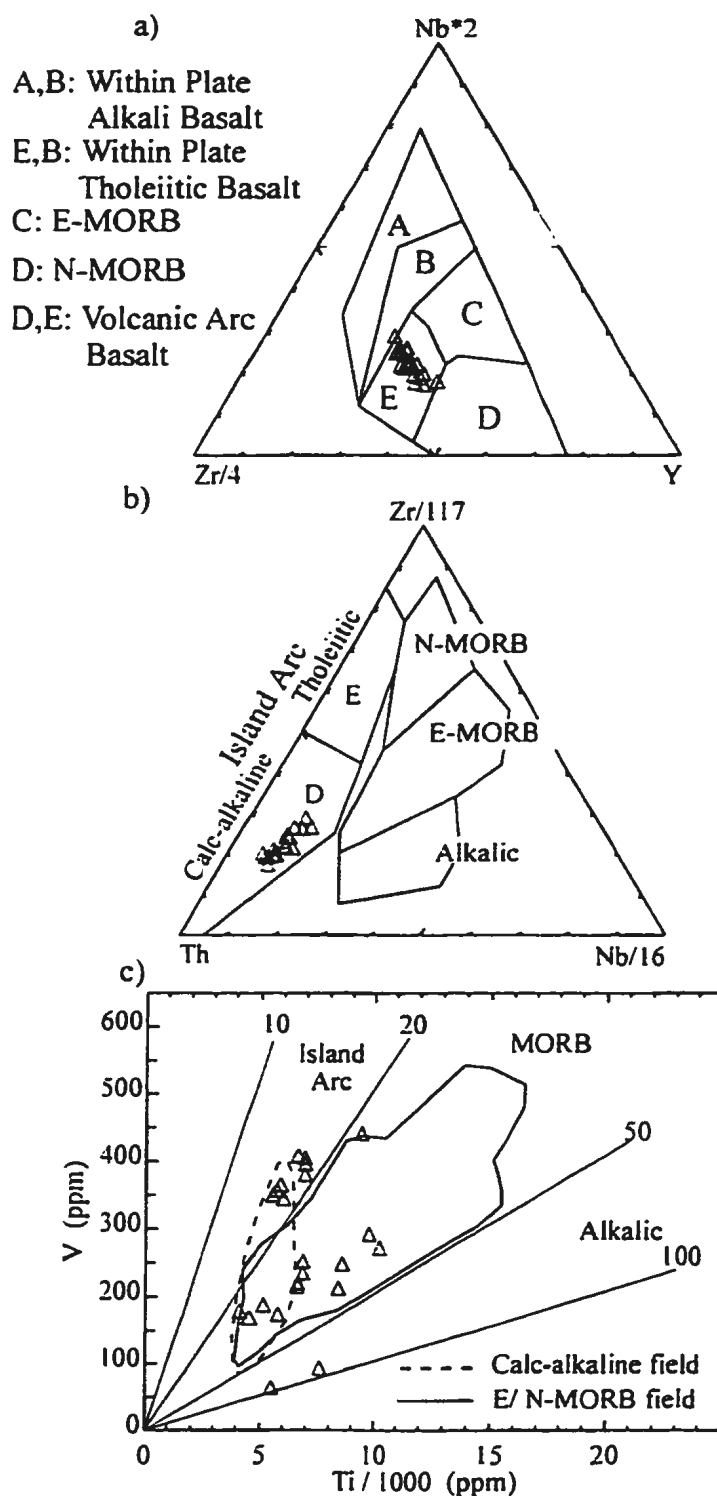
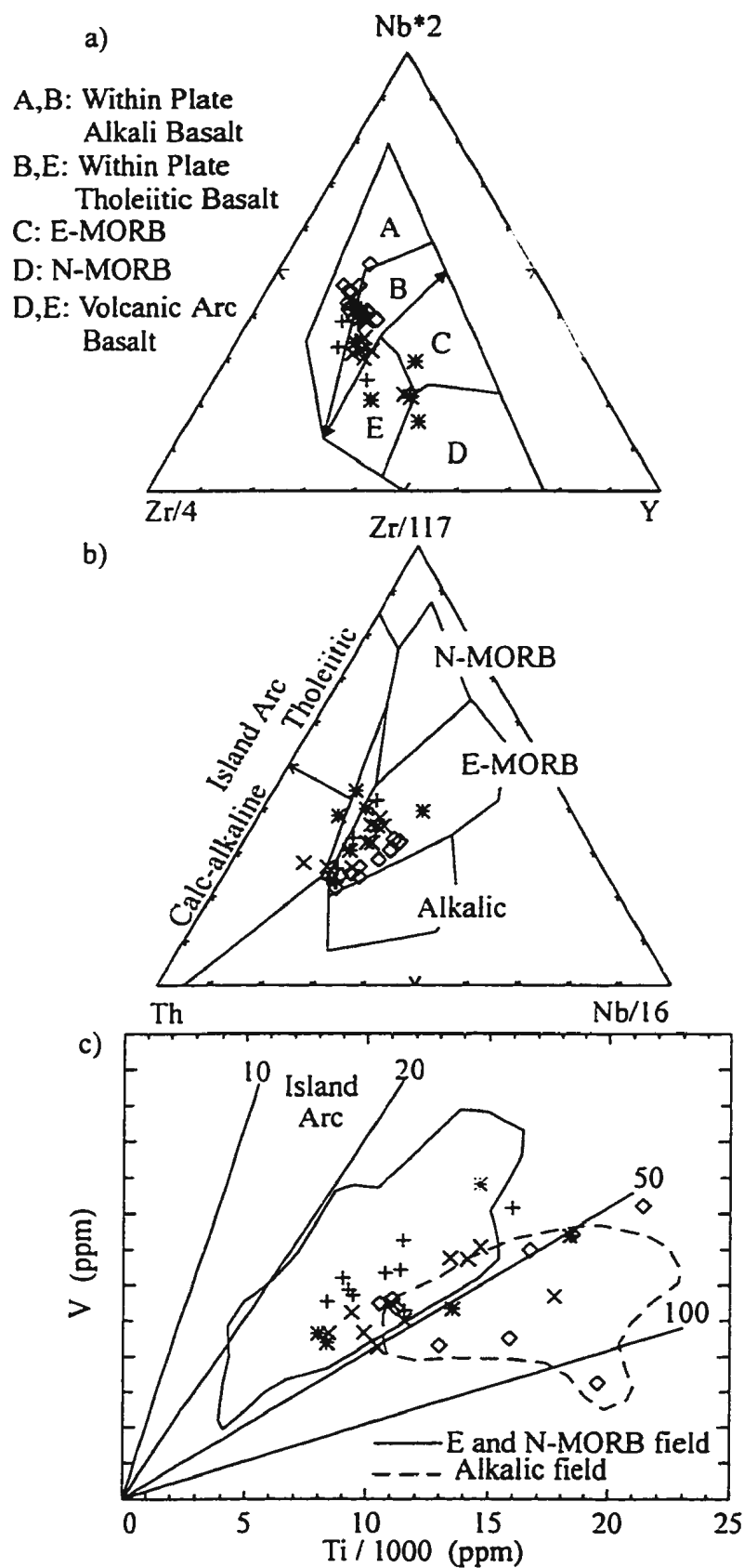


Figure 3.2 Primitive mantle-normalized, extended-REE plots for representative mafic and intermediate samples from the geochemical groups of the younger Wild Bight Group sequence. Numbers beside samples correspond to those in Table 3.2. Normalizing values are from Swinden et al. 1990.



**Figure 3.3** Tectonic discrimination diagrams for all samples from Group 7 calc-alkaline rocks of the younger volcanic sequence of the Wild Bight Group. Fields defined by: a) Shervais 1982; b) Wood 1980; and c) Meschede 1986.



**Figure 3.4** Tectonic discrimination diagrams of all samples from groups 8, 9, 10, and 11 of the younger WBG sequence. Fields defined by: a) Wood 1980; b) Meschede 1986; and c) Shervais 1982.

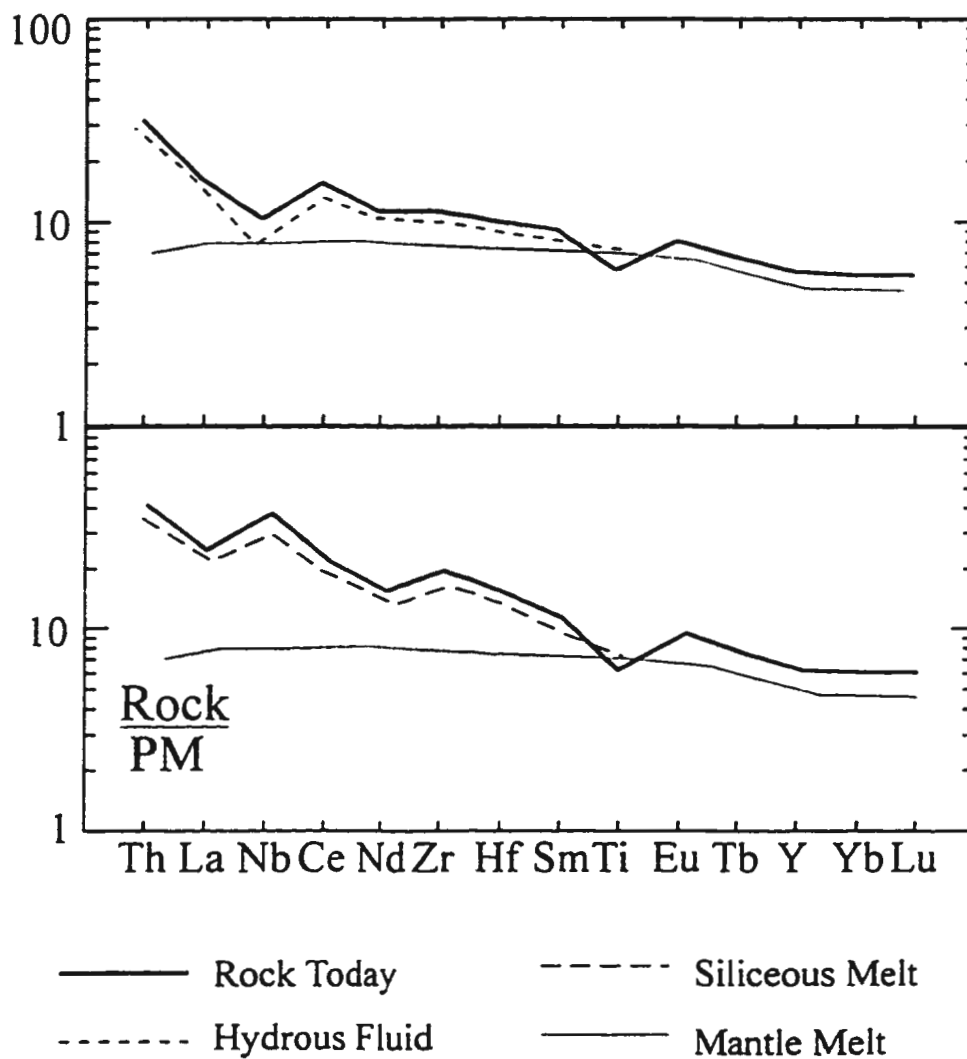


**Figure 3.5** Primitive mantle-normalized, extended-REE plots qualitatively showing the effect of mixing enriched mantle melts with different subduction zone components: a) group 7 calcalkaline rocks by addition of a hydrous fluid; b) group 10 rocks by addition of a partial melt. The mantle melt and rock today are real compositions from the field area. The mantle melt is the most primitive enriched tholeiite analysed with Mg# 58.

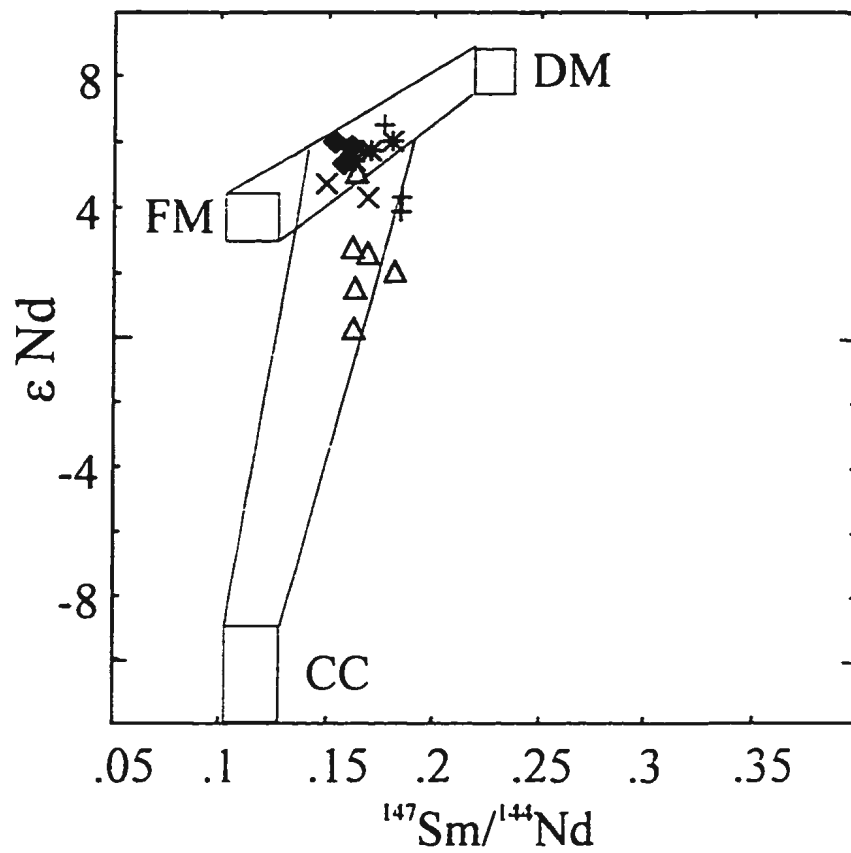
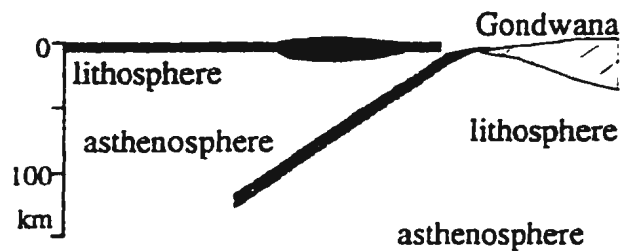
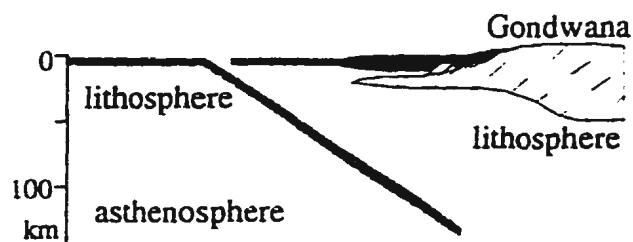


**Figure 3.6**  $\epsilon_{\text{Nd}}$  vs  $^{147}\text{Sm}/^{144}\text{Nd}$  showing the proposed isotopic components combined to create the volcanic rocks of the younger Wild Bight Group sequence. The end-member components are: DM, depleted mantle (MORB source); FM, fertile mantle; CC, continental crust, all calculated for the early Ordovician (Swinden et al. 1990).

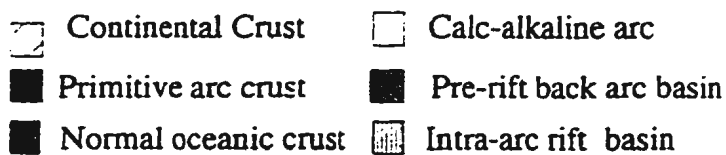
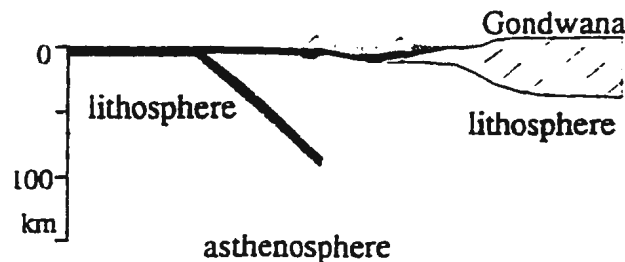
a) *~490-485 Ma.*  
**Formation of Primitive Intra-oceanic Arc**



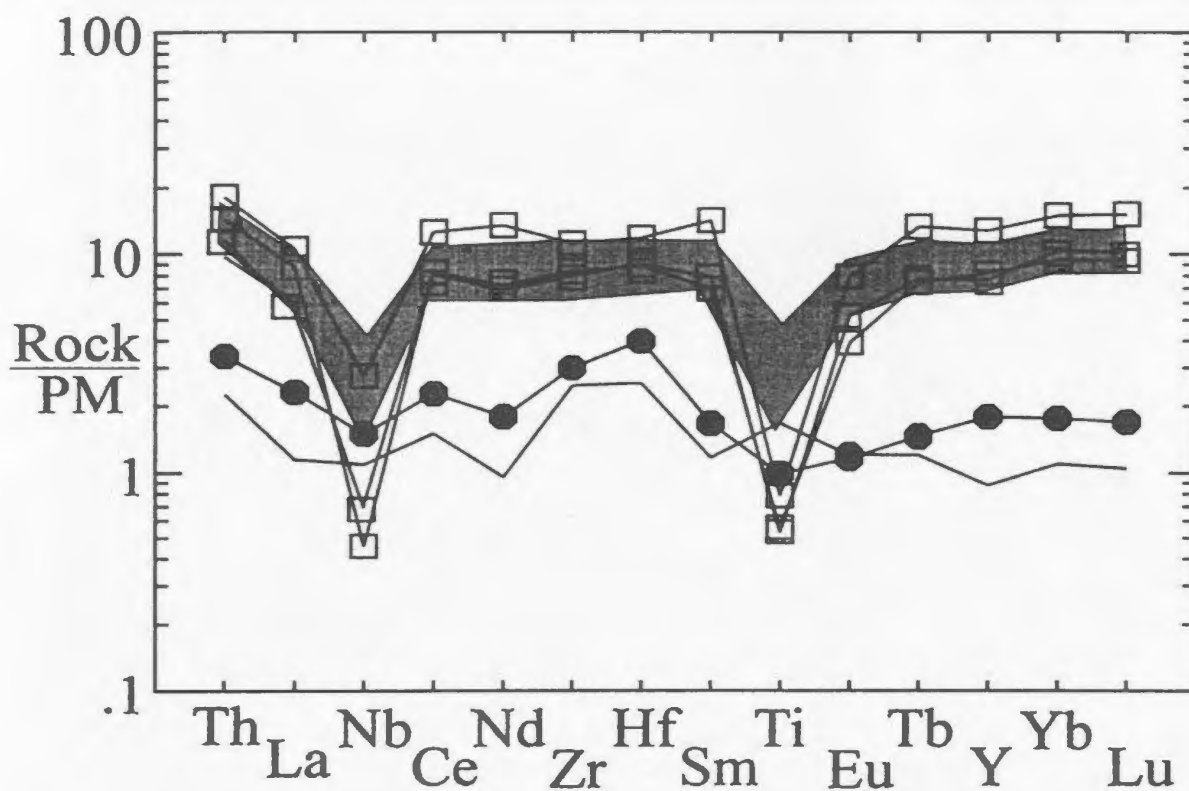
b) *~484 to 475 Ma.*  
**Partial Subduction of Gondwanan Margin and Subduction Polarity Reversal**



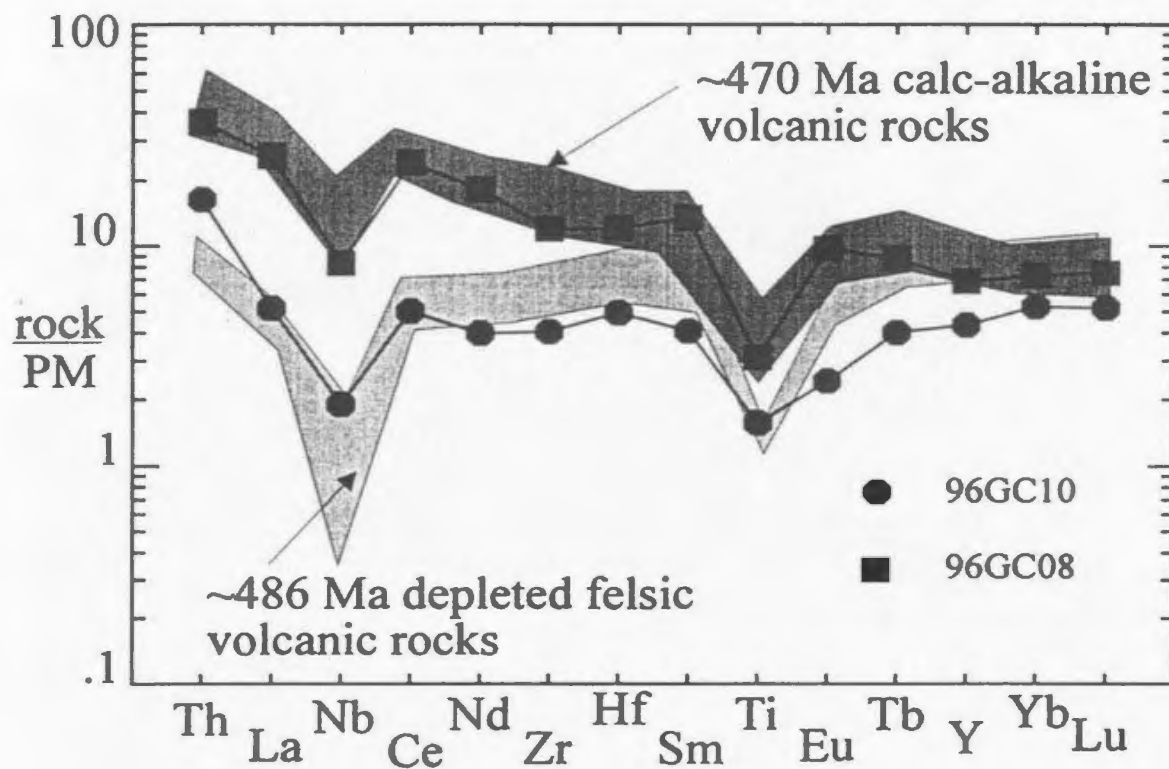
c) *~474 to 465 Ma.*  
**Calc-alkaline Arc and Arc Rifting**



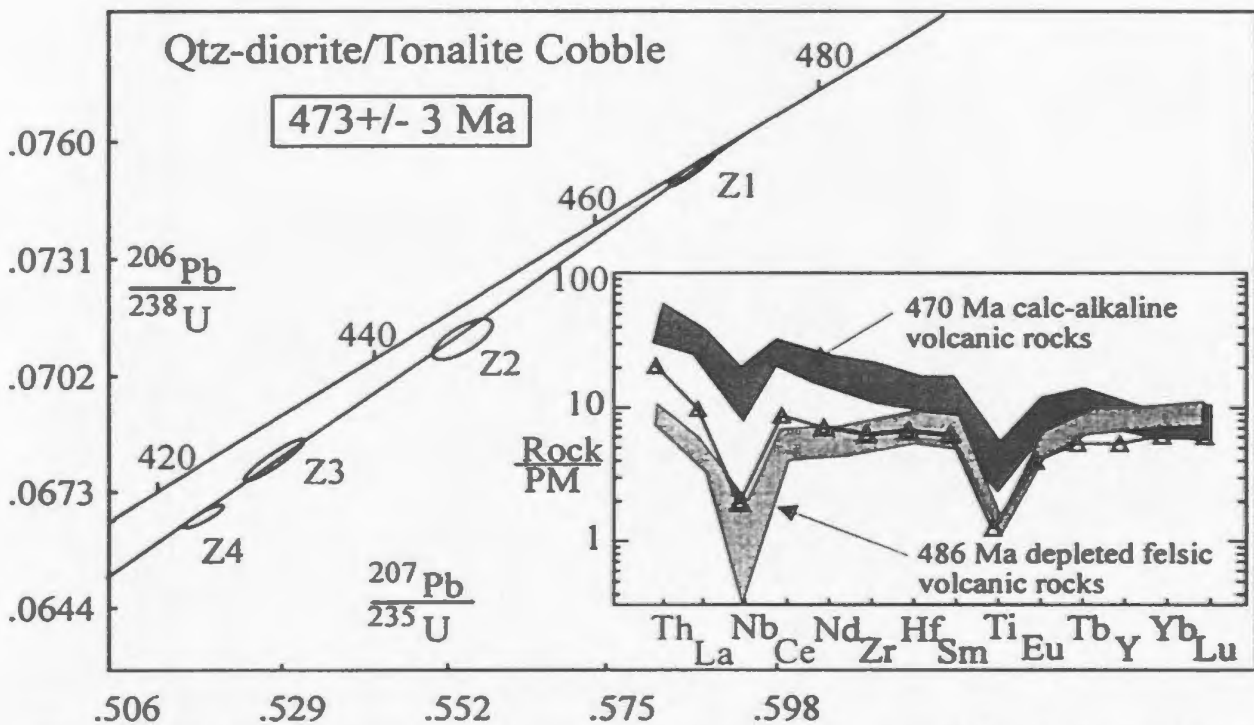
**Figure 3.7.** Plate tectonic model for the evolution of the younger volcanic sequence of the Wild Bight Group.



**Figure 4.1.** Primitive mantle-normalized, extended-REE plots of rhyolite blocks (open squares) from a debris flow and a boninitic olistolith (filled circle) from the younger WBG succession. Field shown is for felsic volcanic rocks of the older WBG sequence, and the plot without symbols is a boninitic volcanic rock from the older WBG package.

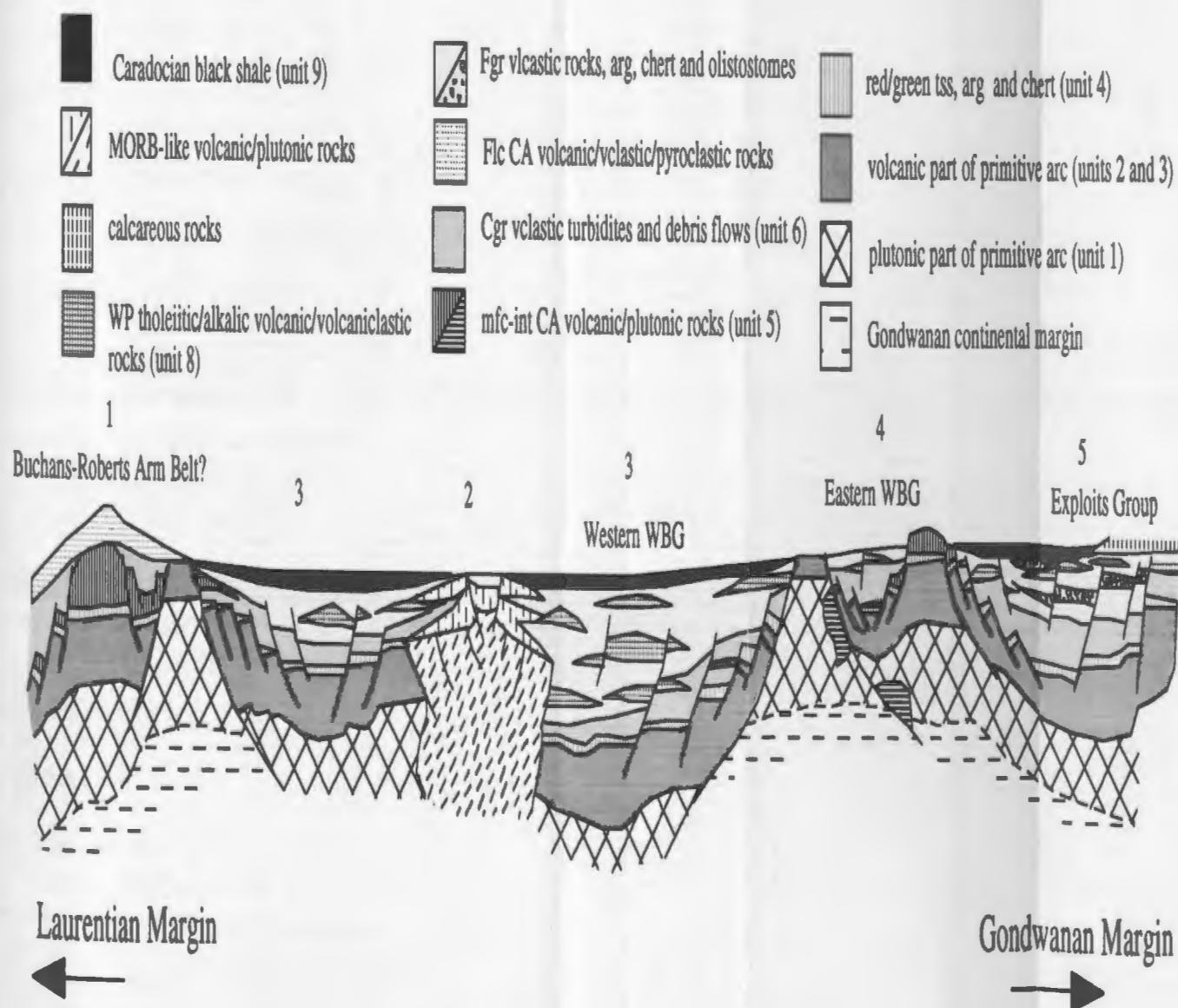


**Fig. 4.2.** Comparison of trace element compositions of rhyolite blocks in a debris flow within the younger WBG succession, compared with fields for felsic to intermediate volcanic rocks of both volcanic sequences of the WBG.



**Figure 4.3.** U-Pb concordia plot and primitive mantle-normalized extended-rare earth element (E-REE) plot for a diorite cobble from a conglomerate in the younger succession of the Wild Bight Group (WBG). Fields on the E-REE plot are for felsic to intermediate calc-alkaline volcanic rocks from the younger WBG sequence.

## Paleogeography of the late Arenig to Llanvirn Wild Bight/Exploits Arc





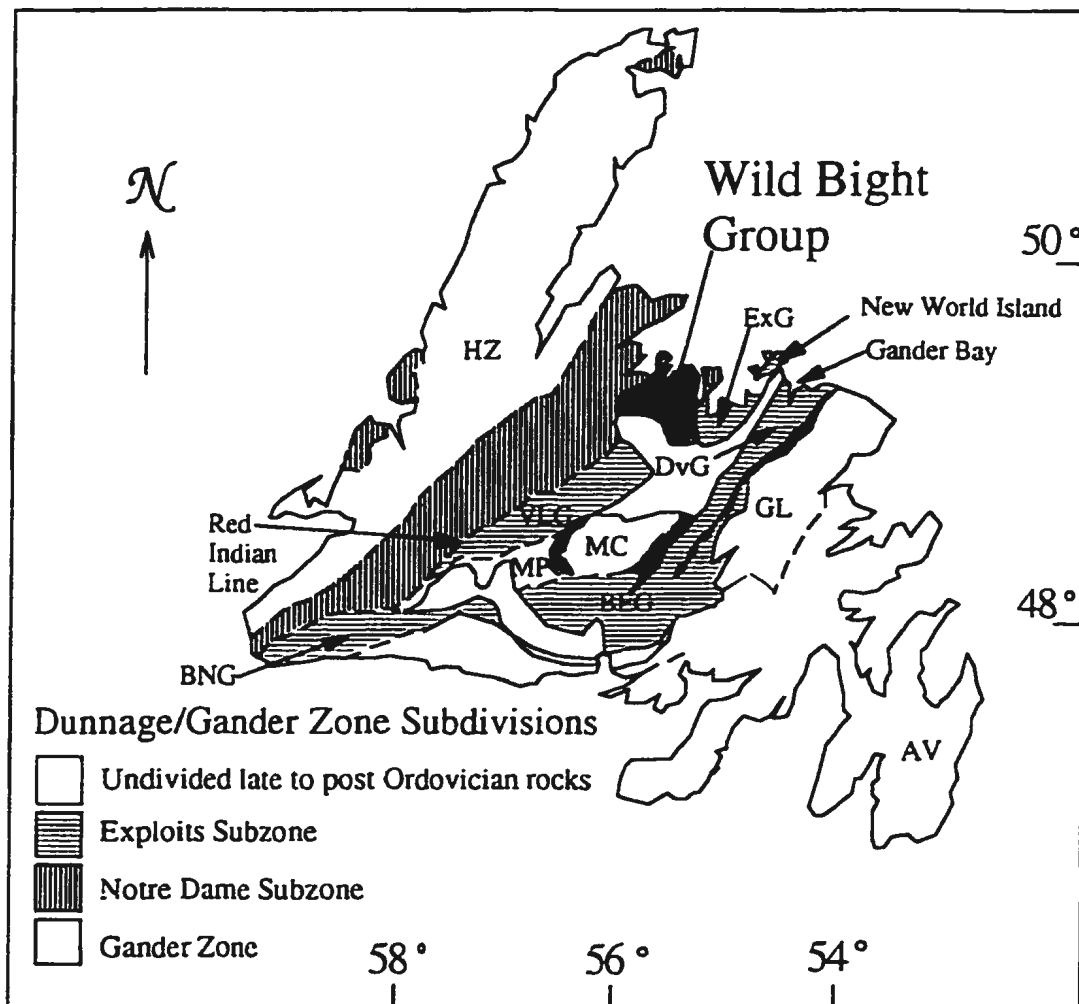
















**Figure 4.4** Schematic representation of possible paleogeography of the late Arenig to Llanvirn Wild Bight/Exploits Arc and rift-related basins. 1, active arc; 2, ensimatic spreading centre; 3, intra-arc rift basin; 4, remnant arc; 5, pre-rift back arc basin; E-thol, enriched tholeiitic; WP, within plate; vlastic, volcanoclastic; Fgr, fine-grained; Cgr, coarse-grained; arg, argillite; CA, calc-alkaline; mfc, mafic; int, intermediate; flc, felsic; tss, tuffaceous sandstone. Dashed lines are assumed structural contacts. Units in brackets refer to Map C1.



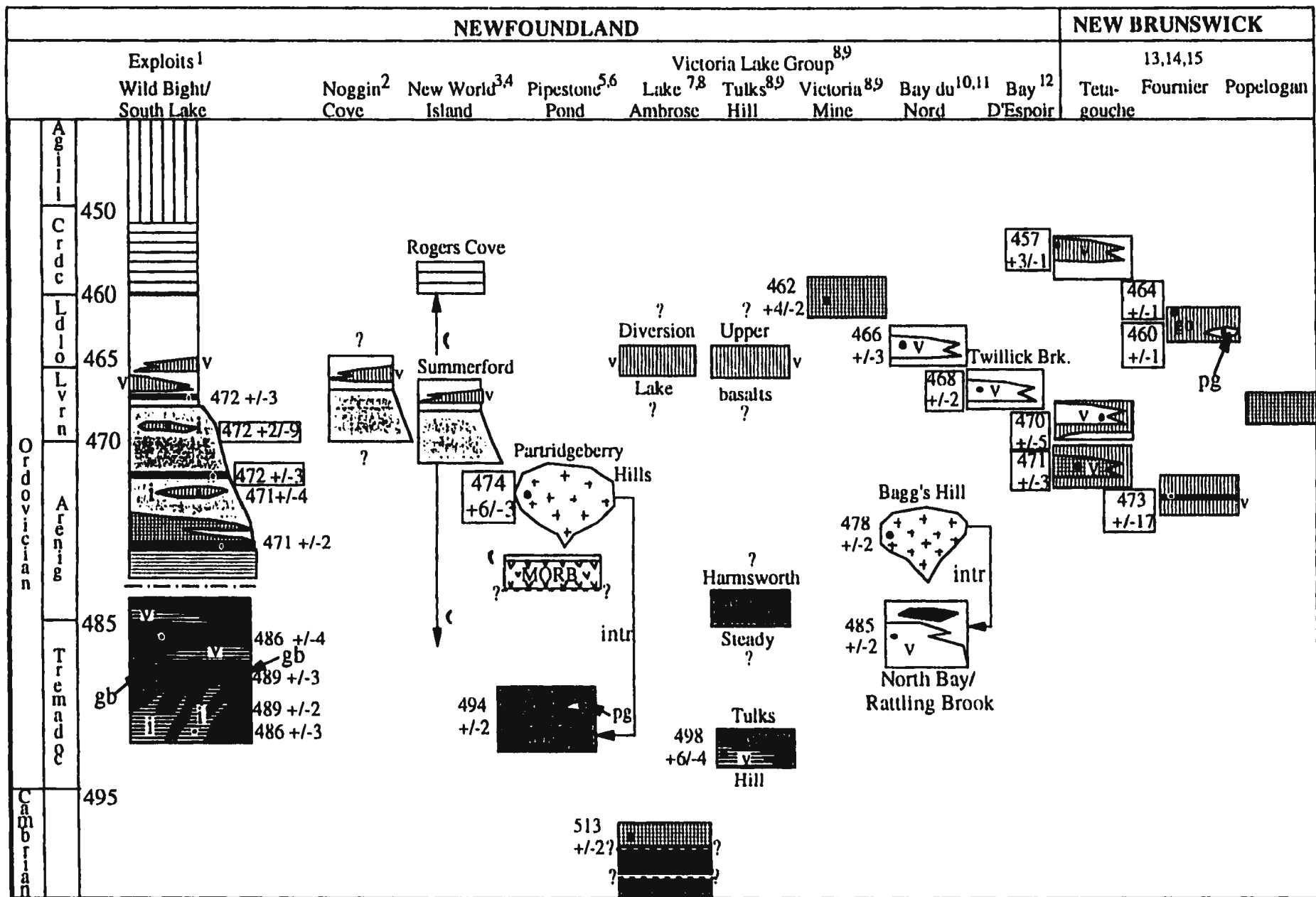
**Figure 5.1.** Tectonostratigraphic zones of the Newfoundland Appalachians. Exploits subzone ophiolites are shown in black. Units within the Avalon Zone (AV) and Humber Zone (HZ) are not differentiated. The pre-late Ordovician rocks of the Exploits and Gander zones are subdivided: ExG, Exploits Group; VLG, Victoria Lake Group; BNG, Bay du Nord Group; BEG, Bay d'Espoir Group; DvG, Davidsville Group; MP, Meelpaeg Subzone; MC Mount Cormack Subzone; and GL, Gander Lake Subzone. Dashed lines are major faults. Simplified from Colman-Sadd et al. 1992.

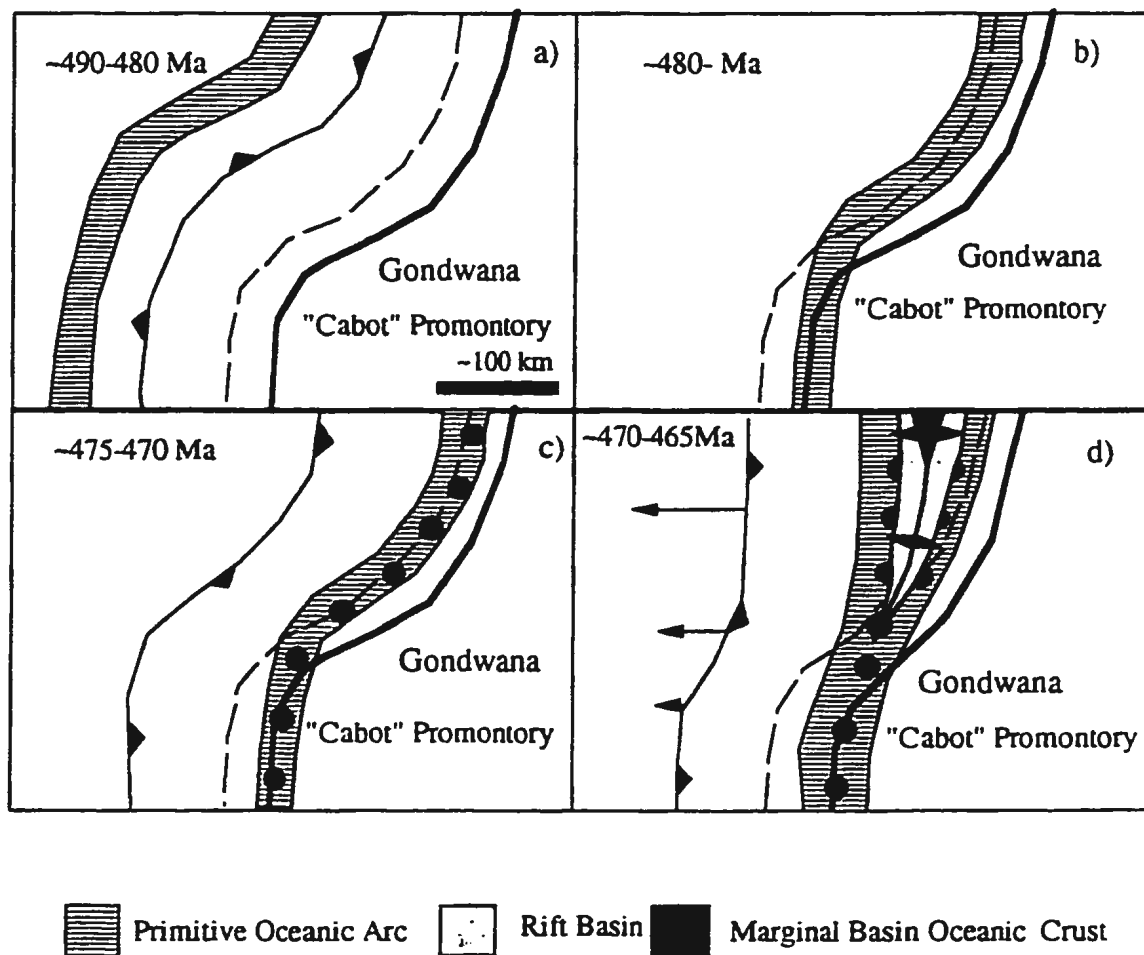
## Legend

	Point Leamington Greywacke		Felsic igneous rock, unknown geochemical type (i, intrusive; v, volcanic; pg, plagiogranite)
	Shoal Arm Formation (black shale)		Gabbro with mafic dyke swarms
	Fine-grained volcanoclastic/epiclastic rocks, +/- chert/argillite		Mafic dyke/amphibolite lense
	Within-plate tholeiitic to alkalic igneous rocks (v, volcanic; i intrusive)		Felsic tuff
	Coarse-grained volcanoclastic rocks		U/Pb dated sample, numbers with a box have Precambrian inheritance
	Calc-alkaline volcanic rocks		Unknown age
	Tuffaceous sandstone and argillite		Faulted contact
	Igneous rocks with island arc tholeiitic (IAT) compositions (v, volcanic; lgb, layered gabbro; gb, gabbro; um, ultramafic bnt, boninitic; n, normal; d, depleted)		Unknown stratigraphic relationship
	Felsic volcanic/plutonic rocks with depleted compositions (v, volcanic; i, intrusive)		Age range known from fossil occurrences

1, O'Brien et al. 1997; 2, Johnston et al. 1994; 3, Jacobi and Wasowski 1985; 4, Elliot et al. 1989; 5, Jenner and Swinden, 1992; 6, Dunning and Krogh 1985; 7, Dunning et al. 1991; 8, Evans et al. 1990; 9, Swinden et al. 1989; 10, Tucker et al. 1994; 11, Dunning et al. 1990; 12, Colman-Sadd et al. 1992; 13, van Staal et al. 1991; 14, Sullivan and van Staal 1996; and 15, Sullivan et al. 1990.

**Figure 5.2.** Compilation of ages and geochemical affiliations of peri-Gondwanan early- to middle-Ordovician volcanic sequences in Newfoundland and New Brunswick, and interpreted correlations with the Wild Bight Group and South Lake Igneous Complex. Time Scale of Tucker and McKerrow 1995.







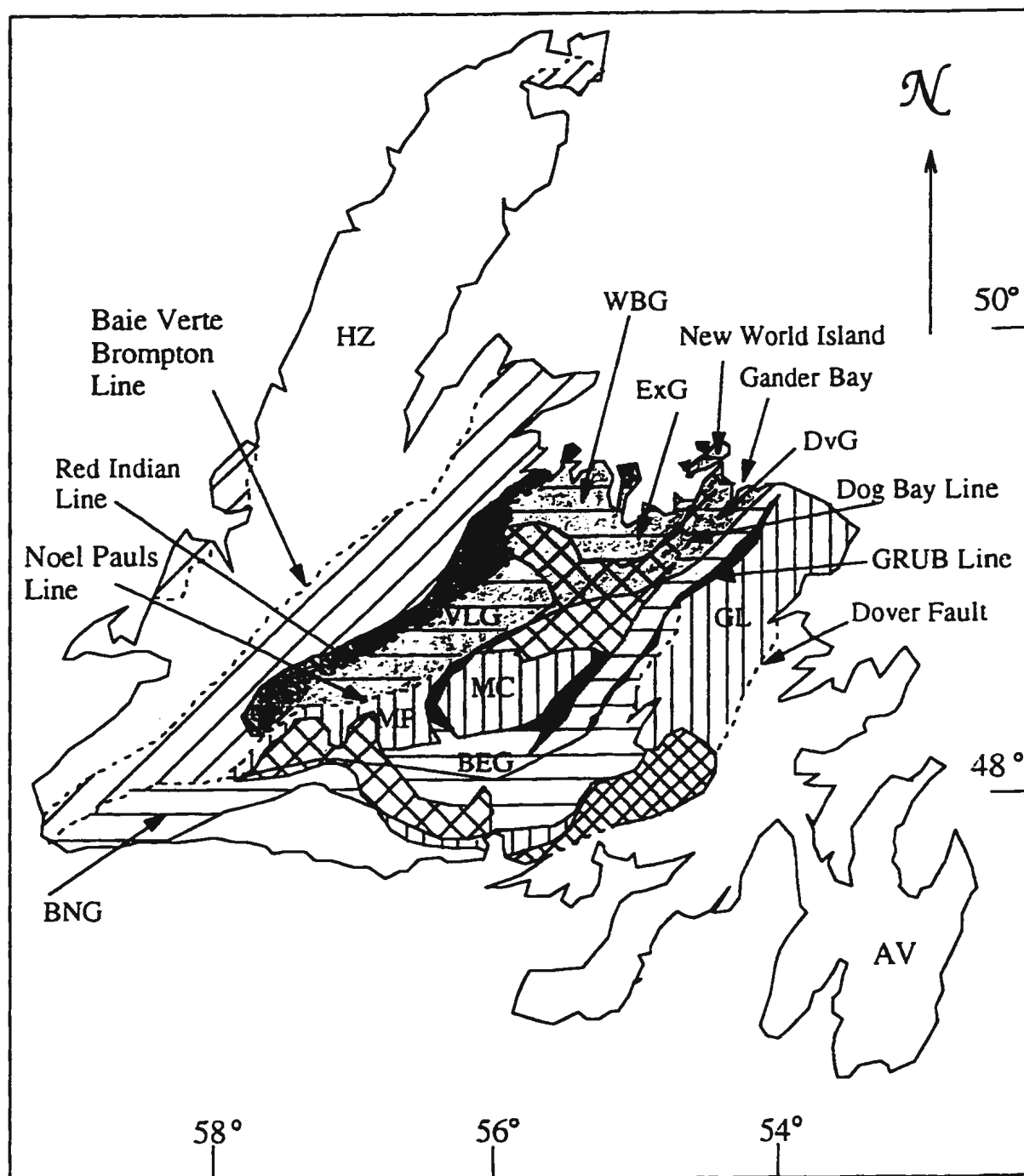







**Figure 5.3** Schematic diagram showing the variable degree to which late Arenig peri-Gondwanan arcs (or arc) might have interacted with the continental margin, as a result of a promontory (e.g., Cabot Promontory Lin et al. 1994). Heavy solid line is the western limit of thick continental crust; dashed line is the limit of thinned continental crust; circles represent a calc-alkaline arc formed on the Gondwanan margin; and the ornamented lines are subduction zones, with ornaments on the overriding plate.



### Possible Ordovician Tectonic Divisions of the Dunnage/Gander Zone

-  Significant Penobscot compression/little or no late Arenig-Llanvirn extension
-  Little or no Penobscot compression/dominated by late Arenig-Llanvirn extension
-  Late Arenig-Llanvirn active arc ? (Buchans-Roberts Arm Belt)

### Dunnage/Gander Zone subdivisions

-  Undivided late to post-Ordovician rocks
-  Exploits Subzone
-  Notre Dame Subzone (mafic belt)
-  Notre Dame Subzone (bimodal belt)
-  Gander Zone
-  Post-Ordovician structural breaks/ tectonic subdivisions of the Dunnage and Gander zones

**Figure 5.4.** Interpretation of possible Ordovician tectonic domains of the Dunnage and Gander zones of the Newfoundland central mobile belt. Post- Ordovician structural breaks and subzone boundaries after Williams 1995 (except Dog Bay Line from Williams et al. 1993). The division of volcanic belts in the Notre Dame Subzone is after Williams 1995. This model only defines broad zones, based on regional structural and stratigraphic relationships. There are no discrete boundaries between regions, they are likely gradational. Various rock groups and subzones of the Dunnage and Gander zones are: BNG, Bay du Nord Group; BEG, Bay d'Espoir Group; DvG, Davidsville Group; ExG, Exploits Group; WBG, Wild Bight Group; GL, Gander Lake; MP, Meelpaeg; and MC, Mount Cormack. The Humber zone (HZ) and Avalon Zone (AZ) are not subdivided. See text for further explanation.

**Table 2.1. U-Pb data for samples from the older volcanic sequence of the Wild Bight Group and the SLIC**

Fractions <sup>a</sup>	weight mg	U ppm	Pb <sub>rad</sub> ppm <sup>b</sup>	Pb <sub>com</sub> pg <sup>c</sup>	<sup>206</sup> Pb <sup>c</sup> <sup>204</sup> Pb	<sup>208</sup> Pb <sup>206</sup> Pb	-----Corrected atomic ratios <sup>d</sup> -----			Age (Ma)		
							<sup>206</sup> Pb <sup>238</sup> U	<sup>207</sup> Pb <sup>235</sup> U	<sup>207</sup> Pb <sup>206</sup> Pb	<sup>206</sup> Pb <sup>238</sup> U	<sup>207</sup> Pb <sup>235</sup> U	<sup>207</sup> Pb <sup>206</sup> Pb
<b>Tonalite (GD91-6 (A) 609800E, 5471800N; D47-10(B) 509350E, 5471375N)</b>												
AZ1 m3 ang clr abr	0.008	1433	110.9	36	1548	0.1052	0.07743 (44)	0.6051 (36)	0.05668 (16)	481	480	479
AZ2 1.7A clr brn frags abr	0.018	1486	112.5	36	3573	0.1039	0.07584 (36)	0.5952 (28)	0.05691 (14)	471	474	488
AZ3 brn crkd abr	0.016	2267	160.1	47	3402	0.1198	0.06977 (50)	0.5446 (38)	0.05661 (18)	435	441	476
AZ4 m3 brn ang abr	0.035	1840	128.8	118	2384	0.1182	0.06924 (42)	0.5405 (32)	0.05662 (10)	432	439	477
AZ5 brn frags abr	0.109	1921	131.2	219	4104	0.1083	0.06813 (26)	0.5343 (22)	0.05687 (06)	425	435	487
BZ1 abr	0.043	911	67.6	12	15262	0.0586	0.07747 (28)	0.6071 (22)	0.05684 (08)	481	482	485
BZ2 frags abr	0.010	555	40.7	11	2508	0.0474	0.07725 (58)	0.6059 (40)	0.05689 (26)	480	481	487
BZ3 brn frags abr	0.026	1395	101.9	21	8268	0.0647	0.07573 (50)	0.5936 (38)	0.05685 (14)	471	473	486
BZ4 clr frags abr	0.034	921	66.8	10	14533	0.0612	0.07551 (30)	0.5913 (24)	0.05680 (06)	469	472	484
BZ5 brn frags abr	0.024	2471	177.3	15	18401	0.0714	0.07397 (46)	0.5785 (36)	0.05672 (12)	460	464	481
BZ6 frags abr	0.070	1358	91.1	47	8775	0.0620	0.06977 (24)	0.5443 (20)	0.05658 (06)	435	441	475
<b>Gabbro pegmatite (94GC03 608400E, 5464500N)</b>												
Z1 clr prisms abr	0.150	178	13.5	4	31173	0.0702	0.07805 (26)	0.6126 (22)	0.05693 (10)	484	485	489
Z2 clr mf abr	0.299	279	20.9	6	64238	0.0556	0.07802 (26)	0.6118 (22)	0.05687 (06)	484	485	487
Z3 clr mf abr	0.306	204	15.2	28	10857	0.0580	0.07796 (22)	0.6114 (20)	0.05688 (06)	484	484	487
Z4 clr prisms abr	0.131	214	16.1	3	50555	0.0685	0.07772 (24)	0.6091 (20)	0.05684 (08)	483	483	485
Z5 unabr clr needles	0.105	810	57.2	21	19500	0.0081	0.07718 (24)	0.6048 (20)	0.05683 (06)	479	480	485
Z6 unabr clr prisms	0.307	413	30.5	36	16611	0.0774	0.07578 (24)	0.5928 (20)	0.05674 (06)	471	473	481

**Hornblende Diorite (94G C04 610150E, 5470150N)**

Z1 clr prisms abr	0.040	206	15.6	29	1380	0.0746	0.07799 (44)	0.6137 (36)	0.05707 (18)	484	486	494
Z2 clr frags abr	0.015	701	53.4	4	11878	0.0835	0.07763 (48)	0.6080 (36)	0.05680 (16)	482	482	484
Z3 clr frags abr	0.030	337	25.4	4	10967	0.0717	0.07749 (30)	0.6085 (22)	0.05695 (12)	481	483	490
Z4 clr prisms abr	0.126	237	17.8	10	14467	0.0771	0.07720 (22)	0.6056 (18)	0.05690 (08)	479	481	488
Z5 clr prisms abr	0.107	227	17.1	10	11155	0.0815	0.07708 (30)	0.6053 (24)	0.05696 (10)	479	481	490

**Alkalic Gabbro Dyke (GHG 610200E, 5480650N)**

B1 nm3 lrg ang subh unabr	0.045	615	43.5	241	557	0.0413	0.07485 (28)	0.5868 (30)	0.05686 (18)	465	469	486
B2 dk plates unabr	0.024	870	62.6	120	808	0.0957	0.07262 (34)	0.5678 (30)	0.05671 (18)	452	457	480
B3 nm3 small clr plates abr	0.029	722	49.0	258	383	0.0415	0.07190 (32)	0.5646 (32)	0.05695 (22)	448	454	489
B4 m3/5 weakly abr	0.031	761	50.6	53	1945	0.0658	0.06893 (36)	0.5402 (28)	0.05683 (18)	430	439	485
B5 clr eq brn abr	0.045	885	57.2	108	1586	0.0499	0.06793 (58)	0.5313 (40)	0.05672 (32)	424	433	481

<sup>a</sup> Z, zircon; B, baddeleyite; mf, multifaceted; ang, angular; crkd, cracked; eq, equant; subh, subhedral; clr, clear; lrg, large; brn, brown; dk, dark; frags, fragments; unabr, unabraded ; m3, magnetic 3 $\infty$  fraction; non magnetic 3 $\infty$  fraction; 1.7A, 1.7amp fraction

<sup>b</sup> Total radiogenic Pb after correction for blank, common Pb and spike.

<sup>c</sup> measured.

<sup>d</sup> Ratios corrected for fractionation, spike, 5-10 pg laboratory blank, initial common Pb (calculated with Stacey and Kramers (1975) for the age of the sample), and 1pg U blank.

**Table 2.2.** Major oxide and trace element data for samples plotted on E-REE diagrams.

	bon. <sup>a</sup>	IAT <sup>b</sup>	N- MORB <sup>c</sup>	95025B gr5	96005 gr5	95149 gr4	96054 gr4	94014 gr3	94GC03 gr3
Mg# <sup>d</sup>	56	50	NR	65	62	49	46	80	73
SiO <sub>2</sub> wt%	58.44	50.70	NR	51.32	53.17	55.04	53.23	49.27	49.66
TiO <sub>2</sub>	0.15	1.29	1.36	0.32	0.16	0.70	0.47	0.28	0.13
Al <sub>2</sub> O <sub>3</sub>	10.99	16.60	NR	16.23	15.28	13.77	16.00	10.93	15.45
Fe <sub>2</sub> O <sub>3</sub> T	9.50	1.01	NR	13.45	9.49	14.19	13.78	9.52	8.74
FeO*	NR	6.68	NR	ND	ND	ND	ND	ND	ND
MnO	0.17	0.16	NR	0.20	0.17	0.25	0.21	0.16	0.18
MgO	12.09	7.70	NR	11.55	7.21	6.29	5.44	17.08	10.99
CaO	7.32	11.12	NR	2.74	7.63	4.80	3.29	11.26	13.78
Na <sub>2</sub> O	1.70	3.20	NR	5.34	5.44	3.92	4.88	1.04	0.32
K <sub>2</sub> O	0.50	0.34	NR	0.08	0.08	0.20	0.44	0.14	0.17
P <sub>2</sub> O <sub>5</sub>	0.02	0.19	NR	0.01	0.01	0.03	0.02	0.02	0.01
LOI	3.81	NR	NR	4.73	3.90	2.98	3.83	2.38	1.92
total	100.88	NR	NR	97.53	98.74	99.27	97.84	99.98	99.52
V (ppm)	191	NR	NR	228	268	455	483	213	172
Nb	BD	5.0	0.7	0.7	0.5	0.5	0.4	0.2	0.2
Hf	NR	NR	0.3	0.7	0.3	0.5	0.2	0.3	0.2
Zr	22.0	107.0	9.8	24.2	11.4	15.9	4.0	8.7	6.3
Y	4.6	29.0	3.9	3.4	3.5	10.9	6.8	7.1	6.3
Th	NR	0.5	0.1	0.2	0.1	0.2	BD	0.1	0.1
La	1.1	5.0	0.6	0.7	0.5	0.8	0.2	0.4	0.3
Ce	2.6	16.1	NR	2.4	1.2	2.3	0.7	1.2	1.1
Pr	NR	NR	NR	0.3	0.2	0.4	0.1	0.2	0.2
Nd	1.5	11.1	1.2	1.2	0.8	2.2	0.9	1.2	1.2
Sm	0.5	3.3	0.4	0.5	0.3	1.0	0.6	0.5	0.5
Eu	0.2	1.3	0.2	0.2	0.1	0.4	0.2	0.2	0.2
Tb	NR	NR	0.1	0.1	0.1	0.3	0.2	0.2	0.2
Dy	0.8	4.7	NR	0.8	0.6	1.9	1.1	1.1	1.2
Ho	NR	NR	NR	0.2	0.1	0.4	0.3	0.3	0.3
Er	0.6	NR	NR	0.5	0.4	1.4	0.8	0.8	0.8
Tm	NR	NR	NR	0.1	0.1	0.2	0.1	0.1	0.1
Yb	0.7	2.9	0.4	0.5	0.5	1.4	1.0	0.8	0.8
Lu	0.1	NR	0.1	0.1	0.1	0.2	0.2	0.1	0.1

NR, not reported; ND, not determined; BD, below detection limit.

Fe<sub>2</sub>O<sub>3</sub>T, total Fe as Fe<sub>2</sub>O<sub>3</sub>; FeO\* FeO and Fe<sub>2</sub>O<sub>3</sub> were measured for some samples.<sup>a</sup> sample 780/59, Taylor et al. 1994.<sup>b</sup> East Scotia Sea dredge 20, from Saunders and Tarney 1991.<sup>c</sup> commonly used MORB normalizing values from Sun and McDonough, 1989.<sup>d</sup> Mg# is cation %, with FeO=0.7xFe<sub>2</sub>O<sub>3</sub>T and Fe<sub>2</sub>O<sub>3</sub>=0.3xFe<sub>2</sub>O<sub>3</sub>T

	94007	94044	94009	94012	94043	94013	94045	96010	96055	96057
	gr3	gr3	gr2	gr2	gr2	gr1	gr1	gr1	gr1	gr1
Mg#	69	66	62	59	70	50	50	46	39	43
SiO <sub>2</sub> wt%	49.75	49.54	49.73	47.00	51.75	46.81	50.20	45.39	51.11	52.60
TiO <sub>2</sub>	0.29	0.49	0.61	0.46	0.29	1.29	1.24	0.01	1.53	1.31
Al <sub>2</sub> O <sub>3</sub>	15.83	14.01	15.45	15.45	13.87	16.92	15.41	16.66	15.10	15.35
Fe <sub>2</sub> O <sub>3</sub> T	9.28	12.38	10.52	10.17	9.12	15.38	13.05	13.95	15.72	14.40
FeO*	ND	ND	ND	ND	ND	ND	ND	ND	ND	ND
MnO	0.15	0.24	0.18	0.17	0.16	0.22	0.19	0.33	0.13	0.19
MgO	9.74	11.18	8.22	6.97	9.82	7.22	6.28	5.52	4.71	5.06
CaO	11.64	10.12	12.09	12.24	10.91	6.19	9.62	5.53	5.57	4.48
Na <sub>2</sub> O	2.73	1.55	1.71	0.75	2.04	4.02	2.67	5.00	5.66	5.50
K <sub>2</sub> O	0.37	0.27	0.43	0.17	0.61	0.02	0.43	0.65	0.07	0.26
P <sub>2</sub> O <sub>5</sub>	0.02	0.02	0.04	0.03	0.02	0.10	0.08	0.08	0.14	0.17
LOI	1.95	2.05	2.07	2.07	1.75	5.59	1.24	6.62	2.24	2.37
total	99.89	99.93	99.06	92.52	98.71	98.24	99.93	93.22	99.84	99.39
V (ppm)	264	354	370	343	270	520	483	510	511	460
Nb	0.5	0.6	0.5	0.5	0.3	1.0	1.2	0.9	2.9	2.6
Hf	0.3	BD	0.7	0.7	0.4	1.6	1.1	1.2	2.3	2.1
Zr	6.3	6.0	21.8	21.9	9.7	55.4	44.5	40.6	93.3	82.0
Y	7.1	8.5	12.4	12.6	8.2	23.8	23.6	21.7	25.8	27.8
Th	0.1	BD	0.2	0.2	0.1	0.5	0.4	0.3	0.8	0.6
La	0.5	0.4	1.1	1.1	0.6	2.9	2.4	2.6	5.4	2.7
Ce	1.4	1.3	3.2	3.2	1.7	8.3	7.0	6.8	14.5	8.4
Pr	0.2	0.2	0.5	0.5	0.3	1.3	1.1	1.1	2.1	1.4
Nd	1.1	1.4	3.2	3.1	1.6	7.1	6.1	6.2	10.9	7.9
Sm	0.6	0.6	1.3	1.2	0.6	2.6	2.1	2.4	3.3	2.9
Eu	0.3	0.4	0.5	0.5	0.3	1.0	1.0	1.0	1.1	0.9
Tb	0.2	0.2	0.3	0.3	0.2	0.6	0.6	0.6	0.7	0.7
Dy	1.2	1.4	2.4	2.3	1.4	4.4	3.8	3.8	4.5	4.8
Ho	0.3	0.3	0.5	0.5	0.3	0.9	0.8	0.8	1.0	1.1
Er	0.8	1.0	1.5	1.5	1.0	2.8	2.5	2.3	3.0	3.4
Tm	0.1	0.1	0.2	0.2	0.1	0.4	0.4	0.3	0.4	0.5
Yb	0.8	1.0	1.5	1.4	1.0	2.7	2.3	2.1	3.0	3.4
Lu	0.1	0.1	0.2	0.2	0.2	0.4	0.3	0.3	0.4	0.5

	96065	94018	94042
	rhy	mlt	mlt
Mg#	18	26	32
SiO <sub>2</sub> wt%	73.58	74.95	76.31
TiO <sub>2</sub>	0.28	0.26	0.15
Al <sub>2</sub> O <sub>3</sub>	12.27	12.92	12.61
Fe <sub>2</sub> O <sub>3</sub> T	4.28	3.40	0.73
FeO*	ND	ND	ND
MnO	0.05	0.07	BD
MgO	0.45	0.56	0.16
CaO	3.13	2.07	3.58
Na <sub>2</sub> O	4.07	4.61	3.69
K <sub>2</sub> O	0.33	0.53	0.25
P <sub>2</sub> O <sub>5</sub>	0.05	0.04	0.02
LOI	0.89	1.27	0.48
total	98.49	99.43	97.50
V (ppm)	20	19	5
Nb	1.8	1.2	1.5
Hf	1.9	1.9	3.6
Zr	61.9	60.2	118.4
Y	30.5	27.3	51.5
Th	1.0	0.9	1.3
La	3.6	3.8	6.0
Ce	9.3	9.8	16.1
Pr	1.4	1.4	2.5
Nd	7.4	7.3	13.1
Sm	2.8	2.5	4.6
Eu	0.8	0.7	0.9
Tb	0.7	0.6	1.2
Dy	5.2	4.7	8.5
Ho	1.2	1.0	1.9
Er	3.8	3.1	5.8
Tm	0.6	0.5	0.9
Yb	3.9	3.3	5.9
Lu	0.6	0.5	0.9

**Table 2.3.** Sm-Nd isotopic data for samples from the old volcanic sequence of the Wild Bight Group and South Lake igneous complex.

Sample	Group	Sm <sup>a</sup>	Nd <sup>a</sup>	<sup>143</sup> Nd/ <sup>144</sup> Nd <sup>b*</sup>	<sup>147</sup> Sm/ <sup>144</sup> Nd <sup>c*</sup>	ε Nd <sup>d</sup>
94056	gr1	2.46	7.19	0.512964 (11)	0.20413 (08)	5.9
94013	gr1	2.56	7.12	0.513001 (12)	0.21906 (07)	5.7
94045	gr1	2.11	5.94	0.513002 (62)	0.21937 (01)	5.7
96055	gr1	3.62	10.55	0.512863 (08)	0.21163 (03)	3.5
96058	gr1	2.15	5.43	0.512919 (06)	0.24376 (08)	2.6
94GC04	gr2	1.59	4.12	0.513008 (13)	0.23063 (07)	5.1
94009	gr2	1.25	3.08	0.513051 (14)	0.24296 (06)	5.2
94042	gr2	4.37	12.66	0.512976 (09)	0.20585 (02)	6.0
95153	gr2	1.39	3.17	0.513180 (51)	0.27017 (09)	6.0
95154	gr2	1.42	3.48	0.513101 (09)	0.25164 (32)	5.6
96009	gr2	0.78	1.59	0.513109 (16)	0.30341 (10)	2.6
94GC03	gr3	0.56	1.35	0.513107 (18)	0.24861 (03)	5.9
94041	gr3	0.58	1.01	0.513061 (11)	0.34161 (03)	-0.7
94014	gr3	0.79	2.38	0.513075 (24)	0.19909 (05)	6.3
94044	gr3	0.60	1.38	0.513141 (260)	0.26944 (04)	5.3
95112	gr3	0.37	0.53	0.513753 (24)	0.4243 (35)	7.7
95149	gr4	0.81	2.07	0.513054 (11)	0.24088 (07)	5.4
96054	gr4	0.44	0.68	0.513626 (84)	0.39772 (09)	6.8
95025B	gr5	0.45	0.81	0.513369 (40)	0.34611 (07)	5.0
95053	gr5	6.96	28.20	0.512741 (09)	0.15245 (04)	4.8
96005	gr5	0.27	0.69	0.513045 (40)	0.24287 (05)	5.1
94018	tnlt	2.49	7.02	0.512879 (12)	0.21121 (04)	3.8
94GC06	tnlt	0.92	2.78	0.513191 (21)	0.19744 (06)	8.6
94051	tnlt	2.58	7.66	0.512895 (09)	0.20773 (03)	4.3
96060	rhy	3.33	8.22	0.512986 (19)	0.24986 (08)	3.5

<sup>a</sup> concentration in ppm from isotope dilution

<sup>b</sup> measured and corrected for mass fractionation

<sup>c</sup> calculated from measured <sup>147</sup>Sm/<sup>149</sup>Sm and <sup>150</sup>Nd/<sup>144</sup>Nd

<sup>d</sup> calculated for UR at 485 Ma

\* number in brackets is the two sigma error in the last two decimal places

**Table 2.4.** Element ratios and abundances which characterize the most primitive rocks used to define the geochemical groups in Fig. 2.4, and examples of similar modern rock types taken from the literature (see table 2.2 for data and references).

	<b>Mg#</b>	<b>CaO/Al<sub>2</sub>O<sub>3</sub></b>	<b>TiO<sub>2</sub></b>	<b>(La/Yb)<sub>N</sub></b>	<b>(Zr/Sm)<sub>N</sub></b>
<b>Group 1</b>	39-50	0.30-0.62	1.1-1.25	0.75-1.0	0.97-1.10
<b>Group 2</b>	59-70	0.8	0.3-0.6	0.75	0.91
<b>Group 3</b>	66-80	0.7-1.0	0.3-0.5	0.3	0.6
<b>Group 4</b>	46-49	0.3-0.35	0.5-0.7	0.14	0.6
<b>Group 5</b>	62-65	0.2-0.5	0.16-0.32	1	1.3
<b>Boninite*</b>	56	0.7	0.15	1	1.25
<b>N-MORB*</b>	46	0.76	1.36	0.6	0.95
<b>IAT*</b>	50	0.67	1.29	1.14	1.17

<sub>N</sub> ratio of primitive mantle-normalized values

\* for data and reference see Table 2.2

**Table 3.1.** U-Pb analytical data for samples from the younger WBG volcanic and intrusive rocks

Fractions <sup>a</sup>	Weight mg	U ppm	Pb <sub>rad</sub> ppm <sup>b</sup>	Pb <sub>con</sub> pg <sup>c</sup>	<sup>206</sup> Pb/ <sup>234</sup> Pb	Corrected Atomic Ratios <sup>d</sup>				Age (Ma) <sup>e</sup>		
						<sup>206</sup> Pb/ <sup>238</sup> U	<sup>206</sup> Pb/ <sup>234</sup> U	<sup>207</sup> Pb/ <sup>235</sup> U	<sup>207</sup> Pb/ <sup>206</sup> Pb	<sup>206</sup> Pb/ <sup>238</sup> U	<sup>207</sup> Pb/ <sup>235</sup> U	<sup>207</sup> Pb/ <sup>206</sup> Pb
Pig Island Tuff (95GC09 610000E, 5479500N)												
Z1 clr prisms abr	0.004	293	22.4	11	563	0.1301	0.07484 (60)	0.5853 (78)	0.05672 (72)	465	468	481
Z2 clr prisms abr	0.004	206	16.0	5	808	0.1409	0.07545 (48)	0.5887 (52)	0.05658 (36)	469	470	475
Z3 clr prisms abr	0.001	4135	326.3	24	831	0.1548	0.07570 (40)	0.5900 (38)	0.05653 (26)	470	471	473
Z4 clr prisms abr	0.001	2768	213.0	29	463	0.1314	0.07530 (34)	0.5886 (36)	0.05670 (26)	468	470	480
Duck Island Tuff (95057 609450E, 5481250N)												
Z1 clr prisms abr	0.001	1528	120.2	30	259	0.1528	0.07562 (44)	0.5880 (80)	0.05639 (70)	470	470	468
Z2 clr prisms abr	NM	—	—	7	4575	0.1531	0.07503 (38)	0.5845 (24)	0.05650 (18)	466	467	472
Z3 clr prisms abr	0.004	1250	96.7	5	5837	0.1441	0.07489 (54)	0.5835 (36)	0.05650 (24)	466	467	472
Z4 trb prism frags abr	0.014	4405	332.5	819	335	0.2127	0.06911 (42)	0.5370 (44)	0.05635 (32)	431	436	466
Z5 single prism tip	0.004	438	288.9	27	303	9.5720	0.07145 (52)	0.8835 (86)	0.08968 (58)	445	643	1419
Locks Harbour Tuff (95092 608050E, 5479950 N)												
Z1 clr prisms abr	0.008	675	52.5	15	1648	0.1394	0.07562 (42)	0.5895 (32)	0.05654 (28)	470	471	473
Z2 clr prisms abr	0.009	512	39.6	16	1320	0.1400	0.07520 (60)	0.5852 (44)	0.05644 (38)	467	468	470
Gabbro Sill (95GC10 611800E, 5478950N)												
B1 flakes unabr	0.001	2581	179.8	36	356	0.0252	0.07494 (38)	0.5832 (54)	0.05644 (44)	466	466	470
B2 frags unabr	0.001	1437	99.2	5	1289	0.0251	0.07427 (44)	0.5779 (40)	0.05643 (36)	462	463	469
Z1 thin clr frags abr	0.001	2728	219.9	26	450	0.3644	0.06587 (30)	0.5090 (40)	0.05605 (34)	411	418	454
Z2 5 mf prisms unabr	0.003	202	21.1	3	1029	0.3721	0.08441 (50)	0.7268 (64)	0.06244 (44)	522	555	689

**Gabbro Sill (95GC03 610200, 5481200N)**

B1 frags unabr	0.005	694	48.7	8	2101	0.0334	0.07494 (34)	0.5840 (26)	0.05652 (18)	466	467	473
B2 frags unabr	0.003	2709	189.3	13	2969	0.0407	0.07409 (42)	0.5749 (32)	0.05628 (22)	461	461	464
B3 frags unabr	0.002	727	49.5	32	255	0.0352	0.07251 (42)	0.5615 (68)	0.05616 (60)	451	453	459
B4 flakes unabr	0.001	4701	327.3	50	454	0.0314	0.07444 (34)	0.5800 (34)	0.05650 (22)	463	464	472
B5 chunks unabr	0.001	7145	495.8	102	338	0.0503	0.07292 (28)	0.5687 (34)	0.05656 (22)	454	457	474

NM: not measured

<sup>a</sup> Z, zircon; B, baddeleyite; mf, multifaceted; clr, clear; trb, turbid; frags, fragments; abr, abraded; unabr, unabraded;

<sup>b</sup> Total radiogenic Pb after correction for blank, common Pb and spike

<sup>c</sup> measured

<sup>d</sup> Ratios corrected for fractionation, spike, 5-10pg laboratory blank, initial common Pb (calculated by Stacey and Kramers (1975) model, for the age of the sample), and 1 pg U blank.

Numbers in brackets are the 2 sigma errors in the last two decimal places

Table 3.2. Major and trace element data for samples plotted in Fig. 3.3

	1	2	3	4	5	6	7	8	9	10
Sample <sup>a</sup>	95001	95016	95164	95166	96033	96063	509	95113	95100	95099
group <sup>b</sup>	Gr7	Gr7	Gr7	Gr7	Gr7	Gr7	Gr11 V	Gr11 V	Gr11 I	Gr11 I
Mg#	54	28	47	39	39	58	35	40	41	61
SiO <sub>2</sub> wt%	51.96	68.95	57.24	54.86	54.10	51.99	50.61	45.95	50.45	50.89
TiO <sub>2</sub>	1.15	0.77	0.98	1.55	0.99	0.68	0.35	2.96	3.21	1.77
Al <sub>2</sub> O <sub>3</sub>	17.39	13.07	18.45	16.37	18.68	20.42	17.33	16.24	14.15	12.13
Fe <sub>2</sub> O <sub>3</sub> T <sup>c</sup>	9.77	5.48	8.32	10.34	9.63	7.56	4.46	14.38	13.74	12.03
FeO <sup>d</sup>	ND	ND	ND	ND	ND	ND	9.58	ND	ND	ND
MnO	0.19	0.14	0.15	0.15	0.14	0.15	0.35	0.20	0.25	0.28
MgO	5.39	0.98	3.44	3.08	2.88	4.89	4.95	4.53	4.40	8.80
CaO	8.71	1.50	3.57	4.77	5.44	7.48	4.71	10.11	6.09	8.51
Na <sub>2</sub> O	4.16	6.43	6.65	6.54	4.99	3.52	6.11	2.84	4.92	3.83
K <sub>2</sub> O	0.34	0.70	0.18	0.41	1.26	1.56	0.09	1.06	1.17	0.35
P <sub>2</sub> O <sub>5</sub>	0.14	0.21	0.13	0.20	0.17	0.08	1.43	0.34	0.56	0.23
LOI	4.21	1.19	2.87	2.46	1.89	4.11	3.02	2.30	1.91	3.07
total	99.26	98.26	99.15	98.35	98.36	98.42	99.73	98.68	99.02	98.97
V ppm	252	29	217	175	408	180	163	350	222	281
Nb	6	8	6	10	7	4	88	27	45	20
Hf	3	5	3	4	3	2	10	5	6	3
Zr	116	230	96	133	108	71	428	212	302	146
Y	25	45	20	24	17	14	59	28	36	22
Th	2.6	5.0	3.0	4.9	3.3	1.8	7.3	2.0	4.1	1.9
La	10.2	22.7	11.4	16.3	13.3	6.5	54.9	16.9	30.4	13.0
Ce	23.3	51.4	26.0	37.8	30.1	15.8	133.5	39.9	68.6	29.4
Pr	2.9	6.5	3.2	4.7	3.6	1.9	NR	5.3	8.8	3.8
Nd	13.0	28.1	13.2	20.3	15.3	8.7	75.5	24.4	37.6	17.0
Sm	3.5	6.9	3.4	5.1	3.6	2.3	15.4	6.0	8.1	4.0
Eu	1.1	1.7	1.0	1.4	1.0	0.8	4.6	2.0	2.5	1.4
Tb	0.7	1.3	0.6	0.8	0.5	0.4	2.2	0.9	1.1	0.6
Dy	4.7	8.2	3.6	5.1	3.3	2.7	NR	5.3	6.6	3.8
Ho	0.8	1.5	0.8	1.1	0.7	0.6	NR	1.0	1.3	0.7
Er	2.4	4.5	2.3	3.3	2.0	1.7	NR	2.7	3.3	1.9
Tm	0.4	0.7	0.3	0.5	0.3	0.2	NR	0.4	0.5	0.3
Yb	2.2	4.4	2.2	2.9	1.9	1.5	5.3	2.2	2.9	1.6
Lu	0.3	0.7	0.3	0.4	0.3	0.2	0.8	0.3	0.4	0.2

<sup>a</sup> three digit numbers are from Swinden et al. 1990; Gb, gabbro sill<sup>b</sup> geochemical groups defined in Fig. 3.3: V, volcanic; I, intrusive<sup>c</sup> total Fe calculated as Fe<sub>2</sub>O<sub>3</sub>, this study; measured for samples from Swinden et al. 1990

ND=not determined; NR=not reported; BD=below detection limit

<sup>d</sup> Mg# in cation %, FeO=0.7xFe<sub>2</sub>O<sub>3</sub>T and Fe<sub>2</sub>O<sub>3</sub>=0.3xFe<sub>2</sub>O<sub>3</sub>T

Table 3.2 cont'd

	11	12	13	14	15	16	17	18	19	20
Sample <sup>a</sup>	96011	497	503	508	511	Gb (D)	549	95076	95077	95081
group <sup>b</sup>	Gr11 I	Gr8 V	Gr8 V	Gr8 I	Gr8 V	Gr8 I	Gr9 V	Gr9 I	Gr9 I	Gr9 I
Mg#	55	44	64	57	66	41	56	57	62	45
SiO <sub>2</sub> wt%	49.21	50.93	50.23	50.35	49.51	48.20	51.75	50.63	50.48	51.42
TiO <sub>2</sub>	2.12	2.43	1.33	2.26	1.39	3.48	1.75	1.87	1.71	2.55
Al <sub>2</sub> O <sub>3</sub>	14.88	14.11	14.04	17.83	14.88	14.24	14.61	14.71	13.61	13.56
Fe <sub>2</sub> O <sub>3</sub> <sup>c</sup>	11.76	3.22	2.74	3.76	2.11	15.54	3.89	11.07	11.20	13.06
FeO	ND	10.67	8.17	7.16	8.67	ND	5.87	ND	ND	ND
MnO	0.18	0.26	0.17	0.29	0.16	0.29	0.11	0.20	0.18	0.21
MgO	6.60	5.31	9.30	6.60	10.35	4.98	5.52	6.92	8.75	4.95
CaO	8.94	7.64	9.68	7.24	9.15	8.21	9.84	7.55	8.59	6.96
Na <sub>2</sub> O	3.25	4.55	2.89	3.74	2.83	4.23	4.66	3.74	2.47	5.20
K <sub>2</sub> O	1.45	0.82	1.60	0.80	1.02	0.28	2.10	1.47	1.78	0.14
P <sub>2</sub> O <sub>5</sub>	0.23	0.35	0.10	0.31	0.11	0.42	0.26	0.28	0.24	0.29
LOI	2.61	2.02	3.99	2.94	3.10	2.44	3.80	2.79	2.87	2.05
total	98.74	99.13	100.42	100.62	100.07	99.94	99.65	98.53	99.14	98.42
V	275	456	232	267	218	369	213	233	233	336
Nb	22	18	3	10	5	16	14	15	13	21
Hf	4	4	2	4	2	3	3	4	4	4
Zr	169	182	60	181	72	144	112	152	149	197
Y	18	35	17	32	19	40	17	26	23	30
Th	1.9	2.3	0.5	1.8	0.6	0.9	1.8	1.4	1.4	2.2
La	13.7	15.8	3.7	12.0	4.8	11.9	12.9	11.5	11.0	16.5
Ce	32.1	38.6	10.0	31.0	13.1	29.5	30.4	28.0	26.2	37.4
Pr	4.2	NR	NR	NR	NR	4.4	0.0	3.9	3.6	5.0
Nd	18.5	22.3	7.4	20.0	9.2	21.5	17.6	18.4	16.9	22.0
Sm	4.6	5.9	2.4	5.2	2.5	5.9	4.3	4.9	4.5	5.6
Eu	1.5	NR	0.9	1.8	1.0	2.3	NR	1.6	1.5	1.8
Tb	0.7	1.1	0.5	0.9	0.6	1.1	0.7	0.8	0.7	0.9
Dy	4.0	NR	NR	NR	NR	6.6	NR	4.8	4.4	5.4
Ho	0.7	NR	NR	NR	NR	1.3	NR	0.9	0.9	1.0
Er	2.0	NR	NR	NR	2.0	3.7	NR	2.6	2.4	2.8
Tm	0.3	NR	NR	NR	NR	0.5	NR	0.3	0.3	0.4
Yb	1.6	3.6	1.6	3.1	2.0	3.3	1.7	2.1	2.0	2.4
Lu	0.2	0.6	0.3	0.5	0.3	0.5	0.3	0.3	0.3	0.4

Table 3.2 cont'd

	21	22	23	24	25	26	27	28
Sample <sup>a</sup>	95114	Gb (E)	95036	96014	96021	96023	96024	96031
group <sup>b</sup>	Gr9 I	Gr9 I	Gr9 I	Gr10 V	Gr10 V	Gr10 V	Gr10 V	Gr10 V
Mg#	61	40	55	43	47	44	43	52
SiO <sub>2</sub> wt%	47.41	49.18	51.89	51.86	55.77	52.28	50.15	52.03
TiO <sub>2</sub>	1.90	3.18	1.64	1.73	1.53	1.75	1.70	1.61
Al <sub>2</sub> O <sub>3</sub>	13.89	14.33	15.19	16.22	15.84	17.43	16.11	14.38
Fe <sub>2</sub> O <sub>3</sub> <sup>c</sup>	11.97	15.09	11.43	13.37	10.25	12.27	13.69	11.39
FeO	ND	ND	ND	ND	ND	ND	ND	ND
MnO	0.17	0.23	0.48	0.34	0.17	0.33	0.36	0.31
MgO	8.63	4.65	6.11	4.69	4.19	4.46	4.86	5.86
CaO	10.98	7.64	5.32	5.75	4.24	4.34	6.98	6.83
Na <sub>2</sub> O	1.75	4.51	5.71	5.48	6.79	5.20	4.47	3.66
K <sub>2</sub> O	1.15	0.13	0.06	0.16	0.17	1.36	0.48	2.37
P <sub>2</sub> O <sub>5</sub>	0.25	0.87	0.24	0.29	0.19	0.31	0.27	0.27
LOI	3.05	2.60	3.34	2.09	2.00	2.86	7.51	2.18
total	98.22	99.88	98.17	99.99	99.18	99.85	99.15	98.83
V	275	285	310	317	486	322	363	294
Nb	15	34	20	36	20	32	29	20
Hf	3	8	6	6	5	6	6	5
Zr	147	388	291	279	210	263	246	229
Y	22	52	48	36	34	36	33	25
Th	1.7	3.3	2.2	5.4	2.1	5.2	4.8	2.7
La	13.3	34.2	16.7	23.3	15.2	22.2	18.4	17.4
Ce	30.4	79.8	40.2	51.4	36.8	49.3	42.2	39.5
Pr	4.0	11.0	5.4	6.4	5.0	6.2	5.4	5.2
Nd	17.7	49.8	24.5	27.1	23.0	25.9	22.9	22.2
Sm	4.4	11.9	6.7	6.3	6.0	6.4	5.8	5.6
Eu	1.5	3.7	2.0	1.8	1.9	1.5	1.6	1.6
Tb	0.7	1.7	1.2	1.1	1.0	1.0	1.0	0.8
Dy	4.0	9.7	7.9	6.8	6.6	6.6	6.3	5.0
Ho	0.8	1.8	1.7	1.4	1.3	1.4	1.3	1.0
Er	2.2	4.7	5.0	4.1	3.8	4.1	3.7	2.7
Tm	0.3	0.6	0.7	0.6	0.5	0.6	0.5	0.4
Yb	1.8	3.7	4.8	4.0	3.5	3.9	3.5	2.5
Lu	0.2	0.5	0.7	0.6	0.5	0.6	0.5	0.4

**Table 3.3.** Sm-Nd isotopic data for samples from the younger volcanic sequence of the Wild Bight Group

Sample*	Group	Nd <sup>a</sup>	Sm <sup>a</sup>	<sup>143</sup> Nd/ <sup>144</sup> Nd <sup>b</sup>	<sup>147</sup> Sm/ <sup>144</sup> Nd <sup>c</sup>	ε Nd <sup>d</sup>
95016	Gr7	29.99	8.18	0.512686 (08)	0.16844 (02)	2.7
95022	Gr7	7.97	2.08	0.512672 (14)	0.16123 (05)	2.9
95026	Gr7	17.34	4.58	0.512795 (13)	0.16296 (05)	5.2
96012	Gr7	12.68	3.34	0.512613 (09)	0.16251 (04)	1.6
96061	Gr7	12.85	3.78	0.512700 (11)	0.18151 (08)	2.1
96064	Gr7	17.65	4.63	0.512546 (09)	0.16175 (05)	0.4
95061	Gr11	8.98	2.98	0.512881 (08)	0.20486 (23)	4.2
95099	Gr11	15.87	3.93	0.512811 (12)	0.15283 (02)	6.1
95128	Gr11	16.19	4.12	0.512828 (17)	0.16067 (05)	5.9
96011	Gr11	17.62	4.48	0.512790 (09)	0.15698 (13)	5.4
Gb (D)	Gr9	21.46	5.90	0.512850 (11)	0.16970 (05)	5.8
497	Gr9	NR	NR	0.512812 (17)	0.162	5.5
511	Gr9	NR	NR	0.512901 (35)	0.180	6.1
Gb (E)	Gr8	43.96	11.98	0.512772 (09)	0.16818 (04)	4.4
549	Gr8	NR	NR	0.512739 (15)	0.149	4.8
96021	Gr10	21.29	6.37	0.512824 (07)	0.18467 (01)	4.4
96031	Gr10	16.34	4.88	0.512801 (08)	0.18427 (03)	4.0
96036	Gr10	23.09	6.59	0.512852 (08)	0.17608 (04)	6.6

<sup>a</sup> concentration in ppm, measured from isotope dilution

<sup>b</sup> measured and corrected for mass fractionation

<sup>c</sup> calculated from measured <sup>147</sup>Sm/<sup>149</sup>Sm and <sup>150</sup>Nd/<sup>144</sup>Nd

<sup>d</sup> calculated for UR at 485 Ma

\* 3 digit sample numbers are from Swinden et al. (1990)

NR, not reported; numbers in brackets are 2 sigma errors

**Table 4.1** U-Pb data for dated samples which occur as detrital fragments within the younger Wild Bight Group succession.

Fractions <sup>a</sup>	Weight mg	U ppm	Pb <sub>rad</sub> ppm <sup>b</sup>	Pb <sub>com</sub> pg <sup>c</sup>	<sup>206</sup> Pb <sup>c</sup> <sup>204</sup> Pb	Corrected Atomic Ratios <sup>d</sup>				Age (Ma)		
						<sup>208</sup> Pb <sup>206</sup> Pb	<sup>206</sup> Pb <sup>238</sup> U	<sup>207</sup> Pb <sup>235</sup> U	<sup>207</sup> Pb <sup>206</sup> Pb	<sup>206</sup> Pb <sup>238</sup> U	<sup>207</sup> Pb <sup>235</sup> U	<sup>207</sup> Pb <sup>206</sup> Pb
<b>95GC08 (610150E, 5481400N)</b>												
Z1 crkd unabr	0.012	566	130	91	1047	0.107	0.22024 (16)	3.2157 (16)	0.10589 (50)	1283	1461	1730
Z2 abr prisms	0.002	231	89	66	155	0.135	0.34989 (25)	7.0389 (76)	0.14591 (106)	1934	2116	2299
Z4 s abr prism	0.002	38	25	4	699	0.231	0.53008 (54)	14.3250 (1370)	0.19600 (88)	2742	2771	2793
Z5 s abr prism	0.002	100	48	5	1107	0.063	0.45260 (33)	10.8689 (58)	0.17417 (58)	2407	2512	2598
Z6 s abr prism	0.002	71	23	5	665	0.014	0.33740 (25)	5.3536 (70)	0.11508 (54)	1874	1877	1881
Z7 s abr prism	0.002	75	28	11	301	0.203	0.33508 (31)	5.3723 (10)	0.11628 (72)	1863	1880	1900
<b>96GC07 (610475E, 5480000N)</b>												
Z1 prisms abr	0.007	2602	178	47	1605	0.112	0.06811 (42)	0.5285 (34)	0.05628 (14)	425	431	464
Z2 prisms abr	0.004	2731	200	31	1399	0.141	0.07113 (42)	0.5547 (34)	0.05656 (24)	443	448	474
Z3 s prism abr	0.010	2359	177	10	10569	0.102	0.07528 (32)	0.5866 (26)	0.05651 (08)	468	469	473
Z4 unabr prisms	0.006	6762	450	222	781	0.103	0.06669 (24)	0.5187 (22)	0.05641 (12)	416	424	469

<sup>a</sup> Z, zircon; abr, abraded; unabr, unabraded; crkd, cracked; s, single grain

<sup>b</sup> total radiogenic Pb after correction for blank, common Pb and spike

<sup>c</sup> measured

<sup>d</sup> ratios corrected for fractionation, spike, 5-10pg laboratory blank, initial common Pb (calculated by Stacey and Kramers (1975) model, for the age of the sample), and 1pg U blank

Numbers in brackets are the two sigma errors in the last decimal places

**Plate 2.1** Field relationships in the South Lake Igneous Complex: a) late mafic dykes cross-cutting a mixed tonalite-hornblende diorite unit; b) sheeted dykes (dark), with 3 chilled margins (arrows) cross-cutting layered gabbro (light); c) 3 mafic dykes (across photo) (1, 2, 3) separated by screens of layered gabbro (layering up and down photo); and d) mylonitized layered gabbro and mafic dykes.



**Plate 2.1** Continued: e) mafic dyke (left) with fracture cleavage (parallel to dashed lines) rotated into the dyke margin (solid line); f) tonalite/trondhjemite net veins in gabbro; g) tonalite with inclusion trains cut by an inclusion-free tonalite sheet (approximate boundaries shown by heavy black lines) which parallels the inclusion trains; and h) xenolith of a mafic dyke in tonalite.



**Plate 2.2** Field relationships and rock types in the older volcanic sequence of the Wild Bight Group: a) pillowed mafic volcanic rocks, tops toward the top of the photo; b) pillow breccia in foreground, with massive flow/synvolcanic sill in the background; c) strongly deformed, hematized pillow basalts with interpillow red argillite (left), adjacent to green argillite of unit 4, along the Winter House Cove Fault (contact shown by white arrows); and d) coarse-grained lapilli tuff, composed entirely of felsic to intermediate clasts in a more mafic matrix.

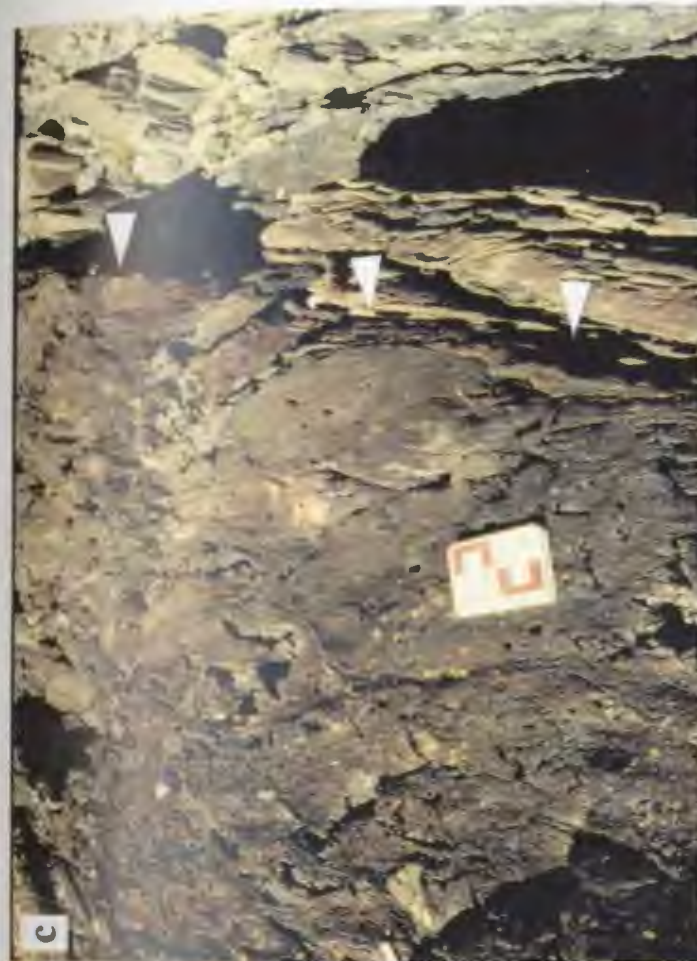


**Plate 2.3** Photomicrographs of gabbro and hornblende diorite from the South Lake igneous complex: a) gabbro pegmatite (94GC03) showing remnants of clinopyroxene (cpx) rimmed by subhedral to euhedral zoned amphibole (am), with interstitial unaltered plagioclase (pc). Totally altered cumulate plagioclase crystals (dark) are overgrown by amphibole also. Field of view is 5mm, plane-polarized light; b) Gabbro pegmatite (94GC03) showing almost completely bastitized orthopyroxene with inclusions of subhedral to euhedral clinopyroxene (cpx) and altered plagioclase (pc). Field of view is 5mm, plane-polarized light; c) hornblende diorite (94GC05) showing totally altered plagioclase laths (mottled black grains) surrounded by ophitic hornblende (hb) crystals, with interstitial quartz (qtz). Field of view is 5 mm, plane polarized light.

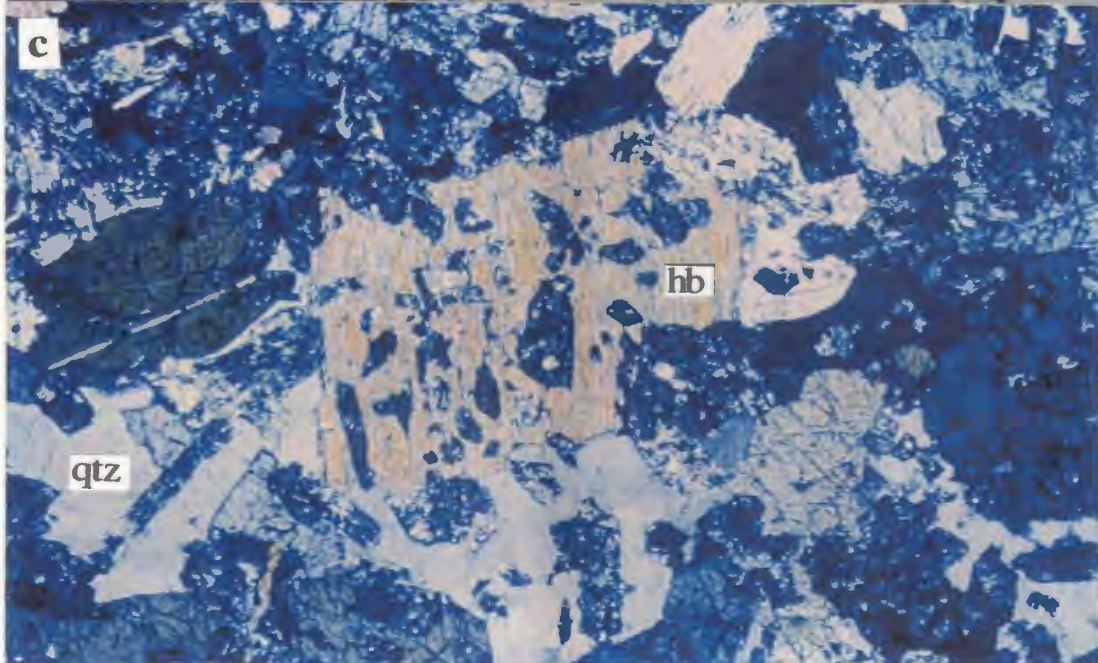
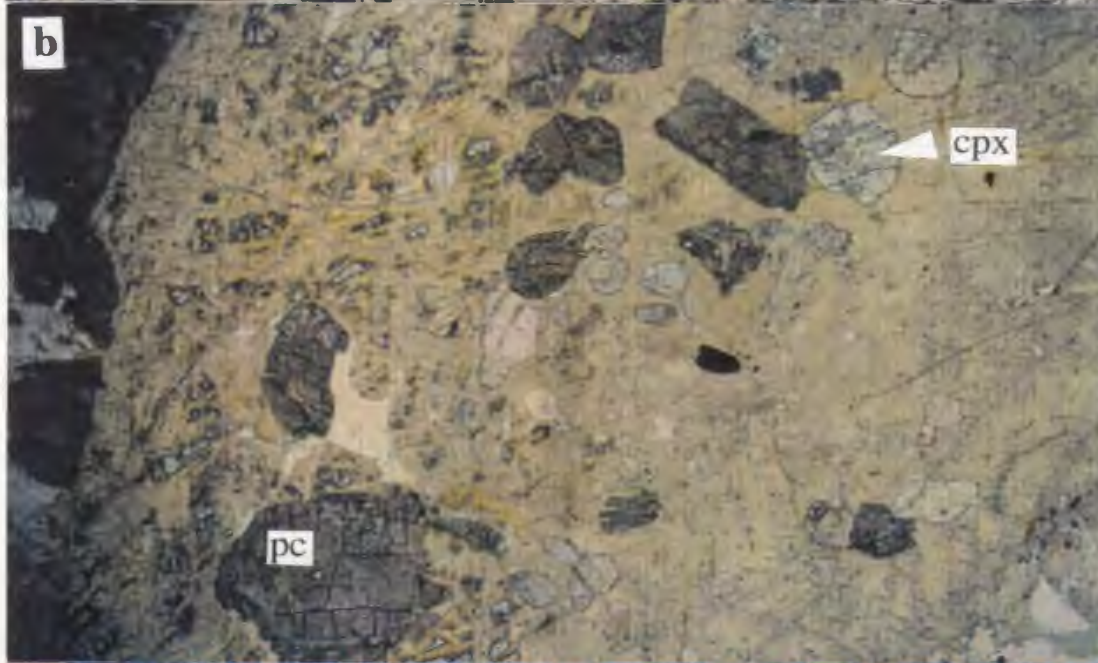
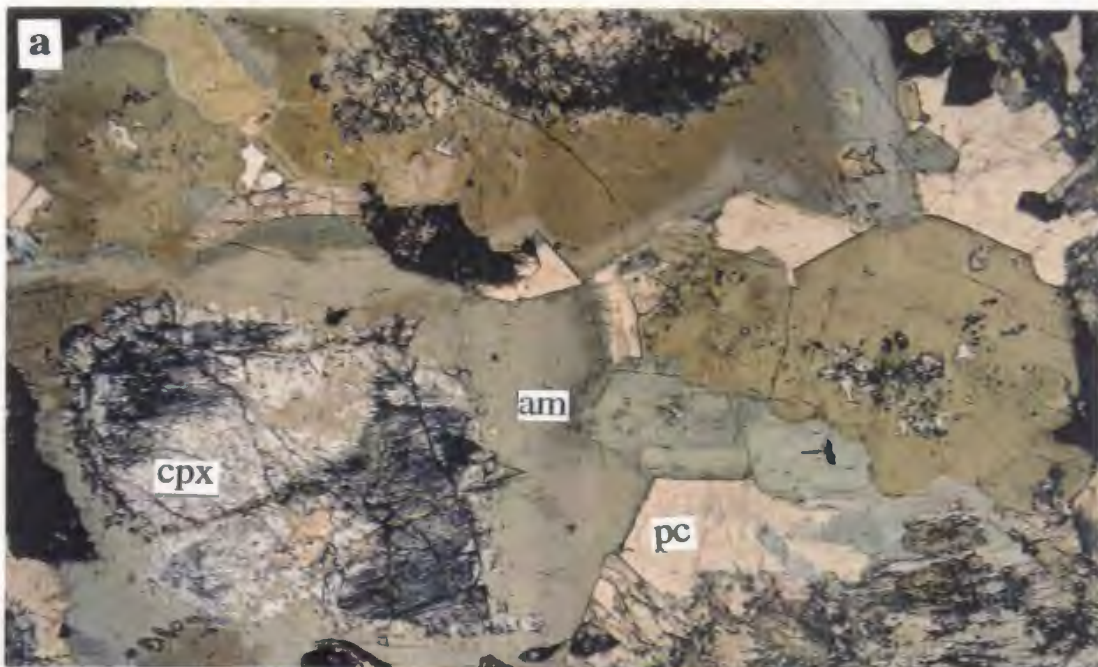


**Plate 3.1** Field relationships and rocks types in the younger Wild Bight Group sequence: a) red tuffaceous sandstone with abundant red argillite rip-up clasts, interbedded with thinly laminated red and green argillite (unit 4); b) coarse-grained volcanoclastic rocks (unit 6) dominated by mafic clasts, with abundant large blocks of plagioclase phyric basalt; c) clast-supported volcanic breccia at the contact between unit 5 pillowed volcanic rocks and the overlying volcanoclastic sequence (unit 6). The matrix is epidotized and silicified pebble conglomerate; d) and e) folded, thinly bedded, red and green argillite (d) and chert (e) (unit 7a) that overlie the volcanoclastic sequence.

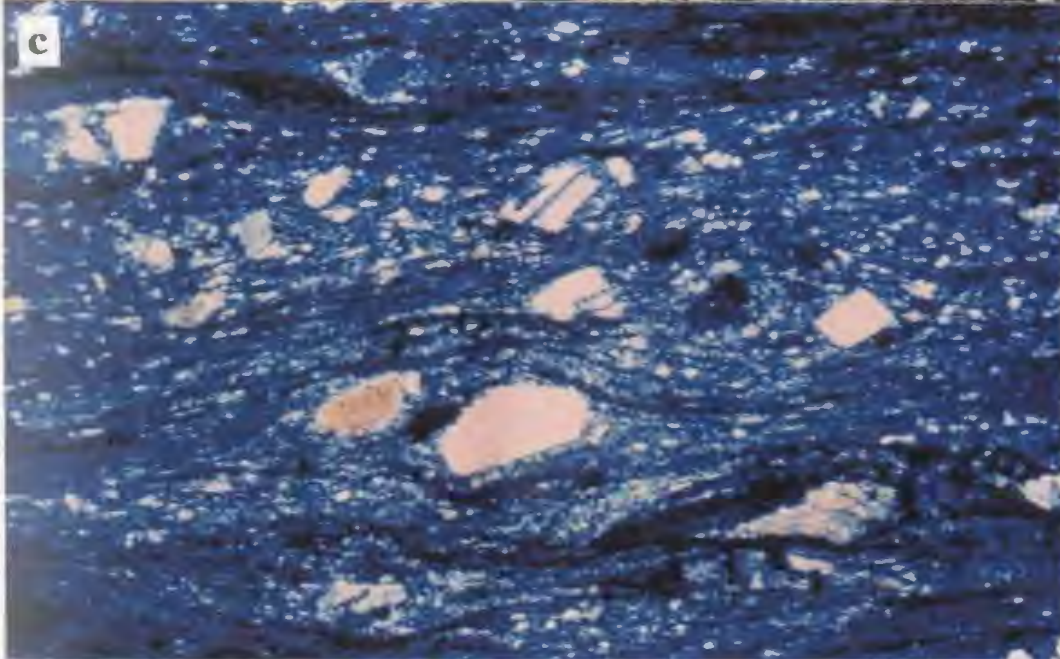
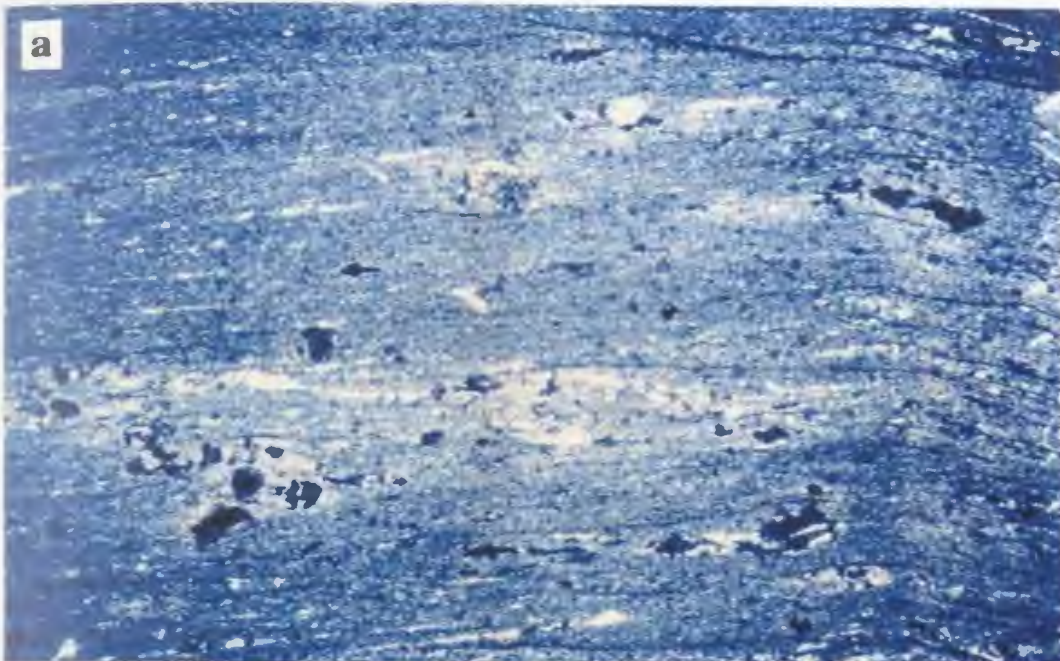




### **Sm-Nd Isotope Analytical Procedure**

Reagents used throughout are doubly distilled in teflon containers. The powdered sample is accurately weighed to the 5<sup>th</sup> decimal place and dissolved with 1 ml each of 8N HNO<sub>3</sub> and HF. The sample is allowed to reflux for a period of 2 to 7 days depending on the rock type. Any white fluoride precipitates from this stage must be redissolved prior to ion exchange chemistry. The sample is then split (and accurately weighed) into isotopic concentration and isotopic dilution fractions. The isotopic dilution fraction is spiked with an accurately weighed ORNL <sup>150</sup>Nd-<sup>147</sup>Sm mixed spike, based on the Nd concentration determined by ICP-MS analysis. The samples (both fractions) are loaded onto EICHROM TRU-Spec resin, and the major and other trace elements are removed immediately with 10 mls of 3N HNO<sub>3</sub>. The REEs are then washed off separately with H<sub>2</sub>O, and the REE solutions from both fractions are evaporated to dryness. Samarium and Nd isotopic concentration and dilution fractions are then pipetted into teflon columns in 0.15N HCl, and the LREEs are stripped off using 0.15N HCl. Both fractions of Nd are removed next, with 0.17N HCl, followed by removal of the isotope dilution fraction of Sm using 0.50 N HCl. Two drops of phosphoric acid are added to each fraction and then they are all evaporated down to a single drop, ready for loading into the mass spectrometer. These drops are loaded separately onto outgassed Re double filaments for the Finnigan MAT 262V thermal ionization mass spectrometer (TI-MS). Neodymium and Sm ratios are measured using faraday multi-collector routines which collect 5 blocks of 20 scans, for a total of 100 scans, with on line drift and mass fractionation correction and statistical analysis. The <sup>147</sup>Sm/<sup>144</sup>Nd reported errors are 2 sigma (of the mean) and are quadratically added using the 2 sigma errors for <sup>147</sup>Sm/<sup>149</sup>Sm and <sup>150</sup>Nd/<sup>144</sup>Nd measured isotopic ratios. εNd values are calculated using <sup>143</sup>Nd/<sup>144</sup>Nd (CHUR) of 0.512638 and <sup>147</sup>Sm/<sup>144</sup>Nd (CHUR) of 0.19659.

**Plate 3.2** Field photos and photomicrographs of dated felsic tuffs of the younger volcanic sequence of the Wild Bight Group: a) photomicrograph of the Pig Island Tuff (95GC09), Field of view is 5mm, cross-polarized light; b) field photo of the Duck Island Tuff (95057) (bottom of photo) intruded by a plagioclase phyric mafic dyke (top of photo). The sample was taken from the fine-grained, siliceous, white weathering top of this graded debris flow; c) photomicrograph of the Duck Island Tuff, showing abundant quartz and plagioclase phenocrysts, but also smaller, rounded grains which suggest the possibility of a detrital component. Field of view is 5 mm, cross-polarized light; d) field photo of the Locks Harbour Tuff showing interbedded mafic and felsic tuffs; and e) photomicrograph of the Locks Harbour Tuff, showing lapilli sized rock fragments and flattened shards with possible cusped terminations. Field of view is 5 mm, cross-polarized light.



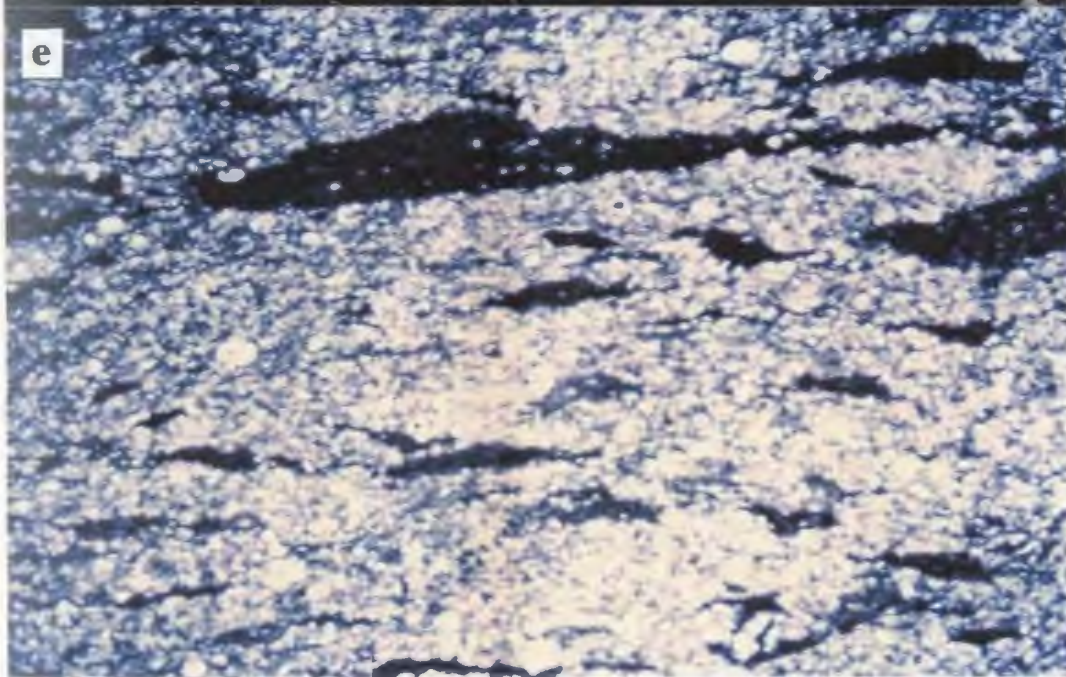


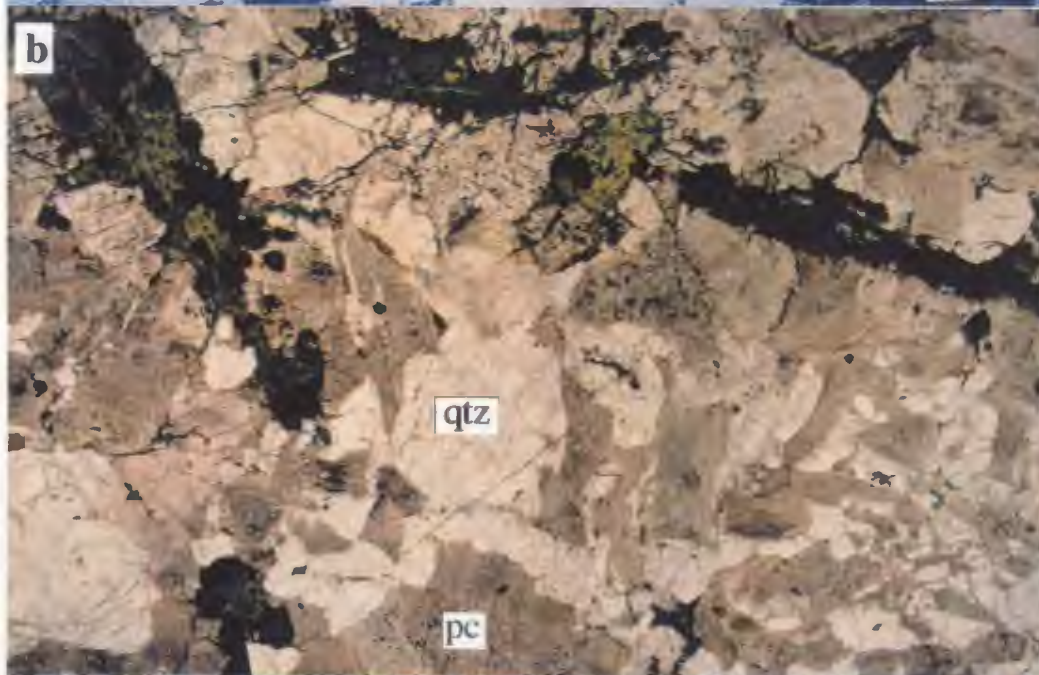
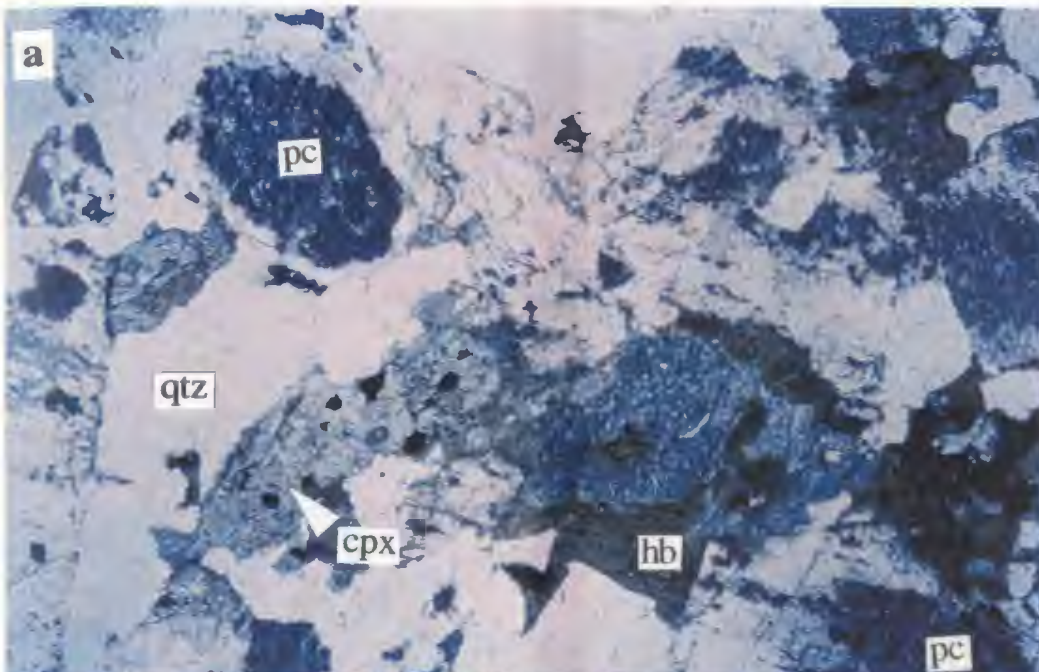
**Plate 4.1** Field photos showing detrital components within sedimentary units of the younger Wild Bight Group sequence: a) pillowed volcanic fragments (with boninitic geochemical signatures) in a dark grey shale olistostrome (unit 4); b) rhyolite block (white) (with a depleted geochemical signature), in a pebbly volcanoclastic bed (unit 6); c) debris flow with abundant rhyolite clasts which are from both the younger and older sequences of the Wild Bight Group; and d) poly lithic pebble conglomerate, with rounded quartz diorite cobbles (white).



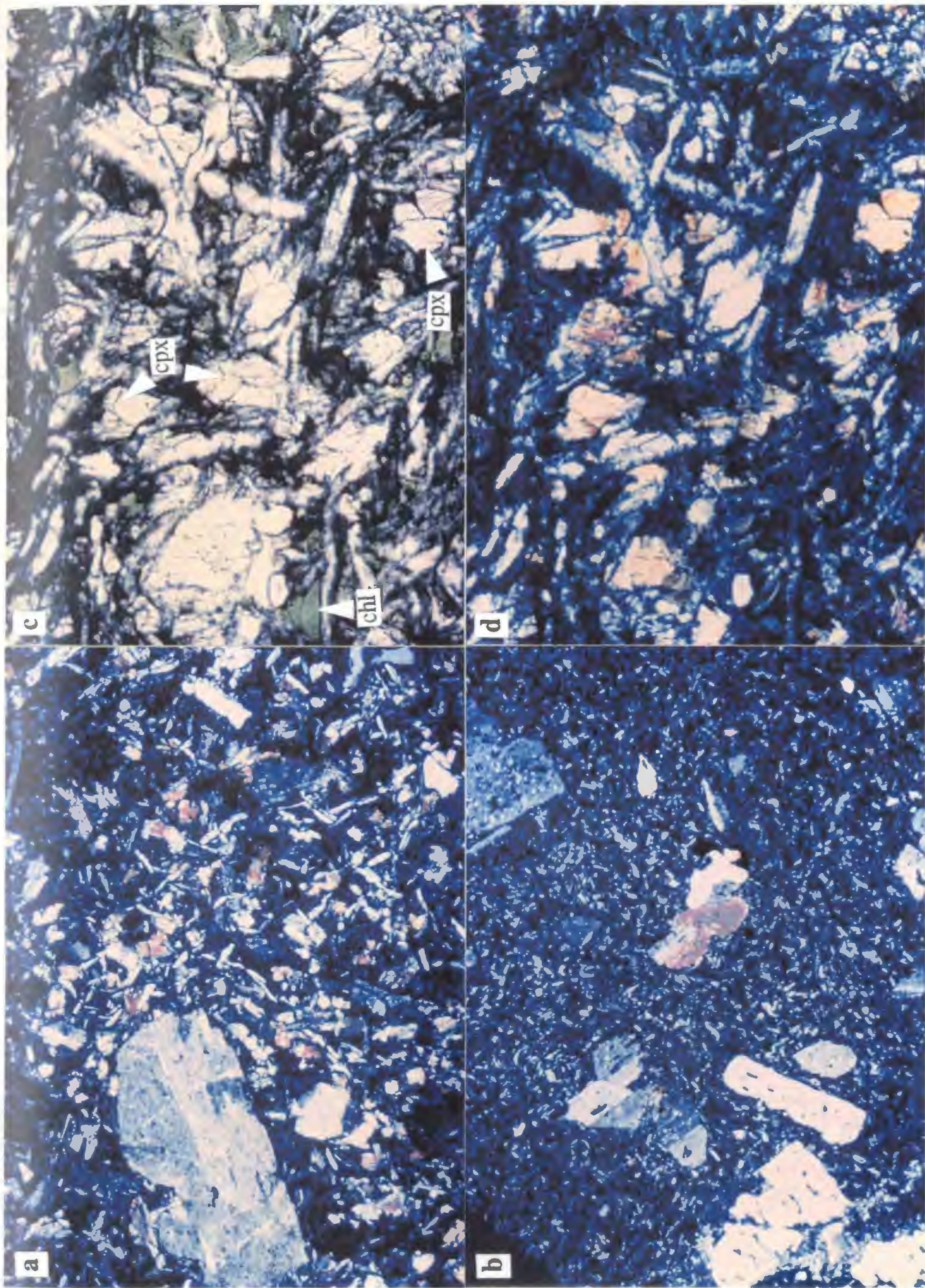
**Plate A6-1** Photomicrographs of various rocks types in the South Lake igneous complex: a) massive gabbro (94037) showing clinopyroxene replaced and rimmed by amphibole, with the rim and replacement amphibole in optical continuity. Field of view is 5mm, cross-polarized light; b) green mafic dyke from the sheeted dyke complex (94014) in which both the groundmass and phenocryst are totally recrystallized to fine-grained pale green, bladed to acicular amphibole. The phenocryst also contains numerous euhedral oxide grains which may be a product of the recrystallization. Field of view is 5 mm, plane-polarized light; c) green mafic dyke from the sheeted dyke complex (94044), showing a phenocryst with a remnant of the original augite in the core, but dominantly replaced by amphibole. Field of view is 5 mm, cross-polarized light; d) grey mafic dyke from the sheeted dyke complex (94009), showing relict diabasic texture. Plagioclase laths are strongly altered, and are partially enclosed by and intergrown with hornblende which is interpreted to be a primary igneous mineral (although it is locally recrystallized). Field of view is 5 mm, plane-polarized light.



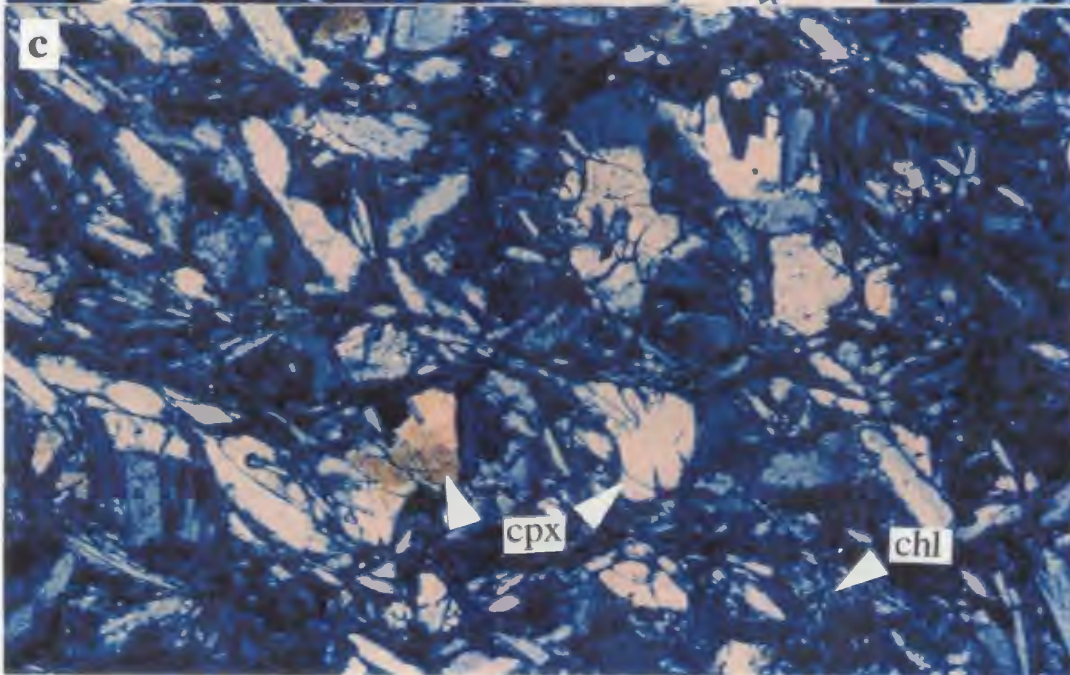
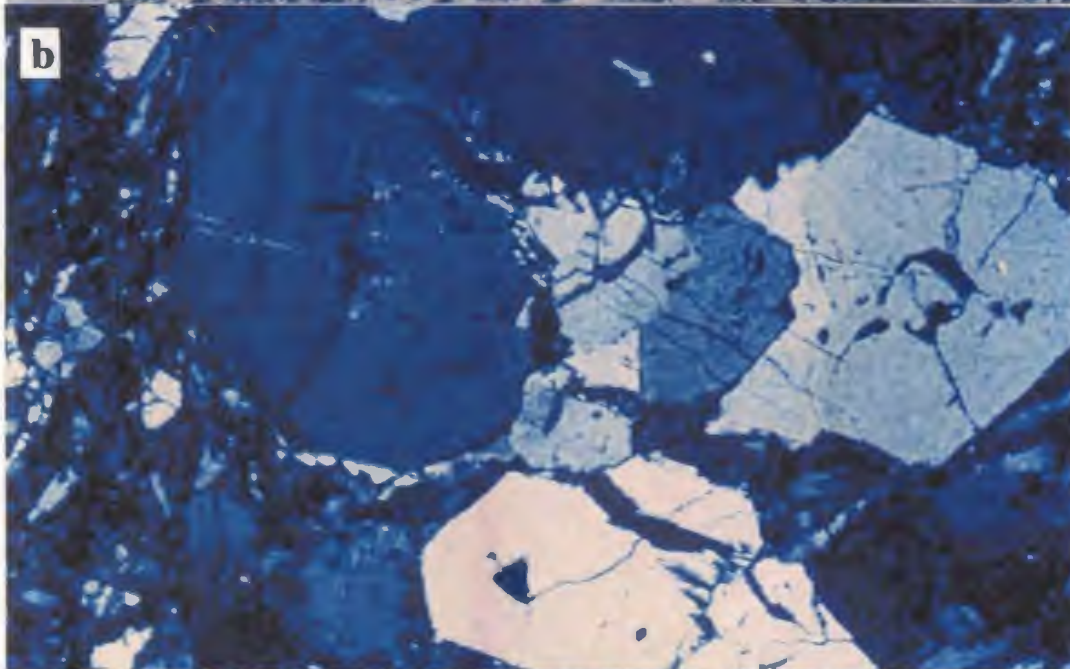
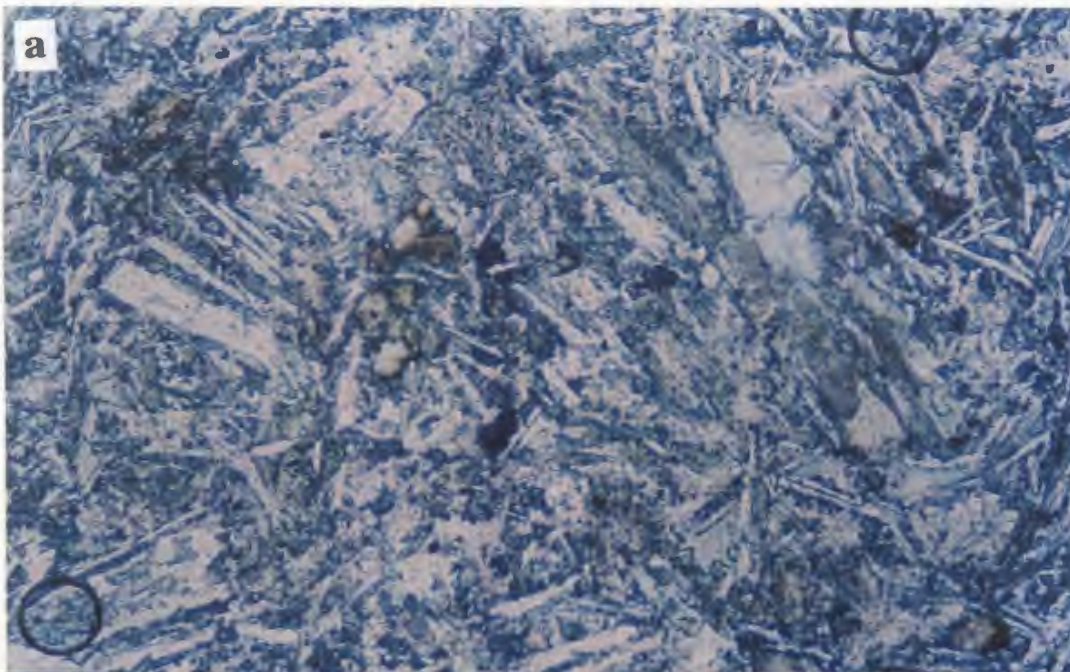
**Plate A6-2** Photomicrographs of various rocks types in the South Lake Igneous Complex: a) tonalite (94GC06) showing cumulate plagioclase (pc) with totally altered core, intergrown with hornblende (hb), clinopyroxene (cpx) and oxide, with interstitial quartz (qtz). Field of view is 5 mm, plane-polarized light; b) tonalite (94061) showing granophyric intergrowth of quartz (qtz) and weakly sericitized plagioclase (pc). Field of view is 5 mm, plane-polarized light; c) late mafic dyke with a diabasic texture, showing relatively fresh plagioclase laths with interstitial clinopyroxene, chlorite and epidote. Field of view is 5 mm, cross-polarized light.

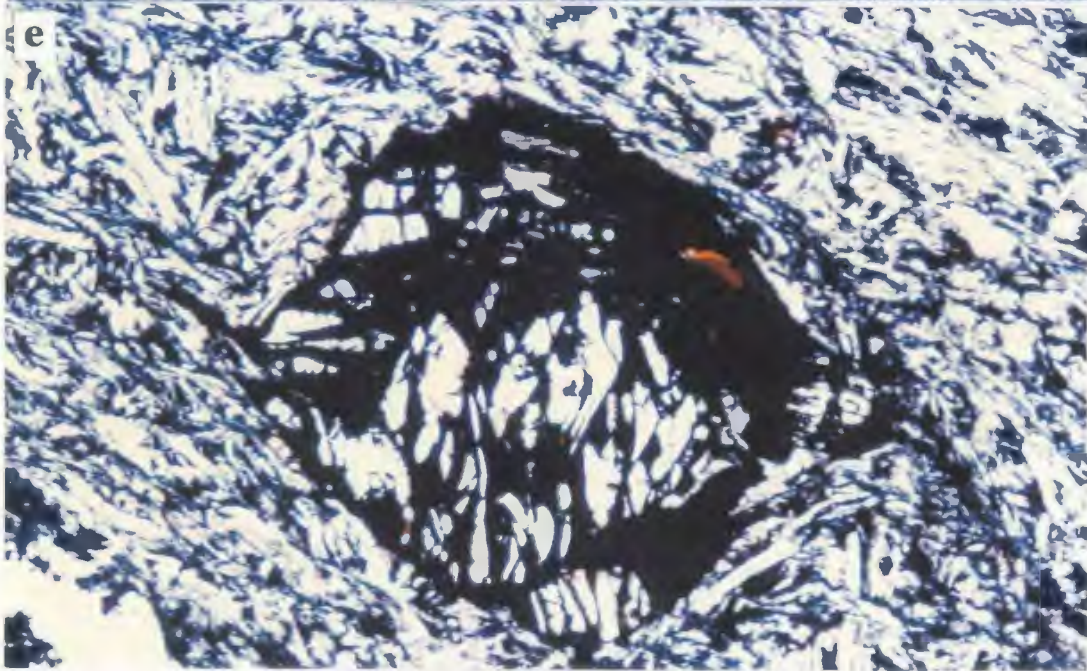
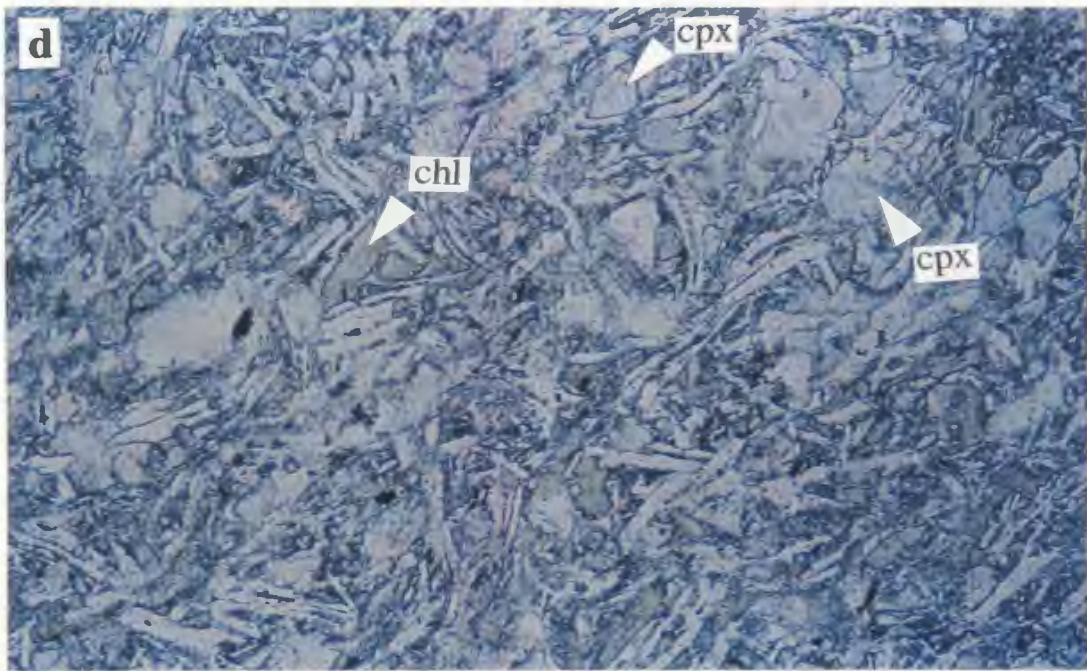


**Plate A6-3** Photomicrographs of various igneous rocks types from the Wild Bight Group: a) calc-alkaline pillowed basalt (95011) showing large, relatively fresh plagioclase phenocrysts in a fine-grained groundmass of plagioclase microlites, clinopyroxene and chlorite. Field of view is 5 mm, cross-polarized light; b) calc-alkaline pillowed basalt with small glomerocrysts of plagioclase and clinopyroxene and plagioclase phenocrysts with sieved textures. Field of view is 5 mm, cross-polarized light; c) and d) pillowed basalt from the upper volcanic sequence (group 10) (96021), showing plagioclase laths with interstitial to subophitic clinopyroxene (cpx) and interstitial chlorite (chl). Field of view is 1.2 mm, c) plane-polarized light and d) cross-polarized light.



**Plate A6-4** Photomicrographs of various igneous rock types from the Wild Bight Group: a) moderately altered, low-Ti, LREE-depleted pillowed basalt (95111) showing plagioclase laths in a totally recrystallized groundmass of fine-grained chlorite and epidote. Field of view is 1.2 mm, plane-polarized light; b) and c) less altered, low-Ti, LREE-depleted IAT (96009) with glomerocrysts of zoned clinopyroxene (b) in a groundmass of plagioclase laths with interstitial to sub-ophitic clinopyroxene (cpx) and interstitial chlorite (chl). Field of view 1.2 mm, cross-polarized light (b and c); d) boninite (96005) showing microlites of plagioclase (pc) with bluish-green interstitial to sub-ophitic clinopyroxene (cpx) and interstitial chlorite (chl). Field of view 1.2 mm, plane-polarized light; e) boninite (95025b) showing phenocryst of what is interpreted to have originally been olivine, but which is now replaced by Mg-rich amphibole. Both the matrix and phenocryst have abundant secondary hematite. Field of view 1.2 mm, plane-polarized light.





### Appendix 1 Sample Lists

This appendix contains two lists of samples in chronological order, one for geochronology samples and one for others. These lists contain a field rock description, stratigraphic unit (where applicable), geographic volcanic unit name (where applicable), other field information and the analytical procedures which have been done (TS, thin section; XRF, X-ray fluorescence spectrometry; ICP, ICP-MS analysis; Nd, Sm-Nd isotopic analysis).

#### Abbreviations (General)

w	with	frag	fragmental
x-cuts	cross-cuts	undef'd	undeformed
vclastic	volcaniclastic	def'd	deformed
vlc	volcanic	alt'd	altered
svlc	sub-volcanic	fol'd	foliated
intr	intrusive	ws	weathered surface
df	debris flow	brn	brown
gw	greywacke	org	orange
tff	tuff	grn	green
agglom	agglomerate	lgt	light
conglom	conglomerate	dk	dark
sd	sheeted dyke	qtz	quartz
peg	pegmatite	pc	plagioclase
xtl	crystal	px	pyroxene
lgb	layered gabbro	hb	hornblende
gb	gabbro	ep	epidote
dt	diorite	cc	calcite
tnlt	tonalite	fsp	feldspar
rhy	rhyolite	amph	amphibole
um	ultramafic	incl	inclusion
mfc	mafic	<b>Geographic Volcanic Units</b>	
flc	felsic	GHE	Glover's Harbour east
int	intermediate	GHW	Glover's Harbour west
fgr	fine-grained	LPS	Long Pond south
mgr	medium-grained	LP	Long Pond
cgr	coarse-grained	KL	Kerry Lake
msv	massive	KLN	Kerry Lake north
bx	breccia	NBL	Nanny Bag Lake
phy	phyric	NB	New Bay
aphy	aphyric	OA	Osmonton Arm
plwd	pillowed	NA	Northern Arm
amyg	amygdular	SBH	Seal Bay Head
sil'd	silicified		
vesic	vesicular		
irreg	irregular		
pheno	phenocryst		

sample	Rock Type (unit)	other	TS	XRF	ICP	Nd
94GC01	cgr gabbro w minor interstitial Qtz					
94GC02	large org ws mgr mfc dyke	in tmlt	*	*		
94GC03	Qtz-rich pegmatitic gb (SLIC)	intr by tmlt and dt	*	*	*	*
94GC04	Qtz hb dt (SLIC)		*	*	*	*
94GC05	hb dt (SLIC)		*	*		
94GC06	tmlt (SLIC)		*	*	*	*
95GC01	peg plagiogranite pod	peg plagiogranite pod				
95GC02	granitoid boulder	in debris flow	*			
95GC03	peg patch in cgr gabbro sill (8)		*	*	*	*
95GC04	mgr gabbro sill	in argillites				
95GC05	silicified int-flc vlc/svlc (5)		*	*		
95GC06	mfc sill in plwd vlcs (3)	w mafic phenos (hbd?)	*			
95GC07	peg plagiogranite pod	peg plagiogranite pod				
95GC08	sil'd flc bx block in df	pc and Qtz phenos	*	*	*	*
95GC09	felsic tuff (Pig Island) (6)		*			
95GC10	peg pod in greenish gb sill	pc is gm, probably choriized	*	*	*	*
96GC01	flsc-int frag in agglom (2)		*			
96GC02	diabase dyke	intr unit 6				
96GC03	flsc-int vlc (?) (2)					
96GC04	lrg flsc block in flsic lappilli tuff (2)					
96GC05	flc tff (2)		*	*	*	
96GC06	cgr org ws mfc dyke	intr lgb and sd (SLIC)	*	*	*	
96GC07	m-cgr Qtz dt/tmlt cobbles	in conglomer of unit 6	*	*	*	*
96GC08	Qtz-phy rhy frag in df	Duck Isl. (unit 6)				
96GC09	m-gr granitoid frag in df	Duck Isl. (unit 6)				
96GC10	Qtz, pc-phy rhy frag in df	flow banded frag Duck Isl. (unit 6)	*	*	*	
96GC11	Qtz-pc-phy rhy	NBL unit	*	*	*	
96GC12	Qtz-pc-phy red rhy	LP unit	*	*	*	
96GC13	cgr peg gb	part of differentiated mfc sill	*			
96GC14	resample of 95GCK-10 gb sill		*			
96GC15	alkalic gb sill		*			
96GC16	plwd mfc vlc	SBH				
96GC17	fgr xtl-rich top of flscvclastic (4)	Omega Point	*			
GHG	pegmatitic part of gabbro sill	cuts pillows of GHW unit	*			
GD-96-1	tonalite	SLIC	*			
D-47-10	tonalite	SLIC	*			

sample	Rock Type (unit)	other	TS	XRF	ICP	Nd
96034	aphy plwd (?) mfc vlc (8)	OA unit				
96035	aphy plwd (?) mfc vlc (8)	OA unit	*	*	*	
96036	aphy plwd (?) mfc vlc (8)	large plws OA unit	*	*	*	*
96037	pc-phy plwd (?) vlcs (8)	SE side SLIC	*	*	*	
96038	str silf'd plwd vlcs (?) (7)	SE side SLIC				
96039	mod silf'd plwd vlcs (?) (7)	SE side SLIC	*			
96040	fgr diabase dyke	intrudes silf'd plws				
96041	str silf'd plwd vlcs (?) (7)	SE side SLIC				
96050	cgr gb	KL unit	*			
96051	msv fgr greenish gb	KL unit				
96052	fgr diabase dyke	KL unit				
96053	plw mfc vlc w cc amygs (3)	LPS unit	*	*	*	
96054	fgr mfc dyke	x-cut LPS mfc vlcs	*	*	*	*
96055	plwd mfc vlcs (3)	LPS unit	*	*	*	*
96056	plwd mfc vlcs (3)	LPS unit				
96057	plwd mfc vlcs (3)	LPS unit	*	*	*	
96058	plwd mfc vlcs	NBL unit	*	*	*	*
96059	pc-hb-phy flc-int dyke	intr NBL mfc vlc	*			
96060	qtz-pc-phy rhy	NBL unit	*	*	*	*
96061	plwd mfc vlcs (3)	NBL unit	*	*	*	*
96062	plwd mfc vlcs (3)	NBL unit				
96063	plwd mfc vlcs (5)	KLN unit	*	*	*	
96064	plwd vlcs (5)	intbd w lower vlcs (N-arc)	*	*	*	*
96065	qtz, pc-phy rhyolite (2)	LP unit	*	*	*	
96066	flc tuff	Pig Island	*	*	*	*
96067	rhy bx frag in cgr vlcastic (7)	frag of Lockport rhyolite (2)	*			*
96068	plw frag in shale olistostrome (4)	Hancock's Isl. olistostrome				
96069	pc-hb-phy int-flc frag	in olistostrome (7)				
96070	flc tuff (7)	same as 95092 (resampled)	*			*
96071	sheared flsc tff xeno in hb dt (SLIC)		*			

sample	Rock Type (unit)	other	TS	XRF	ICP	Nd
95159	mgr pc-phy mfc vlc/svlc (5)	spheroidal text GHE unit				
95160	pc-phy plwd mfc vlc (5)	GHE unit				
95161	pc-phy plwd mfc vlc (5)	GHE unit	*	*		
95162	pc-phy plwd mfc vlc (5)	GHE unit				
95163	bx of pc-phy mfc-vlc (5)	ep grn sil'd matrix GHE unit				
95164	pc-phy plwd mfc vlc (5)	GHE unit				
95165	gritty greywacke					
95166	aphy plwd mfc vlc (5)	GHE unit	*	*		
95167	pebble conglomer (6)					
95168	fgr gb/diabase					
95169	mfc-int agglom (6)					
95170	mfc-int agglom (6)					
96001	aphy mafic dyke	relatively undef'd				
96002	aphy mafic dyke	intrudes Caradoc shale	*	*	*	*
96003	pc, mfc-phy mfc dyke	intrudes Caradoc shale				
96004	fgr diabase dyke	intrudes Caradoc shale	*	*	*	*
96005	plwd mfc vlc (3)	hematized GHW unit	*	*	*	
96006	msv fgr gabbro	part of SLIC				
96007	msv fgr org ws mfc dyke	similar to late dykes in SLIC	*	*	*	
96008	tff/lappilli tff (2)					
96009	mfc vlc (3)		*	*	*	*
96010	fgr msv org ws mfc dyke	x-cuts fol'n in vclastics	*	*	*	
96011	fgr msv org ws mfc dyke	x-cuts fol'n in vclastics	*	*	*	*
96012	pc-phy plwd mfc vlcs (5)		*	*	*	*
96013	fgr aphy mfc dyke	in unit 7				
96014	plwd mfc vlc (8)	OA unit	*	*	*	
96015	plwd mfc vlc (8)	OA unit				
96016	plwd mfc vlc (8)	OA unit				
96017	plwd mfc vlc (8)	OA unit				
96018	plwd mfc vlc (8)	OA unit				
96019	fgr msv orange mafic dyke		*	*	*	
96020	fgr msv orange mafic dyke					
96021	plwd mfc vlc (8)	NA unit	*	*	*	*
96022	plwd mfc vlc (8)	NA unit				
96023	plwd mfc vlc (8)	OA unit	*	*	*	
96024	plwd mfc vlc (8)	OA unit	*	*	*	
96025	pc-hb-phy int-flc frag in melange (7)		*	*	*	*
96026	aph mfc (?) frag in melange		*			
96027	aph mfc (?) frag in melange		*			
96028	pc, hb-phy dyke in unit 7	same as block in melange				
96029	qtz-rich grit (10)					
96030	pc-hb-phy int-flc frag in melange (7)					
96031	msv-plwd mfc flow (5)		*	*	*	*
96032	coarsely pc-phy vlc/svlc (5)	GHE unit	*	*	*	
96033	plwd mfc vlc (5)	GHE unit	*	*	*	

sample	Rock Type (unit)	other	TS	XRF	ICP	Nd
95114	mfc-phy mfc dyke	intr 112, 111	*	*	*	
95115	irreg aphy mfc sill	intr 112	*	*	*	
95116	hbd-phy mfc-int dyke	vesic, glassy margins?	*	*	*	
95117	mgr gbsill					
95118	pebble conglom (6)					
95119	mfc-phy mfc-int dyke		*	*	*	
95120	mfc-phy mfc-int dyke	sparsely phyrlic				*
95121	pc-phy mfc-int dyke	blocky pc-qz-ep-cc bx	*	*		
95122	aphy mfc-int dyke	subvert (post folding?)	*	*		
95123	pc-phy mfc vlc/tff	small pc laths				
95124	pc-phy int-flsc vlc/svlc (5)	sil'd GHE unit	*	*		
95125	irreg aphy mfc dykelets	intr 126	*	*		
95126	pc-phy mfc vlc/svlc (5)	small pc laths GHE unit				
95127	irreg aphy mfc dyke		*	*		
95128	aphy mfc-int dyke	subvert, (post folding?)	*	*	*	*
95129	pc-phy mfc vlc/svlc (5)	small pc laths GHE unit				
95130	pc-phy mfc vlc/svlc (5)	small pc laths GHE unit				
95131	mgr pc-phy mfc svlc (5)	small pc laths GHE unit	*	*		
95132	fgr diabase		*	*		
95133	aphy mfc dyke	intr 132				
95134	bx of pc-phy mfc vlc	ep green siliceous matrix				
95135	pc-phy mfc vlc (5)	frag from 134 GHE unit				
95136	fgr gb					
95137	aphy plwd mfc vlc (5)	large plws GHE unit	*	*		
95138	pc-phy plwd mfc vlcs (5)	GHE unit	*	*		
95139	aphy mfc dyke	intr 138				
95140	pebble conglom (6)	w flc/cherty frags				
95141	mfc-phy mfc dyke	sparsely phy				
95142	pc-phy plwd mfc vlcs (5)	GHE unit	*	*		
95143	pc-phy mfc vlc (5)	small pc laths GHE unit				
95144	pc-phy mfc vlc/svlc (5)	small pc laths GHE unit				
95145	vclastic (6)					
95146	fgr gabbro					
95147	pc-phy mfc vlc/svlc (5)	small pc laths GHE unit				
95148	pebble conglom (6)					
95149	aphy plwd mfc vlc (5)	GHE unit				
95150*	flsc tff (2)	GHW unit	*			
95151	mfc tff ? (2)	GHW unit				
95152	flsc-int vclastic (2)	GHW unit				
95153	aphy plwd mfc vlc (3)	GHW unit	*	*	*	*
95154	aphy plwd mfc vlc (3)	GHW unit	*	*	*	*
95155	aphy plwd mfc vlc (3)	GHW unit				
95156	aphy mfc sill/tff/vlc					
95157	aphy mfc sill/tff/vlc					
95158	pc-phy mfc vlc/svlc (5)	small pc laths GHE unit				

sample	Rock Type (unit)	other	TS	XRF	ICP	Nd
95071	xtl-rich cgr grit (6)		*	*	*	
95072a	pebble conglomer (6)					
95072b	cgr mfc dyke		*			
95073	buff ws fgr mfc-int dyke	x-cuts folding	*			
95074	cgr gb dyke	weakly def'd	*			
95075	cgr gb dyke	strongly def'd	*			
95076	gb sill		*	*	*	
95077	mfc-phy mfc dyke	amyg top, pepperite?	*	*	*	
95078	chert bx/sil'd zone (6)					
95079	qtz-fsp grit/xl tff (6)		*			
95080	msv cgr grits (6)	faintly layered				
95081	diabase dyke/sill		*	*	*	
95082	diabase dyke/sill		*			
95083	pebble conglomer (6)					
95084	pc-phy mfc-int dyke	pc phenos in pockets	*			
95085	aphyc fgr mfc dyke	vesicle trails	*			
95086	aphy fgr mfc dyke		*			
95087	cgr vclastic (6)					
95088	sil'd argillite (7)		*			
95089	sil'd argillite (7)		*			
95090b	pc-phyric mfc dyke/sill		*			
95090a	def'd cgr mfc dyke		*			
95091	def'd cgr mfc dyke		*			
95092*	flsc tff (7)		*			
95093	vesic mfc vlc/sill		*			
95094	vesic mfc vlc/sill		*			
95095	mfc-pc-phy mfc sill	sparsely phy, vesic margin				
95096	diabase sill					
95097	aphy mfc dyke	part of small swarm	*	*		
95098	sil'd bx		*			
95099	pc-mfc-phyric mfc dyke	sparsely phy, chloritic	*	*	*	*
95100	aphy aph mfc-int dyke	part of small swarm	*	*		
95101	mfc-phyric int dyke		*	*		
95102	pebble conglomer (6)					
95103	pc-mfc-phyric aph mfc dyke	sparsely phyric	*			
95104	fgr vclastic (6)					
95105	mfc-phyric fgr mfc dyke	sparsely phyric				
95106	aphy fgr mafic dyke	vesic, bx zones	*	*		
95107	pebble conglomer (6)					
95108	pc-phy fgr mfc sill					
95109	pc-phy fgr mfc sill					
95110	f-mgr pc-phy sill	vesic margins				
95111	irreg aphy fgr mfc sill (3)	intr 112 GHW unit	*	*	*	
95112	pc-phy amyg mfc plwd vlcs (3)	GHW unit	*	*	*	*
95113	pc-phy mfc-int dyke	intr 112, 111	*	*	*	

sample	Rock Type (unit)	other	TS	XRF	ICP	Nd
95026	pc-phy mfc-int dyke	sparsely phyric	*	*	*	*
95027	aphy mfc-int dyke		*			
95028	agglom/conglom (6)					
95029	black shale (4)					
95030	aphyric mfc dyke		*			
95031	aphyric mfc dyke		*			
95032	hb-pc-phy mfc-int dyke	vesic/amyg	*			
95033	mgr gb sill		*	*	*	*
95034	hb-pc-phy mfc dyke	sparsely phyric	*			
95035	pc-phy plwd mfc vlc (3)	GHW unit	*			
95036	flt'd aphy mfc vlc/tff (4)	chloritic	*	*	*	
95037	f-mgr pc-phy mfc sill		*	*		
95038	aph mfc dyke	intrudes 37	*	*	*	
95039	red chert grain grit (6)		*			
95040	red chert grain grit (6)					
95041	red and grn argillite (7)					
95042	mfc-phy mfc dyke	sparsely phyric	*			
95043	argillite w sandy interbed (7)					
95044	aphy mafic dyke		*			
95045	fgr pebble conglomer (6)		*			
95046	chert cobble bed (6)					
95047	fgr vclastic (6)					
95048	debris flow (6)					
95049	qtz-rich grit (6)					
95050	pc-phy plwd mfc vlc (3)	GHW unit	*	*	*	*
95051	red and grn argillite (4)					
95052	pebble conglomer	clast in olistostrome				
95053	plwd mfc vlc	clast in olistostrome	*	*	*	
95054	shale with xtl-rich layers (4)	matrix of olistostrome				
95055	pebble conglomer	lost this sample				
95056	pc-phy mfc-int dyke	irreg margin, syn-sedimentray?	*	*		
95057*	flc tff		*			
95058	aphy f-mgr mfc sill		*	*	*	*
95059	aphric mfc dyke		*			
95060	pc-phyric mfc-int sill		*	*		
95061	def'd mgr gb dyke	serpentinite slickensides	*	*	*	*
95062	fgr diabase sill		*	*		
95063	def'd cgr gb dyke	serpentinite slickensides	*	*		
95064	flc tff (?)		*			
95065	flc-int pebble conglomer/agglom (6)					
95066	plwd mfc vlc (5)	GHE unit	*	*	*	
95067	pc-mfc-phy mfc-int dyke	sparsely phyric	*	*	*	
95068	pc-phy fgr mfc dyke	tiny pc laths	*	*		
95069	pc-phy fgr mfc vlc/svlc (5)	GHE unit	*	*		
95070	pc-phy fgr mfc-int dyke/sill		*	*		

sample	Rock Type (unit)	other	TS	XRF	ICP	Nd
94046	lgb	w gneissic fol'n	*			
94047	def'd msv gb (SLIC)		*	*		
94048	fault bx in mfc dyke	sd intr lgb (SLIC)	*			
94049	msv gb (SLIC)		*	*	*	
94050	lgt grey fgr aphy mfc dyke (SLIC)	sd intr lgb (SLIC)	*	*		
94051	fgr tnlt		*	*	*	*
94052	def'd gb		*			
94053	lgt grey fgr aphy mfc dyke	sd intr lgb (SLIC)	*	*		
94054	lgt grey fgr aphy mfc dyke	sd intr lgb (SLIC)	*	*		
94055	def'd lgb (SLIC)		*	*		
94056	org ws fgr mfc dyke	part of swarm	*	*	*	*
94057	buff ws aph flc-int vlc (?)	screen in dyke swarm	*	*	*	
94058	org ws fgr mfc dyke	sparsely pc phy	*	*	*	
94059	org ws fgr mfc dyke	intr tnlt (SLIC)	*	*		
94060	tnlt (SLIC)		*	*		
94061	pinkish tnlt (SLIC)		*	*	*	
94062	qtz-phy buff ws int dyke	intr tnlt (SLIC)	*	*	*	
94063	def'd lgb (SLIC)		*			
94064	cataclastically def'd hb dt (SLIC)		*			
95001	pc-phy grn ws mfc vlc/svlc (5)	GHE unit	*	*	*	
95002	fgr gb		*			
95003	fgr grn mfc dyke	intrudes 04	*			
95004	flt'd mfc tff (?) (6)		*			
95005	int vclastic/tff (6)		*			
95006	qtz-rich grit (6)		*			
95007	fgr gb		*	*		
95008	fgr aphy mfc dyke		*			
95009	fgr aphy mfc dyke	intr 11	*	*		
95010	fgr aphy mfc dyke	intr 09	*	*	*	*
95011	aphy mfc vlc (5)	GHE unit	*	*		
95012	aphy mfc-int dyke	intr 13	*			
95013	aphy mfc-int vlc/tff		*			
95014	fgr vclastic (6)		*			
95015	qtz-rich grit/vclastic (6)		*			
95016	mfc-int pc-phy vlc/svlc (5)	> 20% phenos GHE unit	*	*	*	*
95017	aphy mfc dyke	intr 16	*			
95018	mfc-int agglom/tff (6)		*			
95019	agglom/conglom (6)	granitoid cobbles				
95020	aphy mfc dyke		*			
95021	plwd vlc (5)	GHE unit	*	*		
95022	pc-phy plwd vlc (5)	GHE unit	*	*	*	*
95023	aphy mfc dyke		*	*		
95024	mfc-int agglom/conglom (6)					
95025	pc-phyric plwd vlcs (5)	GHE unit				
95025b	def'd hematized red plwd vlcs (3)	w inter-plw red argillite GHW unit	*	*	*	*

sample	Rock Type (unit)	other	TS	XRF	ICP	Nd
94001	fgr vclastic (6)	thinly bedded gw and chert	*			
94002	fgr vclastic (6)	thinly bedded gw and chert	*			
94003	fgr vclastic (6)	with minor thinly bedded chert	*	*		
94004	lgb (SLIC)		*			
94005	org ws mfc dyke	relatively undef'd	*	*	*	*
94006	shear zone in tmlt (SLIC)	rextl'd mylonite ?	*			
94007	grey dyke in msv gb (SLIC)	surrounded by lots of tmlt	*	*	*	
94008	org ws fgr mfc dyke	intr lgb and sd (SLIC)	*	*	*	
94009	grey aphy fgr mfc dyke	sd intr lgb (SLIC)	*	*	*	*
94010	lgb		*	*		
94011	lgb		*	*		
94012	aphy mgr grey mfc dyke	sd intr lgb (SLIC)	*	*	*	
94013	org ws mfc dyke	x-cuts def'n in lgb and sd	*	*	*	*
94014	gm pc-phy mfc dyke (SLIC)	sd in lgb (SLIC)	*	*	*	*
94015	qtz-rich hb dt (SLIC)		*	*	*	
94016	tmlt net viens in lgb (SLIC)		*			
94017	qtz-rich hb dt (SLIC)		*	*		
94018	tmlt		*	*	*	*
94019	org ws mfc dyke	relatively undef'd	*	*		
94020	org ws fgr irreg mfc body	mixed with tmlt (SLIC)	*	*	*	
94021	org ws fgr irreg mfc body	intr gb (SLIC)	*	*		
94022	bx of gb w org ws mfc mtrx		*			
94023	hb dt		*	*	*	
94024	org ws fgr mfc dyke	intr hb dt (SLIC)	*	*		
94025	buff ws mfc dyke	intr um part of layered mfc sill	*	*		
94026	um	part of layered mfc sill	*	*		
94027	buff ws mfc dyke	intr gb part of layered mfc sill	*	*		
94028	gb	part of layered mfc sill	*	*	*	*
94029	fgr grey ws irreg intr	intr hb dt (SLIC)	*	*	*	
94030	hb dt		*	*	*	
94031	lgb	only local, surrounded bt tmlt	*			
94032	grey-grn fgr aphy mfc dyke	intr tmlt	*	*	*	*
94033	qtz hb dt		*	*		
94034	def'd org/bm ws mfc incl	in tmlt (SLIC)	*	*		
94035	buff ws undef'd int dyke	intr tmlt and hb dt	*	*	*	
94036	cgr org ws mfc incl	um (?) in tmlt (SLIC)	*	*	*	
94037	cgr gb	px rimmed by amph	*	*	*	
94038	aph dk grey dyke	intr dt and tmlt (SLIC)	*	*	*	*
94039	fgr vclastic (2)					
94040	qtz-phy- flc vlc (2)					
94041	msv gb (SLIC)	intr lgb (SLIC)	*	*	*	*
94042	fgr qtz-fsp-ep (tmlt?) dyke (SLIC)	intr lgb	*	*	*	*
94043	pc and mfc phy gm aph mfc dyke	sd intr lgb (SLIC)	*	*	*	
94044	pc and mfc phy gm aph mfc dyke	sd intr lgb (SLIC)	*	*	*	*
94045	fgr aphy grey mfc dyke (SLIC)	sd intr lgb (SLIC)	*	*	*	*

## **Appendix 2**

### **Sample Locations\***

\*This appendix contains two lists of samples with UTM coordinates from NTS maps, one list for geochronology samples and another for all other samples. There may be minor discrepancies between these numbers and the coordinates of locations taken from the thesis map, because maps were digitized from airphotos which produce some distortion. The UTM coordinates listed are taken from NTS maps and are the correct values.

sample	easting	northing	sample	easting	northing	sample	easting	northing
94001	608500	5471250	94050	608700	5475125	95035	609550	5480875
94002	608500	5469775	94051	608575	5474850	95036	610000	5479425
94003	608650	5469450	94052	607750	5474450	95037	608825	5480225
94004	608750	5469525	94053	607200	5474750	95038	608825	5480225
94005	609450	5469625	94054	607775	5474850	95039	609875	5480400
94006	609500	5469500	94055	607775	5474850	95040	608700	5480375
94007	608950	5469350	94056	608250	5475200	95041	608650	5480500
94008	609475	5472100	94057	608150	5475775	95042	608650	5480500
94009	609475	5472100	94058	608175	5475900	95043	608775	5481150
94010	609475	5472100	94059	610050	5464825	95044	608775	5481150
94011	609425	5471975	94060	609700	5464750	95045	609500	5481040
94012	609575	5472325	94061	610600	5462525	95046	609500	5481040
94013	609350	5472000	94062	610600	5462525	95047	609475	5481000
94014	609400	5472200	95001	610350	5479250	95048	609375	5481025
94015	609875	5470750	95002	610400	5479350	95049	609375	5481025
94016	609250	5472125	95003	610300	5479175	95050	609850	5479825
94017	609000	5472300	95004	610300	5479175	95051	609700	5480500
94018	609525	5473150	95005	610300	5479175	95052	609850	5480675
94019	609075	5472750	95006	610300	5479175	95053	609850	5480675
94020	609075	5472750	95007	610150	5479325	95054	609850	5480675
94021	609500	5469200	95008	610150	5479325	95055	609800	5481275
94022	609457	5469190	95009	610200	5479600	95056	609500	5481250
94023	609275	5468675	95010	610200	5479600	95057	609500	5481250
94024	609275	5468675	95011	610200	5479600	95058	610150	5481300
94025	612000	5483000	95012	610150	5479450	95059	610325	5481325
94026	612000	5483000	95013	610150	5479450	95060	610225	5481600
94027	612000	5483000	95014	609950	5479525	95061	610375	5482325
94028	612000	5483000	95015	609950	5479525	95062	610000	5482550
94029	609100	546855	95016	610425	5480200	95063	610600	5483950
94030	609100	546855	95017	610425	5480200	95064	610650	5483900
94031	609100	546855	95018	610375	5480200	95065	610450	5482450
94032	608150	5467050	95019	610325	5480225	95066	610975	5480850
94033	609500	5466900	95020	610375	5480325	95067	610975	5480850
94034	609150	5465850	95021	610525	5480150	95068	610950	5480925
94035	608925	5465850	95022	610750	5480700	95069	610950	5481075
94036	608840	5465640	95023	610700	5480650	95070	610925	5481375
94037	608850	5465650	95024	610525	5480475	95071	610925	5481375
94038	608625	5464250	95025	610875	5480800	95072	610925	5481450
94039	608150	5463250	95025B	610050	5480650	95073	613525	5483725
94040	608150	5463500	95026	609700	5480450	95074	611125	5481650
94041	608300	5464350	95027	609850	5480675	95075	611125	5481650
94042	607800	5474175	95028	609850	5480675	95076	611050	5481875
94043	607800	5474175	95029	610000	5480725	95077	611050	5481875
94044	607900	5474225	95030	610500	5481750	95078	611206	5482444
94045	607900	5474400	95031	608675	5479975	95079	610950	5482200
94046	607900	5474400	95032	609450	5480000	95080	611050	5482325
94047	607900	5474400	95033	609450	5480000	95081	611300	5482650
94048	608000	5474400	95034	609500	5479850	95082	611600	5483650
94049	608425	5474525				95083	610300	5479000

sample	easting	northing	sample	easting	northing	sample	easting	northing
95084	610300	5479000	95134	611275	5479950	96014	615100	5479850
95085	610300	5479000	95135	611325	5479900	96015	615350	5479450
95086	610250	5479750	95136	611350	5479825	96016	609350	5478300
95087	608300	5477825	95137	611350	5479775	96017	609025	5477875
95088	608075	5477775	95138	611450	5479825	96018	608975	547925
95089	608075	5477775	95139	611450	5479825	96019	608550	5472000
95090	608075	5477775	95140	611525	5479650	96020	608500	5472175
95091	608100	5477825	95141	611550	5479450	96021	616450	5482625
95092	608075	5477950	95142	611550	5479450	96022	616350	5482700
95093	608025	5477975	95143	611225	5478850	96023	617200	5481650
95094	608025	5478000	95144	611050	5479850	96024	617200	5481650
95095	607900	5478650	95145	610975	5479825	96025	616450	5481000
95096	607950	5478650	95146	610825	5478925	96026	616450	5481000
95097	607775	5479325	95147	610650	5479950	96027	616450	5481000
95098	607725	5479750	95148	610275	5478725	96028	616375	5480775
95099	607725	5479950	95149	609550	5478325	96029	613025	5476375
95100	607675	5479725	95150	608725	5478875	96030	616450	5481000
95101	607650	5479725	95151	608725	5478875	96031	615000	5483550
95102	607650	5479725	95152	608750	5478200	96032	613325	5479700
95103	607300	5480100	95153	609775	5478200	96033	612700	5479900
95104	607300	5480100	95154	609000	5478475	96034	614600	5478925
95105	607625	5480800	95155	609050	5478400	96035	614300	5478750
95106	607625	5480800	95156	612875	5482925	96036	614275	5478625
95107	607725	5481925	95157	612825	5482725	96037	610350	5466275
95108	608450	5481250	95158	611250	5480525	96038	610600	5465350
95109	608925	5482375	95159	611250	5480525	96039	610200	5464700
95110	608950	5482500	95160	611050	5480600	96040	610700	5464700
95111	609250	5479800	95161	611075	5480350	96041	610650	5464650
95112	609250	5479800	95162	611075	5480350	96050	607500	5462000
95113	609250	5479800	95163	611225	5480250	96051	607300	5462625
95114	609250	5479800	95164	610150	5478500	96052	607400	5462850
95115	609250	5479800	95165	609850	5478125	96053	607875	5461250
95116	609250	5479800	95166	609700	5478150	96054	608325	5462425
95117	608800	5479600	95167	610350	5478150	96055	608325	5462425
95118	610150	5481400	95168	612500	5482275	96056	608500	5462300
95119	611875	5483425	95169	612525	5482600	96057	608800	5461300
95120	612200	5482575	95170	612600	5483050	96058	609925	5458750
95121	612450	5482000	96001	612175	5478350	96059	610075	5459050
95122	612450	5482000	96002	611500	5475300	96060	610850	5459050
95123	611850	5481225	96003	610850	5474950	96061	611650	5460000
95124	611850	5481225	96004	610050	5473675	96062	611250	5460500
95125	611875	5481125	96005	609500	5477750	96063	607950	5465250
95126	611875	5481125	96006	608950	5474875	96064	607775	5465250
95127	611750	5481000	96007	608825	5474875	96065	608100	5465150
95128	611800	5481000	96008	608800	5476500	96066	609975	5479500
95129	611800	5481000	96009	608750	5476475	96067	610150	5481400
95130	611700	5480900	96010	608600	5476350	96068	610000	5480700
95131	611475	5480525	96011	610250	5477125	96069	616450	5481000
95132	611450	5480350	96012	609825	5477325	96070	608075	5477950
95133	611400	5480300	96013	615600	5480550	96071	608700	5472350

sample	easting	northing	sample	easting	northing	sample	easting	northing
94GC01	609550	5469250	95GC07	609920	5410000	96GC09	608575	5481275
94GC02	609800	5466775	95GC08	610150	5481400	96GC10	608575	5481275
94GC03	608400	5465500	95GC09	609975	5479500	96GC11	610850	5459050
94GC04	609000	5472300	95GC10	611375	5479850	96GC12	608100	5465150
94GC05	610100	5470150	96GC01	609600	5477775	96GC13	612000	5483000
94GC06	609700	5470900	96GC02	608150	5475775	96GC14	611375	5479850
95GC01	608925	5479675	96GC03	608150	5475775	96GC15	610150	5479325
95GC02	609575	5481275	96GC04	608675	5476400	96GC16	605500	5482950
95GC03	610200	5481175	96GC05	608725	5478875	96GC17	603950	5470400
95GC04	607950	5478275	96GC06	609350	5471950	D47-10	609350	5471375
95GC05	610950	5481600	96GC07	610475	5480000	GD-91-6	609800	5471800
95GC06	609250	5479800	96GC08	608575	5481275			

## Appendix 3

### Geochemical Data

This appendix contains a list of all the whole rock geochemical data (XRF major and trace elements and ICP-MS trace elements) from this study (94000, 95000 and 96000 series), and data from Swinden et al. 1990 that was used for comparison (400, 500 and 700 series). Samples are listed by geochemical group as defined in this thesis, and brief rock type descriptions are given. Volcanic and plutonic rocks are also assigned to a geographical volcanic unit as per Fig. 4.1. For the data of Swinden et al. 1990, FeO and Fe<sub>2</sub>O<sub>3</sub> were measured, but for samples from this study,  $\text{FeO} = 0.7 \times \text{Fe}_2\text{O}_3 \text{ T}$  and  $\text{Fe}_2\text{O}_3$  ( $0.3 \times \text{Fe}_2\text{O}_3 \text{ T}$ ). Any elements not measured for a particular sample have nm entered, and for analyses below the detection limit bd is entered. Major elements are given in wt % oxide and trace elements as ppm. Samples with WBG as their geographic unit are within the sedimentary succession and do not belong to a discrete volcanic unit. Samples with PC indicate that they are interpreted to be post Caradocian and thus not part of the WBG stratigraphy. Samples with a ? do not fit easily into a geochemical group and their association is unknown.

#### Abbreviations:

##### General

mfc	mafic
flc	felsic
int	intermediate
vlc	volcanic
svlc	subvolcanic
intr	intrusive
tnlt	tonalite
hb dt	hornblende diorite
gb	gabbro
rhy	rhyolite
peg	pegmatite
xeno	xenolith
bx	breccia
frag	fragment
fgr	fine-grained
PC	post Caradocian
?	unknown

##### Geographic units

GHW	Glover's Harbour west
GHE	Glover's Harbour east
IC	Indian Cove
SLIC	South Lake igneous complex
NBL	Nanny Bag Lake
LPS	Long Pond south
LP	Long Pond
SBB	Seal Bay Bottom
BLL	Big Lewis Lake
NA	Northern Arm
KL	Kerry Lake
KLN	Kerry Lake north
WA	Western Arm
OM	Osmomton Arm
BB	Badger Bay
SH	Side Harbour
WBG	Wild Bight Group
SD	sheeted dykes of SLIC

Sample	Rock Type	Group	Mg #	SiO <sub>2</sub>	TiO <sub>2</sub>	Al <sub>2</sub> O <sub>3</sub>	Fe <sub>2</sub> O <sub>3</sub> *	FeO*	MnO	MgO	CaO
530	mfc vlc NBL	1	47.59	50.58	1.01	15.25	3.33	11.93	0.27	6.84	6.89
532	mfc vlc NBL	1	38.27	54.59	1.59	15.43	5.20	7.87	0.25	3.55	4.68
541	mfc vlc NBL	1	43.88	54.41	1.27	15.26	4.30	8.92	0.21	4.76	4.58
544	mfc vlc NBL	1	45.54	52.40	1.74	14.80	4.44	9.48	0.20	5.38	6.56
94008	mfc dyke SLIC	1	39.19	49.40	1.58	13.84	5.19	12.12	0.26	5.23	9.76
94013	mfc dyke SLIC	1	50.05	46.81	1.29	16.92	4.61	10.77	0.22	7.22	6.19
94045	mfc dyke SLIC	1	50.68	50.20	1.24	15.41	3.92	9.14	0.19	6.28	9.62
94056	mfc dyke SLIC	1	44.91	51.67	1.39	14.92	4.21	9.81	0.25	5.35	6.08
94058	mfc dyke SLIC	1	45.30	52.55	1.33	14.99	4.25	9.91	0.21	5.49	5.43
94GC02	mfc dyke SLIC	1	41.30	48.74	1.69	14.36	5.34	12.45	0.26	5.86	6.80
96010	mfc dyke SLIC	1	46.13	48.70	1.06	16.65	4.16	9.72	0.33	5.57	5.47
96010	mfc dyke SLIC	1	45.78	45.39	0.01	16.66	4.18	9.76	0.33	5.52	5.53
96055	mfc vlc LPS	1	39.02	51.11	1.53	15.10	4.72	11.00	0.13	4.71	5.57
96055	mfc vlc LPS	1	38.72	51.28	1.53	15.25	4.74	11.07	0.13	4.68	5.59
96057	mfc vlc LPS	1	42.84	52.60	1.31	15.35	4.32	10.08	0.19	5.06	4.48
96058	mfc vlc NBL	1	47.74	56.23	1.09	13.79	3.57	8.33	0.19	5.09	6.49
94009	mfc dyke SD	2	62.53	49.73	0.61	15.45	3.16	7.36	0.18	8.22	12.09
94012	mfc dyke SD	2	59.40	47.00	0.46	15.45	3.05	7.12	0.17	6.97	12.24
94015	hbd dt SLIC	2	56.11	50.14	0.29	15.91	3.29	7.68	0.20	6.57	11.80
94020	mfc intr SLIC	2	54.24	53.48	0.59	16.59	3.30	7.71	0.20	6.11	7.78
94036	mfc xeno SLIC	2	73.85	50.03	0.20	9.43	3.90	9.11	0.20	17.21	8.30
94038	mfc dyke SLIC	2	65.38	48.54	0.31	11.58	3.11	7.26	0.22	9.18	12.12
94043	mfc dyke SD	2	69.67	51.75	0.29	13.87	2.74	6.39	0.16	9.82	10.91
94062	mfc dyke SLIC	2	66.41	56.43	0.66	15.45	2.86	6.66	0.17	8.81	5.68
94GC05	hbd dt SLIC	2	51.46	53.41	0.27	15.64	3.40	7.94	0.21	5.63	10.01
94GC05	hbd dt SLIC	2	51.87	54.26	0.28	15.88	3.40	7.94	0.21	5.73	10.19
95153	mfc vlc GHW	2	32.42	55.98	0.93	15.30	4.11	9.60	0.22	3.08	3.83
95153	mfc vlc GHW	2	31.78	55.70	0.93	15.21	4.14	9.65	0.21	3.01	3.82
95153	mfc vlc GHW	2	32.11	56.01	0.94	15.32	4.13	9.64	0.21	3.05	3.83
95154	mfc vlc GHW	2	58.07	50.98	0.83	16.09	3.54	8.27	0.18	7.67	6.69
456	mfc vlc GHW	3	53.14	54.99	0.67	15.34	3.38	7.09	0.13	5.48	6.79
457	mfc intr GHW	3	45.95	45.32	3.96	14.92	4.39	11.06	0.21	6.22	9.96
458	mfc vlc GHW	3	60.02	54.98	0.47	15.66	2.19	7.39	0.12	7.05	8.66
465	mfc intr GHW	3	65.20	52.69	0.49	17.55	1.60	7.75	0.12	8.90	9.19
473	mfc vlc GHW	3	52.49	58.80	0.53	13.58	3.02	7.51	0.16	5.50	8.23
476	mfc vlc GHW	3	48.54	51.99	0.57	16.44	5.18	6.50	0.17	4.67	11.02
492	mfc vlc IC	3	58.98	59.27	0.46	14.34	3.61	4.67	0.10	5.08	8.82
94007	mfc dyke SLIC	3	69.36	49.75	0.29	15.83	2.76	6.43	0.15	9.74	11.64
94014	mfc dyke SD	3	79.45	49.20	0.29	10.89	2.83	6.60	0.17	17.08	11.20
94014	mfc dyke SD	3	79.61	49.31	0.29	10.92	2.81	6.55	0.17	17.10	11.16
94014	mfc dyke SD	3	79.53	49.27	0.28	10.93	2.81	6.57	0.16	17.08	11.26
94023	gb SLIC	3	33.16	44.73	2.15	12.50	7.32	17.07	0.40	5.67	10.52
94029	mfc intr SLIC	3	64.81	49.24	0.40	16.34	2.95	6.88	0.18	8.49	13.01
94030	hbd dt SLIC	3	59.93	48.54	0.41	16.51	3.47	8.09	0.20	8.09	13.13
94037	gb SLIC	3	70.97	52.13	0.24	11.75	3.04	7.10	0.20	11.62	11.40
94041	gb SLIC	3	40.71	42.42	1.11	18.75	5.32	12.42	0.23	5.71	12.56
94044	mfc dyke SD	3	65.84	49.54	0.49	14.01	3.71	8.66	0.24	11.18	10.12
94044	mfc dyke SD	3	65.62	49.34	0.49	13.98	3.72	8.67	0.23	11.08	10.08
94049	gb SLIC	3	42.51	56.23	0.67	14.71	3.75	8.75	0.20	4.33	7.44

Sample	Rock Type	Group	Mg #	SiO <sub>2</sub>	TiO <sub>2</sub>	Al <sub>2</sub> O <sub>3</sub>	Fe <sub>2</sub> O <sub>3</sub> *	FeO*	MnO	MgO	CaO
94049	gb SLIC	3	42.28	56.21	0.68	14.58	3.77	8.79	0.19	4.31	7.44
94049	gb SLIC	3	42.23	56.10	0.67	14.63	3.75	8.75	0.19	4.28	7.45
94gc03	gb peg SLIC	3	72.85	49.66	0.13	15.45	2.62	6.12	0.18	10.99	13.78
94GC04	hbd dt SLIC	3	44.97	58.84	0.53	14.99	2.96	6.91	0.19	3.78	7.47
95050	mfc vlc GHW	3	51.98	50.21	0.32	15.81	2.71	6.32	0.16	4.58	7.47
95111	mfc svlc GHW	3	43.40	52.66	0.59	15.14	3.66	8.54	0.21	4.38	9.27
95112	mfc vlc GHW	3	57.40	47.81	0.37	17.15	3.48	8.12	0.18	7.32	14.67
95115	mfc svlc GHW	3	42.76	50.07	0.49	16.60	3.89	9.07	0.22	4.53	9.82
95116	mfc svlc GHW	3	45.06	49.94	0.51	17.04	4.07	9.50	0.17	5.21	10.14
95GC06	mfc dyke SLIC	3	41.74	53.41	0.63	17.54	3.75	8.75	0.12	4.20	7.13
96009	mfc vlc GHW	3	60.16	50.72	0.54	15.52	3.17	7.39	0.22	7.46	8.39
96009	mfc vlc GHW	3	60.17	46.33	0.55	15.52	3.12	7.28	0.22	7.36	8.30
95149	mfc vlc GHW	4	48.89	55.04	0.70	13.77	4.21	9.83	0.25	6.29	4.80
96054	fgr dyke LP	4	45.99	53.23	0.47	16.00	4.09	9.55	0.21	5.44	3.29
96005	mfc vlc GHW	5	62.09	53.17	0.16	15.28	2.82	6.58	0.17	7.21	7.63
95025B	mfc vlc GHW	5	64.70	51.32	0.32	16.23	4.04	9.42	0.20	11.55	2.74
95053	mfc vlc GHW	5	35.59	65.89	0.21	15.80	1.81	4.23	0.11	1.56	2.80
453	flsc vlc GHW	6	35.95	76.88	0.28	12.36	0.12	2.74	0.03	0.88	0.48
487	flsc vlc GHW	6	16.31	78.51	0.40	11.96	0.92	0.40	0.03	0.09	3.11
538	flsc vlc GHW	6	20.95	77.50	0.23	11.87	0.65	1.86	0.02	0.32	0.54
94060	tnlt SLIC	6	40.60	73.24	0.29	12.38	1.26	2.93	0.06	1.34	1.73
94018	tnlt SLIC	6	26.03	74.95	0.26	12.92	1.02	2.38	0.07	0.56	2.07
94042	tnlt SLIC	6	32.24	76.31	0.15	12.61	0.22	0.51	0.00	0.16	3.58
94051	tnlt SLIC	6	20.70	77.85	0.15	11.72	0.58	1.35	0.03	0.24	0.15
94057	flsc-int vlc (?) GHW	6	18.84	66.06	0.68	13.25	2.84	6.62	0.20	1.03	1.78
94060	tnlt SLIC	6	54.71	73.26	0.27	13.10	1.33	3.10	0.07	2.51	1.95
94061	tnlt SLIC	6	22.63	72.77	0.35	12.71	1.47	3.43	0.10	0.67	1.23
94GC06	tnlt SLIC	6	27.65	70.51	0.37	13.32	1.69	3.95	0.10	1.01	4.60
94GC06	tnlt SLIC	6	27.55	70.20	0.37	13.11	1.68	3.91	0.10	1.00	4.56
94GC06	tnlt SLIC	6	27.55	70.20	0.37	13.11	1.68	3.91	0.10	1.00	4.56
95GC02	tnlt boulder WBG	6	76.80	75.98	0.26	11.73	0.21	0.50	0.03	1.10	1.46
95GC08	rhy bx block WBG	6	32.43	77.94	0.17	10.08	1.21	2.82	0.04	0.90	1.72
96060	rhy NBL	6	42.66	69.95	0.32	12.72	1.98	4.62	0.06	2.30	3.65
96065	rhy LP	6	18.20	73.58	0.28	12.27	1.28	3.00	0.05	0.45	3.13
96065	rhy LP	6	17.78	73.75	0.28	12.36	1.29	3.01	0.05	0.44	3.12
96065	rhy LP	6	17.43	74.17	0.27	12.34	1.29	3.01	0.05	0.43	3.11
96067	rhy bx block WBG	6	33.17	78.44	0.12	8.48	0.83	1.94	0.04	0.65	2.14
96067	rhy bx block WBG	6	33.52	80.42	0.11	8.65	0.85	1.98	0.05	0.67	2.15
96071	rhy tuff xeno SLIC	6	28.07	71.81	0.23	12.47	1.34	3.12	0.06	0.81	5.41
96072	rhy bx block WBG	6	28.33	86.08	0.12	6.43	0.67	1.57	0.03	0.42	1.18
96GC01	rhy block WBG	6	53.84	66.57	0.23	13.26	1.77	4.14	0.10	3.23	4.97
96GC05	flsc tuff WBG	6	39.92	81.45	0.16	9.29	0.38	0.88	0.02	0.39	0.94
96GC07	hbd dt cobble WBG	6	28.69	70.82	0.27	12.84	1.58	3.70	0.10	1.00	2.38
96GC07	hbd dt cobble WBG	6	28.46	66.28	0.27	12.88	1.57	3.66	0.10	0.98	2.38
96GC08	rhy block WBG	6	38.71	76.18	0.23	10.53	1.08	2.53	0.08	1.07	0.75
463	mfc vlc GHE	7	59.45	53.27	0.94	18.52	1.80	5.00	0.17	4.78	9.86
467	mfc vlc GHE	7	40.45	56.13	1.49	16.98	3.08	5.85	0.15	2.76	6.51
481	mfc intr WBG	7	46.03	48.54	1.94	15.01	4.91	10.18	0.27	5.93	8.18
496	mfc intr WBG	7	50.21	53.63	1.16	18.18	2.25	7.38	0.19	4.75	7.39

Sample	Rock Type	Group	Mg #	SiO <sub>2</sub>	TiO <sub>2</sub>	Al <sub>2</sub> O <sub>3</sub>	Fe <sub>2</sub> O <sub>3</sub> *	FeO*	MnO	MgO	CaO
553	mfc vlc SBB	7	49.13	54.09	1.51	16.95	2.06	8.80	0.23	5.27	4.64
554	mfc vlc SBB	7	60.13	53.27	0.99	18.36	1.95	5.87	0.23	5.71	9.62
756	mfc vlc SBB	7	49.15	55.56	1.44	17.20	1.99	8.36	0.19	5.02	6.04
767	mfc vlc BLL	7	61.87	55.11	1.41	14.77	3.50	6.37	0.16	7.23	7.09
772	mfc vlc NA	7	56.21	54.25	0.96	16.09	1.69	6.39	0.16	5.15	10.17
774	mfc vlc NA	7	62.74	52.82	1.02	15.96	1.16	6.92	0.14	7.03	11.34
95001	mfc vlc GHE	7	60.47	50.45	1.14	15.62	3.62	8.44	0.24	8.64	9.08
95001	mfc vlc GHE	7	54.06	51.96	1.15	17.39	2.93	6.84	0.19	5.39	8.71
95011	mfc vlc GHE	7	57.29	52.94	0.90	17.56	2.51	5.85	0.15	5.26	8.35
95016	mfc vlc GHE	7	27.69	68.95	0.77	13.07	1.65	3.84	0.14	0.98	1.50
95021	mfc vlc GHE	7	46.60	55.77	1.53	15.84	3.08	7.18	0.17	4.19	4.24
95022	mfc vlc GHE	7	57.97	54.52	0.74	18.40	2.19	5.11	0.15	4.71	8.53
95026	mfc int GHE	7	49.05	51.25	1.75	14.66	4.35	10.16	0.23	6.54	4.89
95060	int-flsc intr GHE	7	25.10	69.22	0.82	12.97	1.45	3.38	0.12	0.76	1.82
95066	mfc vlc GHE	7	38.91	55.65	1.59	16.48	3.14	7.32	0.15	3.12	4.89
95066	mfc vlc GHE	7	39.11	55.47	1.58	16.47	3.13	7.30	0.15	3.14	4.83
95068	mfc dyke GHE	7	27.95	68.49	0.83	13.12	1.57	3.67	0.19	0.95	2.18
95069	mfc vlc/svlc GHE	7	27.55	70.61	0.36	13.29	1.68	3.93	0.10	1.00	4.60
95071	mfc vlc/tff GHE	7	39.43	54.31	1.03	18.19	3.01	7.02	0.12	3.06	5.38
95124	flsc svlc GHE	7	20.90	72.34	0.38	13.24	0.96	2.23	0.04	0.40	0.34
95131	mfc-int svlc GHE	7	27.72	68.65	0.77	13.00	1.59	3.70	0.17	0.95	1.67
95137	mfc vlc GHE	7	45.30	52.42	1.37	17.21	2.72	6.35	0.15	3.52	10.16
95138	mfc vlc GHE	7	39.47	54.01	0.95	18.74	2.77	6.46	0.14	2.82	6.87
95142	mfc vlc GHE	7	42.51	52.56	1.10	18.41	3.41	7.95	0.14	3.93	4.21
95143	mfc vlc GHE	7	33.84	66.45	0.91	13.52	1.96	4.58	0.15	1.57	2.59
95161	mfc vlc GHE	7	39.54	56.99	0.98	16.98	2.91	6.79	0.17	2.97	3.85
95164	mfc vlc GHE	7	46.86	57.24	0.98	18.45	2.50	5.82	0.15	3.44	3.57
95164	mfc vlc GHE	7	47.01	57.32	0.99	18.35	2.51	5.86	0.15	3.48	3.59
95166	mfc vlc GHE	7	38.83	54.86	1.55	16.37	3.10	7.24	0.15	3.08	4.77
95GC05	flsc svlc GHE	7	28.90	70.77	0.40	13.94	0.84	1.96	0.05	0.53	0.47
95GC05	flsc svlc GHE	7	30.05	70.92	0.40	14.08	0.83	1.94	0.05	0.56	0.48
96012	mfc vlc GHE	7	39.16	53.05	1.00	18.86	2.96	6.90	0.17	2.97	5.71
96019	int dyke WBG	7	34.56	61.93	1.17	14.34	2.58	6.02	0.26	2.13	8.03
96032	mfc vlc/svlc GHE	7	40.24	53.70	0.96	18.37	2.97	6.92	0.13	3.12	4.82
96033	mfc vlc GHE	7	38.96	54.10	0.99	18.68	2.89	6.74	0.14	2.88	5.44
96053	mfc vlc KL	7	61.50	51.30	0.94	16.61	2.65	6.19	0.18	6.62	10.99
96061	mfc vlc WAB	7	58.32	51.78	1.21	15.82	3.23	7.55	0.20	7.07	5.04
96063	mfc vlc KL	7	57.99	51.99	0.68	20.42	2.27	5.29	0.15	4.89	7.48
96064	mfc vlc KL	7	45.14	55.45	1.35	16.86	2.71	6.31	0.17	3.48	6.20
96066	flsc tuff WBG	7	32.69	84.97	0.13	6.58	0.64	1.50	0.06	0.49	1.65
96070	flsc tuff WBG	7	25.71	70.74	0.33	12.04	1.75	4.09	0.18	0.95	2.14
96GC10	rhy block WBG	7	18.07	70.37	0.65	13.72	1.14	2.67	0.13	0.39	1.65
491	mfc intr IC	8	59.28	48.80	1.37	19.11	3.49	5.03	0.15	5.39	12.79
495	intr WBG	8	59.87	48.18	1.29	18.50	1.51	7.89	0.16	7.18	12.89
497	mfc vlc NB	8	43.84	50.93	2.43	14.11	3.22	10.67	0.26	5.31	7.64
498	mfc vlc NB	8	44.75	50.24	2.44	14.45	4.18	10.14	0.22	5.46	7.45
503	mfc vlc BB	8	64.09	50.23	1.33	14.04	2.47	8.17	0.17	9.30	9.68
508	mfc intr BLL	8	57.08	50.35	2.26	17.83	3.76	7.16	0.29	6.60	7.24
511	mfc vlc BLL	8	65.73	49.51	1.39	14.88	2.11	8.67	0.16	10.35	9.15

Sample	Rock Type	Group	Mg #	SiO <sub>2</sub>	TiO <sub>2</sub>	Al <sub>2</sub> O <sub>3</sub>	Fe <sub>2</sub> O <sub>3</sub> *	FeO*	MnO	MgO	CaO
548	mfc vlc SH	8	69.79	49.04	1.95	13.41	2.72	8.03	0.17	11.99	8.48
95GC10	gb sill WBG	8	40.62	48.20	3.48	14.24	4.66	10.88	0.29	4.98	8.21
546	mfc vlc SH	9	56.80	50.48	2.13	14.15	3.35	8.11	0.17	7.09	9.40
549	mfc vlc SH	9	56.36	51.75	1.75	14.61	3.89	5.87	0.11	5.52	9.84
762	mfc vlc SH	9	60.60	49.33	1.74	15.24	3.94	6.93	0.17	7.51	11.70
773	mfc vlc NA	9	64.25	49.92	1.61	14.97	2.64	7.81	0.19	9.07	9.81
95056	mfc dykeWBG	9	56.21	44.03	2.52	15.98	3.88	9.06	0.17	7.78	12.16
95058	mfc sill WBG	9	39.07	52.49	1.71	15.06	4.04	9.42	0.24	4.04	5.94
95076	gb sill WBG	9	57.16	50.63	1.87	14.71	3.32	7.75	0.20	6.92	7.55
95077	mfc dykeWBG	9	62.52	50.48	1.71	13.61	3.36	7.84	0.18	8.75	8.59
95081	mfc dyke WBG	9	44.72	51.42	2.55	13.56	3.92	9.14	0.21	4.95	6.96
95106	mfc dyke WBG	9	44.46	48.44	2.88	13.63	4.46	10.40	0.28	5.57	8.95
95106	mfc dyke WBG	9	44.41	48.23	2.89	13.56	4.47	10.42	0.27	5.57	8.92
95114	mfc dyke WBG	9	60.62	47.41	1.90	13.89	3.59	8.38	0.17	8.63	10.98
95128	mfc dyke WBG	9	56.06	48.11	1.99	15.05	3.55	8.27	0.17	7.06	10.77
95132	mfc dyke WBG	9	44.81	51.64	2.41	13.80	3.77	8.80	0.19	4.78	7.12
95132	mfc dyke WBG	9	44.92	51.86	2.36	14.00	3.78	8.82	0.19	4.82	7.18
95GC03	sill WBG	9	39.67	49.18	3.18	14.33	4.53	10.57	0.23	4.65	7.64
95036	gb sill WBG	10	53.28	51.89	1.64	15.19	3.43	8.00	0.48	6.11	5.32
95036	mfc dykeWBG	10	53.42	52.63	1.63	15.40	3.44	8.03	0.48	6.16	5.39
95036	mfc dyke WBG	10	53.32	52.46	1.63	15.39	3.45	8.04	0.48	6.14	5.40
96014	mfc vlc NB	10	42.84	51.86	1.73	16.22	4.01	9.36	0.34	4.69	5.75
96021	mfc vlc NB	10	46.58	55.77	1.53	15.84	3.08	7.18	0.17	4.19	4.24
96023	mfc vlc NB	10	43.67	52.28	1.75	17.43	3.68	8.59	0.33	4.46	4.34
96024	mfc vlc NB	10	43.09	50.15	1.70	16.11	4.11	9.59	0.36	4.86	6.98
96031	mfc vlc NB	10	52.32	52.03	1.61	14.38	3.42	7.97	0.31	5.86	6.83
96035	mfc vlc NB	10	45.35	52.03	1.66	15.19	3.88	9.06	0.20	5.03	6.95
96036	mfc vlc NB	10	44.35	51.52	1.67	15.52	3.83	8.94	0.19	4.77	6.81
96037	mfc vlc/svlc WA	10	43.87	52.38	1.95	16.96	3.21	7.49	0.20	3.92	6.68
512	mfc vlc BLL	8	73.76	50.77	1.57	11.11	1.98	5.98	0.15	10.84	12.62
450	mfc intr WBG	11	45.94	49.50	2.89	17.80	3.54	7.50	0.32	4.34	7.05
454	mfc intr WBG	11	41.98	49.41	3.81	14.51	4.16	9.95	0.22	4.80	6.90
483	mfc vlc SBH	11	42.56	51.38	0.30	14.76	4.61	10.11	0.30	5.07	6.98
484	mfc vlc SBH	11	40.95	49.74	0.26	16.20	3.27	11.83	0.26	5.18	6.63
502	mfc intr BB	11	45.50	45.37	2.59	21.96	2.27	7.35	0.14	3.92	12.30
506	mfc vlc BB	11	47.64	45.15	1.81	15.18	30.40	10.94	0.17	12.56	9.20
509	mfc vlc BLL	11	35.42	50.61	0.35	17.33	4.46	14.06	0.35	4.95	4.71
551	mfc vlc SH	11	57.60	46.89	2.84	15.39	2.89	8.54	0.19	7.50	11.13
763	mfc vlc SH	11	43.25	50.94	0.19	17.65	3.37	9.47	0.19	4.70	4.68
95007	gb sill WBG	11	43.25	49.43	4.09	13.30	4.20	9.80	0.24	5.00	7.76
95009	mfc dyke WBG	11	37.67	47.51	3.46	13.38	4.86	11.34	0.28	4.59	8.53
95037	mfc intr WBG	11	40.53	49.12	2.48	18.10	3.40	7.94	0.22	3.62	7.62
95061	gb sill WBG	11	76.61	46.67	1.13	10.00	3.50	8.16	0.21	17.90	10.78
95063	gb sill WBG	11	29.44	51.85	2.17	15.15	4.24	9.90	0.22	2.76	5.65
95097	mfc dyke WBG	11	49.72	43.53	2.89	15.06	4.42	10.32	0.21	6.83	10.15
95099	mfc dyke WBG	11	60.96	50.89	1.77	12.13	3.61	8.42	0.28	8.80	8.51
95100	mfc dyke WBG	11	40.61	50.45	3.21	14.15	4.12	9.62	0.25	4.40	6.09
95100	mfc dyke WBG	11	40.30	50.12	3.23	14.24	4.10	9.56	0.24	4.32	6.08
95113	mfc dyke WBG	11	40.19	45.95	2.96	16.24	4.31	10.06	0.20	4.53	10.11

Sample	Rock Type -	Group	Mg #	SiO <sub>2</sub>	TiO <sub>2</sub>	Al <sub>2</sub> O <sub>3</sub>	Fe <sub>2</sub> O <sub>3</sub> *	FeO*	MnO	MgO	CaO
96007	mfc dyke WBG	11	57.82	52.50	1.82	13.56	3.40	7.94	0.23	7.28	7.30
96007	mfc dyke WBG	11	57.94	47.86	1.83	13.50	3.36	7.84	0.23	7.23	7.32
96011	mfc dyke WBG	11	54.48	49.21	2.12	14.88	3.53	8.23	0.18	6.60	8.94
94025	mfc dyke PC	12	52.59	49.32	3.08	15.00	3.50	8.16	0.19	6.06	6.03
95010	mfc dyke WBG PC	12	57.44	45.14	4.16	10.48	4.01	9.35	0.19	8.44	11.87
95023	mfc dyke WBG PC	12	37.82	48.08	3.33	15.69	3.23	7.53	0.18	3.07	10.09
95067	mfc dyke WBG PC	12	47.47	50.56	2.51	16.25	2.96	6.91	0.18	4.18	6.69
95070	mfc dyke WBG PC	12	44.48	48.22	3.24	15.38	3.29	7.68	0.21	4.12	8.88
95101	int dyke WBG PC	12	53.90	51.62	1.11	17.26	2.91	6.80	0.19	5.32	8.71
95119	mfc dyke PC PC	12	67.03	49.52	1.52	13.03	3.43	8.00	0.20	10.89	8.15
95119	mfc dyke PC	12	66.94	49.53	1.53	13.04	3.44	8.04	0.20	10.89	8.26
95122	mfc dyke WBG PC	12	41.20	51.44	2.74	16.69	3.09	7.20	0.15	3.38	6.37
95122	mfc dyke WBG PC	12	40.65	50.82	2.73	16.60	3.08	7.18	0.15	3.29	6.32
95125	mfc dyke WBG PC	12	45.71	42.26	3.55	14.50	7.15	16.69	0.41	9.40	4.49
95127	mfc dyke WBG PC	12	46.34	50.38	2.66	15.70	3.11	7.25	0.20	4.19	8.01
96002	mfc dyke PC	12	45.63	40.76	3.95	13.42	4.11	9.60	0.21	5.39	10.35
96002	mfc dyke PC	12	45.68	44.20	3.90	13.41	4.16	9.70	0.20	5.46	10.41
96002	mfc dyke PC	12	45.53	44.47	3.95	13.54	4.19	9.77	0.21	5.47	10.47
96004	mfc dyke PC	12	48.04	71.20	0.59	13.06	1.63	3.81	0.07	2.36	0.81
96025	flsc frag melange PC	12	36.99	57.47	1.34	16.68	2.05	4.78	0.86	1.88	4.89
96059	flsc dyke NBL PC	12	51.17	65.74	0.53	16.24	1.21	2.81	0.07	1.97	3.48
95033	gb sill GHW	13	42.19	44.79	4.32	13.78	5.09	11.87	0.22	5.80	9.81
94038	mfc dyke SLIC	?	50.70	72.84	0.44	11.77	1.27	2.96	0.20	2.04	0.54
94005	mfc dyke SLIC	?	47.96	49.61	2.40	16.48	3.81	8.89	0.18	5.48	8.62
94005	mfc dyke SLIC	?	47.75	49.40	2.43	16.46	3.81	8.89	0.18	5.44	8.65
94005	mfc dyke SLIC	?	47.96	49.61	2.40	16.48	3.81	8.89	0.18	5.48	8.62
94005	mfc dyke SLIC	?	47.54	48.76	2.36	16.34	3.77	8.80	0.18	5.34	8.48
94028A	gb sill	?	47.75	49.40	2.44	16.46	3.81	8.89	0.18	5.44	8.65
94032	mfc dyke SLIC	?	38.19	58.04	1.95	15.07	3.00	6.99	0.14	2.89	6.44
94035	mfc dyke SLIC	?	41.60	58.68	1.74	15.77	2.79	6.51	0.17	3.10	5.82

Sample	Na <sub>2</sub> O	K <sub>2</sub> O	P <sub>2</sub> O <sub>5</sub>	LOI	total	Cr	Ni	Sc	V	Rb	Ba	Sr	Nb	Hf	Zr
530	3.97	0.15	0.05	2.93	99.32	65	15	44	447	bd	51	63	1.3	0.9	28
532	6.92	0.11	0.25	1.04	98.90	26	2	40	324	1	52	64	1.4	1.6	55
541	5.52	1.00	0.14	1.75	99.04	35	bd	39	463	6	147	86	1.2	1.7	61
544	5.12	0.07	0.19	1.98	98.40	30	3	0	473	3	56	71	2.9	nm	80
94008	2.31	0.11	0.08	2.46	100.00	20	6	45	777	1	16	152	1.7	1.3	51
94013	4.02	0.02	0.10	5.59	98.24	102	31	59	520	bd	13	183	1.0	1.6	55
94045	2.67	0.43	0.08	1.24	99.93	96	29	60	483	4	38	185	1.2	1.1	44
94056	5.18	0.12	0.09	1.98	99.16	20	12	35	411	bd	39	163	1.1	1.5	56
94058	5.13	0.04	0.11	2.36	99.55	30	13	33	496	bd	19	139	1.3	2.0	71
94GC02	3.48	0.27	0.08	3.00	99.45	15	6	57	772	2	51	156	0.9	1.4	43
96010	5.23	0.65	0.08	6.62	97.71	nm	nm	nm	nm	nm	nm	nm	nm	nm	nm
96010	5.00	0.65	0.08	6.62	93.22	95	10	63	510	5	109	142	0.9	1.2	41
96055	5.66	0.07	0.14	2.24	99.84	bd	bd	46	511	1	17	149	2.9	2.3	93
96055	5.64	0.08	0.15	2.24	100.23	bd	bd	44	497	1	17	147	2.9	2.4	96
96057	5.50	0.26	0.17	2.37	99.39	1	bd	45	460	2	19	82	2.6	2.1	82
96058	4.50	0.13	0.10	1.95	99.59	15	bd	42	450	1	24	112	1.9	1.4	52
94009	1.71	0.43	0.04	2.07	99.06	168	63	63	370	4	41	190	0.5	0.7	22
94012	0.75	0.17	0.03	2.07	92.52	368	81	58	343	1	40	119	0.5	0.7	22
94015	1.14	0.11	0.01	2.48	97.22	77	9	69	410	2	23	81	0.3	0.4	13
94020	2.54	0.62	0.05	2.23	98.87	9	23	55	302	7	59	143	0.4	0.6	20
94036	0.32	0.26	0.02	30.40	99.02	251	160	51	203	5	15	56	0.2	0.3	8
94038	0.80	0.09	0.02	1.10	93.39	991	141	53	244	1	14	101	0.4	0.4	12
94043	2.04	0.61	0.02	1.75	98.71	671	84	54	270	5	45	128	0.3	0.4	10
94062	1.60	0.86	0.06	6.91	99.34	373	60	49	314	17	112	513	0.4	1.0	31
94GC05	1.50	0.25	0.01	2.09	98.32	46	4	80	264	4	63	102	0.5	nm	18
94GC05	1.54	0.25	0.01	2.07	99.75	46	6	84	254	4	49	103	0.6	nm	19
95153	6.48	0.20	0.06	2.19	99.86	bd	bd	53	283	4	96	56	0.8	0.9	28
95153	6.33	0.20	0.05	2.19	99.25	bd	bd	51	282	3	109	57	0.4	nm	29
95153	6.27	0.21	0.06	2.13	99.73	bd	bd	62	293	3	76	57	1.0	1.1	29
95154	4.72	0.14	0.07	3.78	99.27	272	39	52	336	1	23	63	0.7	0.9	31
456	6.03	0.12	0.28	5.68	100.18	48	6	41	362	1	38	40	0.6	0.4	11
457	3.41	0.46	0.46	2.44	100.40	26	28	27	377	10	158	385	38.3	4.6	182
458	3.39	0.26	0.03	5.68	99.74	62	12	46	311	3	33	116	0.5	0.2	7
465	1.34	0.48	0.02	5.31	100.35	182	35	0	246	5	32	67	0.5	nm	3
473	2.64	0.12	0.03	3.18	100.10	45	6	47	307	1	22	19	0.3	0.2	4
476	3.85	0.04	0.02	3.44	100.31	45	6	46	327	bd	20	19	0.3	0.3	6
492	3.78	0.17	0.03	5.95	100.42	463	75	42	246	2	10	83	0.3	0.3	6
94007	2.73	0.37	0.02	1.95	99.89	405	80	51	264	4	57	319	0.5	0.3	6
94014	1.02	0.15	0.02	2.42	99.77	1990	406	46	218	1	14	50	0.4	0.3	9
94014	1.03	0.15	0.02	2.40	99.87	2110	415	43	214	2	14	49	0.3	0.2	8
94014	1.04	0.14	0.02	2.38	99.98	2043	408	51	213	1	11	50	0.2	0.3	9
94023	1.61	0.14	0.11	0.78	99.91	7	bd	90	157	2	17	175	0.1	0.4	9
94029	bd	0.04	0.02	2.06	97.61	215	64	64	333	bd	8	104	0.3	0.6	11
94030	1.23	0.08	0.01	1.13	99.82	93	36	64	306	1	17	148	0.5	0.3	7
94037	0.92	0.11	0.00	1.91	98.61	535	77	68	252	1	17	67	0.3	0.5	12
94041	0.66	0.61	0.01	1.65	99.95	14	3	66	720	14	152	149	0.3	0.2	5
94044	1.55	0.27	0.02	2.05	99.93	858	167	57	354	3	19	128	0.6	nm	6
94044	1.53	0.28	0.02	2.02	99.55	864	164	63	348	2	7	126	0.5	0.2	6
94049	2.79	0.44	0.04	1.50	99.42	3	bd	57	415	4	68	140	1.1	1.0	28

Sample	Na <sub>2</sub> O	K <sub>2</sub> O	P <sub>2</sub> O <sub>5</sub>	LOI	total	Cr	Ni	Sc	V	Rb	Ba	Sr	Nb	Hf	Zr
94049	2.71	0.43	0.04	1.42	99.28	bd	bd	60	398	5	76	141	0.8	0.9	25
94049	2.72	0.48	0.03	1.46	99.10	10	bd	57	418	5	68	142	1.4	0.8	26
94gc03	0.32	0.17	0.01	1.92	99.52	519	61	66	172	2	16	97	0.2	0.2	6
94GC04	2.64	0.35	0.03	1.77	98.73	14	3	44	313	4	44	131	1.0	1.0	27
95050	5.67	0.12	0.02	4.34	93.45	42	16	50	302	1	20	98	0.4	0.2	6
95111	4.48	0.05	0.05	3.86	99.12	10	bd	65	416	bd	32	186	0.7	0.5	11
95112	0.70	0.03	0.01	4.51	99.92	61	1	60	408	bd	bd	184	0.5	0.2	3
95115	3.92	0.20	0.03	2.97	98.90	26	5	54	355	3	38	238	0.6	0.3	5
95116	1.38	0.84	0.04	4.92	98.91	28	5	58	373	10	7	389	0.6	0.3	1
95GC06	3.33	0.21	0.05	1.05	99.16	1	bd	46	369	2	38	184	0.8	nm	14
96009	4.47	0.04	0.04	3.38	98.04	nm	nm	nm	nm	nm	nm	nm	nm	nm	nm
96009	4.24	0.04	0.03	3.38	93.08	225	56	44	310	bd	20	56	0.4	0.5	15
95149	3.92	0.20	0.03	2.98	99.27	bd	bd	59	455	2	23	68	0.5	0.5	16
96054	4.88	0.44	0.02	3.83	97.84	bd	bd	63	483	3	98	272	0.4	0.2	4
96005	5.44	0.08	0.01	3.90	98.74	516	107	52	268	1	23	45	0.5	0.3	11
95025B	5.34	0.08	0.01	4.73	98.35	536	108	61	228	bd	16	36	0.7	0.7	24
95053	4.41	1.53	0.04	2.75	98.50	24	7	31	160	32	234	107	1.0	1.1	29
453	6.14	0.07	0.03	1.10	100.24	5	bd	8	bd	3	26	38	0.3	3.1	90
487	2.94	1.68	0.06	1.47	99.69	5	bd	9	24	6	114	46	0.6	1.8	50
538	3.71	3.32	0.04	0.68	99.34	11	bd	16	bd	22	148	38	0.3	2.4	73
94060	3.93	0.63	0.05	1.83	99.21	5	bd	bd	34	bd	bd	100	1.5	1.7	45
94018	4.61	0.53	0.04	1.27	99.43	13	bd	8	19	6	108	102	1.2	1.9	60
94042	3.69	0.25	0.02	0.48	97.50	14	bd	12	5	2	28	265	1.5	3.6	118
94051	5.93	0.20	0.02	0.63	98.21	7	bd	8	bd	2	39	46	0.8	2.9	105
94057	5.66	0.09	0.21	1.50	98.40	bd	bd	23	39	8	20	74	3.7	4.3	175
94060	4.10	0.65	0.06	1.83	99.50	5	bd	10	bd	8	47	100	nm	nm	nm
94061	4.67	0.70	0.08	1.61	98.19	4	bd	16	15	11	72	98	1.5	1.5	49
94GC06	2.92	0.23	0.08	0.95	98.80	6	bd	31	60	4	171	235	1.1	1.1	3
94GC06	2.87	0.23	0.08	0.97	98.12	5	bd	28	60	4	156	239	1.1	nm	3
94GC06	2.87	0.23	0.08	0.97	98.07	bd	bd	23	61	4	150	229	1.2	0.2	6
95GC02	3.35	2.43	0.04	2.28	97.14	4	bd	102	105	50	275	42	0.3	nm	34
95GC08	1.79	1.24	0.02	2.87	97.95	bd	bd	16	2	33	216	41	1.8	3.3	110
96060	1.30	0.24	0.07	2.37	97.21	7	bd	15	6	4	18	125	1.9	2.3	70
96065	4.07	0.33	0.05	0.89	98.49	2	bd	14	20	7	29	113	1.8	1.9	62
96065	4.10	0.35	0.05	0.88	98.79	1	bd	14	22	6	30	111	1.6	2.0	58
96065	4.06	0.35	0.06	0.88	99.13	2	bd	12	20	7	231	113	2.2	1.7	55
96067	2.82	0.43	0.01	2.01	95.90	2	bd	2	3	10	80	49	0.4	2.5	78
96067	2.90	0.43	0.01	2.03	98.22	bd	bd	7	bd	9	79	48	1.2	2.5	78
96071	3.11	0.02	0.02	1.08	98.42	22	bd	14	49	bd	6	122	1.3	1.5	47
96072	1.80	0.53	0.02	1.76	98.86	bd	bd	8	1	12	105	33	0.3	2.5	82
96GC01	2.89	0.75	0.09	2.39	98.06	160	bd	30	209	13	114	218	0.9	0.8	23
96GC05	4.13	0.33	0.03	0.67	98.00	6	bd	9	12	3	39	74	0.9	2.3	72
96GC07	3.03	2.41	0.05	1.58	98.22	nm	nm	nm	nm	nm	nm	nm	nm	nm	nm
96GC07	2.90	2.39	0.05	1.58	93.52	8	bd	14	29	5	85	35	1.3	1.9	62
96GC08	4.72	0.49	0.04	1.08	97.72	22	bd	20	53	69	380	477	1.2	1.4	40
463	5.07	0.67	0.09	4.11	99.84	90	22	30	189	14	158	104	1.3	1.6	61
467	6.59	0.53	0.21	2.49	99.35	34	1	30	288	4	185	79	8.0	3.4	131
481	3.48	1.94	0.31	2.82	99.75	43	17	38	466	0	58	152	6.6	2.4	93
496	4.05	1.16	0.15	4.16	98.99	55	14	31	253	5	106	154	6.0	2.6	100

Sample	Na <sub>2</sub> O	K <sub>2</sub> O	P <sub>2</sub> O <sub>5</sub>	LOI	total	Cr	Ni	Sc	V	Rb	Ba	Sr	Nb	Hf	Zr
553	6.19	0.24	0.20	2.56	99.81	41	2	37	331	3	193	141	7.0	3.2	120
554	3.79	0.26	0.14	4.07	100.35	178	48	21	198	7	107	139	5.0	2.5	95
756	4.17	0.02	0.18	4.01	99.48	532	6	bd	285	3	47	103	6.0	nm	108
767	4.52	0.08	0.06	2.83	100.01	245	239	bd	316	2	33	104	7.0	nm	72
772	4.99	0.14	0.16	3.25	99.86	65	1	bd	bd	3	43	41	2.8	nm	80
774	2.52	1.05	0.14	2.70	99.80	348	127	bd	bd	22	332	228	3.6	nm	79
95001	3.40	0.33	0.12	0.00	99.26	76	18	33	252	5	91	69	6.2	2.6	116
95001	4.16	0.34	0.14	4.21	99.26	72	0	45	257	6	73	70	6.1	nm	115
95011	5.27	0.16	0.09	3.17	99.10	119	26	33	188	4	97	87	4.3	nm	88
95016	6.43	0.70	0.21	1.19	98.26	3	bd	18	29	11	164	36	7.6	4.9	230
95021	6.79	0.17	0.19	2.00	99.18	34	bd	40	272	3	63	64	10.4	nm	172
95022	4.77	0.42	0.09	3.81	99.67	117	27	37	170	11	185	125	4.1	1.6	70
95026	1.08	3.50	0.31	4.73	98.84	7	11	43	442	51	282	225	6.0	2.6	110
95060	5.66	1.63	0.27	1.28	98.15	2	bd	14	30	23	351	99	14.3	nm	218
95066	6.70	0.43	0.20	5.26	99.74	24	bd	38	293	7	112	102	11.8	4.0	165
95066	6.54	0.43	0.21	2.45	99.31	27	4	41	289	7	125	102	9.2	4.0	175
95068	5.44	1.90	0.24	1.51	98.64	bd	bd	13	28	30	335	86	13.9	nm	221
95069	2.90	0.24	0.08	7.17	98.82	4	12	36	365	41	406	158	6.2	nm	108
95071	5.90	0.43	0.17	2.79	98.70	2	10	32	380	10	158	126	7.1	2.7	113
95124	4.44	3.81	0.04	0.64	98.28	8	bd	12	5	80	520	53	27.6	nm	383
95131	5.40	1.99	0.21	0.82	98.13	bd	bd	13	26	39	358	93	14.9	nm	234
95137	4.92	0.09	0.21	2.18	99.19	55	2	35	248	1	28	79	10.5	nm	151
95138	5.40	0.77	0.15	2.67	99.17	9	bd	22	357	29	131	211	6.2	nm	100
95142	5.77	0.46	0.16	3.15	98.18	bd	2	36	396	14	125	120	7.2	nm	122
95143	5.38	1.01	0.29	1.41	98.46	bd	bd	25	65	13	237	101	12.7	nm	198
95161	6.62	0.57	0.17	1.82	99.08	3	2	33	344	13	280	150	6.6	nm	107
95164	6.65	0.18	0.13	2.87	99.15	58	bd	32	217	5	89	89	5.6	2.5	96
95164	6.71	0.17	0.14	2.86	99.32	57	bd	36	216	4	93	89	4.8	2.6	98
95166	6.54	0.41	0.20	2.46	98.35	179	5	31	175	21	114	250	10.1	3.7	133
95GC05	5.22	3.39	0.05	0.70	97.67	7	bd	1	7	55	377	48	29.6	nm	395
95GC05	5.21	3.41	0.04	0.70	97.98	nm	nm	nm	nm	nm	nm	nm	nm	nm	nm
96012	5.43	0.78	0.17	2.93	98.07	3	1	35	405	21	223	230	7.4	2.5	106
96019	1.27	1.22	0.33	3.28	99.31	bd	bd	27	94	45	163	528	14.8	5.0	204
96032	5.94	0.60	0.17	0.89	97.78	5	2	33	350	15	120	214	7.2	2.5	102
96033	4.99	1.26	0.17	1.89	98.36	4	3	26	408	27	208	172	7.3	2.8	108
96053	2.98	0.53	0.12	4.07	99.22	485	131	36	220	23	47	136	6.5	2.7	112
96061	4.83	0.78	0.14	2.87	97.73	136	18	62	235	12	155	125	6.5	2.8	119
96063	3.52	1.56	0.08	4.11	98.42	195	47	33	180	66	218	435	4.3	1.8	71
96064	5.07	1.49	0.27	2.69	99.46	62	5	38	213	33	299	248	12.2	3.5	148
96066	0.89	1.47	0.03	1.50	98.43	bd	bd	6	14	55	233	30	37.3	3.2	105
96070	4.46	0.89	0.07	0.41	97.68	63	bd	9	43	27	230	580	7.3	2.7	134
96GC10	6.94	0.22	0.21	0.66	98.15	8	bd	18	41	2	377	222	5.4	3.4	118
491	2.67	1.37	0.17	2.65	99.60	69	35	31	227	4	110	346	10.0	2.2	89
495	2.46	1.29	0.15	3.10	100.19	143	79	32	184	15	91	288	8.0	2.0	78
497	4.55	0.82	0.35	2.02	99.13	50	14	40	456	15	178	193	18.1	4.4	182
498	4.90	0.50	0.37	1.45	98.38	54	15	41	441	8	165	100	18.1	4.5	185
503	2.89	1.60	0.10	3.99	100.42	590	196	29	232	27	303	91	3.0	1.7	60
508	3.74	0.80	0.31	2.94	100.62	72	49	28	267	22	351	415	10.0	4.1	181
511	2.83	1.02	0.11	3.10	100.07	488	218	33	218	24	136	174	5.0	2.0	72

Sample	Na <sub>2</sub> O	K <sub>2</sub> O	P <sub>2</sub> O <sub>5</sub>	LOI	total	Cr	Ni	Sc	V	Rb	Ba	Sr	Nb	Hf	Zr
548	2.95	1.25	0.25	4.22	99.93	581	213	33	281	20	133	95	16.0	3.1	117
95GC10	4.23	0.28	0.42	2.44	99.94	bd	bd	54	369	9	108	197	15.8	3.3	144
546	4.51	0.60	0.30	2.85	100.04	104	62	31	289	6	163	360	20.1	3.4	138
549	4.66	2.10	0.26	3.80	99.65	229	1247	28	213	21	198	87	14.1	2.9	112
762	2.63	0.92	0.24	2.18	100.19	188	72	bd	bd	15	244	426	11.0	nm	109
773	3.34	0.65	0.22	2.58	99.13	56	176	bd	222	10	116	120	19.1	nm	105
95056	2.09	0.67	0.34	3.73	98.79	116	110	37	354	17	206	397	25.3	nm	181
95058	4.78	0.76	0.41	2.11	98.96	bd	bd	31	262	16	247	439	10.2	3.4	145
95076	3.74	1.47	0.28	2.79	98.53	89	92	33	233	41	463	191	14.8	3.5	152
95077	2.47	1.78	0.24	2.87	99.14	377	171	26	233	46	260	511	13.0	3.8	149
95081	5.20	0.14	0.29	2.05	98.42	21	31	15	336	2	79	103	21.1	4.4	197
95106	3.50	1.00	0.35	3.14	99.55	nm	nm	nm	nm	nm	nm	nm	nm	nm	nm
95106	3.46	0.98	0.34	3.14	99.22	37	31	26	344	25	215	980	26.4	nm	220
95114	1.75	1.15	0.25	3.05	98.22	421	144	34	275	20	147	328	15.1	3.3	147
95128	2.82	1.07	0.22	2.97	99.18	289	107	36	251	47	208	279	14.2	3.4	153
95132	4.80	0.84	0.28	2.16	98.52	46	13	26	342	18	285	149	23.0	nm	233
95132	4.80	0.84	0.28	2.19	99.01	40	15	24	338	18	270	149	22.8	nm	233
95GC03	4.51	0.13	0.87	2.60	99.88	bd	bd	28	285	3	164	250	33.6	7.9	388
95036	5.71	0.06	0.24	3.34	98.17	114	44	33	310	1	272	150	20.2	6.1	291
95036	5.76	0.06	0.24	3.30	99.31	nm	nm	nm	nm	nm	nm	nm	nm	nm	nm
95036	5.75	0.06	0.24	2.37	99.14	124	60	38	312	bd	273	153	19.1	nm	293
96014	5.48	0.16	0.29	2.09	99.99	40	23	39	317	3	101	163	36.3	6.2	279
96021	6.79	0.17	0.19	2.00	99.18	40	5	37	486	28	281	272	20.2	4.7	210
96023	5.20	1.36	0.31	2.86	99.85	43	27	36	322	27	452	225	32.4	5.9	263
96024	4.47	0.48	0.27	7.51	99.15	46	23	41	363	9	140	374	28.9	5.6	246
96031	3.66	2.37	0.27	2.18	98.83	39	25	28	294	63	650	313	19.7	4.8	229
96035	3.53	1.49	0.25	2.75	99.36	29	30	24	278	34	293	192	32.5	5.6	244
96036	2.97	1.92	0.27	2.50	98.53	29	27	33	286	53	347	237	35.2	5.9	259
96037	4.12	2.13	0.29	3.24	99.45	29	bd	31	264	56	359	638	28.0	5.5	253
512	2.96	0.19	0.17	5.38	99.11	648	445	bd	190	3	59	137	10.0	nm	84
450	3.91	2.78	0.68	3.96	100.07	9	4	18	227	43	499	235	47.2	5.7	247
454	4.64	1.30	0.66	2.48	100.04	3	1	22	294	18	445	168	53.5	6.4	274
483	5.56	0.02	0.86	2.05	99.24	3	1	26	194	33	162	143	41.4	7.7	322
484	3.43	2.25	0.73	3.30	99.02	3	1	25	227	31	286	324	60.2	8.0	349
502	3.26	0.59	0.29	4.16	100.08	8	8	24	303	13	165	406	15.0	2.6	101
506	2.01	0.38	0.21	5.88	98.50	825	421	bd	256	7	55	267	10.1	nm	116
509	6.11	0.09	1.43	3.02	99.73	3	1	19	163	2	132	261	88.0	9.7	428
551	3.54	0.95	0.39	7.85	98.74	21	32	bd	bd	8	96	267	21.1	nm	180
763	4.56	2.88	1.35	3.47	99.33	7	3	bd	98	bd	718	490	68.0	nm	408
95007	4.01	1.04	0.30	1.96	99.28	bd	22	24	411	21	256	151	28.1	nm	223
95009	3.79	0.50	0.46	2.26	98.80	16	10	30	371	10	271	156	34.7	nm	265
95037	4.44	1.27	0.45	3.09	98.75	1	4	19	215	37	493	214	41.3	nm	282
95061	0.84	0.25	0.12	4.94	99.84	1786	697	31	193	5	50	172	10.2	1.9	77
95063	5.21	1.59	0.80	2.45	99.63	bd	bd	8	63	26	455	258	97.0	nm	647
95097	1.50	2.38	0.25	3.32	97.69	80	69	35	479	75	551	163	23.3	nm	143
95099	3.83	0.35	0.23	3.07	98.97	603	267	28	281	5	238	94	20.1	3.2	146
95100	4.92	1.17	0.56	1.91	99.02	bd	bd	23	222	28	455	211	44.6	6.3	302
95100	4.82	1.19	0.56	1.89	98.53	bd	bd	20	225	29	469	209	39.7	nm	297
95113	2.84	1.06	0.34	2.30	98.68	9	10	33	350	21	216	367	27.2	4.8	212

Sample	Na <sub>2</sub> O	K <sub>2</sub> O	P <sub>2</sub> O <sub>5</sub>	LOI	total	Cr	Ni	Sc	V	Rb	Ba	Sr	Nb	Hf	Zr
96007	4.24	1.23	0.22	2.13	99.82	nm	nm	nm	nm	nm	nm	nm	nm	nm	nm
96007	4.10	1.20	0.21	2.13	94.80	326	174	38	268	22	253	105	17.7	3.3	146
96011	3.25	1.45	0.23	2.61	98.74	215	71	36	275	42	295	163	22.4	3.8	169
94025	4.20	2.37	0.67	2.97	98.76	bd	34	22	323	43	1235	623	76.4	nm	389
95010	2.49	1.98	0.74	4.46	99.09	511	190	29	354	45	1127	1029	73.1	8.3	391
95023	3.39	3.53	0.88	8.39	99.21	3	6	16	317	100	1102	1187	116.5	nm	485
95067	3.32	4.06	0.95	1.18	98.77	bd	2	14	245	117	1437	867	121.3	11.2	589
95070	3.40	3.30	0.97	3.26	98.86	bd	bd	26	327	73	1296	1117	111.8	nm	542
95101	4.09	0.34	0.13	4.21	98.56	16	30	28	334	132	810	124	6.2	2.9	237
95119	3.02	1.09	0.22	4.50	99.24	nm	nm	nm	nm	nm	nm	nm	nm	nm	nm
95119	3.04	1.09	0.23	4.50	99.47	758	359	24	232	34	475	170	12.4	3.1	143
95122	4.41	2.70	0.95	2.06	99.25	bd	bd	17	257	42	953	773	102.8	nm	524
95122	4.27	2.65	0.94	2.19	98.17	bd	bd	22	256	44	945	781	102.1	nm	528
95125	2.97	0.29	0.45	0.00	98.70	55	15	48	340	10	43	57	52.2	nm	634
95127	3.37	2.72	0.77	7.65	98.51	25	5	24	257	63	1008	962	91.9	nm	391
96002	2.63	2.77	0.97	9.94	94.54	6	9	27	379	86	2233	1471	132.8	10.4	489
96002	2.75	2.76	1.00	9.94	98.31	2	8	25	394	86	2132	1472	147.8	10.1	500
96002	2.72	2.73	0.97	9.87	98.83	nm	nm	nm	nm	nm	nm	nm	nm	nm	nm
96004	3.70	1.23	0.08	2.42	98.61	165	19	29	169	43	282	178	8.9	3.3	151
96025	4.42	2.81	0.59	4.09	98.11	bd	bd	12	134	50	2463	1257	121.6	11.4	554
96059	4.06	1.89	0.12	3.25	98.17	36	bd	15	93	29	361	399	4.6	2.0	69
95033	3.26	0.35	0.48	5.66	99.85	9	31	35	386	12	89	374	46.1	4.7	213
94038	4.39	0.83	0.10	1.64	97.42	99	64	12	66	24	130	37	10.9	3.0	142
94005	3.19	0.70	0.38	2.93	99.82	16	41	24	239	13	248	441	13.2	nm	205
94005	3.18	0.70	0.37	2.90	99.58	4	35	27	234	14	229	445	76.4	nm	200
94005	3.19	0.70	0.38	2.93	98.12	13	43	30	236	14	236	444	13.7	4.1	203
94005	3.25	0.70	0.36	2.96	98.42	9	35	28	241	14	246	443	13.2	4.4	200
94028A	3.18	0.70	0.37	2.86	99.58	422	238	46	203	1	37	126	5.6	1.4	57
94032	4.68	0.08	0.34	2.17	99.69	1	4	33	266	1	54	283	4.4	3.9	157
94035	3.98	0.68	0.39	2.47	99.63	32	7	21	198	10	189	353	12.2	4.7	218

Sample	Y	Th	La	Ce	Pr	Nd	Sm	Eu	Tb	Dy	Ho	Er	Tm	Yb	Lu
530	17	0.29	1.06	3.31	nm	3.81	1.47	0.62	0.40	nm	nm	nm	nm	1.78	0.28
532	27	0.44	2.77	8.85	nm	7.55	2.77	1.14	0.69	nm	nm	nm	nm	3.07	0.47
541	26	0.65	5.02	12.76	nm	8.44	2.78	1.03	0.64	nm	nm	nm	nm	2.82	0.44
544	31	nm	nm	nm	nm	nm	nm	nm	nm	nm	nm	nm	nm	nm	nm
94008	25	0.36	2.27	6.50	1.05	5.94	2.21	0.88	0.56	4.00	0.82	2.48	0.35	2.44	0.35
94013	24	0.53	2.85	8.29	1.32	7.14	2.63	1.05	0.62	4.38	0.93	2.84	0.40	2.73	0.42
94045	24	0.37	2.42	7.00	1.10	6.14	2.14	0.97	0.56	3.82	0.82	2.49	0.37	2.34	0.34
94056	23	0.45	2.81	8.36	1.29	7.13	2.47	1.04	0.65	4.27	0.89	2.68	0.40	2.61	0.41
94058	28	0.58	3.61	10.37	1.63	8.57	2.81	1.15	0.75	5.16	1.11	3.24	0.50	3.30	0.49
94GC02	20	0.35	2.13	6.25	1.03	5.48	2.13	0.80	0.52	3.65	0.79	2.37	0.35	2.36	0.34
96010	nm	nm	nm	nm	nm	nm	nm	nm	nm	nm	nm	nm	nm	nm	nm
96010	22	0.28	2.63	6.85	1.12	6.21	2.36	0.97	0.58	3.77	0.79	2.32	0.33	2.10	0.33
96055	26	0.80	5.44	14.53	2.14	10.89	3.29	1.08	0.67	4.49	1.01	3.02	0.44	3.01	0.45
96055	26	0.79	5.12	13.60	2.02	10.32	3.15	1.00	0.65	4.46	1.01	2.99	0.45	2.99	0.45
96057	28	0.56	2.69	8.39	1.42	7.86	2.95	0.91	0.70	4.82	1.11	3.38	0.50	3.38	0.51
96058	19	0.45	2.72	7.54	1.17	6.09	2.18	0.77	0.51	3.44	0.77	2.42	0.35	2.28	0.35
94009	12	0.18	1.07	3.24	0.55	3.21	1.27	0.50	0.31	2.36	0.49	1.55	0.22	1.48	0.23
94012	13	0.18	1.11	3.19	0.54	3.09	1.15	0.49	0.31	2.33	0.49	1.52	0.23	1.37	0.23
94015	11	0.13	0.33	1.70	0.23	1.61	0.82	0.41	0.24	1.79	0.40	1.21	0.17	1.21	0.18
94020	12	0.26	1.12	3.12	0.52	2.81	1.03	0.54	0.28	2.15	0.49	1.46	0.23	1.62	0.24
94036	5	0.14	0.44	1.33	0.20	1.17	0.39	0.20	0.11	0.74	0.17	0.59	0.08	0.59	0.09
94038	9	0.13	0.64	1.92	0.31	1.81	0.78	0.31	0.21	1.51	0.38	1.09	0.17	1.09	0.19
94043	8	0.11	0.56	1.67	0.27	1.55	0.64	0.26	0.20	1.40	0.31	0.97	0.14	1.03	0.16
94062	18	0.28	1.62	4.89	0.81	4.46	1.60	0.58	0.45	3.16	0.69	2.09	0.30	2.06	0.32
94GC05	16	2.97	nm	nm	nm	nm	nm	nm	nm	nm	nm	nm	nm	nm	nm
94GC05	16	1.68	nm	nm	nm	nm	nm	nm	nm	nm	nm	nm	nm	nm	nm
95153	17	0.28	1.44	4.11	0.64	3.49	1.41	0.53	0.38	2.59	0.64	1.88	0.29	1.95	0.31
95153	17	bd	nm	nm	nm	nm	nm	nm	nm	nm	nm	nm	nm	nm	nm
95153	15	0.30	1.44	4.03	0.64	3.43	1.45	0.51	0.37	2.58	0.59	1.83	0.29	1.92	0.30
95154	17	0.21	1.22	3.71	0.65	3.74	1.44	0.65	0.38	2.65	0.56	1.68	0.25	1.67	0.25
456	28	0.50	2.11	5.02	nm	3.91	1.61	0.66	0.55	nm	nm	nm	nm	3.31	0.50
457	24	2.82	24.71	56.65	nm	31.24	6.72	2.27	0.96	nm	nm	nm	nm	2.31	0.32
458	5	0.14	0.59	1.50	nm	1.00	0.58	0.29	0.19	nm	nm	nm	nm	0.76	0.15
465	55	nm	nm	nm	nm	nm	nm	nm	nm	nm	nm	nm	nm	nm	nm
473	7	0.14	0.40	1.20	nm	0.90	0.52	0.25	0.18	nm	nm	nm	nm	0.87	0.18
476	7	0.16	0.55	1.41	nm	1.31	0.65	0.29	0.19	nm	nm	nm	nm	0.87	0.16
492	8	0.24	0.81	2.11	nm	1.40	0.71	0.29	0.21	nm	nm	nm	nm	0.87	0.14
94007	7	0.10	0.50	1.38	0.22	1.13	0.59	0.26	0.17	1.22	0.28	0.79	0.13	0.77	0.12
94014	6	0.09	0.42	1.25	0.21	1.23	0.69	0.23	0.16	1.08	0.26	0.83	0.11	0.82	0.12
94014	7	0.07	0.44	1.28	0.21	1.43	0.56	0.22	0.15	1.13	0.24	0.74	0.12	0.79	0.12
94014	7	0.08	0.44	1.23	0.23	1.19	0.53	0.22	0.15	1.11	0.26	0.77	0.11	0.83	0.12
94023	9	0.06	0.44	1.53	0.30	1.89	0.84	0.76	0.26	1.78	0.42	1.20	0.15	1.11	0.14
94029	9	0.10	0.56	1.75	0.30	1.84	0.77	0.34	0.23	1.62	0.37	1.17	0.17	1.07	0.17
94030	10	0.02	0.33	1.18	0.23	1.61	0.82	0.41	0.24	1.75	0.36	1.14	0.15	1.09	0.17
94037	14	0.16	0.71	2.60	0.48	2.90	1.27	0.34	0.33	2.38	0.56	1.79	0.28	1.92	0.29
94041	5	0.04	0.33	1.02	0.17	1.13	0.41	0.28	0.13	0.94	0.22	0.71	0.11	0.76	0.11
94044	8	0.03	nm	nm	nm	nm	nm	nm	nm	nm	nm	nm	nm	nm	nm
94044	9	0.03	0.45	1.33	0.25	1.41	0.65	0.36	0.19	1.39	0.31	0.97	0.14	1.03	0.15
94049	23	0.29	1.56	4.68	0.79	4.84	2.19	0.58	0.58	4.12	0.92	2.77	0.41	2.64	0.40

Sample	Y	Th	La	Ce	Pr	Nd	Sm	Eu	Tb	Dy	Ho	Er	Tm	Yb	Lu
94049	27	0.25	1.60	4.61	0.82	4.86	2.10	0.57	0.60	4.08	0.96	2.87	0.42	2.69	0.39
94049	26	0.30	1.55	4.65	0.81	4.81	2.09	0.52	0.57	4.12	0.90	2.64	0.39	2.68	0.39
94gc03	6	0.12	0.33	1.14	0.19	1.23	0.53	0.19	0.15	1.19	0.26	0.77	0.12	0.81	0.15
94GC04	19	0.28	1.62	4.93	0.84	4.47	1.78	0.53	0.48	3.32	0.71	2.15	0.34	2.21	0.35
95050	7	0.07	0.50	1.21	0.19	1.13	0.46	0.22	0.17	1.24	0.25	0.79	0.12	0.80	0.12
95111	14	0.19	0.87	2.24	0.36	2.02	0.90	0.39	0.29	2.08	0.47	1.50	0.23	1.63	0.24
95112	6	0.07	0.23	0.63	0.11	0.68	0.47	0.23	0.12	0.97	0.24	0.65	0.10	0.67	0.10
95115	11	0.10	0.55	1.36	0.24	1.42	0.69	0.34	0.23	1.67	0.39	1.20	0.19	1.23	0.19
95116	11	0.11	0.54	1.44	0.25	1.47	0.77	0.36	0.23	1.70	0.38	1.31	0.19	1.27	0.21
95GC06	14	bd	nm	nm	nm	nm	nm	nm	nm	nm	nm	nm	nm	nm	nm
96009	nm	nm	nm	nm	nm	nm	nm	nm	nm	nm	nm	nm	nm	nm	nm
96009	10	0.12	0.64	2.04	0.36	2.23	0.99	0.36	0.26	1.86	0.42	1.29	0.19	1.27	0.20
95149	11	0.23	0.82	2.33	0.39	2.20	1.02	0.42	0.27	1.91	0.44	1.36	0.21	1.43	0.21
96054	7	0.04	0.24	0.74	0.13	0.89	0.55	0.23	0.15	1.14	0.28	0.84	0.13	0.96	0.15
96005	3	0.12	0.54	1.21	0.17	0.81	0.34	0.12	0.08	0.57	0.13	0.45	0.07	0.49	0.08
95025B	3	0.20	0.72	2.39	0.26	1.16	0.47	0.18	0.12	0.79	0.16	0.47	0.06	0.48	0.07
95053	7	0.30	1.46	3.63	0.48	2.16	0.66	0.17	0.14	0.98	0.23	0.72	0.10	0.76	0.11
453	31	1.12	2.60	10.40	nm	8.50	2.94	0.64	0.71	nm	nm	nm	nm	3.80	0.52
487	30	0.68	3.78	10.34	nm	7.46	2.61	0.67	0.69	nm	nm	nm	nm	3.54	0.54
538	43	0.75	4.10	12.01	nm	9.61	3.91	1.05	1.05	nm	nm	nm	nm	5.30	0.84
94060	27	0.81	2.63	6.89	1.06	5.73	2.20	0.63	0.70	4.91	0.97	3.02	0.48	3.14	0.50
94018	27	0.86	3.80	9.84	1.44	7.26	2.46	0.70	0.64	4.66	1.01	3.14	0.50	3.34	0.52
94042	52	1.28	5.99	16.09	2.51	13.11	4.56	0.86	1.21	8.52	1.92	5.83	0.88	5.88	0.88
94051	30	1.34	3.56	11.18	1.41	7.22	2.50	0.39	0.67	4.67	1.08	3.40	0.54	3.68	0.57
94057	49	2.00	12.12	31.30	4.60	22.70	6.52	1.63	1.31	8.85	1.93	5.79	0.90	5.71	0.87
94060	nm	nm	nm	nm	nm	nm	nm	nm	nm	nm	nm	nm	nm	nm	nm
94061	26	0.76	2.73	7.57	1.20	6.68	2.42	0.78	0.66	4.55	1.01	3.32	0.48	3.20	0.50
94GC06	20	0.60	0.82	2.65	0.48	3.24	1.68	0.70	0.49	3.39	0.73	2.22	0.30	1.89	0.28
94GC06	20	1.40	nm	nm	nm	nm	nm	nm	nm	nm	nm	nm	nm	nm	nm
94GC06	20	0.02	0.87	2.63	0.50	3.57	1.63	0.70	0.51	3.41	0.77	2.23	0.31	1.89	0.29
95GC02	83	3.00	nm	nm	nm	nm	nm	nm	nm	nm	nm	nm	nm	nm	nm
95GC08	50	1.60	6.68	20.02	3.22	16.32	5.68	1.19	1.31	8.99	2.02	6.30	0.94	6.49	1.00
96060	35	0.67	2.69	8.25	1.39	7.91	3.17	1.08	0.86	6.25	1.42	4.35	0.66	4.46	0.69
96065	31	0.96	3.65	9.30	1.39	7.36	2.80	0.77	0.73	5.20	1.21	3.77	0.58	3.94	0.60
96065	31	1.01	3.83	9.63	1.48	7.55	2.76	0.76	0.73	5.19	1.20	3.73	0.56	3.84	0.52
96065	31	0.96	3.73	9.36	1.43	7.52	2.90	0.75	0.75	5.33	1.21	3.80	0.58	3.96	0.60
96067	30	1.02	3.43	9.86	1.57	8.29	3.13	0.79	0.76	5.54	1.27	3.98	0.65	4.50	0.68
96067	30	1.03	3.43	10.18	1.71	8.69	3.13	0.78	0.82	5.80	1.31	4.21	0.66	4.51	0.73
96071	28	0.79	2.49	6.61	0.95	5.15	2.02	0.58	0.58	4.27	0.98	3.12	0.49	3.27	0.51
96072	32	1.27	5.51	13.18	1.81	8.73	2.78	0.59	0.73	5.06	1.20	3.76	0.61	4.08	0.62
96GC01	14	0.28	1.92	4.19	0.57	2.97	1.06	0.26	0.24	1.88	0.48	1.53	0.26	1.77	0.29
96GC05	21	0.77	1.85	4.75	0.79	4.21	1.73	0.28	0.44	3.29	0.80	2.66	0.43	2.94	0.47
96GC07	nm	nm	nm	nm	nm	nm	nm	nm	nm	nm	nm	nm	nm	nm	nm
96GC07	21	1.82	6.17	13.87	1.83	8.61	2.50	0.60	0.52	3.59	0.83	2.49	0.39	2.63	0.40
96GC08	17	1.45	3.29	8.00	1.10	4.83	1.64	0.37	0.39	2.79	0.67	2.13	0.34	2.29	0.34
463	14	1.80	7.41	16.83	nm	8.82	2.51	0.88	0.48	nm	nm	nm	nm	1.70	0.28
467	27	4.31	15.75	36.31	nm	18.86	4.69	1.42	0.82	nm	nm	nm	nm	2.75	0.44
481	28	2.07	13.32	30.97	nm	18.64	4.77	1.66	0.85	nm	nm	nm	nm	2.70	0.43
496	23	3.18	12.12	27.51	nm	13.61	3.59	1.13	0.68	nm	nm	nm	nm	2.42	0.39

Sample	Y	Th	La	Ce	Pr	Nd	Sm	Eu	Tb	Dy	Ho	Er	Tm	Yb	Lu
553	29	4.11	13.63	33.87	nm	17.63	4.49	1.39	0.84	nm	nm	nm	nm	2.85	0.46
554	21	3.63	12.12	28.95	nm	14.32	3.53	1.09	0.63	nm	nm	nm	nm	2.16	0.34
756	26	nm	nm	nm	nm	nm	nm	nm	nm	nm	nm	nm	nm	nm	nm
767	16	nm	10.55	21.50	nm	13.26	3.72	1.31	nm	3.72	nm	1.81	nm	1.31	nm
772	21	nm	10.32	24.45	nm	15.03	4.01	1.10	nm	4.41	nm	2.51	nm	nm	nm
774	19	nm	10.42	21.74	nm	11.82	3.11	0.70	1.00	3.41	nm	2.10	nm	nm	nm
95001	25	2.62	10.20	23.33	2.90	12.99	3.50	1.12	0.72	4.68	0.84	2.38	0.35	2.24	0.32
95001	25	bd	nm	nm	nm	nm	nm	nm	nm	nm	nm	nm	nm	nm	nm
95011	20	bd	nm	nm	nm	nm	nm	nm	nm	nm	nm	nm	nm	nm	nm
95016	45	4.98	22.66	51.43	6.52	28.06	6.88	1.73	1.30	8.25	1.52	4.53	0.67	4.35	0.68
95021	32	4.00	nm	nm	nm	nm	nm	nm	nm	nm	nm	nm	nm	nm	nm
95022	16	1.65	6.47	14.97	1.91	8.41	2.23	0.81	0.46	3.07	0.55	1.62	0.23	1.46	0.22
95026	28	1.95	12.96	29.35	3.88	17.86	4.64	1.51	0.91	5.66	1.02	2.95	0.42	2.76	0.40
95060	43	4.00	nm	nm	nm	nm	nm	nm	nm	nm	nm	nm	nm	nm	nm
95066	28	4.48	16.27	38.19	4.77	20.32	5.02	1.48	0.83	5.27	1.10	3.19	0.45	2.93	0.44
95066	33	4.70	16.68	38.17	4.76	20.31	4.88	1.46	0.85	5.42	1.11	3.21	0.46	3.01	0.45
95068	42	6.00	nm	nm	nm	nm	nm	nm	nm	nm	nm	nm	nm	nm	nm
95069	19	bd	nm	nm	nm	nm	nm	nm	nm	nm	nm	nm	nm	nm	nm
95071	21	3.65	14.63	32.68	3.97	16.25	3.62	1.08	0.56	3.44	0.71	2.07	0.31	2.03	0.29
95124	59	12.00	nm	nm	nm	nm	nm	nm	nm	nm	nm	nm	nm	nm	nm
95131	45	7.00	nm	nm	nm	nm	nm	nm	nm	nm	nm	nm	nm	nm	nm
95137	26	4.00	nm	nm	nm	nm	nm	nm	nm	nm	nm	nm	nm	nm	nm
95138	18	bd	nm	nm	nm	nm	nm	nm	nm	nm	nm	nm	nm	nm	nm
95142	21	4.01	nm	nm	nm	nm	nm	nm	nm	nm	nm	nm	nm	nm	nm
95143	41	4.00	nm	nm	nm	nm	nm	nm	nm	nm	nm	nm	nm	nm	nm
95161	20	bd	nm	nm	nm	nm	nm	nm	nm	nm	nm	nm	nm	nm	nm
95164	20	3.04	11.36	25.96	3.17	13.16	3.42	0.98	0.56	3.63	0.78	2.30	0.32	2.17	0.31
95164	20	3.06	11.95	26.85	3.33	13.95	3.39	1.05	0.59	3.69	0.78	2.23	0.33	2.16	0.32
95166	24	4.87	16.31	37.79	4.69	20.27	5.07	1.45	0.83	5.10	1.15	3.26	0.47	2.90	0.44
95GC05	57	12.00	nm	nm	nm	nm	nm	nm	nm	nm	nm	nm	nm	nm	nm
95GC05	nm	nm	nm	nm	nm	nm	nm	nm	nm	nm	nm	nm	nm	nm	nm
96012	17	3.35	14.21	30.89	3.72	15.34	3.51	1.03	0.53	3.21	0.67	1.98	0.28	1.90	0.29
96019	37	3.94	21.86	50.31	6.50	28.13	6.87	2.02	1.09	6.89	1.44	4.23	0.63	4.06	0.62
96032	18	3.14	14.36	30.75	3.69	15.13	3.58	1.05	0.51	3.23	0.67	2.00	0.29	1.94	0.30
96033	17	3.33	13.32	30.12	3.64	15.30	3.57	1.03	0.53	3.26	0.69	2.02	0.28	1.89	0.28
96053	19	3.21	11.46	25.62	3.13	12.97	3.33	1.00	0.57	3.66	0.76	2.25	0.32	2.10	0.31
96061	24	2.45	7.95	21.44	2.90	12.99	3.74	1.08	0.71	4.64	0.97	2.89	0.40	2.65	0.39
96063	14	1.78	6.49	15.76	1.95	8.71	2.31	0.77	0.42	2.66	0.56	1.68	0.23	1.50	0.23
96064	23	3.97	14.68	34.10	4.26	18.32	4.56	1.42	0.72	4.47	0.90	2.60	0.36	2.34	0.34
96066	26	4.33	11.32	26.80	3.53	15.22	4.18	0.76	0.76	5.07	1.11	3.52	0.55	4.05	0.62
96070	16	8.86	16.54	34.89	3.76	14.36	2.93	0.65	0.49	2.66	0.57	1.67	0.25	1.81	0.28
96GC10	27	3.19	16.16	38.09	5.06	22.05	5.41	1.47	0.86	5.15	1.10	3.25	0.47	3.16	0.50
491	16	1.15	8.70	20.61	nm	12.40	3.21	1.22	0.54	nm	nm	nm	nm	1.58	0.25
495	15	10.85	7.17	16.92	nm	10.55	2.82	1.07	0.48	nm	nm	nm	nm	1.41	0.22
497	35	2.27	15.75	38.62	nm	22.27	5.95	nm	1.12	nm	nm	nm	nm	3.62	0.60
498	25	2.46	15.76	38.86	nm	24.10	6.20	nm	1.13	nm	nm	nm	nm	3.64	0.56
503	17	0.46	3.71	10.03	nm	7.42	2.44	0.89	0.51	nm	nm	nm	nm	1.56	0.25
508	32	1.85	12.04	31.01	nm	19.97	5.20	1.82	0.93	nm	nm	nm	nm	3.05	0.48
511	19	0.61	4.81	13.13	nm	9.22	2.48	0.97	0.57	nm	nm	1.98	nm	1.98	0.30

Sample	Y	Th	La	Ce	Pr	Nd	Sm	Eu	Tb	Dy	Ho	Er	Tm	Yb	Lu
548	17	1.92	13.74	32.29	nm	18.25	4.47	nm	0.72	nm	nm	nm	nm	1.63	0.26
95GC10	40	0.91	11.89	29.52	4.38	21.50	5.89	2.31	1.06	6.63	1.32	3.71	0.53	3.33	0.47
546	21	2.41	18.56	41.54	nm	22.38	5.21	nm	0.82	nm	nm	nm	nm	1.99	0.30
549	17	1.78	12.85	30.42	nm	17.57	4.33	nm	0.71	nm	nm	nm	nm	1.72	0.25
762	20	nm	11.65	25.30	nm	14.66	3.92	1.00	nm	3.41	0.00	2.11	nm	1.20	nm
773	17	nm	nm	nm	nm	nm	nm	nm	nm	nm	nm	nm	nm	nm	nm
95056	20	bd	nm	nm	nm	nm	nm	nm	nm	nm	nm	nm	nm	nm	nm
95058	36	2.60	16.10	36.91	4.94	22.40	5.72	1.91	0.95	5.93	1.27	3.58	0.52	3.40	0.49
95076	26	1.38	11.50	27.96	3.88	18.35	4.86	1.64	0.78	4.76	0.94	2.58	0.34	2.12	0.30
95077	23	1.42	11.00	26.16	3.63	16.91	4.49	1.46	0.74	4.44	0.87	2.44	0.33	2.02	0.29
95081	30	2.22	16.47	37.45	4.98	22.04	5.57	1.82	0.89	5.38	1.03	2.85	0.38	2.44	0.37
95106	nm	nm	nm	nm	nm	nm	nm	nm	nm	nm	nm	nm	nm	nm	nm
95106	28	bd	nm	nm	nm	nm	nm	nm	nm	nm	nm	nm	nm	nm	nm
95114	22	1.69	13.31	30.44	4.02	17.74	4.41	1.49	0.70	4.02	0.80	2.15	0.28	1.78	0.24
95128	23	1.44	10.48	25.05	3.56	16.68	4.28	1.54	0.72	4.32	0.82	2.22	0.32	1.90	0.26
95132	32	3.00	nm	nm	nm	nm	nm	nm	nm	nm	nm	nm	nm	nm	nm
95132	32	4.01	nm	nm	nm	nm	nm	nm	nm	nm	nm	nm	nm	nm	nm
95GC03	52	3.32	34.16	79.80	11.05	49.78	11.94	3.67	1.69	9.72	1.75	4.68	0.63	3.65	0.53
95036	48	2.17	16.69	40.15	5.44	24.54	6.73	2.04	1.24	7.93	1.69	4.97	0.72	4.82	0.70
95036	nm	nm	nm	nm	nm	nm	nm	nm	nm	nm	nm	nm	nm	nm	nm
95036	49	bd	nm	nm	nm	nm	nm	nm	nm	nm	nm	nm	nm	nm	nm
96014	36	5.41	23.29	51.38	6.43	27.07	6.33	1.80	1.08	6.77	1.43	4.12	0.60	3.97	0.59
96021	34	2.08	15.24	36.83	5.03	22.97	6.02	1.91	1.04	6.58	1.34	3.83	0.54	3.45	0.51
96023	36	5.19	22.20	49.26	6.21	25.86	6.38	1.48	1.04	6.59	1.39	4.07	0.59	3.94	0.59
96024	33	4.81	18.37	42.18	5.42	22.92	5.80	1.59	0.99	6.28	1.30	3.74	0.54	3.49	0.54
96031	25	2.67	17.40	39.49	5.16	22.15	5.56	1.65	0.83	4.97	0.98	2.75	0.38	2.46	0.36
96035	33	4.88	20.80	45.43	5.67	23.58	5.84	1.64	0.97	6.14	1.28	3.77	0.56	3.65	0.54
96036	35	5.17	22.44	49.49	6.22	26.16	6.14	1.76	1.04	6.61	1.35	4.03	0.58	3.83	0.59
96037	27	4.27	21.38	49.40	6.26	26.26	6.17	1.75	0.93	5.53	1.08	3.00	0.41	2.54	0.36
512	13	nm	9.22	22.15	nm	14.43	3.01	1.30	nm	3.91	nm	2.21	nm	1.10	nm
450	30	4.01	34.52	76.27	nm	39.74	8.64	2.71	1.18	nm	nm	nm	nm	2.63	0.40
454	36	3.78	34.64	80.33	nm	42.38	9.11	3.11	1.35	nm	nm	nm	nm	3.18	0.45
483	42	3.73	31.60	79.77	nm	49.73	11.71	3.88	1.72	nm	nm	nm	nm	3.62	0.55
484	39	5.39	38.59	89.21	nm	46.68	10.58	3.38	1.55	nm	nm	nm	nm	3.62	0.56
502	11	1.44	13.61	31.11	nm	18.01	3.92	1.41	0.55	nm	nm	nm	nm	1.21	0.17
506	19	0.00	9.17	22.07	nm	13.30	3.73	1.21	0.91	3.53	nm	2.12	nm	nm	nm
509	59	7.35	54.94	133.48	nm	75.54	15.42	4.64	2.19	nm	nm	nm	nm	5.28	0.79
551	22	nm	26.77	60.87	nm	36.80	8.93	2.61	nm	1.80	nm	3.21	nm	1.10	nm
763	49	nm	54.59	115.98	nm	59.23	12.46	2.99	nm	7.62	nm	4.43	nm	2.99	nm
95007	25	4.01	nm	nm	nm	nm	nm	nm	nm	nm	nm	nm	nm	nm	nm
95009	37	4.01	nm	nm	nm	nm	nm	nm	nm	nm	nm	nm	nm	nm	nm
95037	29	6.01	nm	nm	nm	nm	nm	nm	nm	nm	nm	nm	nm	nm	nm
95061	13	0.85	7.17	16.34	2.19	10.00	2.61	0.87	0.41	2.48	0.47	1.23	0.17	0.99	0.15
95063	60	11.02	nm	nm	nm	nm	nm	nm	nm	nm	nm	nm	nm	nm	nm
95097	18	4.01	nm	nm	nm	nm	nm	nm	nm	nm	nm	nm	nm	nm	nm
95099	22	1.89	12.99	29.36	3.82	16.99	4.03	1.35	0.64	3.78	0.74	1.93	0.28	1.63	0.22
95100	36	4.08	30.40	68.62	8.76	37.55	8.11	2.49	1.13	6.63	1.26	3.34	0.46	2.87	0.40
95100	35	5.01	nm	nm	nm	nm	nm	nm	nm	nm	nm	nm	nm	nm	nm
95113	28	2.05	16.91	39.88	5.35	24.41	6.03	2.03	0.91	5.33	1.01	2.68	0.37	2.16	0.31

Sample	Y	Th	La	Ce	Pr	Nd	Sm	Eu	Tb	Dy	Ho	Er	Tm	Yb	Lu
96007	nm	nm	nm	nm	nm	nm	nm	nm	nm	nm	nm	nm	nm	nm	nm
96007	18	1.42	10.65	25.53	3.48	15.67	4.03	1.27	0.66	3.98	0.74	2.01	0.27	1.72	0.24
96011	18	1.87	13.70	32.09	4.22	18.54	4.61	1.52	0.69	3.99	0.74	1.99	0.26	1.64	0.23
94025	32	6.01	nm	nm	nm	nm	nm	nm	nm	nm	nm	nm	nm	nm	nm
95010	29	5.23	56.28	123.01	15.11	61.92	11.78	3.42	1.37	7.10	1.07	2.58	0.32	1.74	0.23
95023	34	10.01	nm	nm	nm	nm	nm	nm	nm	nm	nm	nm	nm	nm	nm
95067	38	8.81	87.14	183.62	21.65	82.60	14.07	4.02	1.40	7.55	1.36	3.59	0.47	2.68	0.38
95070	38	8.01	nm	nm	nm	nm	nm	nm	nm	nm	nm	nm	nm	nm	nm
95101	29	2.71	10.29	23.61	2.98	13.07	3.46	1.16	0.63	4.00	0.88	2.47	0.36	2.27	0.32
95119	nm	nm	nm	nm	nm	nm	nm	nm	nm	nm	nm	nm	nm	nm	nm
95119	23	1.46	10.52	24.55	3.39	15.45	3.94	1.31	0.67	3.97	0.76	2.13	0.28	1.83	0.25
95122	40	5.01	nm	nm	nm	nm	nm	nm	nm	nm	nm	nm	nm	nm	nm
95122	41	6.01	nm	nm	nm	nm	nm	nm	nm	nm	nm	nm	nm	nm	nm
95125	81	10.02	nm	nm	nm	nm	nm	nm	nm	nm	nm	nm	nm	nm	nm
95127	32	8.01	nm	nm	nm	nm	nm	nm	nm	nm	nm	nm	nm	nm	nm
96002	31	8.65	91.51	189.14	22.09	83.44	13.87	3.94	1.39	7.26	1.27	3.15	0.40	2.40	0.34
96002	31	8.52	90.31	188.57	21.79	83.01	13.86	3.89	1.36	7.08	1.28	3.25	0.41	2.41	0.33
96002	nm	nm	nm	nm	nm	nm	nm	nm	nm	nm	nm	nm	nm	nm	nm
96004	16	8.01	24.10	44.76	5.28	19.50	3.75	0.95	0.50	3.11	0.63	1.89	0.28	1.90	0.30
96025	30	11.70	97.17	190.94	21.12	75.54	11.93	3.13	1.14	6.27	1.14	3.02	0.41	2.61	0.38
96059	12	2.39	11.28	24.22	2.88	11.20	2.58	0.78	0.37	2.20	0.45	1.23	0.18	1.23	0.18
95033	30	2.53	24.06	53.72	6.97	30.00	6.90	2.33	1.09	6.42	1.02	2.81	0.36	2.27	0.33
94038	16	7.21	17.25	31.84	3.63	13.58	3.02	0.60	0.46	2.90	0.52	1.51	0.22	1.43	0.24
94005	33	1.40	nm	nm	nm	nm	nm	nm	nm	nm	nm	nm	nm	nm	nm
94005	33	6.01	nm	nm	nm	nm	nm	nm	nm	nm	nm	nm	nm	nm	nm
94005	33	1.50	13.44	33.70	4.56	20.59	5.20	1.85	0.89	5.43	1.09	3.16	0.44	2.85	0.39
94005	33	1.54	13.70	33.22	4.67	21.65	5.50	1.87	0.92	5.60	1.17	3.34	0.46	2.80	0.43
94028A	13	0.60	4.70	11.60	1.65	7.83	2.34	0.83	0.40	2.18	0.43	1.07	0.16	0.98	0.13
94032	30	3.68	16.39	36.98	4.84	21.27	5.14	1.82	0.91	5.79	1.18	3.43	0.46	2.97	0.44
94035	35	2.97	18.56	43.55	5.69	24.61	6.01	2.02	0.98	6.20	1.23	3.54	0.50	3.26	0.52

## Appendix 4

### Analysis of Precision and Accuracy of Geochemical Data\*

#### Assessment of Precision

Several duplicate samples were included in each batch of samples submitted for analysis, for each whole rock geochemical analytical technique, to facilitate an independent assessment of data precision. An average, standard deviation (stdev) and relative standard deviation (rstdev %) were calculated for each set of replicate analyses. This data is tabulated separately for each geochemical technique.

For *major elements analysed by XRF* on fused glass beads, the rstdev is typically: < 1% for SiO<sub>2</sub>, Al<sub>2</sub>O<sub>3</sub>, Fe<sub>2</sub>O<sub>3</sub>, CaO and MgO (except at very low levels, <1 wt %); < 3% for TiO<sub>2</sub>, MnO and Na<sub>2</sub>O; < 5% for K<sub>2</sub>O (except at very low levels, <0.1 wt%); and < 10% for P<sub>2</sub>O<sub>5</sub>. For *trace elements analysed by XRF* on pressed pellets, when element abundances are well above the detection limit (det limit), the rstdev is typically: < 2% for Sr and Zr; < 3% for Y; < 5% for V, Cr, Ni and Rb; and < 10% for Ba and Sc. For the elements Nb, Ce, Pb, Th and U, levels are generally too close to the detection limit to give reliable analyses by XRF. For *trace elements analysed by ICP-MS*, the rstdev varies considerably with the amount of element present. This is shown by plots of average values versus rstdev for all elements, which are presented after the data table. In general, except at very low levels, the rstdev is < 5% for all elements except Nb, for which it is slightly higher because of the low levels of Nb in many of the samples analysed.

#### Assessment of Accuracy

As part of normal lab procedure, several standards are included in each analytical run. An average, and standard deviation (stdev) have been calculated for all the standards included in runs with my samples. This data is tabulated for each geochemical technique, and compared with accepted values, and in some cases lab average values (lab\*), compiled from hundreds of runs.

Average values of *XRF major element standards* are generally within approximately 1 stdev of the accepted value, for amounts well above the detection limit, with the exception of Na<sub>2</sub>O, which is a bit erratic. For some elements, at low levels (P<sub>2</sub>O<sub>5</sub> < 0.2wt%, Fe<sub>2</sub>O<sub>3</sub> < 1wt%, CaO < 1wt%, Na<sub>2</sub>O < 0.5wt% and K<sub>2</sub>O < 0.2wt%) there is a greater discrepancy between average and accepted values. Average values for *XRF trace element standards* are generally within approximately 1 stdev of the accepted values, for amounts well above the detection limit (DL); except for Rb, Sr, Zr and Nb, which are consistently a bit above, and Y which is slightly below the accepted values. The elements U and Th are below the detection limit for many of the standards and thus the accuracy is not as well constrained for these elements. Average values for trace element standards are generally within approximately 1 stdev of the accepted values, at levels well above the detection limit, although Ba, Ce, Nd and Eu tend to be a bit low. For the standard MRG-1, Zr, Nb and Yb are consistently high and Y, Ba, La, Ce, Pr, Nd, Sm and Th are consistently low compared to accepted values. However, they are all within 1 stdev of the lab average value, except Zr which is a bit high.

\* For more information on lab precision and accuracy see Lonerich et al. 1993 and Jenner et al. 1990.

**Assessment of Precision of XRF-Major Element Oxide Data**  
**Replicate Analyses**

Sample	SiO <sub>2</sub>	TiO <sub>2</sub>	Al <sub>2</sub> O <sub>3</sub>	Fe <sub>2</sub> O <sub>3</sub>	MnO	MgO	CaO	Na <sub>2</sub> O	K <sub>2</sub> O	P <sub>2</sub> O <sub>5</sub>
95066	55.65	1.59	16.48	10.46	0.15	3.12	4.89	6.70	0.43	0.20
95066	55.47	1.58	16.47	10.43	0.15	3.14	4.83	6.54	0.43	0.21
average	55.56	1.59	16.48	10.44	0.15	3.13	4.86	6.62	0.43	0.21
stdev	0.128	0.008	0.011	0.024	0.003	0.011	0.037	0.111	0.001	0.003
rstdev (%)	<b>0.23</b>	<b>0.47</b>	<b>0.07</b>	<b>0.23</b>	<b>2.26</b>	<b>0.35</b>	<b>0.77</b>	<b>1.67</b>	<b>0.21</b>	<b>1.31</b>
95164	57.24	0.98	18.45	8.32	0.15	3.44	3.57	6.65	0.18	0.13
95164	57.32	0.99	18.35	8.37	0.15	3.48	3.59	6.71	0.17	0.14
average	57.28	0.99	18.40	8.34	0.15	3.46	3.58	6.68	0.17	0.13
stdev	0.055	0.008	0.068	0.032	0.002	0.028	0.014	0.045	0.005	0.004
rstdev (%)	<b>0.10</b>	<b>0.85</b>	<b>0.37</b>	<b>0.38</b>	<b>1.17</b>	<b>0.82</b>	<b>0.39</b>	<b>0.67</b>	<b>2.71</b>	<b>3.36</b>
95GC05	70.77	0.40	13.94	2.80	0.05	0.53	0.47	5.22	3.39	0.05
95GC05	70.92	0.40	14.08	2.78	0.05	0.56	0.48	5.21	3.41	0.04
average	70.84	0.40	14.01	2.79	0.05	0.55	0.48	5.21	3.40	0.04
stdev	0.106	0.000	0.101	0.014	0.001	0.019	0.002	0.006	0.017	0.001
rstdev (%)	<b>0.15</b>	<b>0.02</b>	<b>0.72</b>	<b>0.50</b>	<b>1.58</b>	<b>3.42</b>	<b>0.36</b>	<b>0.11</b>	<b>0.49</b>	<b>2.16</b>
95106	48.44	2.88	13.63	14.86	0.28	5.57	8.95	3.50	1.00	0.35
95106	48.23	2.89	13.56	14.89	0.27	5.57	8.92	3.46	0.98	0.34
average	48.34	2.89	13.59	14.88	0.27	5.57	8.94	3.48	0.99	0.34
stdev	0.147	0.005	0.044	0.023	0.003	0.001	0.024	0.032	0.017	0.006
rstdev (%)	<b>0.30</b>	<b>0.18</b>	<b>0.32</b>	<b>0.16</b>	<b>1.24</b>	<b>0.01</b>	<b>0.26</b>	<b>0.92</b>	<b>1.71</b>	<b>1.65</b>
95132	51.64	2.41	13.80	12.56	0.19	4.78	7.12	4.80	0.84	0.28
95132	51.86	2.36	14.00	12.61	0.19	4.82	7.18	4.80	0.84	0.28
average	51.75	2.38	13.90	12.59	0.19	4.80	7.15	4.80	0.84	0.28
stdev	0.156	0.036	0.140	0.029	0.003	0.026	0.041	0.002	0.002	0.004
rstdev (%)	<b>0.30</b>	<b>1.52</b>	<b>1.00</b>	<b>0.23</b>	<b>1.37</b>	<b>0.54</b>	<b>0.57</b>	<b>0.04</b>	<b>0.22</b>	<b>1.35</b>
95036	51.89	1.64	15.19	11.43	0.48	6.11	5.32	5.71	0.06	0.24
95036	52.63	1.63	15.40	11.47	0.48	6.16	5.39	5.76	0.06	0.24
95036	52.46	1.63	15.39	11.48	0.48	6.14	5.40	5.75	0.06	0.24
average	52.33	1.63	15.33	11.46	0.48	6.14	5.37	5.74	0.06	0.24
stdev	0.386	0.002	0.116	0.026	0.002	0.026	0.044	0.030	0.003	0.003
rstdev (%)	<b>0.74</b>	<b>0.14</b>	<b>0.76</b>	<b>0.23</b>	<b>0.49</b>	<b>0.42</b>	<b>0.81</b>	<b>0.52</b>	<b>4.92</b>	<b>1.32</b>
94005	49.40	2.43	16.46	12.70	0.18	5.44	8.65	3.18	0.70	0.37
94005	48.76	2.36	16.34	12.57	0.18	5.34	8.48	3.25	0.70	0.36
average	49.08	2.40	16.40	12.64	0.18	5.39	8.57	3.22	0.70	0.37
stdev	0.453	0.053	0.086	0.088	0.001	0.068	0.116	0.052	0.001	0.007
rstdev (%)	<b>0.92</b>	<b>2.23</b>	<b>0.52</b>	<b>0.70</b>	<b>0.33</b>	<b>1.27</b>	<b>1.35</b>	<b>1.61</b>	<b>0.18</b>	<b>2.03</b>
95119	49.52	1.52	13.03	11.43	0.20	10.89	8.15	3.02	1.09	0.22
95119	49.53	1.53	13.04	11.48	0.20	10.89	8.26	3.04	1.09	0.23
average	49.52	1.52	13.04	11.46	0.20	10.89	8.20	3.03	1.09	0.23
stdev	0.008	0.011	0.008	0.035	0.002	0.000	0.078	0.014	0.003	0.007
rstdev (%)	<b>0.02</b>	<b>0.73</b>	<b>0.06</b>	<b>0.30</b>	<b>0.96</b>	<b>0.00</b>	<b>0.95</b>	<b>0.45</b>	<b>0.29</b>	<b>3.02</b>
96002	44.20	3.90	13.41	13.86	0.20	5.46	10.41	2.75	2.76	1.00
96002	44.47	3.95	13.54	13.96	0.21	5.47	10.47	2.72	2.73	0.97
average	44.34	3.92	13.47	13.91	0.20	5.46	10.44	2.73	2.75	0.99
stdev	0.187	0.033	0.092	0.070	0.007	0.004	0.044	0.018	0.021	0.019
rstdev (%)	<b>0.42</b>	<b>0.85</b>	<b>0.68</b>	<b>0.51</b>	<b>3.25</b>	<b>0.07</b>	<b>0.42</b>	<b>0.67</b>	<b>0.75</b>	<b>1.90</b>
95100	50.45	3.21	14.15	13.74	0.25	4.40	6.09	4.92	1.17	0.56
95100	50.12	3.23	14.24	13.65	0.24	4.32	6.08	4.82	1.19	0.56
average	50.28	3.22	14.20	13.69	0.25	4.36	6.08	4.87	1.18	0.56
stdev	0.232	0.014	0.065	0.059	0.007	0.059	0.003	0.072	0.008	0.002
rstdev (%)	<b>0.46</b>	<b>0.45</b>	<b>0.46</b>	<b>0.43</b>	<b>2.68</b>	<b>1.35</b>	<b>0.04</b>	<b>1.48</b>	<b>0.66</b>	<b>0.35</b>
95122	51.44	2.74	16.69	10.29	0.15	3.38	6.37	4.41	2.70	0.95
95122	50.82	2.73	16.60	10.26	0.15	3.29	6.32	4.27	2.65	0.94
average	51.13	2.74	16.65	10.27	0.15	3.33	6.35	4.34	2.68	0.94
stdev	0.437	0.006	0.065	0.020	0.000	0.060	0.034	0.102	0.035	0.005
rstdev (%)	<b>0.85</b>	<b>0.21</b>	<b>0.39</b>	<b>0.19</b>	<b>0.06</b>	<b>1.81</b>	<b>0.53</b>	<b>2.34</b>	<b>1.31</b>	<b>0.50</b>

Sample	SiO <sub>2</sub>	TiO <sub>2</sub>	Al <sub>2</sub> O <sub>3</sub>	Fe <sub>2</sub> O <sub>3</sub>	MnO	MgO	CaO	Na <sub>2</sub> O	K <sub>2</sub> O	P <sub>2</sub> O <sub>5</sub>
94014	49.20	0.29	10.89	9.48	0.17	17.08	11.20	1.02	0.15	0.02
94014	49.31	0.29	10.92	9.44	0.17	17.10	11.16	1.03	0.15	0.02
94014	49.27	0.28	10.93	9.52	0.16	17.08	11.26	1.04	0.14	0.02
average	49.26	0.29	10.91	9.48	0.17	17.08	11.21	1.03	0.15	0.02
stdev	0.056	0.004	0.020	0.040	0.002	0.015	0.046	0.012	0.005	0.001
rstdev (%)	0.11	1.51	0.18	0.42	1.22	0.09	0.41	1.20	3.58	6.03
94044	49.54	0.49	14.01	12.38	0.24	11.18	10.12	1.55	0.27	0.02
94044	49.34	0.49	13.98	12.39	0.23	11.08	10.08	1.53	0.28	0.02
average	49.44	0.49	13.99	12.38	0.23	11.13	10.10	1.54	0.28	0.02
stdev	0.146	0.001	0.022	0.009	0.006	0.071	0.028	0.013	0.010	0.001
rstdev (%)	0.29	0.15	0.16	0.08	2.46	0.64	0.27	0.86	3.60	4.10
94049	56.23	0.67	14.71	12.50	0.20	4.33	7.44	2.79	0.44	0.04
94049	56.21	0.68	14.58	12.56	0.19	4.31	7.44	2.71	0.43	0.04
94049	56.10	0.67	14.63	12.50	0.19	4.28	7.45	2.72	0.48	0.03
average	56.18	0.67	14.64	12.52	0.20	4.31	7.44	2.74	0.45	0.04
stdev	0.071	0.004	0.067	0.035	0.005	0.025	0.007	0.044	0.026	0.003
rstdev (%)	0.13	0.64	0.46	0.28	2.41	0.59	0.10	1.62	5.75	7.86
94GC05	53.41	0.27	15.64	11.34	0.21	5.63	10.01	1.50	0.25	0.01
94GC05	54.26	0.28	15.88	11.35	0.21	5.73	10.19	1.54	0.25	0.01
average	53.83	0.27	15.76	11.34	0.21	5.68	10.10	1.52	0.25	0.01
stdev	0.603	0.006	0.169	0.005	0.002	0.070	0.127	0.026	0.003	0.000
rstdev (%)	1.12	2.08	1.07	0.05	1.15	1.23	1.26	1.73	1.30	2.05
95153	55.98	0.93	15.30	13.72	0.22	3.08	3.83	6.48	0.20	0.06
95153	55.70	0.93	15.21	13.79	0.21	3.01	3.82	6.33	0.20	0.05
95153	56.01	0.94	15.32	13.77	0.21	3.05	3.83	6.27	0.21	0.06
average	55.89	0.93	15.28	13.76	0.21	3.05	3.83	6.36	0.20	0.06
stdev	0.169	0.004	0.060	0.038	0.003	0.036	0.008	0.109	0.008	0.005
rstdev (%)	0.30	0.41	0.39	0.28	1.43	1.19	0.20	1.71	4.15	8.92
96055	51.11	1.53	15.10	15.72	0.13	4.71	5.57	5.66	0.07	0.14
96055	51.28	1.53	15.25	15.81	0.13	4.68	5.59	5.64	0.08	0.15
average	51.20	1.53	15.18	15.77	0.13	4.70	5.58	5.65	0.08	0.15
stdev	0.119	0.000	0.104	0.064	0.000	0.024	0.018	0.012	0.007	0.001
rstdev (%)	0.23	0.03	0.69	0.41	0.27	0.51	0.33	0.22	9.57	0.72
94GC06	70.51	0.37	13.32	5.64	0.10	1.01	4.60	2.92	0.23	0.08
94GC06	70.20	0.37	13.11	5.59	0.10	1.00	4.56	2.87	0.23	0.08
average	70.35	0.37	13.21	5.61	0.10	1.00	4.58	2.90	0.23	0.08
stdev	0.219	0.000	0.143	0.035	0.001	0.010	0.031	0.038	0.001	0.001
rstdev (%)	0.31	0.10	1.08	0.62	1.51	1.00	0.69	1.31	0.62	1.50
96065	73.58	0.28	12.27	4.28	0.05	0.45	3.13	4.07	0.33	0.05
96065	73.75	0.28	12.36	4.30	0.05	0.44	3.12	4.10	0.35	0.05
96065	74.17	0.27	12.34	4.30	0.05	0.43	3.11	4.06	0.35	0.06
average	73.83	0.28	12.32	4.29	0.05	0.44	3.12	4.07	0.34	0.05
stdev	0.304	0.009	0.045	0.010	0.003	0.011	0.012	0.021	0.010	0.004
rstdev (%)	0.41	3.21	0.37	0.22	5.65	2.43	0.38	0.52	2.94	8.17
96067	78.44	0.12	8.48	2.78	0.04	0.65	2.14	2.82	0.43	0.01
96067	80.42	0.11	8.65	2.83	0.05	0.67	2.15	2.90	0.43	0.01
average	79.43	0.11	8.56	2.80	0.05	0.66	2.14	2.86	0.43	0.01
stdev	1.397	0.006	0.126	0.036	0.003	0.016	0.011	0.061	0.000	0.002
rstdev (%)	1.76	5.74	1.47	1.27	7.48	2.39	0.52	2.12	0.03	22.15
95001	51.62	1.11	17.26	9.71	0.19	5.32	8.71	4.09	0.34	0.13
95001	51.96	1.15	17.39	9.77	0.19	5.39	8.71	4.16	0.34	0.14
average	51.79	1.13	17.32	9.74	0.19	5.35	8.71	4.12	0.34	0.13
stdev	0.240	0.026	0.089	0.042	0.003	0.047	0.002	0.047	0.003	0.004
rstdev (%)	0.46	2.29	0.52	0.43	1.53	0.87	0.02	1.13	0.90	3.21

**Assessment of Precision of XRF-Trace Element Data**  
**Replicate Analyses**

Element	Sc	V	Cr	Ni	Rb	Sr	Y	Zr	Nb	Ba	Ce	Pb	Th	U
det limit	7	6	7	5	0.7	1.2	0.6	1.3	0.7	24	44	4	3	4
94GC06	23	60	BD	BD	3.7	224.2	19.5	BD	0.8	147	BD	BD	BD	BD
94GC06	30	57	BD	BD	3.7	221.6	18.7	3.2	1.0	162	BD	BD	BD	BD
94GC06	26	56	BD	BD	3.6	223.0	18.4	2.7	1.0	145	BD	BD	BD	BD
avg	26	58	NA	NA	3.7	222.9	18.9	2.9	0.9	151	BD	BD	BD	BD
stdv	3	2	NA	NA	0.1	1.3	0.5	0.4	0.1	9	NA	NA	NA	NA
rstdv (%)	13	3	NA	NA	2.2	0.6	2.9	12.4	13.2	6	NA	NA	NA	NA
94GC05	78	236	43	BD	3.6	95.3	15.1	17.2	0.6	46	BD	BD	BD	BD
94GC05	74	244	42	BD	3.7	94.2	14.6	16.6	0.5	58	BD	BD	BD	BD
avg	76	240	43	NA	3.7	94.7	14.9	16.9	0.5	52	NA	NA	NA	NA
stdv	3	5	1	NA	0.1	0.8	0.3	0.4	0.1	8	NA	NA	NA	NA
rstdv (%)	4	2	2	NA	1.9	0.9	2.3	2.6	14.8	16	NA	NA	NA	NA
94005	26	218	BD	32	12.9	400.5	29.8	181.0	12.4	223	BD	BD	BD	BD
94005	24	213	BD	32	12.3	405.3	30.2	182.6	13.0	209	BD	10	BD	BD
94005	27	213	12	39	12.7	401.5	29.5	183.8	12.4	213	BD	BD	BD	BD
94005	21	213	14	37	12.0	393.4	29.6	182.4	11.8	221	BD	BD	BD	BD
avg	25	214	13	35	12.5	400.2	29.8	182.4	12.4	216	NA	NA	NA	NA
stdv	2	2	1	4	0.4	5.0	0.3	1.2	0.5	6	NA	NA	NA	NA
rstdv (%)	9	1	9	11	3.2	1.2	1.1	0.6	4.0	3	NA	NA	NA	NA
94014	48	201	1930	386	1.0	46.8	6.8	8.2	0.4	11	BD	BD	BD	BD
94014	43	205	1866	381	1.3	46.8	6.8	7.1	0.6	27	BD	BD	BD	BD
94014	40	199	1957	385	1.4	45.3	6.6	7.2	0.4	13	BD	BD	BD	BD
avg	44	202	1918	384	1.3	46.3	6.7	7.5	0.5	17	NA	NA	NA	NA
stdv	4	3	47	3	0.2	0.9	0.1	0.6	0.1	9	NA	NA	NA	NA
rstdv (%)	9	1	2	1	17.9	1.9	1.3	8.3	16.4	54	NA	NA	NA	NA
94032	31	244	BD	BD	1.3	259.5	29.4	151.4	5.6	43	54	6	5	BD
94032	30	229	BD	BD	1.0	261.1	29.6	150.4	6.3	50	35	7	4	BD
avg	30	237	NA	NA	1.2	260.3	29.5	150.9	5.9	47	45	7	5	NA
stdv	0	10	NA	NA	0.2	1.1	0.1	0.7	0.5	5	14	1	1	NA
rstdv (%)	0	4	NA	NA	19.8	0.4	0.3	0.5	8.4	11	31	12	14	NA
94036	50	197	244	155	4.4	53.9	4.6	8.8	BD	12	BD	BD	BD	BD
94036	43	198	246	157	4.7	54.6	4.4	7.5	BD	12	BD	BD	BD	BD
avg	46	198	245	156	4.5	54.2	4.5	8.1	NA	12	NA	NA	NA	NA
stdv	5	1	2	1	0.2	0.5	0.1	0.9	NA	1	NA	NA	NA	NA
rstdv (%)	10	1	1	1	3.8	1.0	1.9	11.5	NA	5	NA	NA	NA	NA
94037	63	234	499	71	0.8	62.2	15.5	11.5	BD	23	BD	BD	BD	BD
94037	58	234	484	66	0.7	64.0	15.9	11.8	BD	9	BD	BD	BD	BD
avg	61	234	491	69	0.7	63.1	15.7	11.7	NA	16	NA	BD	NA	NA
stdv	4	0	11	4	0.1	1.3	0.3	0.2	NA	10	NA	0	NA	NA
rstdv (%)	6	0	2	6	9.6	2.0	1.8	1.7	NA	62	NA	NA	NA	NA
94038	51	238	964	137	0.7	98.7	9.0	11.6	BD	BD	BD	BD	BD	BD
94038	57	244	958	140	0.6	100.3	9.3	11.7	BD	BD	BD	BD	BD	BD
avg	54	241	961	139	0.6	99.5	9.1	11.6	NA	NA	NA	NA	NA	NA
stdv	4	4	5	2	0.1	1.1	0.2	0.1	NA	NA	NA	NA	NA	NA
rstdv (%)	8	2	0	2	14.1	1.2	2.1	0.6	NA	NA	NA	NA	NA	NA
94044	57	319	793	151	2.0	116.0	8.2	5.6	BD	BD	BD	BD	BD	BD
94044	52	324	786	153	2.4	117.6	7.8	5.5	BD	BD	BD	BD	BD	BD
avg	55	322	790	152	2.2	116.8	8.0	5.6	NA	NA	NA	NA	NA	NA
stdv	4	3	5	2	0.3	1.1	0.3	0.1	NA	NA	NA	NA	NA	NA
rstdv (%)	7	1	1	1	12.4	1.0	4.0	1.3	NA	NA	NA	NA	NA	NA

Element	Sc	V	Cr	Ni	Rb	Sr	Y	Zr	Nb	Ba	Ce	Pb	Th	U
94049	56	373	BD	BD	4.4	131.7	25.1	23.0	1.0	71	BD	BD	BD	BD
94049	54	390	BD	BD	3.9	131.4	25.4	24.0	0.9	71	BD	BD	BD	BD
94049	53	386	NA	BD	4.5	131.2	24.1	24.2	1.2	63	BD	BD	BD	BD
avg	54	383	NA	NA	4.2	131.4	24.9	23.7	1.1	68	NA	NA	NA	NA
stdv	2	9	NA	NA	0.3	0.3	0.7	0.7	0.2	5	NA	NA	NA	NA
rstdv (%)	3	2	NA	NA	8.1	0.2	2.6	2.8	16.0	7	NA	NA	NA	NA
95001	40	227	64	BD	5.0	61.4	22.2	101.4	5.9	64	BD	BD	BD	BD
95001	30	223	68	BD	4.4	60.9	22.2	102.4	6.1	81	BD	BD	BD	BD
avg	35	225	66	NA	4.7	61.2	22.2	101.9	6.0	73	NA	NA	NA	NA
stdv	7	3	3	NA	0.4	0.3	0.1	0.7	0.2	11	NA	NA	NA	NA
rstdv (%)	21	1	4	NA	9.1	0.5	0.3	0.7	2.9	16	NA	NA	NA	NA
950100	21	202	BD	BD	25.4	192.0	32.4	274.4	39.6	414	101	BD	BD	BD
950100	18	209	BD	BD	26.7	193.0	32.7	274.7	40.4	434	84	BD	BD	BD
avg	20	205	NA	NA	26.1	192.5	32.6	274.5	40.0	424	93	NA	NA	NA
stdv	2	5	NA	NA	0.9	0.7	0.2	0.2	0.6	15	12	NA	NA	NA
rstdv (%)	10	2	NA	NA	3.5	0.4	0.5	0.1	1.4	3	13	NA	NA	NA
95122	20	236	BD	BD	40.1	719.5	38.1	486.9	102.2	870	213	4	6	BD
95122	15	238	BD	BD	39.0	717.1	36.7	485.6	102.7	883	173	5	5	BD
avg	18	237	NA	NA	39.5	718.3	37.4	486.2	102.4	877	193	5	6	NA
stdv	3	2	NA	NA	0.8	1.7	0.9	0.9	0.4	9	29	1	1	NA
rstdv (%)	19	1	NA	NA	2.0	0.2	2.5	0.2	0.4	1	15	15	17	NA
95132	22	303	36	13	16.3	133.3	28.4	208.6	22.8	242	23	6	4	BD
95132	23	302	40	12	15.9	132.2	28.0	206.0	23.0	252	42	7	3	BD
avg	23	303	38	12	16.1	132.8	28.2	207.3	22.9	247	33	7	4	NA
stdv	1	0	3	1	0.3	0.8	0.3	1.8	0.1	7	13	1	0	NA
rstdv (%)	5	0	9	NA	1.8	0.6	1.1	0.9	0.4	3	NA	8	11	NA
95153	47	258	BD	BD	3.1	51.8	15.4	26.5	0.7	100	BD	BD	BD	BD
95153	49	261	BD	BD	3.2	51.6	15.3	26.1	0.5	88	5	4	BD	BD
95153	57	269	BD	BD	3.1	51.9	15.9	26.6	1.2	109	BD	4	BD	BD
avg	51	263	NA	NA	3.1	51.8	15.5	26.4	0.8	99	NA	4	NA	NA
stdv	5	6	NA	NA	0.1	0.1	0.3	0.3	0.4	10	NA	0	NA	NA
rstdv (%)	10	2	NA	NA	2.9	0.2	2.2	1.1	43.9	10	NA	12	NA	NA
95164	28	186	49	BD	3.9	76.6	20.7	98.6	4.9	76	32	14	5	BD
95164	31	188	50	BD	3.7	77.3	21.3	99.1	5.5	81	19	13	5	BD
avg	29	187	50	NA	3.8	76.9	21.0	98.9	5.2	79	26	14	5	NA
stdv	2	1	0	NA	0.1	0.5	0.4	0.4	0.4	4	9	1	0	NA
rstdv (%)	8	1	1	NA	2.9	0.7	2.0	0.4	7.5	5	36	5	1	NA
95036	30	280	103	39	BD	135.8	43.7	262.3	19.3	245	BD	BD	BD	BD
95036	33	276	110	53	BD	135.9	43.1	260.0	19.1	242	BD	BD	BD	BD
avg	32	278	106	46	NA	135.8	43.4	261.1	19.2	244	NA	NA	NA	NA
stdv	3	3	5	10	NA	0.1	0.5	1.6	0.2	2	NA	NA	NA	NA
rstdv (%)	9	1	4	21	NA	0.0	1.1	0.6	0.8	1	NA	NA	NA	NA
95066	38	265	25	4	6.7	93.5	30.7	160.6	10.2	115	38	10	4	BD
95066	36	272	19	BD	6.6	91.5	30.1	154.5	9.8	141	2	9	4	BD
95066	35	268	22	BD	6.3	93.6	30.4	156.9	9.6	164	17	10	4	BD
avg	36	268	22	NA	6.5	92.9	30.4	157.3	9.9	140	19	10	4	NA
stdv	1	4	3	NA	0.2	1.2	0.3	3.1	0.3	24	18	0	0	NA
rstdv (%)	4	1	14	NA	3.7	1.3	1.0	2.0	3.0	17	94	5	2	NA

Element	Sc	V	Cr	Ni	Rb	Sr	Y	Zr	Nb	Ba	Ce	Pb	Th	U
96002	24	338	BD	8	76.9	1308.6	32.1	464.3	122.6	2917	279	10	7	BD
96002	22	347	BD	7	76.1	1295.7	31.5	458.1	121.7	2869	179	10	8	BD
avg	23	342	NA	8	76.5	1302.1	31.8	461.2	122.2	2893	229	10	7	NA
stdv	1	7	NA	1	0.6	9.1	0.4	4.3	0.7	34	71	0	0	NA
rstdv (%)	5	2	NA	7	0.7	0.7	1.1	0.9	0.5	1	31	1	4	NA
96055	39	448	BD	BD	0.6	132.4	26.8	85.2	2.4	30	BD	6	BD	BD
96055	42	460	BD	BD	0.7	134.2	27.6	86.3	2.7	30	BD	4	BD	BD
avg	41	454	NA	NA	0.6	133.3	27.2	85.7	2.5	30	NA	5	NA	NA
stdv	2	9	NA	NA	0.1	1.3	0.6	0.8	0.2	0	NA	1	NA	NA
rstdv (%)	4	2	NA	NA	11.3	1.0	2.1	1.0	9.4	0	NA	26	NA	NA
96065	12	19	BD	BD	6.5	108.6	31.7	57.4	1.4	54	BD	6	BD	BD
96065	14	19	BD	BD	6.5	108.4	31.9	57.7	1.5	54	BD	6	BD	BD
96065	14	21	NA	BD	6.0	107.6	32.2	57.5	1.1	29	BD	7	NA	BD
avg	13	20	NA	NA	6.3	108.2	32.0	57.5	1.3	46	NA	7	NA	NA
stdv	1	1	NA	NA	0.3	0.5	0.2	0.2	0.2	14	NA	1	NA	NA
rstdv (%)	9	6	NA	NA	4.7	0.5	0.7	0.3	18.3	31	NA	12	NA	NA
96067	BD	BD	BD	BD	9.7	49.2	31.6	79.5	1.3	81	BD	BD	BD	BD
96067	BD	BD	BD	BD	9.6	48.5	31.8	79.4	1.4	79	BD	BD	BD	BD
avg	NA	NA	NA	NA	9.6	48.8	31.7	79.5	1.4	80	NA	NA	NA	NA
stdv	NA	NA	NA	NA	0.1	0.5	0.2	0.1	0.0	1	NA	NA	NA	NA
rstdv (%)	NA	NA	NA	NA	0.7	1.0	0.5	0.1	3.3	1	NA	NA	NA	NA

**Assessment of Precision of ICP-MS Trace Element Data**  
**Replicate Analyses**

## Replicate ICP-MS analyses-Assessment of precision

sample#	Y	Zr	Nb	Ba	La	Ce	Pr	Nd	Sm	Eu	Gd
det limit	0.010	0.227	0.026	0.234	0.020	0.043	0.008	0.109	0.058	0.016	0.030
94GC03	6.24	6.22	0.15	15.78	0.33	1.13	0.18	1.22	0.53	0.19	0.80
94GC03	6.18	6.10	0.29	16.09	0.36	1.17	0.20	1.17	0.54	0.20	0.73
average	6.21	6.16	0.22	15.94	0.34	1.15	0.19	1.19	0.54	0.20	0.76
stdev	0.04	0.08	0.10	0.22	0.02	0.02	0.01	0.03	0.01	0.01	0.05
rstdev (%)	0.67	1.36	46.70	1.38	5.71	2.12	6.75	2.51	2.31	3.48	6.53
94GC04	18.35	26.66	1.02	43.66	1.60	4.88	0.83	4.42	1.76	0.52	2.54
94GC04	18.31	27.76	1.05	44.71	1.67	5.08	0.87	4.80	1.79	0.55	2.47
average	18.33	27.21	1.03	44.18	1.63	4.98	0.85	4.61	1.78	0.53	2.51
stdev	0.03	0.78	0.02	0.74	0.05	0.15	0.03	0.27	0.02	0.02	0.05
rstdev (%)	0.15	2.86	1.73	1.67	2.83	2.94	3.08	5.76	1.35	3.97	1.91
94GC06	18.15	4.80	1.21	145.34	0.87	2.62	0.50	3.57	1.62	0.70	2.56
94GC06	18.40	4.71	1.11	146.65	0.81	2.62	0.49	3.52	1.56	0.68	2.61
94GC06	17.55	4.87	0.92	147.00	0.80	2.64	0.50	3.38	1.57	0.70	2.72
94GC06	18.11	4.55	1.07	147.80	0.81	2.63	0.48	3.22	1.67	0.70	2.57
94GC06	17.86	4.76	1.01	147.46	0.84	2.60	0.51	3.17	1.49	0.69	2.69
average	18.01	4.74	1.06	146.85	0.83	2.62	0.49	3.37	1.58	0.69	2.63
stdev	0.32	0.12	0.11	0.95	0.03	0.02	0.01	0.18	0.07	0.01	0.07
rstdev (%)	1.80	2.57	10.43	0.65	3.49	0.65	2.10	5.25	4.19	1.18	2.72
94005	28.76	198.09	13.22	185.02	13.68	33.17	4.67	21.62	5.49	1.87	5.66
94005	27.74	187.11	13.41	178.91	13.24	33.21	4.50	20.28	5.12	1.82	5.77
94005	28.19	190.80	12.26	183.39	13.33	33.56	4.65	21.10	5.21	1.91	5.87
average	28.23	192.00	12.97	182.44	13.42	33.31	4.60	21.00	5.28	1.87	5.76
stdev	0.51	5.59	0.62	3.16	0.23	0.22	0.09	0.67	0.19	0.04	0.10
rstdev (%)	1.81	2.91	4.77	1.73	1.74	0.65	2.01	3.21	3.68	2.34	1.80
94018	27.14	59.95	1.22	107.16	3.78	9.80	1.43	7.23	2.45	0.70	3.57
94018	26.58	58.03	0.63	105.83	3.68	9.34	1.40	7.01	2.51	0.69	3.44
average	26.86	58.99	0.93	106.49	3.73	9.57	1.42	7.12	2.48	0.70	3.51
stdev	0.40	1.36	0.42	0.94	0.07	0.33	0.02	0.16	0.04	0.01	0.09
rstdev (%)	1.48	2.31	44.83	0.88	1.88	3.40	1.61	2.22	1.72	1.16	2.64
94035	31.05	204.41	12.06	163.83	18.36	43.09	5.63	24.35	5.94	2.00	6.22
94035	31.03	205.46	12.08	163.52	18.49	42.87	5.62	24.49	5.96	1.97	6.20
average	31.04	204.93	12.07	163.68	18.43	42.98	5.63	24.42	5.95	1.98	6.21
stdev	0.01	0.74	0.02	0.22	0.09	0.16	0.00	0.10	0.01	0.02	0.02
rstdev (%)	0.04	0.36	0.16	0.13	0.51	0.36	0.05	0.39	0.23	1.18	0.28
94041	5.36	4.56	0.34	149.99	0.32	1.00	0.17	1.11	0.40	0.28	0.74
94041	5.32	4.57	0.33	152.23	0.36	0.96	0.18	0.93	0.42	0.33	0.72
average	5.34	4.56	0.34	151.11	0.34	0.98	0.17	1.02	0.41	0.30	0.73
stdev	0.03	0.00	0.01	1.59	0.03	0.03	0.01	0.13	0.02	0.04	0.01
rstdev (%)	0.50	0.10	1.77	1.05	7.75	2.56	3.88	12.30	3.75	12.51	1.58
94049	23.76	29.76	0.80	68.05	1.60	4.60	0.82	4.85	2.09	0.57	3.17
94049	23.03	25.80	0.80	66.86	1.53	4.58	0.80	4.74	2.06	0.52	3.28
94049	23.06	25.48	0.78	74.92	1.58	4.72	0.81	4.82	2.08	0.58	2.96
94049	23.22	27.83	1.07	68.10	1.55	4.67	0.79	4.84	2.19	0.58	3.10
average	23.27	27.22	0.86	69.48	1.56	4.64	0.80	4.81	2.11	0.56	3.13
stdev	0.34	1.99	0.14	3.67	0.03	0.06	0.01	0.05	0.06	0.03	0.14
rstdev (%)	1.46	7.31	16.27	5.28	2.00	1.38	1.78	1.05	2.68	5.52	4.34

## Replicate IC

sample#	Tb	Dy	Ho	Er	Tm	Yb	Lu	Hf	Th
det limit	0.009	0.022	0.007	0.021	0.007	0.044	0.003	0.077	0.023
94GC03	0.15	1.17	0.25	0.76	0.12	0.81	0.14	0.24	0.12
94GC03	0.14	1.07	0.24	0.81	0.11	0.76	0.12	0.23	0.10
average	0.15	1.12	0.25	0.78	0.12	0.78	0.13	0.23	0.11
stdev	0.01	0.07	0.01	0.04	0.01	0.03	0.02	0.00	0.02
rstdev (%)	6.12	6.35	5.36	4.58	5.15	4.23	14.77	1.83	15.28
94GC04	0.47	3.28	0.70	2.12	0.33	2.18	0.35	0.98	0.28
94GC04	0.46	3.20	0.69	2.13	0.34	2.19	0.32	0.96	0.32
average	0.46	3.24	0.70	2.13	0.34	2.19	0.33	0.97	0.30
stdev	0.01	0.06	0.00	0.01	0.00	0.00	0.02	0.02	0.03
rstdev (%)	1.71	1.81	0.66	0.39	0.75	0.13	6.13	1.60	10.47
94GC06	0.51	3.41	0.77	2.23	0.31	1.89	0.29	0.15	0.02
94GC06	0.50	3.33	0.75	2.20	0.30	1.96	0.28	0.16	0.02
94GC06	0.48	3.33	0.72	2.10	0.31	1.93	0.27	0.20	0.04
94GC06	0.49	3.37	0.72	2.21	0.30	1.88	0.28	0.22	0.03
94GC06	0.49	3.18	0.75	2.19	0.29	1.93	0.29	0.18	0.04
average	0.49	3.32	0.74	2.18	0.30	1.92	0.28	0.18	0.03
stdev	0.01	0.09	0.02	0.05	0.01	0.03	0.01	0.03	0.01
rstdev (%)	2.33	2.60	2.76	2.37	3.12	1.76	2.47	15.89	41.45
94005	0.92	5.59	1.16	3.33	0.46	2.79	0.43	4.44	1.54
94005	0.87	5.35	1.07	3.11	0.44	2.81	0.38	4.01	1.46
94005	0.88	5.44	1.09	3.06	0.43	2.71	0.42	4.08	1.36
average	0.89	5.46	1.11	3.17	0.44	2.77	0.41	4.17	1.45
stdev	0.02	0.12	0.05	0.15	0.01	0.06	0.02	0.23	0.09
rstdev (%)	2.59	2.28	4.47	4.61	3.33	2.01	5.75	5.48	6.27
94018	0.64	4.64	1.01	3.12	0.50	3.33	0.52	1.93	0.86
94018	0.61	4.30	1.02	3.13	0.47	3.15	0.51	1.96	0.86
average	0.62	4.47	1.01	3.12	0.49	3.24	0.51	1.95	0.86
stdev	0.02	0.24	0.01	0.00	0.02	0.13	0.01	0.02	0.00
rstdev (%)	3.28	5.44	0.97	0.05	4.15	3.97	1.18	1.22	0.37
94035	0.97	6.14	1.21	3.51	0.49	3.22	0.52	4.62	2.91
94035	0.97	6.06	1.23	3.45	0.50	3.21	0.49	4.65	2.89
average	0.97	6.10	1.22	3.48	0.49	3.21	0.50	4.63	2.90
stdev	0.00	0.05	0.01	0.04	0.00	0.01	0.02	0.01	0.01
rstdev (%)	0.51	0.87	0.79	1.05	0.93	0.35	3.74	0.32	0.50
94041	0.13	0.93	0.22	0.70	0.11	0.75	0.11	0.18	0.04
94041	0.14	0.99	0.24	0.72	0.09	0.73	0.11	0.15	0.03
average	0.13	0.96	0.23	0.71	0.10	0.74	0.11	0.16	0.03
stdev	0.01	0.04	0.01	0.01	0.01	0.01	0.00	0.02	0.00
rstdev (%)	6.89	4.32	5.18	1.63	11.01	1.86	0.51	11.87	12.20
94049	0.60	4.08	0.96	2.87	0.42	2.69	0.39	0.88	0.25
94049	0.56	4.06	0.88	2.60	0.39	2.64	0.39	0.86	0.29
94049	0.59	4.18	0.91	2.71	0.40	2.63	0.39	0.94	0.31
94049	0.58	4.11	0.92	2.77	0.41	2.63	0.40	0.96	0.29
average	0.58	4.11	0.92	2.74	0.40	2.65	0.39	0.91	0.29
stdev	0.02	0.05	0.03	0.11	0.01	0.03	0.01	0.05	0.03
rstdev (%)	2.79	1.31	3.49	4.13	3.51	1.02	1.61	5.08	9.22

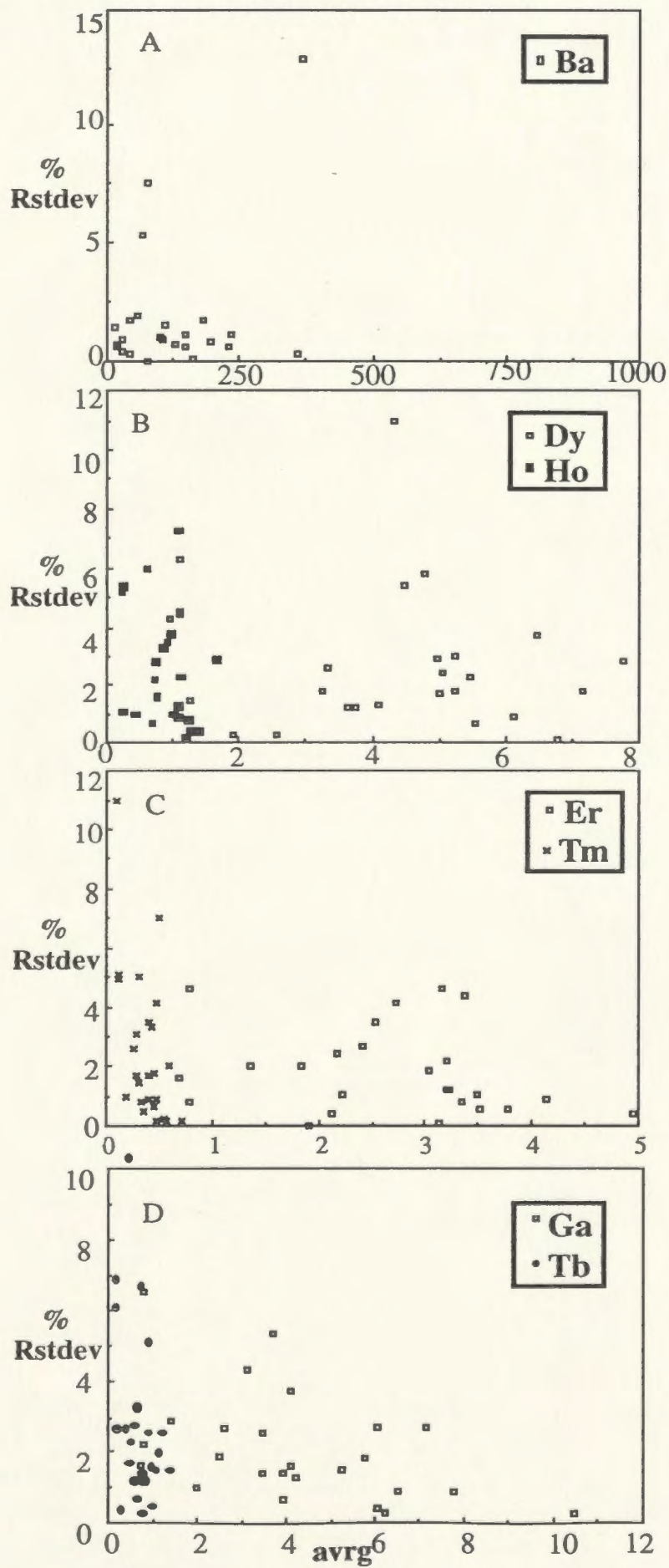
sample#	Y	Zr	Nb	Ba	La	Ce	Pr	Nd	Sm	Eu	Gd
94058	27.76	69.92	1.25	19.14	3.56	10.20	1.60	8.43	2.77	1.13	3.98
94058	27.90	68.15	1.33	18.94	3.52	10.11	1.59	8.45	3.00	1.05	4.20
average	27.83	69.04	1.29	19.04	3.54	10.16	1.59	8.44	2.89	1.09	4.09
stdev	0.10	1.25	0.05	0.14	0.02	0.06	0.01	0.01	0.17	0.06	0.15
rstdev (%)	<b>0.35</b>	<b>1.81</b>	<b>4.25</b>	<b>0.74</b>	<b>0.61</b>	<b>0.61</b>	<b>0.70</b>	<b>0.14</b>	<b>5.76</b>	<b>5.31</b>	<b>3.70</b>
94061	26.22	49.05	1.50	71.91	2.72	7.54	1.20	6.64	2.41	0.78	3.49
94061	27.88	54.55	1.11	79.00	2.71	7.65	1.23	6.84	2.64	0.78	3.81
94061	29.65	49.99	1.75	83.47	2.85	8.20	1.32	7.03	2.77	0.84	3.85
average	27.92	51.19	1.45	78.13	2.76	7.80	1.25	6.84	2.61	0.80	3.71
stdev	1.72	2.94	0.32	5.83	0.08	0.35	0.06	0.20	0.19	0.03	0.20
rstdev (%)	<b>6.15</b>	<b>5.74</b>	<b>22.06</b>	<b>7.46</b>	<b>2.95</b>	<b>4.54</b>	<b>5.07</b>	<b>2.85</b>	<b>7.12</b>	<b>4.26</b>	<b>5.32</b>
95001	21.04	104.58	6.20	58.63	10.19	23.31	2.90	12.97	3.50	1.12	3.96
95001	21.67	108.40	6.22	60.23	10.27	23.58	2.98	13.05	3.46	1.16	3.88
average	21.36	106.49	6.21	59.43	10.23	23.44	2.94	13.01	3.48	1.14	3.92
stdev	0.44	2.70	0.01	1.13	0.06	0.19	0.06	0.06	0.03	0.03	0.06
rstdev (%)	<b>2.08</b>	<b>2.54</b>	<b>0.17</b>	<b>1.91</b>	<b>0.55</b>	<b>0.82</b>	<b>1.93</b>	<b>0.45</b>	<b>0.80</b>	<b>2.37</b>	<b>1.41</b>
95100	30.93	296.59	44.53	339.88	30.36	68.52	8.75	37.50	8.10	2.49	7.73
95100	30.85	294.68	44.86	421.15	30.17	68.31	8.74	37.09	8.09	2.50	7.82
95100	31.29	286.60	40.31	338.19	30.42	68.43	8.76	37.23	8.07	2.52	7.70
average	31.03	292.62	43.23	366.41	30.31	68.42	8.75	37.27	8.09	2.50	7.75
stdev	0.23	5.30	2.54	47.42	0.13	0.11	0.01	0.21	0.02	0.02	0.07
rstdev (%)	<b>0.75</b>	<b>1.81</b>	<b>5.87</b>	<b>12.94</b>	<b>0.43</b>	<b>0.16</b>	<b>0.15</b>	<b>0.55</b>	<b>0.19</b>	<b>0.67</b>	<b>0.85</b>
95149	10.88	15.88	0.54	22.47	0.82	2.33	0.39	2.20	1.02	0.42	1.38
95149	10.89	16.15	0.50	22.67	0.84	2.35	0.39	2.19	0.95	0.41	1.44
average	10.89	16.01	0.52	22.57	0.83	2.34	0.39	2.19	0.99	0.41	1.41
stdev	0.01	0.19	0.03	0.14	0.02	0.02	0.00	0.00	0.05	0.01	0.04
rstdev (%)	<b>0.10</b>	<b>1.20</b>	<b>6.00</b>	<b>0.63</b>	<b>2.30</b>	<b>0.76</b>	<b>0.09</b>	<b>0.19</b>	<b>4.77</b>	<b>1.62</b>	<b>2.91</b>
95153	15.09	27.48	0.85	75.93	1.43	4.11	0.64	3.48	1.41	0.53	1.99
95153	14.53	28.62	0.98	75.99	1.44	4.02	0.64	3.42	1.45	0.51	1.97
average	14.81	28.05	0.91	75.96	1.44	4.06	0.64	3.45	1.43	0.52	1.98
stdev	0.40	0.81	0.09	0.04	0.00	0.06	0.00	0.04	0.03	0.02	0.02
rstdev (%)	<b>2.68</b>	<b>2.88</b>	<b>10.07</b>	<b>0.05</b>	<b>0.23</b>	<b>1.53</b>	<b>0.10</b>	<b>1.24</b>	<b>1.83</b>	<b>3.35</b>	<b>1.00</b>
95036	42.53	277.19	20.16	236.17	16.66	40.09	5.43	24.50	6.72	2.04	7.31
95036	41.65	271.23	19.49	232.57	16.68	39.47	5.43	24.09	6.39	1.94	7.03
average	42.09	274.21	19.82	234.37	16.67	39.78	5.43	24.29	6.56	1.99	7.17
stdev	0.62	4.21	0.47	2.54	0.01	0.44	0.00	0.29	0.23	0.07	0.20
rstdev (%)	<b>1.48</b>	<b>1.54</b>	<b>2.39</b>	<b>1.08</b>	<b>0.05</b>	<b>1.11</b>	<b>0.01</b>	<b>1.21</b>	<b>3.57</b>	<b>3.42</b>	<b>2.72</b>
95050	6.43	7.55	0.36	29.35	0.50	1.21	0.19	1.13	0.46	0.22	0.76
95050	6.48	8.75	0.38	28.98	0.49	1.21	0.20	1.08	0.51	0.24	0.78
average	6.45	8.15	0.37	29.16	0.49	1.21	0.19	1.10	0.48	0.23	0.77
stdev	0.04	0.85	0.01	0.26	0.01	0.00	0.01	0.04	0.04	0.01	0.02
rstdev (%)	<b>0.56</b>	<b>10.41</b>	<b>3.94</b>	<b>0.89</b>	<b>1.46</b>	<b>0.06</b>	<b>4.65</b>	<b>3.38</b>	<b>8.42</b>	<b>4.83</b>	<b>2.16</b>
95066	28.94	168.30	9.21	115.06	16.66	38.12	4.76	20.29	4.88	1.46	5.36
95066	28.92	159.13	10.12	112.05	16.30	37.76	4.69	20.25	5.07	1.44	5.21
95066	28.15	165.23	11.75	112.10	16.25	38.15	4.77	20.29	5.01	1.48	5.25
average	28.67	164.22	10.36	113.07	16.40	38.01	4.74	20.28	4.99	1.46	5.27
stdev	0.45	4.67	1.28	1.73	0.23	0.22	0.04	0.02	0.10	0.02	0.08
rstdev (%)	<b>1.59</b>	<b>2.85</b>	<b>12.40</b>	<b>1.53</b>	<b>1.37</b>	<b>0.58</b>	<b>0.94</b>	<b>0.11</b>	<b>1.96</b>	<b>1.28</b>	<b>1.48</b>

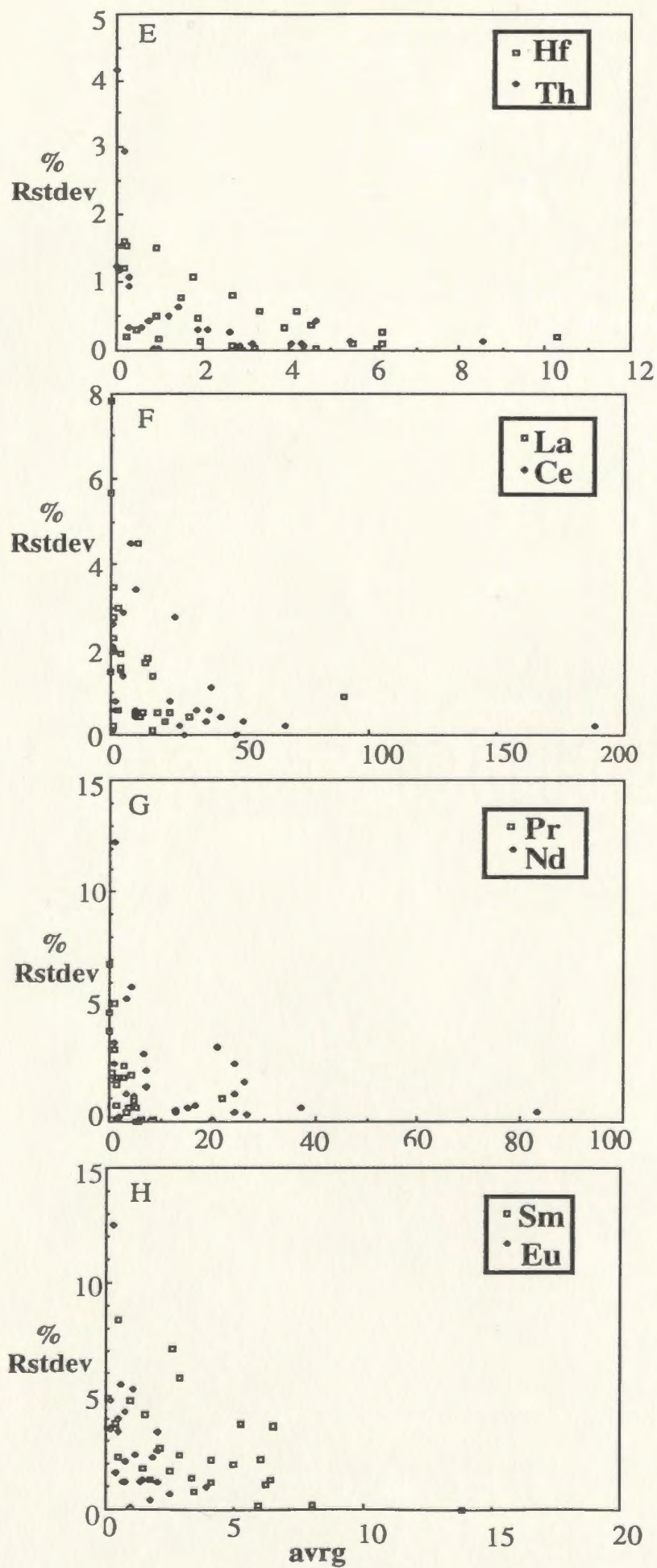
sample#	Tb	Dy	Ho	Er	Tm	Yb	Lu	Hf	Th
94058	0.73	5.08	1.10	3.19	0.49	3.25	0.48	1.98	0.57
94058	0.73	4.87	1.08	3.24	0.49	3.19	0.48	1.86	0.54
average	0.73	4.98	1.09	3.21	0.49	3.22	0.48	1.92	0.56
stdev	0.00	0.14	0.01	0.04	0.00	0.04	0.00	0.09	0.02
rstdev (%)	<b>0.31</b>	<b>2.90</b>	<b>1.30</b>	<b>1.20</b>	<b>0.21</b>	<b>1.29</b>	<b>0.79</b>	<b>4.61</b>	<b>3.45</b>
94061	0.65	4.53	1.01	3.30	0.47	3.18	0.50	1.44	0.75
94061	0.71	4.72	1.10	3.26	0.50	3.44	0.49	1.65	0.71
94061	0.75	5.08	1.17	3.54	0.54	3.69	0.57	1.45	0.77
average	0.70	4.78	1.09	3.37	0.51	3.44	0.52	1.51	0.74
stdev	0.05	0.28	0.08	0.15	0.04	0.25	0.04	0.12	0.03
rstdev (%)	<b>6.72</b>	<b>5.80</b>	<b>7.25</b>	<b>4.44</b>	<b>7.01</b>	<b>7.38</b>	<b>8.53</b>	<b>7.70</b>	<b>4.39</b>
95001	0.72	4.67	0.84	2.38	0.35	2.24	0.32	2.56	2.61
95001	0.63	4.00	0.88	2.47	0.36	2.27	0.32	2.86	2.71
average	0.68	4.33	0.86	2.43	0.35	2.25	0.32	2.71	2.66
stdev	0.07	0.48	0.03	0.06	0.00	0.02	0.00	0.21	0.07
rstdev (%)	<b>9.87</b>	<b>10.96</b>	<b>3.26</b>	<b>2.66</b>	<b>0.52</b>	<b>0.96</b>	<b>0.32</b>	<b>7.87</b>	<b>2.57</b>
95100	1.13	6.62	1.26	3.34	0.46	2.86	0.40	6.32	4.07
95100	1.12	6.62	1.24	3.35	0.45	2.80	0.42	6.30	4.07
95100	1.09	6.20	1.24	3.39	0.46	2.78	0.40	6.04	4.14
average	1.11	6.48	1.25	3.36	0.46	2.81	0.40	6.22	4.09
stdev	0.02	0.24	0.01	0.03	0.00	0.04	0.01	0.16	0.04
rstdev (%)	<b>1.96</b>	<b>3.71</b>	<b>0.81</b>	<b>0.75</b>	<b>0.71</b>	<b>1.59</b>	<b>2.60</b>	<b>2.53</b>	<b>1.04</b>
95149	0.27	1.91	0.44	1.35	0.20	1.43	0.21	0.51	0.22
95149	0.27	1.92	0.44	1.39	0.20	1.38	0.21	0.49	0.15
average	0.27	1.91	0.44	1.37	0.20	1.40	0.21	0.50	0.19
stdev	0.00	0.01	0.00	0.03	0.00	0.03	0.00	0.01	0.05
rstdev (%)	<b>0.40</b>	<b>0.35</b>	<b>1.03</b>	<b>2.00</b>	<b>1.00</b>	<b>2.48</b>	<b>1.30</b>	<b>2.89</b>	<b>29.34</b>
95153	0.38	2.59	0.64	1.88	0.29	1.95	0.31	0.85	0.28
95153	0.37	2.58	0.59	1.82	0.29	1.92	0.30	1.05	0.30
average	0.37	2.58	0.62	1.85	0.29	1.93	0.30	0.95	0.29
stdev	0.01	0.01	0.04	0.04	0.00	0.02	0.01	0.14	0.01
rstdev (%)	<b>2.66</b>	<b>0.27</b>	<b>6.04</b>	<b>2.00</b>	<b>1.68</b>	<b>1.20</b>	<b>2.30</b>	<b>14.93</b>	<b>3.27</b>
95036	1.24	7.92	1.69	4.97	0.72	4.81	0.70	6.12	2.17
95036	1.19	7.61	1.62	4.94	0.72	4.67	0.71	6.08	2.09
average	1.21	7.76	1.66	4.95	0.72	4.74	0.70	6.10	2.13
stdev	0.03	0.22	0.05	0.02	0.00	0.10	0.00	0.02	0.06
rstdev (%)	<b>2.64</b>	<b>2.83</b>	<b>2.92</b>	<b>0.42</b>	<b>0.24</b>	<b>2.09</b>	<b>0.56</b>	<b>0.39</b>	<b>2.83</b>
95050	0.17	1.24	0.25	0.79	0.12	0.80	0.12	0.24	0.07
95050	0.16	1.26	0.25	0.78	0.11	0.79	0.12	0.30	0.09
average	0.17	1.25	0.25	0.79	0.12	0.79	0.12	0.27	0.08
stdev	0.00	0.02	0.00	0.01	0.01	0.01	0.00	0.04	0.01
rstdev (%)	<b>2.72</b>	<b>1.51</b>	<b>1.09</b>	<b>0.84</b>	<b>4.94</b>	<b>1.01</b>	<b>0.21</b>	<b>15.43</b>	<b>11.72</b>
95066	0.85	5.41	1.11	3.21	0.46	3.01	0.44	3.97	4.69
95066	0.83	5.09	1.15	3.26	0.47	2.90	0.44	3.74	4.87
95066	0.83	5.26	1.10	3.18	0.45	2.93	0.44	3.95	4.47
average	0.84	5.26	1.12	3.22	0.46	2.94	0.44	3.89	4.68
stdev	0.01	0.16	0.03	0.04	0.01	0.06	0.00	0.13	0.20
rstdev (%)	<b>1.16</b>	<b>3.04</b>	<b>2.32</b>	<b>1.16</b>	<b>1.84</b>	<b>1.90</b>	<b>0.95</b>	<b>3.31</b>	<b>4.24</b>

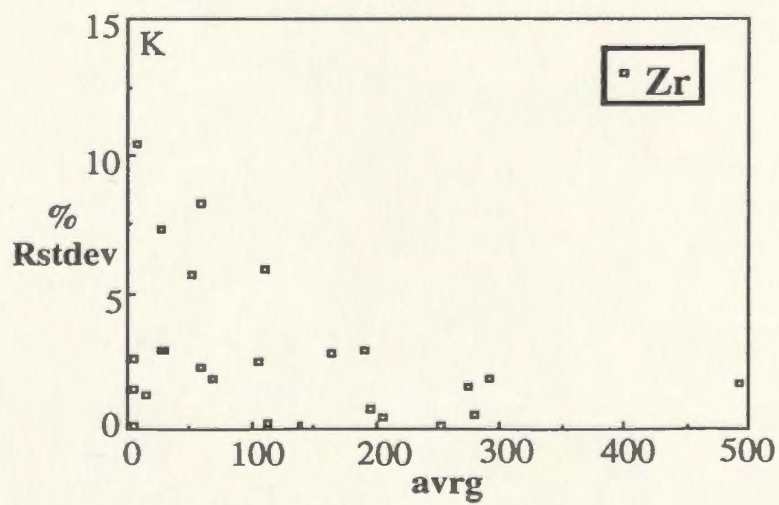
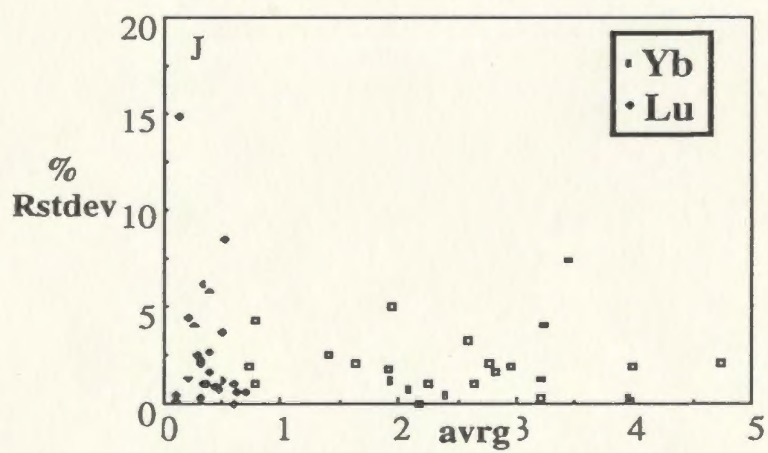
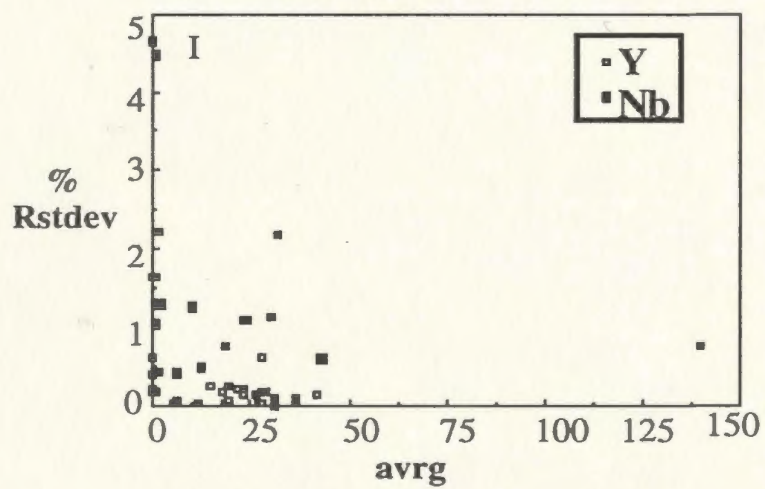
sample#	Y	Zr	Nb	Ba	La	Ce	Pr	Nd	Sm	Eu	Gd
95099	18.26	138.87	20.03	195.62	12.97	29.31	3.81	16.96	4.03	1.35	4.18
95099	18.13	139.09	18.00	193.53	13.06	29.31	3.84	16.81	4.15	1.33	4.26
average	18.19	138.98	19.01	194.57	13.01	29.31	3.83	16.88	4.09	1.34	4.22
stdev	0.09	0.15	1.43	1.48	0.06	0.00	0.02	0.11	0.09	0.02	0.06
rstdev (%)	<b>0.50</b>	<b>0.11</b>	<b>7.55</b>	<b>0.76</b>	<b>0.46</b>	<b>0.01</b>	<b>0.55</b>	<b>0.65</b>	<b>2.19</b>	<b>1.24</b>	<b>1.34</b>
96002	31.13	487.86	132.60	2230.05	91.37	188.85	22.06	83.32	13.85	3.93	10.49
96002	31.45	498.98	147.60	2128.50	90.17	188.28	21.76	82.89	13.84	3.88	10.44
average	31.29	493.42	140.10	2179.28	90.77	188.56	21.91	83.10	13.84	3.91	10.46
stdev	0.23	7.86	10.61	71.80	0.85	0.41	0.21	0.30	0.00	0.04	0.04
rstdev (%)	<b>0.73</b>	<b>1.59</b>	<b>7.57</b>	<b>3.29</b>	<b>0.94</b>	<b>0.22</b>	<b>0.96</b>	<b>0.37</b>	<b>0.02</b>	<b>0.95</b>	<b>0.34</b>
96014	36.32	278.47	36.26	100.43	23.26	51.30	6.42	27.02	6.32	1.79	6.50
96014	36.47	280.51	36.73	99.02	23.43	51.51	6.43	26.92	6.43	1.78	6.58
average	36.39	279.49	36.49	99.73	23.34	51.40	6.42	26.97	6.37	1.79	6.54
stdev	0.11	1.44	0.33	0.99	0.12	0.15	0.01	0.08	0.08	0.01	0.06
rstdev (%)	<b>0.30</b>	<b>0.51</b>	<b>0.91</b>	<b>0.99</b>	<b>0.53</b>	<b>0.30</b>	<b>0.09</b>	<b>0.28</b>	<b>1.28</b>	<b>0.41</b>	<b>0.90</b>
96037	26.84	252.53	27.98	358.31	21.35	49.33	6.25	26.22	6.16	1.75	6.02
9607	27.07	252.15	32.74	360.03	21.44	49.29	6.24	26.86	6.25	1.72	6.06
average	26.96	252.34	30.36	359.17	21.40	49.31	6.25	26.54	6.21	1.74	6.04
stdev	0.17	0.27	3.37	1.21	0.07	0.02	0.01	0.46	0.07	0.02	0.02
rstdev (%)	<b>0.63</b>	<b>0.11</b>	<b>11.10</b>	<b>0.34</b>	<b>0.31</b>	<b>0.04</b>	<b>0.13</b>	<b>1.71</b>	<b>1.07</b>	<b>1.25</b>	<b>0.40</b>
96053	19.39	111.80	6.50	46.64	11.45	25.59	3.13	12.96	3.33	1.00	3.49
96053	19.20	111.46	6.15	46.44	10.74	24.60	3.02	13.05	3.39	1.00	3.42
average	19.29	111.63	6.33	46.54	11.10	25.10	3.07	13.00	3.36	1.00	3.45
stdev	0.13	0.24	0.25	0.14	0.50	0.70	0.08	0.07	0.05	0.00	0.05
rstdev (%)	<b>0.70</b>	<b>0.21</b>	<b>3.97</b>	<b>0.30</b>	<b>4.53</b>	<b>2.79</b>	<b>2.45</b>	<b>0.53</b>	<b>1.36</b>	<b>0.11</b>	<b>1.37</b>
96065	30.98	55.04	2.16	28.87	3.73	9.35	1.43	7.51	2.90	0.74	3.91
96065	30.53	61.89	1.80	29.01	3.64	9.29	1.39	7.35	2.80	0.77	3.94
average	30.75	58.46	1.98	28.94	3.69	9.32	1.41	7.43	2.85	0.76	3.92
stdev	0.32	4.84	0.25	0.10	0.06	0.04	0.03	0.11	0.07	0.02	0.03
rstdev (%)	<b>1.05</b>	<b>8.28</b>	<b>12.78</b>	<b>0.36</b>	<b>1.60</b>	<b>0.44</b>	<b>1.92</b>	<b>1.53</b>	<b>2.43</b>	<b>2.09</b>	<b>0.66</b>
96066	26.39	105.46	37.27	231.17	11.32	26.80	3.53	15.21	4.18	0.76	4.15
96066	25.92	114.65	27.38	232.98	11.38	26.71	3.51	15.34	4.11	0.77	4.06
average	26.16	110.05	32.33	232.08	11.35	26.75	3.52	15.28	4.14	0.77	4.10
stdev	0.33	6.50	6.99	1.28	0.05	0.06	0.01	0.09	0.05	0.01	0.07
rstdev (%)	<b>1.27</b>	<b>5.91</b>	<b>21.62</b>	<b>0.55</b>	<b>0.43</b>	<b>0.23</b>	<b>0.40</b>	<b>0.56</b>	<b>1.23</b>	<b>1.20</b>	<b>1.60</b>

sample#	Tb	Dy	Ho	Er	Tm	Yb	Lu	Hf	Th
95099	0.64	3.78	0.74	1.93	0.28	1.62	0.22	3.24	1.88
95099	0.63	3.72	0.71	1.93	0.27	1.67	0.24	3.22	1.96
average	0.64	3.75	0.72	1.93	0.27	1.65	0.23	3.23	1.92
stdev	0.00	0.04	0.02	0.00	0.01	0.03	0.01	0.01	0.06
rstdev (%)	<b>0.67</b>	<b>1.15</b>	<b>2.19</b>	<b>0.04</b>	<b>2.57</b>	<b>2.03</b>	<b>4.38</b>	<b>0.36</b>	<b>2.90</b>
96002	1.38	7.25	1.27	3.15	0.40	2.39	0.33	10.38	8.64
96002	1.36	7.06	1.28	3.25	0.41	2.41	0.33	10.10	8.51
average	1.37	7.16	1.27	3.20	0.41	2.40	0.33	10.24	8.58
stdev	0.02	0.13	0.01	0.07	0.01	0.01	0.00	0.20	0.09
rstdev (%)	<b>1.48</b>	<b>1.82</b>	<b>0.44</b>	<b>2.18</b>	<b>1.74</b>	<b>0.48</b>	<b>0.98</b>	<b>1.95</b>	<b>1.06</b>
96014	1.08	6.76	1.42	4.11	0.59	3.97	0.59	6.16	5.41
96014	1.06	6.77	1.42	4.16	0.61	3.98	0.60	6.24	5.50
average	1.07	6.77	1.42	4.14	0.60	3.97	0.60	6.20	5.45
stdev	0.02	0.00	0.01	0.04	0.01	0.01	0.01	0.06	0.06
rstdev (%)	<b>1.48</b>	<b>0.07</b>	<b>0.39</b>	<b>0.89</b>	<b>1.98</b>	<b>0.20</b>	<b>1.02</b>	<b>0.90</b>	<b>1.16</b>
96037	0.93	5.52	1.08	2.99	0.41	2.53	0.36	5.47	4.27
9607	0.95	5.58	1.09	3.07	0.42	2.65	0.37	5.55	4.31
average	0.94	5.55	1.09	3.03	0.41	2.59	0.37	5.51	4.29
stdev	0.02	0.04	0.01	0.06	0.00	0.08	0.00	0.05	0.03
rstdev (%)	<b>1.64</b>	<b>0.69</b>	<b>0.95</b>	<b>1.86</b>	<b>0.95</b>	<b>3.17</b>	<b>0.98</b>	<b>0.96</b>	<b>0.81</b>
96053	0.57	3.65	0.76	2.24	0.32	2.10	0.31	2.73	3.20
96053	0.56	3.59	0.75	2.21	0.32	2.08	0.30	2.70	3.16
average	0.57	3.62	0.75	2.23	0.32	2.09	0.31	2.72	3.18
stdev	0.01	0.04	0.01	0.03	0.00	0.02	0.01	0.02	0.03
rstdev (%)	<b>1.24</b>	<b>1.19</b>	<b>1.62</b>	<b>1.13</b>	<b>1.45</b>	<b>0.77</b>	<b>2.03</b>	<b>0.60</b>	<b>1.04</b>
96065	0.75	5.33	1.21	3.80	0.57	3.96	0.59	1.68	0.96
96065	0.73	5.19	1.21	3.77	0.58	3.94	0.60	1.95	0.96
average	0.74	5.26	1.21	3.78	0.58	3.95	0.59	1.81	0.96
stdev	0.01	0.09	0.00	0.02	0.00	0.01	0.00	0.19	0.00
rstdev (%)	<b>1.43</b>	<b>1.80</b>	<b>0.19</b>	<b>0.61</b>	<b>0.22</b>	<b>0.30</b>	<b>0.04</b>	<b>10.48</b>	<b>0.26</b>
96066	0.76	5.07	1.11	3.52	0.55	4.05	0.62	3.21	4.33
96066	0.75	4.95	1.09	3.49	0.56	3.94	0.61	3.48	4.36
average	0.76	5.01	1.10	3.51	0.56	3.99	0.62	3.35	4.35
stdev	0.01	0.08	0.01	0.02	0.00	0.08	0.00	0.19	0.02
rstdev (%)	<b>1.21</b>	<b>1.70</b>	<b>1.28</b>	<b>0.58</b>	<b>0.28</b>	<b>1.89</b>	<b>0.56</b>	<b>5.69</b>	<b>0.50</b>

Plots of average versus % relative standard deviation for replicate ICP-MS analyses, showing the variation of precision with the amount of an element that is present.







**Assessment of Accuracy of XRF Major Element Data**

**Analyses of Standards**

sample	SiO <sub>2</sub>	Al <sub>2</sub> O <sub>3</sub>	TiO <sub>2</sub>	Fe <sub>2</sub> O <sub>3</sub> T	MnO	MgO	CaO	Na <sub>2</sub> O	K <sub>2</sub> O	P <sub>2</sub> O <sub>5</sub>
DL	0.02	0.05	0.01	0.01	0.00	0.02	0.01	0.04	0.01	0.01
BIR-1-G	47.77	15.60	0.97	11.44	0.17	9.64	13.17	1.16	0.04	0.03
BIR-1-G	47.65	15.56	0.94	11.43	0.18	9.64	13.19	1.07	0.04	0.02
BIR-1-G	47.64	15.47	0.93	11.43	0.16	9.59	13.13	0.94	0.04	0.02
BIR-1-G	47.64	15.43	0.95	11.48	0.17	9.63	13.21	1.04	0.04	0.03
BIR-1-G	47.60	15.49	0.96	11.51	0.17	9.73	13.26	2.00	0.04	0.03
BIR-1-G	47.56	15.52	0.95	11.48	0.17	9.69	13.09	2.02	0.04	0.03
BIR-1-G	47.67	15.40	0.96	11.50	0.17	9.65	13.15	1.99	0.04	0.03
BIR-1-G	47.77	15.58	0.95	11.47	0.17	9.63	13.11	1.98	0.04	0.03
BIR-1-G	47.50	15.35	0.94	11.54	0.17	9.53	13.17	1.99	0.04	0.03
BIR-1-G	47.56	15.43	0.96	11.43	0.17	9.67	13.01	2.04	0.03	0.03
BIR-1-G	47.18	15.30	0.93	11.48	0.17	9.54	13.16	1.98	0.04	0.03
BIR-1-G	47.77	15.60	0.97	11.44	0.17	9.64	13.17	1.16	0.04	0.03
BIR-1-G	47.65	15.56	0.94	11.43	0.18	9.64	13.19	1.07	0.04	0.02
BIR-1-G	47.64	15.47	0.93	11.43	0.16	9.59	13.13	0.94	0.04	0.02
BIR-1-G	47.64	15.43	0.95	11.48	0.17	9.63	13.21	1.04	0.04	0.03
BIR-1-G	47.56	15.52	0.95	11.48	0.17	9.69	13.09	2.02	0.04	0.03
BIR-1-G	47.67	15.40	0.96	11.50	0.17	9.65	13.15	1.99	0.04	0.03
BIR-1-G	38.26	10.40	0.96	12.05	0.18	6.93	12.89	0.85	0.04	0.03
BIR-1-G	47.77	15.58	0.95	11.47	0.17	9.63	13.11	1.98	0.04	0.03
BIR-1-G	47.50	15.35	0.94	11.54	0.17	9.53	13.17	1.99	0.04	0.03
BIR-1-G	47.56	15.43	0.96	11.43	0.17	9.67	13.01	2.04	0.03	0.03
BIR-1-G	47.18	15.30	0.93	11.48	0.17	9.54	13.16	1.98	0.04	0.03
BIR-1-G	47.84	15.56	0.95	11.48	0.17	9.68	13.22	2.22	0.04	0.03
BIR-1-G	47.72	15.33	0.98	11.54	0.17	9.65	13.24	2.17	0.04	0.03
BIR-1-G	47.73	15.50	0.93	11.52	0.17	9.67	13.27	2.15	0.05	0.03
BIR-1-G	47.77	15.50	0.95	11.51	0.17	9.71	13.26	2.20	0.04	0.03
BIR-1-G	47.90	15.57	0.97	11.52	0.17	9.70	13.19	2.13	0.04	0.03
BIR-1-G	47.78	15.59	0.95	11.55	0.17	9.66	13.19	2.15	0.04	0.03
BIR-1-G	47.61	15.52	0.95	11.50	0.17	9.65	13.12	2.17	0.04	0.03
BIR-1-G	47.74	15.54	0.94	11.52	0.17	9.68	13.18	2.14	0.04	0.03
BIR-1-G	47.72	15.51	0.95	11.47	0.17	9.69	13.10	2.27	0.04	0.03
BIR-1-G	47.61	15.46	0.95	11.47	0.17	9.64	13.17	2.25	0.04	0.03
BIR-1-G	47.59	15.43	0.93	11.49	0.17	9.71	13.24	2.20	0.04	0.04
BIR-1-G	47.70	15.38	0.94	11.51	0.17	9.70	13.17	2.23	0.04	0.03
BIR-1-G	47.85	15.38	0.95	11.49	0.17	9.71	13.15	2.26	0.05	0.03
BIR-1-G	47.80	15.47	0.97	11.49	0.17	9.67	13.21	2.25	0.04	0.03
BIR-1-G	47.60	15.38	0.97	11.53	0.17	9.65	13.28	2.23	0.04	0.03
BIR-1-G	47.81	15.60	0.96	11.47	0.17	9.66	13.13	2.20	0.04	0.03
BIR-1-G	47.74	15.52	0.96	11.47	0.17	9.71	13.15	2.20	0.04	0.03
BIR-1-G	47.75	15.48	0.94	11.49	0.17	9.68	13.15	2.18	0.04	0.03
BIR-1-G	47.86	15.45	0.95	11.52	0.17	9.66	13.16	2.27	0.04	0.04
BIR-1-G	47.80	15.42	0.94	11.52	0.17	9.70	13.10	2.24	0.04	0.03
BIR-1-G	47.74	15.37	0.95	11.49	0.17	9.72	13.24	2.25	0.04	0.03
BIR-1-G	47.50	15.36	0.97	11.52	0.17	9.65	13.09	2.26	0.04	0.03
BIR-1-G	47.76	15.40	0.95	11.48	0.17	9.69	13.17	2.24	0.04	0.03
BIR-1-G	47.80	15.50	0.97	11.45	0.17	9.66	13.21	2.23	0.05	0.03
BIR-1-G	47.60	15.53	0.97	11.52	0.17	9.65	13.11	2.24	0.04	0.03
BIR-1-G	47.69	15.43	0.94	11.50	0.17	9.70	13.12	2.20	0.04	0.04
BIR-1-G	47.47	15.41	0.94	11.51	0.17	9.64	13.16	2.22	0.04	0.04
BIR-1-G	47.44	15.28	0.94	11.50	0.17	9.66	13.16	2.26	0.04	0.03
BIR-1-G	47.76	15.51	0.95	11.48	0.17	9.66	13.19	2.29	0.04	0.04
BIR-1-G	47.79	15.50	0.95	11.44	0.17	9.68	13.17	2.28	0.04	0.03
BIR-1-G	47.85	15.53	0.93	11.48	0.17	9.64	13.21	2.24	0.04	0.03
BIR-1-G	47.58	15.49	0.94	11.46	0.17	9.64	13.12	2.26	0.04	0.03

sample	SiO <sub>2</sub>	Al <sub>2</sub> O <sub>3</sub>	TiO <sub>2</sub>	Fe <sub>2</sub> O <sub>3</sub> T	MnO	MgO	CaO	Na <sub>2</sub> O	K <sub>2</sub> O	P <sub>2</sub> O <sub>5</sub>
BIR-1-G	47.65	15.51	0.94	11.49	0.17	9.68	13.13	2.26	0.04	0.03
BIR-1-G	47.74	15.53	0.94	11.45	0.17	9.64	13.20	2.26	0.04	0.03
BIR-1-G	47.37	15.32	0.96	11.50	0.17	9.63	13.20	2.20	0.04	0.03
BIR-1-G	47.53	15.48	0.96	11.50	0.17	9.62	13.11	2.20	0.04	0.03
BIR-1-G	47.61	15.43	0.95	11.49	0.17	9.64	13.08	2.24	0.04	0.03
BIR-1-G	47.53	15.50	0.95	11.49	0.17	9.59	13.11	2.27	0.04	0.03
BIR-1-G	47.74	15.50	0.95	11.51	0.17	9.66	13.19	2.22	0.04	0.03
BIR-1-G	47.98	15.53	0.95	11.49	0.17	9.68	13.15	2.26	0.04	0.03
BIR-1-G	47.80	15.47	0.94	11.46	0.17	9.69	13.13	2.23	0.04	0.03
BIR-1-G	47.58	15.36	0.96	11.52	0.17	9.62	13.15	2.26	0.04	0.03
average	47.52	15.39	0.95	11.50	0.17	9.61	13.16	2.01	0.04	0.03
stdev	1.18	0.64	0.01	0.08	0.00	0.34	0.06	0.41	0.00	0.00
acpctd	47.49	15.26	0.95	11.19	0.17	9.62	13.16	1.74	0.03	0.05
JB-1A-G	53.30	14.81	1.30	9.16	0.14	7.89	9.37	2.68	1.42	0.24
JB-1A-G	53.18	14.75	1.29	9.17	0.15	7.91	9.37	2.50	1.42	0.26
JB-1A-G	53.05	14.68	1.28	9.14	0.15	7.92	9.38	2.64	1.44	0.25
JB-1A-G	53.17	14.67	1.29	9.10	0.15	7.92	9.33	2.95	1.45	0.25
JB-1A-G	53.24	14.84	1.31	9.19	0.15	7.91	9.41	3.26	1.43	0.25
JB-1A-G	53.29	14.70	1.29	9.16	0.14	7.94	9.39	3.28	1.44	0.27
JB-1A-G	52.95	14.65	1.29	9.25	0.15	7.87	9.36	3.21	1.46	0.25
JB-1A-G	53.25	14.80	1.28	9.16	0.14	7.91	9.35	3.24	1.42	0.26
JB-1A-G	53.09	14.79	1.30	9.14	0.15	7.88	9.37	3.31	1.42	0.25
JB-1A-G	53.28	14.73	1.30	9.19	0.15	7.89	9.35	3.19	1.42	0.26
JB-1A-G	53.10	14.75	1.28	9.18	0.15	7.89	9.35	3.20	1.43	0.27
JB-1A-G	53.12	14.62	1.30	9.14	0.15	7.92	9.26	3.22	1.43	0.26
JB-1A-G	53.30	14.81	1.30	9.16	0.14	7.89	9.37	2.68	1.42	0.24
JB-1A-G	53.18	14.75	1.29	9.17	0.15	7.91	9.37	2.50	1.42	0.26
JB-1A-G	53.05	14.68	1.28	9.14	0.15	7.92	9.38	2.64	1.44	0.25
JB-1A-G	53.17	14.67	1.29	9.10	0.15	7.92	9.33	2.95	1.45	0.25
JB-1A-G	53.24	14.84	1.31	9.19	0.15	7.91	9.41	3.26	1.43	0.25
JB-1A-G	53.29	14.70	1.29	9.16	0.14	7.94	9.39	3.28	1.44	0.27
JB-1A-G	52.95	14.65	1.29	9.25	0.15	7.87	9.36	3.21	1.46	0.25
JB-1A-G	53.25	14.80	1.28	9.16	0.14	7.91	9.35	3.24	1.42	0.26
JB-1A-G	53.09	14.79	1.30	9.14	0.15	7.88	9.37	3.31	1.42	0.25
JB-1A-G	53.28	14.73	1.30	9.19	0.15	7.89	9.35	3.19	1.42	0.26
JB-1A-G	53.10	14.75	1.28	9.18	0.15	7.89	9.35	3.20	1.43	0.27
JB-1A-G	53.12	14.62	1.30	9.14	0.15	7.92	9.26	3.22	1.43	0.26
JB-1A-G	52.95	14.61	1.29	9.24	0.15	7.83	9.42	3.26	1.45	0.26
JB-1A-G	53.13	14.64	1.29	9.18	0.15	7.85	9.34	3.31	1.42	0.25
JB-1A-G	53.14	14.55	1.29	9.19	0.15	7.88	9.46	3.32	1.42	0.26
JB-1A-G	53.10	14.60	1.30	9.19	0.15	7.88	9.43	3.37	1.42	0.27
JB-1A-G	53.32	14.77	1.30	9.21	0.14	7.84	9.36	3.30	1.44	0.27
JB-1A-G	53.07	14.71	1.28	9.22	0.14	7.85	9.36	3.23	1.40	0.26
JB-1A-G	53.06	14.62	1.31	9.21	0.14	7.86	9.32	3.27	1.40	0.25
JB-1A-G	52.89	14.66	1.27	9.22	0.15	7.85	9.38	3.27	1.43	0.25
JB-1A-G	53.03	14.63	1.28	9.15	0.14	7.90	9.31	3.34	1.43	0.26
JB-1A-G	53.13	14.66	1.29	9.16	0.15	7.90	9.28	3.33	1.42	0.25
JB-1A-G	53.04	14.71	1.27	9.15	0.15	7.91	9.32	3.33	1.45	0.25
JB-1A-G	52.93	14.57	1.28	9.14	0.14	7.88	9.33	3.38	1.41	0.26
JB-1A-G	53.02	14.66	1.30	9.19	0.14	7.87	9.39	3.31	1.43	0.26
JB-1A-G	53.19	14.60	1.28	9.16	0.14	7.91	9.35	3.31	1.43	0.26
JB-1A-G	53.11	14.66	1.30	9.19	0.14	7.86	9.32	3.35	1.43	0.26
JB-1A-G	52.82	14.56	1.29	9.21	0.15	7.89	9.34	3.25	1.42	0.25
JB-1A-G	53.32	14.78	1.29	9.15	0.15	7.85	9.31	3.32	1.42	0.25
JB-1A-G	53.29	14.65	1.27	9.18	0.15	7.90	9.33	3.34	1.41	0.26

sample	SiO <sub>2</sub>	Al <sub>2</sub> O <sub>3</sub>	TiO <sub>2</sub>	Fe <sub>2</sub> O <sub>3</sub> T	MnO	MgO	CaO	Na <sub>2</sub> O	K <sub>2</sub> O	P <sub>2</sub> O <sub>5</sub>
JB-1A-G	53.26	14.60	1.29	9.14	0.15	7.89	9.30	3.38	1.40	0.26
JB-1A-G	53.04	14.65	1.28	9.16	0.15	7.87	9.32	3.31	1.41	0.25
JB-1A-G	53.17	14.63	1.29	9.17	0.15	7.83	9.39	3.32	1.40	0.27
JB-1A-G	53.09	14.71	1.26	9.19	0.15	7.93	9.30	3.29	1.46	0.26
JB-1A-G	53.02	14.63	1.29	9.21	0.14	7.90	9.34	3.32	1.42	0.25
JB-1A-G	53.05	14.60	1.27	9.15	0.15	7.86	9.34	3.43	1.43	0.25
JB-1A-G	53.00	14.72	1.28	9.19	0.15	7.85	9.32	3.35	1.42	0.26
JB-1A-G	53.13	14.76	1.29	9.17	0.14	7.90	9.33	3.37	1.42	0.25
JB-1A-G	52.99	14.66	1.27	9.18	0.14	7.87	9.35	3.38	1.44	0.25
JB-1A-G	53.01	14.64	1.30	9.18	0.15	7.90	9.36	3.32	1.41	0.27
JB-1A-G	52.99	14.48	1.27	9.15	0.15	7.84	9.32	3.29	1.40	0.25
JB-1A-G	52.83	14.56	1.26	9.15	0.15	7.89	9.27	3.38	1.43	0.25
JB-1A-G	53.06	14.63	1.27	9.19	0.14	7.94	9.30	3.37	1.43	0.26
JB-1A-G	53.17	14.68	1.28	9.17	0.14	7.92	9.28	3.39	1.41	0.26
JB-1A-G	53.26	14.77	1.26	9.14	0.15	7.87	9.29	3.40	1.44	0.26
JB-1A-G	53.02	14.60	1.28	9.18	0.15	7.83	9.35	3.35	1.41	0.26
JB-1A-G	52.95	14.69	1.28	9.20	0.15	7.86	9.25	3.35	1.45	0.25
JB-1A-G	53.00	14.77	1.29	9.18	0.14	7.88	9.40	3.30	1.44	0.26
JB-1A-G	53.16	14.70	1.27	9.17	0.14	7.83	9.34	3.28	1.43	0.26
JB-1A-G	52.80	14.60	1.29	9.18	0.14	7.90	9.38	3.32	1.45	0.26
JB-1A-G	52.80	14.67	1.26	9.20	0.15	7.83	9.37	3.32	1.45	0.27
JB-1A-G	53.05	14.64	1.30	9.21	0.15	7.85	9.37	3.32	1.43	0.26
JB-1A-G	53.13	14.69	1.28	9.16	0.15	7.89	9.37	3.32	1.44	0.25
JB-1A-G	52.90	14.73	1.27	9.17	0.15	7.89	9.32	3.34	1.42	0.27
JB-1A-G	53.15	14.63	1.28	9.17	0.15	7.87	9.35	3.24	1.42	0.26
JB-1A-G	53.24	14.65	1.27	9.16	0.15	7.85	9.37	3.35	1.43	0.25
JB-1A-G	53.08	14.63	1.29	9.17	0.14	7.83	9.39	3.32	1.42	0.25
JB-1A-G	53.10	14.58	1.29	9.18	0.15	7.87	9.31	3.34	1.42	0.26
average	53.10	14.68	1.29	9.17	0.15	7.88	9.35	3.23	1.43	0.26
stdev	0.13	0.08	0.01	0.03	0.00	0.03	0.04	0.21	0.01	0.01
acptd	<b>52.81</b>	<b>14.69</b>	<b>1.32</b>	<b>9.21</b>	<b>0.15</b>	<b>7.85</b>	<b>9.34</b>	<b>2.77</b>	<b>1.44</b>	<b>0.26</b>
JG-1A-G	71.68	14.12	0.24	2.04	0.06	0.71	2.19	3.75	4.11	0.08
JG-1A-G	71.39	13.99	0.25	2.07	0.06	0.72	2.16	3.65	4.06	0.08
JG-1A-G	71.29	14.03	0.25	2.06	0.06	0.71	2.13	3.66	4.08	0.09
JG-1A-G	71.44	14.04	0.24	2.05	0.06	0.72	2.17	3.59	4.07	0.08
JG-1A-G	71.43	14.09	0.24	2.06	0.06	0.73	2.17	3.69	4.01	0.08
JG-1A-G	71.68	14.12	0.24	2.04	0.06	0.71	2.19	3.75	4.11	0.08
JG-1A-G	71.39	13.99	0.25	2.07	0.06	0.72	2.16	3.65	4.06	0.08
JG-1A-G	71.29	14.03	0.25	2.06	0.06	0.71	2.13	3.66	4.08	0.09
JG-1A-G	71.49	14.15	0.24	2.05	0.06	0.70	2.14	3.69	4.00	0.08
JG-1A-G	71.48	14.03	0.24	2.06	0.06	0.71	2.12	3.63	4.03	0.08
JG-1A-G	71.49	14.03	0.24	2.06	0.06	0.72	2.16	3.68	3.98	0.09
JG-1A-G	71.49	14.07	0.24	2.08	0.06	0.73	2.15	3.65	4.09	0.08
JG-1A-G	71.35	14.08	0.25	2.06	0.06	0.71	2.14	3.73	4.04	0.08
JG-1A-G	71.20	13.99	0.23	2.06	0.06	0.74	2.15	3.70	4.01	0.09
JG-1A-G	71.74	14.07	0.25	2.05	0.06	0.72	2.14	3.65	3.95	0.09
JG-1A-G	71.42	14.05	0.25	2.05	0.06	0.70	2.10	3.66	3.98	0.08
JG-1A-G	71.36	14.02	0.23	2.05	0.06	0.72	2.11	3.62	4.01	0.08
JG-1A-G	71.64	14.01	0.23	2.06	0.06	0.72	2.15	3.65	4.03	0.08
average	71.46	14.05	0.24	2.06	0.06	0.72	2.15	3.67	4.04	0.08
stdev	0.15	0.05	0.01	0.01	0.00	0.01	0.02	0.04	0.05	0.00
acptd	<b>72.68</b>	<b>14.32</b>	<b>0.25</b>	<b>2.06</b>	<b>0.06</b>	<b>0.69</b>	<b>2.14</b>	<b>3.43</b>	<b>4.04</b>	<b>0.08</b>
JG-2-G	76.70	12.51	0.05	0.98	0.02	0.06	0.73	3.52	4.98	0.01
JG-2-G	76.24	12.43	0.04	0.98	0.02	0.06	0.71	3.63	4.87	0.02
JG-2-G	76.17	12.35	0.05	0.99	0.02	0.03	0.70	3.64	4.85	0.02

sample	SiO <sub>2</sub>	Al <sub>2</sub> O <sub>3</sub>	TiO <sub>2</sub>	Fe <sub>2</sub> O <sub>3</sub> T	MnO	MgO	CaO	Na <sub>2</sub> O	K <sub>2</sub> O	P <sub>2</sub> O <sub>5</sub>
JG-2-G	76.70	12.51	0.05	0.98	0.02	0.06	0.73	3.52	4.98	0.01
JG-2-G	76.24	12.43	0.04	0.98	0.02	0.06	0.71	3.63	4.87	0.02
JG-2-G	76.17	12.35	0.05	0.99	0.02	0.03	0.70	3.64	4.85	0.02
JG-2-G	76.01	12.32	0.04	0.99	0.02	0.08	0.71	3.58	4.83	0.01
JG-2-G	76.23	12.39	0.05	0.99	0.02	0.07	0.70	3.60	4.79	0.01
JG-2-G	76.53	12.40	0.05	0.97	0.02	0.08	0.70	3.63	4.78	0.02
JG-2-G	76.25	12.40	0.04	0.98	0.02	0.07	0.70	3.63	4.76	0.00
JG-2-G	76.15	12.41	0.04	0.98	0.02	0.07	0.69	3.66	4.74	0.01
JG-2-G	76.30	12.45	0.05	0.98	0.02	0.07	0.71	3.63	4.77	0.02
JG-2-G	76.21	12.48	0.04	0.97	0.02	0.07	0.69	3.62	4.79	0.02
JG-2-G	76.37	12.51	0.05	0.97	0.02	0.06	0.71	3.62	4.80	0.01
JG-2-G	76.33	12.43	0.04	0.98	0.02	0.05	0.71	3.62	4.80	0.02
JG-2-G	75.93	12.34	0.05	0.97	0.01	0.06	0.71	3.61	4.80	0.01
JG-2-G	76.26	12.34	0.04	0.97	0.02	0.06	0.69	3.62	4.77	0.02
average	76.28	12.41	0.04	0.98	0.02	0.06	0.71	3.61	4.83	0.01
stdev	0.20	0.06	0.00	0.01	0.00	0.01	0.01	0.04	0.07	0.00
acptd	77.20	12.45	0.04	0.92	0.02	0.04	0.80	3.56	4.74	0.00
JP-1-G	43.39	0.62	0.00	8.86	0.13	45.88	0.57	BD	0.01	0.01
JP-1-G	43.73	0.56	0.00	8.77	0.12	46.22	0.58	0.20	0.01	0.01
JP-1-G	43.54	0.57	0.00	8.82	0.12	46.59	0.59	0.18	0.01	0.01
JP-1-G	43.39	0.62	0.00	8.86	0.13	45.88	0.57	BD	0.01	0.01
JP-1-G	43.73	0.56	0.00	8.77	0.12	46.22	0.58	0.20	0.01	0.01
JP-1-G	43.54	0.57	0.00	8.82	0.12	46.59	0.59	0.18	0.01	0.01
JP-1-G	43.53	0.59	0.00	8.82	0.12	46.35	0.57	0.47	0.01	0.01
JP-1-G	43.57	0.58	0.00	8.85	0.12	46.52	0.58	0.42	0.02	0.01
JP-1-G	43.57	0.64	0.00	8.84	0.12	46.61	0.58	0.51	0.01	0.01
JP-1-G	43.50	0.67	0.00	8.85	0.12	46.45	0.60	0.53	0.01	0.01
JP-1-G	43.72	0.59	0.00	8.84	0.12	46.61	0.57	0.46	0.01	0.01
JP-1-G	43.57	0.60	0.01	8.88	0.12	46.59	0.58	0.48	0.01	0.00
JP-1-G	43.43	0.65	0.00	8.83	0.13	46.54	0.59	0.45	0.02	0.01
JP-1-G	43.50	0.62	0.00	8.85	0.12	46.59	0.57	0.53	0.02	0.01
JP-1-G	43.62	0.61	0.01	8.84	0.12	46.56	0.57	0.49	0.01	0.01
JP-1-G	43.44	0.65	0.00	8.86	0.12	46.38	0.58	0.48	0.01	0.01
JP-1-G	43.65	0.64	0.01	8.87	0.12	46.58	0.55	0.52	0.01	0.01
average	43.55	0.61	0.00	8.84	0.12	46.42	0.58	0.41	0.01	0.01
stdev	0.11	0.03	0.00	0.03	0.00	0.24	0.01	0.14	0.00	0.00
acptd	43.50	0.64	0.00	8.56	0.12	45.89	0.57	0.02	0.00	0.00
MRG-1-G	39.76	8.49	3.83	18.26	0.17	13.78	14.90	BD	0.19	0.07
MRG-1-G	39.67	8.48	3.84	18.23	0.17	13.74	14.96	BD	0.19	0.07
MRG-1-G	39.73	8.48	3.81	18.16	0.17	13.73	14.95	BD	0.19	0.07
MRG-1-G	39.67	8.46	3.84	18.20	0.17	13.79	14.95	BD	0.18	0.07
MRG-1-G	39.75	8.46	3.85	18.19	0.17	13.77	14.89	0.91	0.20	0.07
MRG-1-G	39.69	8.43	3.81	18.20	0.17	13.81	15.06	0.90	0.19	0.08
MRG-1-G	39.49	8.43	3.85	18.21	0.17	13.76	14.89	0.90	0.18	0.07
MRG-1-G	39.47	8.40	3.82	18.24	0.18	13.71	14.91	0.90	0.20	0.06
MRG-1-G	39.66	8.45	3.82	18.20	0.18	13.76	15.01	0.93	0.19	0.07
MRG-1-G	39.62	8.40	3.85	18.20	0.17	13.75	14.89	0.91	0.19	0.08
MRG-1-G	39.69	8.40	3.81	18.22	0.18	13.81	14.97	0.85	0.19	0.07
MRG-1-G	39.41	8.36	3.84	18.22	0.17	13.72	14.89	0.89	0.20	0.07
MRG-1-G	39.76	8.49	3.83	18.26	0.17	13.78	14.90	BD	0.19	0.07
MRG-1-G	39.67	8.48	3.84	18.23	0.17	13.74	14.96	BD	0.19	0.07
MRG-1-G	39.73	8.48	3.81	18.16	0.17	13.73	14.95	BD	0.19	0.07
MRG-1-G	39.67	8.46	3.84	18.20	0.17	13.79	14.95	BD	0.18	0.07
MRG-1-G	39.75	8.46	3.85	18.19	0.17	13.77	14.89	0.91	0.20	0.07
MRG-1-G	39.69	8.43	3.81	18.20	0.17	13.81	15.06	0.90	0.19	0.08

sample	SiO <sub>2</sub>	Al <sub>2</sub> O <sub>3</sub>	TiO <sub>2</sub>	Fe <sub>2</sub> O <sub>3</sub> T	MnO	MgO	CaO	Na <sub>2</sub> O	K <sub>2</sub> O	P <sub>2</sub> O <sub>5</sub>
MRG-1-G	39.49	8.43	3.85	18.21	0.17	13.76	14.89	0.90	0.18	0.07
MRG-1-G	39.47	8.40	3.82	18.24	0.18	13.71	14.91	0.90	0.20	0.06
MRG-1-G	39.66	8.45	3.82	18.20	0.18	13.76	15.01	0.93	0.19	0.07
MRG-1-G	39.62	8.40	3.85	18.20	0.17	13.75	14.89	0.91	0.19	0.08
MRG-1-G	39.69	8.40	3.81	18.22	0.18	13.81	14.97	0.85	0.19	0.07
MRG-1-G	39.41	8.36	3.84	18.22	0.17	13.72	14.89	0.89	0.20	0.07
MRG-1-G	39.86	8.45	3.86	18.25	0.17	13.79	14.97	1.10	0.20	0.07
MRG-1-G	39.74	8.45	3.81	18.19	0.17	13.75	14.97	1.15	0.18	0.07
MRG-1-G	39.78	8.43	3.82	18.21	0.17	13.78	14.92	1.15	0.19	0.07
MRG-1-G	39.69	8.42	3.83	18.19	0.17	13.72	14.90	1.13	0.19	0.07
MRG-1-G	39.83	8.48	3.79	18.24	0.18	13.73	14.93	1.18	0.19	0.08
MRG-1-G	39.88	8.52	3.85	18.21	0.17	13.79	14.97	1.14	0.19	0.07
MRG-1-G	39.91	8.47	3.82	18.16	0.17	13.75	14.93	1.15	0.19	0.07
MRG-1-G	39.76	8.44	3.86	18.23	0.17	13.77	14.93	1.17	0.19	0.07
MRG-1-G	39.66	8.47	3.83	18.21	0.17	13.76	14.94	1.17	0.19	0.08
MRG-1-G	39.74	8.52	3.85	18.23	0.17	13.78	14.98	1.17	0.18	0.08
MRG-1-G	39.63	8.43	3.82	18.23	0.17	13.71	14.95	1.13	0.20	0.08
MRG-1-G	39.58	8.43	3.82	18.17	0.17	13.79	14.90	1.21	0.19	0.08
MRG-1-G	39.72	8.50	3.87	18.17	0.17	13.73	14.95	1.24	0.19	0.08
MRG-1-G	39.68	8.43	3.83	18.23	0.17	13.78	14.91	1.24	0.18	0.07
MRG-1-G	39.62	8.44	3.82	18.24	0.18	13.77	15.00	1.20	0.20	0.08
MRG-1-G	39.61	8.40	3.79	18.20	0.17	13.76	14.91	1.17	0.19	0.08
MRG-1-G	39.86	8.48	3.85	18.29	0.17	13.76	15.00	1.16	0.19	0.07
MRG-1-G	39.77	8.40	3.80	18.20	0.17	13.76	14.94	1.21	0.19	0.07
MRG-1-G	39.76	8.41	3.82	18.16	0.17	13.77	14.94	1.19	0.19	0.07
MRG-1-G	39.76	8.39	3.85	18.20	0.17	13.75	14.89	1.15	0.19	0.07
MRG-1-G	39.76	8.47	3.84	18.15	0.17	13.77	14.90	1.22	0.19	0.07
MRG-1-G	39.70	8.39	3.80	18.26	0.17	13.75	15.00	1.19	0.19	0.07
MRG-1-G	39.86	8.49	3.85	18.23	0.17	13.76	14.95	1.20	0.19	0.07
MRG-1-G	39.69	8.45	3.82	18.20	0.17	13.76	14.91	1.20	0.18	0.08
MRG-1-G	39.71	8.43	3.85	18.23	0.18	13.74	14.93	1.18	0.20	0.08
MRG-1-G	39.81	8.47	3.82	18.18	0.18	13.76	14.98	1.20	0.18	0.07
MRG-1-G	39.70	8.40	3.82	18.17	0.17	13.77	14.88	1.17	0.19	0.08
MRG-1-G	39.73	8.49	3.83	18.25	0.17	13.77	14.98	1.19	0.19	0.08
MRG-1-G	39.61	8.35	3.81	18.20	0.17	13.67	14.94	1.21	0.18	0.08
MRG-1-G	39.54	8.42	3.89	18.19	0.17	13.78	14.91	1.22	0.18	0.08
MRG-1-G	39.64	8.51	3.85	18.18	0.17	13.76	14.89	1.24	0.18	0.08
MRG-1-G	39.74	8.50	3.82	18.23	0.18	13.77	14.96	1.24	0.19	0.08
MRG-1-G	39.74	8.46	3.80	18.20	0.17	13.76	14.99	1.25	0.18	0.07
MRG-1-G	39.53	8.41	3.86	18.24	0.17	13.75	14.92	1.24	0.20	0.07
MRG-1-G	39.80	8.45	3.84	18.23	0.17	13.75	14.96	1.16	0.19	0.08
MRG-1-G	39.74	8.47	3.82	18.22	0.17	13.80	14.97	1.20	0.18	0.07
MRG-1-G	39.69	8.41	3.82	18.20	0.17	13.69	14.92	1.17	0.20	0.07
MRG-1-G	39.39	8.41	3.85	18.19	0.18	13.80	14.91	1.16	0.18	0.08
MRG-1-G	39.64	8.45	3.83	18.27	0.17	13.70	14.98	1.14	0.20	0.08
MRG-1-G	39.68	8.45	3.83	18.20	0.17	13.74	14.94	1.15	0.20	0.08
MRG-1-G	39.67	8.44	3.80	18.21	0.17	13.81	14.97	1.20	0.18	0.08
MRG-1-G	39.73	8.48	3.85	18.17	0.17	13.79	14.88	1.19	0.20	0.08
MRG-1-G	39.71	8.42	3.83	18.21	0.17	13.76	14.93	1.12	0.17	0.08
MRG-1-G	39.76	8.45	3.86	18.22	0.17	13.79	14.95	1.18	0.18	0.07
MRG-1-G	39.83	8.44	3.82	18.21	0.17	13.74	14.91	1.22	0.19	0.07
MRG-1-G	39.51	8.39	3.81	18.20	0.17	13.74	14.97	1.25	0.18	0.07
average	39.69	8.44	3.83	18.21	0.17	13.76	14.94	1.11	0.19	0.07
stdev	0.11	0.04	0.02	0.03	0.00	0.03	0.04	0.13	0.01	0.00
accptd	39.71	8.59	3.83	18.21	0.17	13.76	14.94	0.75	0.18	0.08

sample	SiO <sub>2</sub>	Al <sub>2</sub> O <sub>3</sub>	TiO <sub>2</sub>	Fe <sub>2</sub> O <sub>3</sub> T	MnO	MgO	CaO	Na <sub>2</sub> O	K <sub>2</sub> O	P <sub>2</sub> O <sub>5</sub>
SY-2-G	60.92	12.30	0.14	6.39	0.31	2.68	7.96	4.35	4.53	0.42
SY-2-G	60.64	12.11	0.13	6.42	0.32	2.66	8.01	4.46	4.47	0.45
SY-2-G	60.11	11.95	0.14	6.42	0.33	2.65	7.92	4.35	4.42	0.43
SY-2-G	60.75	12.16	0.14	6.47	0.32	2.68	8.08	4.33	4.46	0.42
SY-2-G	60.83	12.14	0.14	6.49	0.32	2.68	8.05	4.33	4.51	0.43
SY-2-G	60.56	12.23	0.13	6.48	0.32	2.67	7.98	4.42	4.49	0.44
SY-2-G	60.69	12.15	0.14	6.47	0.32	2.67	8.06	4.35	4.50	0.43
SY-2-G	60.79	12.14	0.14	6.48	0.32	2.64	8.04	4.31	4.45	0.43
SY-2-G	60.71	12.19	0.14	6.45	0.32	2.69	7.99	4.39	4.52	0.42
SY-2-G	60.59	12.21	0.14	6.46	0.32	2.66	7.98	4.35	4.46	0.44
SY-2-G	60.74	12.14	0.14	6.47	0.32	2.67	8.02	4.39	4.54	0.43
SY-2-G	61.17	12.32	0.14	6.43	0.32	2.67	8.12	4.28	4.53	0.42
SY-2-G	60.92	12.30	0.14	6.39	0.31	2.68	7.96	4.35	4.53	0.42
SY-2-G	60.64	12.11	0.13	6.42	0.32	2.66	8.01	4.46	4.47	0.45
SY-2-G	60.11	11.95	0.14	6.42	0.33	2.65	7.92	4.35	4.42	0.43
SY-2-G	60.75	12.16	0.14	6.47	0.32	2.68	8.08	4.33	4.46	0.42
SY-2-G	60.83	12.14	0.14	6.49	0.32	2.68	8.05	4.33	4.51	0.43
SY-2-G	60.56	12.23	0.13	6.48	0.32	2.67	7.98	4.42	4.49	0.44
SY-2-G	60.69	12.15	0.14	6.47	0.32	2.67	8.06	4.35	4.50	0.43
SY-2-G	60.79	12.14	0.14	6.48	0.32	2.64	8.04	4.31	4.45	0.43
SY-2-G	60.71	12.19	0.14	6.45	0.32	2.69	7.99	4.39	4.52	0.42
SY-2-G	60.59	12.21	0.14	6.46	0.32	2.66	7.98	4.35	4.46	0.44
SY-2-G	60.74	12.14	0.14	6.47	0.32	2.67	8.02	4.39	4.54	0.43
SY-2-G	60.89	12.24	0.13	6.48	0.32	2.67	8.02	4.36	4.49	0.42
SY-2-G	60.70	12.16	0.14	6.46	0.32	2.70	8.00	4.39	4.47	0.44
SY-2-G	60.59	12.11	0.14	6.46	0.32	2.70	8.03	4.39	4.54	0.43
SY-2-G	60.66	12.17	0.14	6.48	0.32	2.69	8.03	4.29	4.46	0.43
SY-2-G	60.99	12.25	0.13	6.46	0.31	2.70	8.02	4.43	4.50	0.42
SY-2-G	60.69	12.20	0.13	6.48	0.32	2.71	8.00	4.31	4.50	0.43
SY-2-G	60.57	12.13	0.13	6.48	0.32	2.68	7.99	4.34	4.47	0.44
SY-2-G	60.60	12.10	0.14	6.46	0.33	2.71	8.08	4.35	4.49	0.43
SY-2-G	60.71	12.17	0.14	6.46	0.32	2.69	7.99	4.40	4.49	0.43
SY-2-G	60.89	12.18	0.14	6.46	0.31	2.68	8.01	4.30	4.48	0.44
SY-2-G	60.69	12.21	0.13	6.48	0.32	2.69	7.98	4.38	4.51	0.42
SY-2-G	60.56	12.12	0.14	6.43	0.32	2.68	7.99	4.37	4.48	0.43
SY-2-G	60.77	12.17	0.14	6.45	0.32	2.70	8.02	4.33	4.50	0.44
SY-2-G	60.75	12.22	0.14	6.44	0.32	2.69	8.06	4.41	4.50	0.43
SY-2-G	60.69	12.11	0.13	6.49	0.32	2.68	8.00	4.36	4.47	0.44
SY-2-G	60.63	12.18	0.14	6.50	0.32	2.68	8.01	4.34	4.49	0.41
SY-2-G	60.84	12.21	0.14	6.46	0.32	2.67	8.00	4.35	4.45	0.43
SY-2-G	60.75	12.23	0.14	6.46	0.32	2.68	8.04	4.38	4.53	0.43
SY-2-G	60.72	12.11	0.14	6.47	0.32	2.67	8.03	4.35	4.49	0.43
SY-2-G	60.53	12.13	0.13	6.47	0.32	2.67	8.00	4.37	4.48	0.43
SY-2-G	60.77	12.21	0.14	6.46	0.32	2.68	8.06	4.35	4.48	0.42
SY-2-G	60.66	12.20	0.14	6.50	0.32	2.68	7.99	4.37	4.50	0.44
SY-2-G	60.71	12.12	0.14	6.46	0.33	2.69	7.97	4.38	4.48	0.43
SY-2-G	60.70	12.15	0.14	6.50	0.32	2.69	8.04	4.33	4.50	0.43
SY-2-G	60.68	12.21	0.13	6.48	0.32	2.68	7.99	4.34	4.52	0.43
SY-2-G	60.79	12.19	0.13	6.43	0.32	2.67	8.01	4.34	4.46	0.42
SY-2-G	60.65	12.15	0.14	6.50	0.32	2.70	8.00	4.41	4.48	0.43
SY-2-G	60.71	12.12	0.14	6.46	0.32	2.67	8.03	4.36	4.50	0.43
SY-2-G	60.59	12.11	0.13	6.49	0.32	2.67	7.96	4.33	4.53	0.44
SY-2-G	60.49	12.10	0.13	6.45	0.32	2.70	7.95	4.38	4.46	0.42
SY-2-G	60.78	12.20	0.13	6.46	0.33	2.69	7.99	4.36	4.51	0.44
SY-2-G	60.76	12.19	0.13	6.46	0.32	2.68	8.00	4.38	4.48	0.43

sample	SiO <sub>2</sub>	Al <sub>2</sub> O <sub>3</sub>	TiO <sub>2</sub>	Fe <sub>2</sub> O <sub>3</sub> T	MnO	MgO	CaO	Na <sub>2</sub> O	K <sub>2</sub> O	P <sub>2</sub> O <sub>5</sub>
SY-2-G	60.63	12.14	0.14	6.49	0.32	2.68	8.03	4.34	4.45	0.42
SY-2-G	60.68	12.15	0.14	6.48	0.32	2.68	8.01	4.36	4.53	0.43
SY-2-G	60.77	12.21	0.14	6.47	0.32	2.68	8.03	4.35	4.46	0.43
SY-2-G	60.80	12.26	0.14	6.50	0.32	2.66	8.04	4.33	4.51	0.44
SY-2-G	60.78	12.15	0.13	6.47	0.32	2.69	8.06	4.41	4.53	0.43
SY-2-G	60.49	12.06	0.14	6.48	0.32	2.64	7.96	4.35	4.46	0.42
SY-2-G	60.71	12.14	0.14	6.47	0.32	2.66	7.99	4.37	4.53	0.42
SY-2-G	60.77	12.19	0.13	6.50	0.33	2.65	7.98	4.36	4.50	0.43
SY-2-G	60.56	12.16	0.13	6.48	0.32	2.69	7.99	4.33	4.48	0.43
SY-2-G	60.80	12.20	0.14	6.49	0.31	2.70	7.96	4.38	4.45	0.44
SY-2-G	60.70	12.17	0.13	6.45	0.32	2.68	7.99	4.33	4.49	0.43
SY-2-G	60.85	12.21	0.13	6.44	0.31	2.67	8.02	4.42	4.49	0.43
SY-2-G	60.69	12.17	0.13	6.46	0.32	2.68	7.96	4.35	4.50	0.43
SY-2-G	60.60	12.13	0.13	6.45	0.32	2.67	7.98	4.34	4.48	0.43
average	60.70	12.17	0.14	6.47	0.32	2.68	8.01	4.36	4.49	0.43
stdev	0.15	0.06	0.00	0.02	0.00	0.02	0.04	0.04	0.03	0.01
accptd	60.71	12.17	0.14	6.38	0.32	2.72	8.05	4.36	4.49	0.43
SY-3-G	59.74	11.65	0.13	6.56	0.32	2.63	8.10	3.94	4.20	0.49
SY-3-G	59.96	11.62	0.14	6.55	0.33	2.64	8.13	4.20	4.20	0.50
SY-3-G	59.58	11.58	0.13	6.53	0.33	2.66	8.10	4.20	4.22	0.51
SY-3-G	59.44	11.50	0.14	6.55	0.33	2.61	8.11	4.09	4.17	0.50
SY-3-G	59.69	11.63	0.13	6.61	0.33	2.64	8.15	4.08	4.16	0.52
SY-3-G	57.14	10.88	0.14	6.69	0.33	2.27	8.16	2.94	4.16	0.51
SY-3-G	59.55	11.55	0.13	6.60	0.33	2.63	8.18	4.07	4.13	0.51
SY-3-G	55.47	10.43	0.13	6.78	0.33	1.95	8.05	2.36	4.15	0.50
SY-3-G	59.56	11.61	0.13	6.61	0.33	2.65	8.20	4.11	4.17	0.52
SY-3-G	59.69	11.53	0.13	6.57	0.33	2.63	8.09	4.14	4.17	0.52
SY-3-G	59.59	11.54	0.14	6.57	0.33	2.66	8.11	4.18	4.17	0.51
SY-3-G	59.23	11.49	0.13	6.61	0.33	2.64	8.14	4.12	4.17	0.52
SY-3-G	59.74	11.65	0.13	6.56	0.32	2.63	8.10	3.94	4.20	0.49
SY-3-G	59.96	11.62	0.14	6.55	0.33	2.64	8.13	4.20	4.20	0.50
SY-3-G	59.58	11.58	0.13	6.53	0.33	2.66	8.10	4.20	4.22	0.51
SY-3-G	59.44	11.50	0.14	6.55	0.33	2.61	8.11	4.09	4.17	0.50
SY-3-G	59.69	11.63	0.13	6.61	0.33	2.64	8.15	4.08	4.16	0.52
SY-3-G	57.14	10.88	0.14	6.69	0.33	2.27	8.16	2.94	4.16	0.51
SY-3-G	59.55	11.55	0.13	6.60	0.33	2.63	8.18	4.07	4.13	0.51
SY-3-G	55.47	10.43	0.13	6.78	0.33	1.95	8.05	2.36	4.15	0.50
SY-3-G	59.56	11.61	0.13	6.61	0.33	2.65	8.20	4.11	4.17	0.52
SY-3-G	59.69	11.53	0.13	6.57	0.33	2.63	8.09	4.14	4.17	0.52
SY-3-G	59.59	11.54	0.14	6.57	0.33	2.66	8.11	4.18	4.17	0.51
SY-3-G	59.23	11.49	0.13	6.61	0.33	2.64	8.14	4.12	4.17	0.52
SY-3-G	59.79	11.57	0.13	6.62	0.33	2.67	8.24	4.12	4.16	0.52
SY-3-G	59.68	11.56	0.14	6.61	0.33	2.67	8.16	4.09	4.19	0.51
SY-3-G	59.78	11.62	0.14	6.62	0.33	2.67	8.25	4.20	4.22	0.51
SY-3-G	59.75	11.53	0.14	6.63	0.33	2.68	8.27	4.14	4.17	0.51
SY-3-G	59.91	11.59	0.14	6.62	0.33	2.68	8.15	4.10	4.15	0.51
SY-3-G	59.80	11.62	0.13	6.62	0.33	2.66	8.20	4.12	4.18	0.52
SY-3-G	59.81	11.63	0.14	6.61	0.33	2.66	8.14	4.12	4.19	0.52
SY-3-G	59.49	11.50	0.14	6.63	0.32	2.65	8.19	4.16	4.19	0.51
SY-3-G	59.79	11.61	0.14	6.63	0.32	2.68	8.19	4.17	4.22	0.52
SY-3-G	59.77	11.60	0.14	6.62	0.33	2.68	8.15	4.15	4.23	0.51
SY-3-G	59.61	11.56	0.13	6.60	0.33	2.68	8.19	4.16	4.19	0.52
SY-3-G	59.53	11.53	0.14	6.62	0.32	2.65	8.20	4.16	4.19	0.50
SY-3-G	59.67	11.53	0.13	6.62	0.33	2.67	8.26	4.11	4.20	0.52
SY-3-G	59.70	11.60	0.14	6.60	0.33	2.69	8.17	4.20	4.23	0.51

sample	SiO <sub>2</sub>	Al <sub>2</sub> O <sub>3</sub>	TiO <sub>2</sub>	Fe <sub>2</sub> O <sub>3</sub> T	MnO	MgO	CaO	Na <sub>2</sub> O	K <sub>2</sub> O	P <sub>2</sub> O <sub>5</sub>
SY-3-G	59.56	11.48	0.14	6.66	0.33	2.66	8.20	4.16	4.24	0.51
SY-3-G	59.45	11.52	0.13	6.63	0.33	2.65	8.23	4.20	4.24	0.51
SY-3-G	59.85	11.66	0.14	6.63	0.33	2.64	8.14	4.14	4.19	0.50
SY-3-G	59.77	11.57	0.14	6.63	0.33	2.67	8.14	4.16	4.16	0.52
SY-3-G	59.69	11.58	0.14	6.63	0.33	2.67	8.14	4.22	4.14	0.51
SY-3-G	59.75	11.53	0.14	6.60	0.33	2.68	8.17	4.16	4.16	0.51
SY-3-G	59.62	11.54	0.13	6.63	0.33	2.67	8.21	4.25	4.20	0.51
SY-3-G	59.63	11.58	0.14	6.63	0.33	2.69	8.18	4.19	4.18	0.52
SY-3-G	59.51	11.53	0.14	6.58	0.33	2.66	8.18	4.19	4.22	0.51
SY-3-G	59.52	11.52	0.14	6.62	0.32	2.68	8.16	4.11	4.19	0.52
SY-3-G	59.32	11.48	0.13	6.62	0.32	2.65	8.14	4.17	4.21	0.50
SY-3-G	59.55	11.59	0.14	6.63	0.33	2.67	8.14	4.18	4.20	0.50
SY-3-G	59.55	11.61	0.14	6.61	0.33	2.65	8.17	4.16	4.22	0.51
SY-3-G	59.49	11.57	0.14	6.57	0.33	2.68	8.16	4.19	4.20	0.51
SY-3-G	59.43	11.49	0.14	6.59	0.32	2.68	8.21	4.20	4.16	0.51
SY-3-G	59.31	11.43	0.13	6.61	0.33	2.66	8.16	4.18	4.18	0.49
SY-3-G	59.72	11.56	0.13	6.61	0.33	2.66	8.13	4.22	4.15	0.52
SY-3-G	59.64	11.59	0.13	6.60	0.33	2.66	8.24	4.19	4.23	0.50
SY-3-G	59.62	11.58	0.13	6.64	0.33	2.65	8.26	4.14	4.20	0.50
SY-3-G	59.49	11.50	0.13	6.59	0.33	2.67	8.21	4.16	4.14	0.51
SY-3-G	59.60	11.61	0.14	6.60	0.33	2.67	8.19	4.23	4.18	0.50
SY-3-G	59.59	11.57	0.14	6.63	0.33	2.64	8.19	4.10	4.19	0.51
SY-3-G	59.82	11.54	0.13	6.61	0.33	2.67	8.24	4.20	4.22	0.51
SY-3-G	59.33	11.45	0.14	6.62	0.33	2.64	8.19	4.10	4.20	0.50
SY-3-G	59.56	11.55	0.13	6.65	0.33	2.65	8.19	4.14	4.19	0.50
SY-3-G	59.51	11.62	0.13	6.62	0.33	2.65	8.12	4.12	4.24	0.50
SY-3-G	59.58	11.51	0.14	6.61	0.33	2.65	8.14	4.11	4.14	0.50
SY-3-G	59.64	11.63	0.14	6.64	0.32	2.66	8.18	4.20	4.20	0.51
SY-3-G	59.70	11.57	0.14	6.59	0.33	2.67	8.18	4.13	4.21	0.51
SY-3-G	59.56	11.61	0.14	6.62	0.33	2.66	8.22	4.16	4.22	0.49
SY-3-G	59.70	11.55	0.13	6.63	0.33	2.67	8.22	4.15	4.20	0.51
SY-3-G	59.48	11.56	0.14	6.61	0.33	2.66	8.16	4.16	4.19	0.51
average	59.43	11.51	0.14	6.61	0.33	2.63	8.17	4.06	4.19	0.51
stdev	0.81	0.22	0.00	0.04	0.00	0.13	0.05	0.36	0.03	0.01
acpptd	<b>60.32</b>	<b>11.89</b>	<b>0.15</b>	<b>6.57</b>	<b>0.32</b>	<b>2.70</b>	<b>8.36</b>	<b>4.17</b>	<b>4.28</b>	<b>0.55</b>
W-2-G	52.27	15.31	1.08	11.06	0.17	6.42	11.18	2.35	0.65	0.13
W-2-G	52.04	15.24	1.09	11.13	0.17	6.44	11.15	2.91	0.66	0.13
W-2-G	52.05	15.20	1.07	11.09	0.17	6.37	11.07	2.94	0.66	0.13
W-2-G	52.27	15.31	1.08	11.06	0.17	6.42	11.18	2.35	0.65	0.13
W-2-G	52.04	15.24	1.09	11.13	0.17	6.44	11.15	2.91	0.66	0.13
W-2-G	52.05	15.20	1.07	11.09	0.17	6.37	11.07	2.94	0.66	0.13
W-2-G	52.22	15.19	1.06	11.08	0.17	6.43	11.12	3.03	0.65	0.12
W-2-G	52.08	15.26	1.07	11.12	0.17	6.38	11.14	3.03	0.65	0.13
W-2-G	52.09	15.19	1.07	11.03	0.17	6.42	10.98	3.01	0.66	0.14
W-2-G	52.17	15.07	1.10	11.05	0.17	6.41	10.97	3.00	0.66	0.13
W-2-G	52.18	15.25	1.06	11.05	0.17	6.42	11.01	3.02	0.63	0.13
W-2-G	52.21	15.10	1.05	11.05	0.16	6.42	10.98	3.01	0.64	0.12
W-2-G	52.10	15.17	1.09	11.03	0.16	6.44	10.95	3.05	0.65	0.13
W-2-G	51.98	15.23	1.06	11.04	0.17	6.41	10.99	3.03	0.66	0.13
W-2-G	52.12	15.21	1.06	10.99	0.17	6.42	10.95	3.03	0.65	0.13
W-2-G	51.95	15.15	1.07	11.08	0.16	6.38	10.96	2.98	0.63	0.13
W-2-G	52.11	15.27	1.05	11.00	0.17	6.37	10.98	3.01	0.64	0.13
average	52.11	15.21	1.07	11.06	0.17	6.41	11.05	2.92	0.65	0.13
stdev	0.09	0.06	0.01	0.04	0.00	0.03	0.09	0.22	0.01	0.00
acpptd	<b>52.45</b>	<b>15.53</b>	<b>1.06</b>	<b>10.74</b>	<b>0.16</b>	<b>6.37</b>	<b>10.87</b>	<b>2.14</b>	<b>0.63</b>	<b>0.13</b>

## **Assessment of Accuracy of XRF Trace Element Data**

### **Analyses of Standards**

element	Sc	V	Cr	Ni	Rb	Sr	Y	Zr	Nb	Ba	Ce	Pb	Th	U
det limit	7	6	7	5	0.7	1.2	0.6	1.4	0.7	24	44	4	3	4
AGV-1	16	121	9	15	69.6	691.0	17.7	253.3	16.8	1165	98	37	7	BD
AGV-1	16	114	8	17	70.6	687.9	18.0	253.6	16.5	1212	75	35	6	BD
AGV-1	15	119	16	12	70.0	690.0	17.7	252.5	16.7	1275	101	33	8	BD
AGV-1	14	117	BD	18	70.4	686.4	17.4	251.0	16.4	1263	80	35	6	BD
AGV-1	BD	121	BD	15	70.0	685.6	17.9	249.8	16.9	1256	66	38	6	BD
AGV-1	18	116	BD	BD	70.6	689.7	17.6	245.9	16.4	1288	78	36	6	BD
AGV-1	14	118	BD	BD	70.2	689.7	17.1	245.3	16.7	1289	77	37	7	BD
AGV-1	13	118	BD	BD	69.5	686.3	17.8	246.8	17.0	1284	82	35	5	BD
AGV-1	14	116	BD	BD	70.3	686.5	17.3	246.4	16.6	1271	94	39	5	BD
AGV-1	15	111	BD	BD	70.1	687.7	17.6	246.7	16.3	1266	66	36	6	BD
AGV-1	15	112	BD	6	70.1	690.7	17.7	249.1	16.7	1241	67	38	8	BD
AGV-1	20	120	BD	8	69.8	688.7	17.5	246.7	16.7	1333	69	38	6	BD
average	15	117	NA	13	70.1	688.4	17.6	248.9	16.6	1262	79	36	6	NA
stdev	2	3	NA	5	0.35	1.88	0.25	3.05	0.23	42	12	2	1	NA
accptd	12	121	10	16	67.3	662.0	20.0	227.0	15	1226	67	36	7	2
BCR-1	36	417	17	13	49.3	350.1	35.1	208.8	15.2	701	65	13	5	BD
BCR-1	30	408	9	10	49.9	347.6	34.3	207.6	14.5	712	43	13	6	BD
BCR-1	37	418	15	10	49.5	348.0	34.8	209.6	14.6	748	54	16	7	BD
BCR-1	35	413	14	13	49.5	348.6	34.0	209.0	14.4	729	BD	16	6	BD
BCR-1	27	404	9	16	49.6	347.3	34.2	206.7	14.8	722	BD	16	4	BD
BCR-1	44	403	BD	BD	50.2	348.0	34.9	205.8	14.8	759	74	19	6	BD
BCR-1	34	412	BD	6	49.6	347.8	34.7	205.4	15.0	752	BD	19	6	BD
BCR-1	32	421	BD	BD	49.4	348.8	34.7	203.9	15.0	711	55	21	5	BD
BCR-1	33	412	BD	BD	49.6	347.8	34.9	206.1	14.8	758	67	19	4	BD
BCR-1	29	407	BD	BD	50.6	350.3	35.0	205.6	14.8	734	BD	21	7	BD
BCR-1	31	397	BD	BD	49.8	349.4	34.3	207.0	15.3	717	72	18	5	BD
BCR-1	35	399	BD	6	49.7	349.0	35.2	206.3	14.4	770	54	17	6	BD
average	34	409	13	NA	49.7	348.6	34.7	206.8	14.8	734	60	18	6	NA
stdev	4	8	4	NA	0.37	0.98	0.39	1.68	0.29	23	11	3	1	NA
accptd	33	407	16	13	47.2	330.0	38.0	190.0	14.0	681	54	14	6	2
BHVO-1	32	318	323	125	8.9	405.7	24.9	189.4	21.8	128	51	BD	BD	BD
BHVO-1	34	312	321	124	9.2	407.9	24.7	190.3	21.3	152	38	BD	BD	BD
BHVO-1	36	318	324	122	9.0	410.6	25.2	188.1	22.4	118	13	BD	BD	BD
BHVO-1	28	315	310	125	9.3	412.7	24.9	187.5	21.8	133	41	BD	BD	BD
BHVO-1	34	309	317	122	9.3	410.2	25.3	186.6	21.9	137	37	BD	BD	BD
BHVO-1	32	326	316	123	9.3	409.9	25.3	184.7	22.0	124	39	BD	BD	BD
BHVO-1	35	316	316	121	9.8	408.4	24.9	187.9	22.0	134	16	5	4	BD
BHVO-1	29	311	317	126	9.3	406.9	24.5	187.0	21.7	135	21	BD	BD	BD
BHVO-1	32	324	315	121	9.9	410.4	24.7	187.3	22.2	131	27	BD	BD	BD
BHVO-1	34	317	321	122	9.4	408.2	24.7	185.7	21.8	139	22	BD	4	BD
BHVO-1	39	322	316	118	9.4	410.6	25.1	186.7	21.5	138	32	BD	BD	BD
BHVO-1	28	313	318	121	9.6	411.9	24.7	186.4	21.9	142	46	BD	BD	BD
BHVO-1	31	323	323	122	9.2	410.2	25.0	186.4	21.7	152	51	BD	BD	BD
BHVO-1	32	310	318	123	9.4	409.4	24.5	187.1	21.9	140	25	BD	4	BD
BHVO-1	29	314	310	123	9.5	409.0	24.8	186.3	21.9	160	36	5	BD	BD
BHVO-1	33	324	312	121	9.4	411.2	24.7	185.1	21.6	129	31	4	BD	BD
BHVO-1	36	315	314	124	9.3	407.1	24.9	187.4	22.0	126	41	4	BD	BD
BHVO-1	32	315	309	123	9.0	409.4	25.3	185.8	22.0	153	17	5	BD	BD
BHVO-1	34	311	321	122	9.0	407.5	24.9	184.6	22.3	144	BD	5	BD	BD
BHVO-1	31	326	316	119	9.3	409.1	24.4	185.4	22.2	124	4	7	BD	BD
BHVO-1	30	320	321	121	9.2	408.9	24.6	185.0	22.0	141	16	6	BD	BD
BHVO-1	35	310	314	123	9.4	411.8	25.1	186.1	22.2	131	34	6	BD	BD
BHVO-1	27	326	301	114	9.3	412.3	25.0	183.6	22.1	108	38	7	BD	BD
BHVO-1	32	316	293	109	9.9	411.7	25.4	183.4	21.8	130	45	5	BD	BD

element	Sc	V	Cr	Ni	Rb	Sr	Y	Zr	Nb	Ba	Ce	Pb	Th	U
BHVO-1	32	315	304	108	9.4	411.2	25.2	184.6	21.4	137	BD	10	BD	BD
BHVO-1	38	311	307	108	10.1	409.1	25.0	183.4	22.0	130	9	6	BD	BD
BHVO-1	32	316	296	110	9.4	411.5	25.7	182.9	22.1	168	39	5	BD	BD
BHVO-1	32	318	302	115	9.3	412.6	25.3	184.9	22.3	127	48	10	4	BD
BHVO-1	32	311	302	107	10.4	410.3	25.4	183.3	22.1	137	33	9	BD	BD
BHVO-1	34	322	301	114	9.2	410.4	25.0	181.8	22.3	140	18	9	BD	BD
BHVO-1	30	326	304	111	9.1	409.7	24.9	184.7	22.2	141	30	5	BD	BD
BHVO-1	32	314	302	114	9.1	410.6	25.5	183.8	22.3	116	50	7	BD	BD
BHVO-1	35	314	300	112	9.5	408.8	25.0	184.4	22.5	136	17	5	BD	BD
BHVO-1	33	314	300	113	8.5	410.3	25.1	184.1	22.1	155	34	5	BD	BD
BHVO-1	27	320	310	112	9.7	410.8	24.8	183.9	21.8	140	54	8	BD	BD
BHVO-1	35	320	314	114	9.5	411.4	25.1	185.4	22.2	118	70	8	BD	BD
BHVO-1	39	315	299	114	9.3	411.6	25.9	185.4	22.3	122	34	12	BD	BD
BHVO-1	28	313	307	111	9.5	412.2	25.2	184.6	22.0	136	48	6	BD	BD
BHVO-1	34	317	309	115	9.1	409.3	25.2	185.2	22.1	181	19	BD	BD	BD
BHVO-1	31	309	305	111	9.3	410.6	25.3	183.2	22.0	153	16	6	BD	BD
BHVO-1	35	323	299	113	9.0	410.1	26.0	184.1	22.0	133	47	6	BD	BD
BHVO-1	30	319	312	111	9.4	413.1	25.9	182.8	22.5	155	9	7	BD	BD
BHVO-1	30	317	315	113	8.8	414.0	24.9	184.9	22.0	119	28	7	BD	BD
BHVO-1	31	320	305	115	8.7	411.7	24.9	185.4	22.6	127	44	9	BD	BD
BHVO-1	34	311	320	116	9.5	414.3	25.3	186.7	22.6	128	54	6	BD	BD
BHVO-1	35	321	300	114	9.0	412.0	26.1	184.5	21.7	125	43	6	BD	BD
BHVO-1	35	321	305	117	9.3	411.7	25.4	185.3	22.0	123	53	5	BD	BD
BHVO-1	33	315	312	119	9.6	413.5	25.4	185.5	22.2	122	52	8	BD	BD
BHVO-1	36	309	306	116	9.7	413.1	25.1	184.2	22.1	111	42	6	BD	BD
BHVO-1	26	323	305	114	8.9	411.6	25.5	183.4	22.1	123	60	BD	BD	BD
average	33	317	310	117	9.3	410.5	25.1	185.3	22.0	135	35	7	NA	NA
stdev	3	5	8	5	0.34	1.87	0.37	1.71	0.28	14	15	BD	NA	NA
accptd	32	317	289	121	11.0	403.0	27.6	179.0	19.0	139	39	3	1	ND
DNC-1	33	148	311	247	3.2	144.5	15.6	37.1	1.3	119	BD	5	BD	BD
DNC-1	31	148	304	252	3.4	146.1	16.4	37.1	1.4	122	27	8	BD	BD
DNC-1	31	142	308	249	4.4	143.7	16.0	36.2	1.5	103	BD	6	5	BD
DNC-1	28	146	305	248	3.8	146.5	16.2	35.5	1.7	120	11	6	BD	BD
DNC-1	27	147	295	249	3.4	143.5	16.0	36.6	1.8	125	6	8	BD	BD
DNC-1	30	138	308	251	3.5	143.8	16.2	36.4	2.1	118	BD	8	BD	BD
DNC-1	35	133	294	242	3.8	144.4	16.2	34.4	1.7	140	BD	9	BD	BD
DNC-1	28	153	300	243	3.8	144.4	16.2	34.6	1.7	112	BD	10	BD	BD
DNC-1	33	142	293	243	3.4	143.9	16.5	34.7	1.7	121	14	8	BD	BD
DNC-1	41	143	296	241	3.4	144.6	16.0	35.4	1.4	116	7	8	BD	BD
DNC-1	34	149	302	242	4.1	143.2	16.8	35.9	1.7	140	BD	11	BD	BD
DNC-1	30	145	306	243	4.0	144.2	16.1	35.4	1.5	117	BD	11	BD	BD
DNC-1	27	142	295	240	3.5	144.3	16.4	35.7	1.5	110	BD	8	0	BD
average	31	144	301	245	3.7	144.4	16.2	35.8	1.6	120	NA	8	NA	NA
stdev	4	5	6	4	0.34	0.96	0.29	0.90	0.23	10	NA	2	NA	NA
accptd	31	148	285	247	ND	145.0	18.0	41.0	3.0	114	11	6	ND	ND
DTS-1	BD	9	4040	2352	BD	BD	BD	BD	BD	BD	BD	5	BD	BD
DTS-1	BD	11	4052	2361	BD	BD	BD	BD	BD	BD	BD	8	BD	BD
DTS-1	BD	10	4019	2352	BD	BD	BD	BD	BD	BD	BD	6	BD	BD
DTS-1	BD	14	3969	2351	BD	BD	BD	BD	BD	BD	BD	6	BD	BD
DTS-1	BD	10	3982	2372	BD	BD	BD	BD	BD	BD	BD	5	BD	BD
DTS-1	BD	9	3990	2366	BD	BD	BD	BD	BD	BD	BD	5	BD	BD
DTS-1	BD	12	4000	2349	BD	BD	BD	BD	BD	BD	BD	7	BD	BD
DTS-1	BD	8	3982	2358	BD	BD	BD	BD	BD	BD	BD	6	BD	BD
DTS-1	BD	11	3975	2364	BD	BD	BD	BD	BD	BD	BD	7	BD	BD
DTS-1	BD	13	4003	2369	BD	BD	BD	BD	BD	BD	BD	7	BD	BD

element	Sc	V	Cr	Ni	Rb	Sr	Y	Zr	Nb	Ba	Ce	Pb	Th	U
DTS-1	BD	14	3985	2350	BD	BD	BD	BD	BD	BD	BD	6	BD	BD
DTS-1	BD	12	3989	2354	BD	BD	BD	BD	BD	BD	BD	5	BD	BD
DTS-1	BD	16	3998	2365	BD	BD	BD	BD	BD	BD	BD	6	BD	BD
DTS-1	BD	13	3988	2370	BD	BD	BD	BD	BD	BD	BD	5	BD	BD
DTS-1	BD	10	4019	2339	BD	BD	BD	BD	BD	BD	BD	9	BD	BD
DTS-1	BD	13	3992	2344	BD	BD	BD	BD	BD	BD	BD	6	BD	BD
DTS-1	BD	9	3976	2369	BD	BD	BD	BD	BD	BD	BD	6	BD	BD
DTS-1	BD	10	3972	2388	BD	BD	BD	BD	BD	BD	BD	6	BD	BD
DTS-1	BD	12	3992	2362	BD	BD	BD	BD	BD	BD	BD	8	BD	BD
DTS-1	BD	14	3992	2370	0.0	BD	BD	BD	BD	BD	BD	8	BD	BD
DTS-1	BD	11	3991	2349	BD	BD	BD	BD	BD	BD	BD	8	BD	BD
DTS-1	BD	11	3985	2360	BD	BD	BD	BD	BD	BD	BD	8	BD	BD
DTS-1	BD	12	4001	2374	BD	BD	BD	BD	BD	BD	BD	11	BD	BD
DTS-1	BD	13	3988	2354	BD	BD	BD	BD	BD	BD	BD	8	BD	BD
DTS-1	BD	13	3979	2359	BD	BD	BD	BD	BD	BD	BD	7	BD	BD
DTS-1	BD	11	3992	2352	BD	BD	BD	BD	BD	BD	BD	9	BD	BD
DTS-1	BD	13	3994	2345	BD	BD	BD	BD	BD	BD	BD	8	BD	BD
DTS-1	BD	15	4000	2354	BD	BD	BD	BD	BD	BD	BD	9	BD	BD
DTS-1	BD	12	3969	2366	BD	BD	BD	BD	BD	BD	BD	9	BD	BD
DTS-1	BD	11	3996	2375	BD	BD	BD	BD	BD	BD	BD	9	BD	BD
DTS-1	BD	13	3986	2358	BD	BD	BD	BD	BD	BD	BD	9	BD	BD
DTS-1	BD	12	4008	2368	BD	BD	BD	BD	BD	BD	BD	8	BD	BD
DTS-1	BD	15	3989	2360	BD	BD	BD	BD	BD	BD	BD	7	BD	BD
DTS-1	BD	16	3977	2354	BD	BD	BD	BD	BD	BD	BD	10	BD	BD
DTS-1	BD	9	4004	2354	BD	BD	BD	BD	BD	BD	BD	9	BD	BD
DTS-1	BD	8	3988	2365	BD	BD	BD	BD	BD	BD	BD	8	BD	BD
DTS-1	BD	8	3983	2367	BD	BD	BD	BD	BD	BD	BD	8	BD	BD
DTS-1	BD	9	3984	2354	BD	BD	BD	BD	BD	BD	BD	11	BD	BD
DTS-1	BD	13	3995	2356	BD	BD	BD	BD	BD	BD	BD	8	BD	BD
DTS-1	BD	13	3988	2367	BD	BD	BD	BD	BD	BD	BD	8	BD	BD
DTS-1	BD	10	4003	2356	BD	BD	BD	BD	BD	BD	BD	9	BD	BD
DTS-1	BD	17	3974	2361	BD	BD	BD	BD	BD	BD	BD	9	BD	BD
DTS-1	BD	11	3969	2357	BD	BD	BD	BD	BD	BD	BD	9	BD	BD
DTS-1	BD	9	3999	2368	BD	BD	BD	BD	BD	BD	BD	10	BD	BD
DTS-1	BD	12	4026	2357	BD	BD	BD	BD	BD	BD	BD	9	BD	BD
DTS-1	BD	10	3966	2359	BD	BD	BD	BD	BD	BD	BD	9	BD	BD
DTS-1	BD	10	3961	2368	BD	BD	BD	BD	BD	BD	BD	8	BD	BD
DTS-1	BD	12	3992	2370	BD	BD	BD	BD	BD	BD	BD	7	BD	BD
DTS-1	BD	13	4020	2353	BD	BD	BD	BD	BD	BD	BD	9	BD	BD
DTS-1	BD	12	3987	2350	BD	BD	BD	BD	BD	BD	BD	9	BD	BD
average	NA	12	3992	2360	NA	NA	NA	NA	NA	NA	NA	8	NA	NA
stdev	NA	2	18	9	NA	NA	NA	NA	NA	NA	NA	2	NA	NA
accptd		11	3990	2360	0.1	0.3	ND	4.0	202	2	ND	12	ND	ND
JG-2	BD	BD	9	15	289.9	15.6	72.4	89.4	15.7	56	52	29	30	13
JG-2	BD	BD	7	13	286.9	15.8	73.2	89.9	16.2	57	44	29	29	14
JG-2	BD	BD	6	8	287.7	15.9	73.4	88.8	16.0	62	32	29	29	11
JG-2	BD	BD	7	9	287.9	15.5	73.0	89.6	15.6	80	48	29	30	13
JG-2	BD	BD	9	9	288.4	15.9	73.0	89.2	15.9	64	34	30	26	12
JG-2	BD	BD	8	10	288.7	16.2	73.2	88.1	15.6	65	31	30	28	13
JG-2	BD	BD	BD	1	289.0	15.6	71.9	88.2	15.4	64	44	30	29	12
JG-2	BD	BD	BD	0	288.5	15.8	72.0	89.2	15.6	62	41	31	29	13
JG-2	BD	BD	BD	0	288.1	16.2	72.0	89.4	15.7	72	40	31	29	13
JG-2	BD	BD	BD	0	289.7	16.1	71.7	91.4	15.5	69	65	33	27	13
JG-2	BD	BD	BD	1	288.3	15.5	72.6	93.8	15.7	81	43	32	29	13
JG-2	BD	BD	BD	3	288.6	16.3	72.4	92.9	16.1	63	26	30	27	11

element	Sc	V	Cr	Ni	Rb	Sr	Y	Zr	Nb	Ba	Ce	Pb	Th	U
JG-2	BD	BD	BD	4	289.0	15.8	71.9	85.1	15.4	57	64	30	29	11
average	NA	NA	BD	6	288.5	15.9	72.5	89.6	15.7	66	43	30	28	12
stdev	NA	NA	BD	5	0.80	0.27	0.61	2.19	0.25	8	12	1	1	1
accptd	2	3	8	2	288.0	16.0	89.0	97.0	15	67	46	33	30	13
PACS-1	17	148	133	48	46.1	271.2	15.8	135.9	9.5	675	70	357	BD	BD
PACS-1	13	148	135	47	46.2	272.5	15.7	135.5	9.5	695	35	361	BD	BD
PACS-1	17	150	139	47	45.5	274.9	15.7	135.1	10.1	617	62	351	BD	BD
PACS-1	16	148	130	49	46.7	277.0	15.8	134.9	9.6	616	66	357	BD	BD
PACS-1	16	144	130	46	46.3	274.7	15.9	133.6	9.8	618	47	355	BD	BD
PACS-1	13	151	138	47	46.0	274.9	15.7	132.5	10.0	664	59	355	BD	BD
PACS-1	17	147	132	45	46.9	274.0	15.6	134.1	10.0	634	58	354	BD	BD
PACS-1	15	150	137	44	46.2	274.3	15.6	134.2	10.0	660	29	356	BD	BD
PACS-1	19	150	137	46	46.9	273.6	15.3	134.9	9.1	659	67	356	BD	BD
PACS-1	16	152	131	44	46.3	273.6	15.6	134.4	9.8	642	46	352	BD	BD
PACS-1	14	153	131	46	46.4	275.6	15.5	133.5	9.8	665	60	354	BD	BD
PACS-1	10	153	133	43	46.6	276.0	15.6	135.7	9.7	669	73	355	BD	BD
PACS-1	16	151	131	46	46.2	275.2	15.5	134.9	9.6	675	79	354	BD	BD
PACS-1	14	157	130	48	46.3	276.4	15.5	136.5	9.8	654	52	353	BD	BD
PACS-1	12	149	134	47	45.5	277.2	16.0	132.9	9.8	670	60	351	BD	BD
PACS-1	10	148	134	51	45.9	277.5	16.0	136.1	9.6	667	64	354	BD	BD
PACS-1	12	149	131	51	46.4	276.2	16.1	137.0	10.0	681	62	356	BD	BD
PACS-1	14	146	132	48	46.4	277.5	15.9	134.8	9.9	682	30	357	BD	BD
PACS-1	13	152	135	51	46.2	276.3	16.1	135.4	9.8	666	66	350	BD	BD
PACS-1	20	149	138	50	45.9	276.3	16.2	134.7	9.3	673	40	346	BD	BD
PACS-1	17	154	133	49	46.0	277.2	15.5	134.5	10.3	661	60	352	BD	BD
PACS-1	12	153	128	52	46.2	276.9	15.9	134.7	9.5	692	60	352	BD	BD
PACS-1	14	154	122	39	46.8	277.5	15.7	132.1	9.2	712	52	346	BD	BD
PACS-1	18	150	121	38	46.7	278.7	15.9	133.6	9.9	703	88	347	BD	BD
PACS-1	13	152	121	35	47.1	278.2	16.0	132.7	9.5	681	43	346	BD	BD
PACS-1	21	151	114	37	47.4	277.8	15.9	132.9	9.5	690	75	352	BD	BD
PACS-1	14	154	121	37	46.9	277.5	15.9	132.2	10.0	695	61	344	BD	BD
PACS-1	22	149	118	37	47.4	277.9	15.7	131.7	9.9	672	63	347	BD	BD
PACS-1	11	156	125	39	47.2	277.2	15.8	131.6	10.0	679	51	345	BD	BD
PACS-1	16	153	125	37	47.5	279.2	16.1	132.0	10.2	667	45	345	BD	BD
PACS-1	9	158	129	38	46.8	276.7	15.9	134.1	10.3	685	71	344	BD	BD
PACS-1	14	153	123	40	46.5	278.4	16.0	132.0	10.1	642	73	348	BD	BD
PACS-1	17	152	123	40	46.2	276.2	16.3	133.1	9.7	658	65	344	BD	BD
PACS-1	18	149	126	40	46.7	276.4	15.7	133.7	9.7	680	62	347	BD	BD
PACS-1	18	153	131	38	47.0	276.8	15.6	133.2	9.8	671	51	346	BD	BD
PACS-1	15	149	121	42	47.1	277.0	15.8	131.9	10.2	658	88	352	BD	BD
PACS-1	20	144	128	39	47.5	278.7	15.6	132.2	9.9	689	89	354	BD	BD
PACS-1	15	145	125	43	47.0	278.5	15.5	134.5	9.4	694	79	350	BD	BD
PACS-1	17	152	125	45	47.3	277.2	15.9	131.2	9.9	677	52	352	BD	BD
PACS-1	16	154	123	36	47.2	278.0	16.0	132.4	10.3	670	65	348	BD	BD
PACS-1	21	151	119	41	47.0	278.1	16.1	133.4	10.0	680	60	352	BD	BD
PACS-1	16	151	127	41	46.6	278.8	16.3	132.1	10.1	690	52	349	BD	BD
PACS-1	19	150	125	44	46.5	279.2	16.0	134.3	10.1	663	36	347	BD	BD
PACS-1	16	143	124	43	46.8	278.8	15.7	133.5	10.2	650	52	344	BD	BD
PACS-1	15	141	127	47	46.5	280.8	16.1	134.9	9.7	688	99	347	BD	BD
PACS-1	12	149	129	42	46.7	280.5	16.1	133.8	10.2	665	78	351	BD	BD
PACS-1	12	144	127	44	46.5	277.8	15.8	135.2	9.7	685	33	356	BD	BD
PACS-1	20	150	126	45	46.6	277.6	15.4	131.8	9.7	702	64	356	BD	BD
PACS-1	18	151	120	42	46.5	278.7	16.1	136.1	9.8	715	52	350	BD	BD
PACS-1	14	151	131	44	46.8	279.1	16.1	134.2	9.8	729	58	352	BD	BD
average	15	150	128	44	46.6	276.9	15.8	133.8	9.8	672	60	351	NA	NA

element	Sc	V	Cr	Ni	Rb	Sr	Y	Zr	Nb	Ba	Ce	Pb	Th	U
stdev	3	4	6	4	0.49	1.93	0.24	1.46	0.29	23	15	4	NA	NA
acptd	ND	127	113	44	ND	227.0	ND	ND	ND	ND	ND	404	ND	ND
SY-2	11	46	14	9	220.4	269.7	118.2	298.4	34.4	456	180	87	345	289
SY-2	10	45	10	11	220.2	270.9	117.3	299.1	34.6	467	155	86	344	288
SY-2	3	51	15	12	221.0	272.5	118.8	298.2	35.3	449	183	87	352	290
SY-2	11	47	BD	9	220.5	271.9	117.8	296.2	34.4	450	179	86	347	292
SY-2	8	49	8	8	220.6	271.6	118.2	298.0	34.2	457	162	86	347	289
SY-2	BD	47	8	9	218.0	268.0	117.2	291.7	34.5	444	188	85	343	289
SY-2	8	52	13	7	220.5	270.1	117.9	294.9	34.3	460	168	86	347	290
SY-2	BD	46	12	BD	219.3	270.3	117.7	296.3	34.7	453	165	88	346	291
SY-2	9	45	11	BD	220.1	271.6	118.2	296.9	34.2	443	139	86	347	290
SY-2	11	47	8	8	220.2	272.1	118.2	295.9	34.4	444	178	84	348	289
SY-2	4	47	BD	7	219.5	270.2	117.9	296.2	35.0	448	177	87	347	286
SY-2	13	48	12	6	220.3	271.3	117.5	297.1	33.9	446	183	85	346	290
SY-2	13	49	12	BD	220.6	269.9	118.5	296.5	35.0	440	135	88	346	292
SY-2	12	46	10	BD	219.7	272.6	118.2	294.3	34.4	466	181	84	349	292
SY-2	BD	49	9	9	220.4	270.5	118.0	296.0	34.5	442	151	83	347	287
SY-2	BD	43	BD	7	219.6	271.4	118.0	294.8	34.7	430	168	86	345	291
SY-2	13	48	10	9	221.0	271.4	118.1	296.0	35.4	472	173	88	347	292
SY-2	BD	50	12	7	219.1	270.7	117.9	297.2	34.8	456	151	87	348	291
SY-2	10	52	10	9	220.1	270.8	117.8	295.4	34.8	434	146	85	347	290
SY-2	BD	48	4	10	219.2	271.2	117.3	295.3	34.7	454	146	86	345	289
SY-2	8	50	11	8	220.5	271.0	118.5	296.7	35.5	465	150	87	350	291
SY-2	9	50	9	8	220.2	271.0	118.4	296.6	34.8	446	200	86	346	291
SY-2	8	53	BD	BD	220.2	271.1	117.6	294.1	35.3	468	166	85	348	292
SY-2	17	49	BD	BD	219.1	270.8	118.2	297.4	35.0	429	119	88	345	291
SY-2	BD	50	BD	BD	220.2	271.3	118.2	295.3	35.4	451	165	85	346	290
SY-2	8	52	BD	BD	220.5	270.9	117.9	297.2	35.4	451	162	86	349	287
SY-2	9	49	BD	BD	220.3	271.7	118.0	295.3	35.5	440	155	89	348	290
SY-2	BD	47	BD	BD	220.1	270.9	118.0	296.2	35.3	451	176	84	347	290
SY-2	BD	50	BD	BD	219.6	269.9	118.1	295.8	34.9	472	161	84	346	291
SY-2	BD	54	BD	BD	220.0	271.5	117.9	296.8	34.9	436	147	87	348	290
SY-2	11	53	BD	BD	219.9	270.1	118.5	295.5	35.0	447	146	84	347	291
SY-2	11	51	BD	BD	219.7	271.7	117.9	296.5	35.2	448	120	87	347	293
SY-2	11	50	BD	BD	220.5	271.6	117.9	296.3	35.0	439	166	87	347	288
SY-2	9	52	BD	BD	220.0	270.5	117.6	295.8	35.8	465	163	86	348	288
SY-2	15	47	BD	BD	220.3	269.7	117.5	297.0	35.3	457	170	86	344	290
SY-2	15	46	BD	BD	220.0	270.7	118.1	293.9	35.2	442	173	86	349	292
SY-2	9	49	BD	BD	219.9	270.9	118.2	295.0	35.3	449	179	85	346	291
SY-2	10	51	BD	BD	219.7	272.7	118.1	298.1	34.7	453	199	87	348	288
SY-2	8	50	BD	BD	219.6	270.8	118.4	297.7	35.6	463	148	85	348	290
SY-2	BD	51	BD	BD	220.0	270.8	118.4	295.7	35.4	429	154	88	348	291
SY-2	14	55	BD	BD	220.1	272.3	118.0	294.8	35.4	450	156	86	346	290
SY-2	8	49	BD	BD	220.3	270.1	117.1	295.9	35.3	459	122	84	346	290
SY-2	15	50	BD	BD	221.0	271.2	118.6	297.6	34.8	465	173	89	346	293
SY-2	BD	47	BD	BD	220.5	271.4	117.7	296.6	35.0	455	152	85	349	288
SY-2	9	49	BD	BD	219.2	270.5	117.8	295.7	35.2	443	158	88	346	289
SY-2	11	52	BD	BD	219.2	270.9	117.9	294.1	35.4	438	185	81	346	290
SY-2	12	45	BD	BD	220.9	271.2	118.1	296.4	35.0	435	173	86	349	290
SY-2	9	46	BD	BD	218.6	269.2	117.9	295.5	35.0	434	201	87	344	289
SY-2	8	50	BD	BD	220.4	271.9	118.1	296.7	35.3	461	189	85	347	291
SY-2	10	56	BD	BD	220.1	271.8	117.9	295.4	35.0	470	183	87	348	290
average	10	49	10	NA	220.0	271.0	118.0	296.1	35.0	450	164	86	347	290
stdev	3	3	3	NA	0.61	0.88	0.35	1.32	0.42	12	19	1	2	1
acptd	7	50	10	10	217.0	271.0	128.0	280.0	29.0	460	175	85	379	284

element	Sc	V	Cr	Ni	Rb	Sr	Y	Zr	Nb	Ba	Ce	Pb	Th	U
SY-3	BD	12	BD	12	203.2	298.7	600.1	358.4	252.7	437	2199	146	929	745
SY-3	BD	13	BD	13	202.9	298.2	601.0	357.0	252.8	466	2226	144	919	742
SY-3	BD	15	BD	8	203.8	301.2	603.3	353.2	253.8	451	2241	141	926	746
SY-3	BD	14	BD	10	201.5	298.3	602.4	355.8	254.6	447	2251	143	916	745
SY-3	BD	15	BD	11	200.8	295.1	590.3	351.2	249.9	431	2233	142	912	739
SY-3	BD	15	BD	10	203.9	303.1	607.0	355.8	253.8	429	2195	143	931	749
SY-3	BD	9	BD	BD	203.0	299.4	602.4	354.1	253.8	461	2258	144	918	748
SY-3	BD	15	BD	BD	203.1	299.5	600.8	353.0	252.6	419	2215	142	924	743
SY-3	BD	10	BD	BD	203.2	297.7	600.6	352.3	253.0	437	2209	143	924	740
SY-3	BD	12	BD	BD	202.5	298.8	600.8	353.1	252.7	455	2239	143	922	743
SY-3	BD	23	BD	BD	203.1	299.5	601.0	353.5	252.7	433	2245	142	925	749
SY-3	BD	18	BD	BD	202.8	299.2	599.3	353.0	253.2	445	2201	145	920	747
SY-3	BD	17	BD	BD	203.2	299.7	599.7	353.4	253.4	452	2230	138	922	745
SY-3	BD	18	BD	BD	202.6	299.6	599.7	351.6	252.8	425	2243	143	915	744
SY-3	BD	17	BD	BD	201.9	298.0	599.6	352.2	253.3	439	2196	143	925	748
SY-3	BD	13	BD	BD	202.7	297.4	598.5	351.0	252.6	455	2229	142	922	745
SY-3	BD	22	BD	BD	202.2	297.6	598.1	351.2	252.8	445	2224	144	916	749
SY-3	BD	20	BD	6	202.5	297.7	599.2	352.6	253.3	443	2271	142	922	746
SY-3	BD	19	BD	6	202.6	297.6	598.3	351.8	253.0	425	2206	143	925	747
SY-3	BD	16	BD	8	203.0	298.8	597.9	351.5	252.9	477	2236	139	923	744
SY-3	BD	15	BD	BD	202.9	297.7	598.0	351.7	252.8	465	2211	146	924	746
SY-3	BD	13	BD	BD	204.0	298.8	599.1	352.1	253.3	450	2268	142	926	746
SY-3	BD	20	BD	BD	202.4	299.1	605.4	354.0	253.4	467	2291	139	921	752
SY-3	BD	13	BD	BD	201.9	298.7	604.6	354.1	252.6	484	2253	142	921	743
SY-3	BD	21	BD	BD	202.2	296.6	604.1	352.3	252.7	507	2177	139	923	746
SY-3	BD	17	BD	BD	201.3	298.1	603.5	351.7	253.3	448	2200	139	925	743
SY-3	8	19	BD	BD	201.8	299.1	606.3	352.1	252.5	433	2267	137	924	740
SY-3	8	13	BD	BD	200.5	298.1	604.5	350.9	252.0	470	2239	140	920	740
SY-3	BD	15	BD	BD	201.3	300.0	607.4	352.2	253.6	462	2193	143	922	746
SY-3	8	18	BD	BD	202.0	296.9	607.1	353.5	253.9	463	2221	143	925	738
SY-3	BD	19	BD	BD	200.9	296.9	602.2	353.0	253.8	431	2206	141	921	742
SY-3	BD	19	BD	BD	202.0	299.2	602.2	354.3	253.1	464	2221	139	925	747
SY-3	BD	18	BD	BD	200.4	297.7	600.7	351.8	252.4	451	2221	138	922	747
SY-3	BD	22	BD	BD	201.3	298.9	602.5	352.5	252.7	450	2272	138	921	751
SY-3	BD	9	BD	BD	203.3	298.3	603.9	356.7	252.9	448	2255	140	932	747
SY-3	BD	10	BD	BD	201.0	297.8	602.6	357.0	251.5	466	2220	138	929	742
SY-3	BD	9	BD	BD	203.0	298.4	607.6	353.7	253.0	446	2211	142	934	744
SY-3	BD	9	BD	BD	202.5	297.5	605.4	355.3	254.5	483	2233	141	936	743
SY-3	BD	17	BD	BD	202.1	297.8	606.0	359.0	253.5	480	2205	141	925	745
SY-3	BD	20	BD	BD	202.0	296.5	601.7	353.0	253.1	475	2193	141	932	746
SY-3	BD	19	BD	BD	202.6	297.6	603.9	353.2	253.2	459	2265	143	929	740
SY-3	BD	18	BD	BD	201.7	296.7	602.0	356.7	252.2	457	2257	140	921	745
SY-3	13	15	BD	BD	202.2	300.1	604.7	354.6	254.1	421	2226	139	929	744
SY-3	BD	17	BD	BD	201.8	298.6	605.2	356.0	251.4	464	2219	137	926	745
SY-3	BD	15	BD	BD	201.6	298.5	604.2	351.5	252.2	456	2232	140	923	744
SY-3	BD	15	BD	BD	201.3	299.5	602.9	355.6	254.3	487	2244	138	927	744
SY-3	BD	17	BD	BD	201.0	298.6	605.2	355.6	252.0	475	2160	140	917	752
SY-3	BD	20	BD	BD	201.5	298.0	602.1	352.9	252.2	497	2267	140	917	747
SY-3	BD	13	BD	BD	202.4	298.1	601.5	354.3	254.5	485	2248	144	918	751
SY-3	9	12	BD	BD	200.7	297.0	601.6	350.9	253.3	501	2245	142	916	751
average	NA	16	NA	NA	202.2	298.4	602.2	353.6	253.0	456	2229	141	923	745
stdev	NA	4	NA	NA	0.90	1.28	3.18	2.02	0.84	21	27	2	5	3
accptd	7	50	11	11	206.0	302.0	718.0	320.0	148.0	450	2230	133	1002	650

## **Assessment of ICP-MS Trace Element Data**

### **Analysis of Standards**

## ICP-MS

Name	Name	Ho	Er	Tm	Yb	Lu	Hf	Th
DL	DL	0.00	0.01	0.00	0.01	0.00	0.01	0.01
BCR-2	BCR-2	1.27	3.62	0.51	3.29	0.48	4.76	6.03
BCR-2	BCR-2	1.28	3.56	0.51	3.33	0.49	4.77	5.95
BCR-2	BCR-2	1.28	3.66	0.53	3.39	0.48	4.38	6.01
avrg	avrg	1.28	3.61	0.52	3.34	0.49	4.63	6.00
stdev	stdev	0.01	0.05	0.01	0.05	0.00	0.22	0.04
lab*	lab*	1.27	3.63	0.52	3.27	0.49	4.90	5.77
BR-688	BR-688	0.68	1.97	0.29	2.08	0.29	1.43	0.27
BR-688	BR-688	0.67	2.07	0.30	1.91	0.30	1.50	0.32
BR-688	BR-688	0.69	2.08	0.29	1.99	0.31	1.43	0.28
BR-688	BR-688	0.73	2.15	0.31	2.01	0.30	1.78	0.34
BR-688	BR-688	0.72	2.12	0.31	2.05	0.31	1.84	0.34
BR-688	BR-688	0.70	2.00	0.30	2.05	0.32	1.50	0.35
BR-688	BR-688	0.69	2.07	0.32	1.97	0.32	1.51	0.33
BR-688	BR-688	0.72	2.12	0.32	2.04	0.31	1.45	0.36
BR-688	BR-688	0.70	2.06	0.30	1.98	0.30	1.59	0.34
BR-688	BR-688	0.72	2.14	0.31	2.01	0.31	1.57	0.33
avrg	avrg	0.70	2.08	0.30	2.01	0.31	1.56	0.33
stdev	stdev	0.02	0.06	0.01	0.05	0.01	0.14	0.03
accptd	accptd	0.81	2.11	0.29	2.09	0.34	1.60	0.33
MRG-1	MRG-1	0.50	1.13	0.14	0.82	0.11	3.79	0.81
MRG-1	MRG-1	0.46	1.22	0.14	0.85	0.11	4.07	0.79
MRG-1	MRG-1	0.48	1.14	0.13	0.73	0.11	3.84	0.75
MRG-1	MRG-1	0.49	1.05	0.15	0.80	0.11	3.82	0.79
MRG-1	MRG-1	0.51	1.20	0.15	0.80	0.11	3.94	0.76
MRG-1	MRG-1	0.50	1.19	0.16	0.81	0.12	4.19	0.80
MRG-1	MRG-1	0.50	1.16	0.14	0.81	0.12	3.96	0.76
MRG-1	MRG-1	0.48	1.21	0.15	0.84	0.11	3.95	0.77
MRG-1	MRG-1	0.49	1.18	0.14	0.82	0.10	3.42	0.81
MRG-1	MRG-1	0.50	1.18	0.14	0.82	0.11	3.57	0.74
MRG-1	MRG-1	0.51	1.22	0.15	0.84	0.11	4.12	0.77
avrg	avrg	0.49	1.17	0.15	0.81	0.11	3.88	0.78
stdev	stdev	0.01	0.05	0.01	0.03	0.00	0.23	0.02
accptd	accptd	0.49	1.12	0.11	0.60	0.12	3.76	0.93
lab*	lab*	0.49	1.16	0.14	0.79	0.11	3.89	0.82

Name	Y	Zr	Nb	Ba	La	Ce	Pr	Nd	Sm	Eu	Gd	Tb	Dy
<b>DL</b>	<b>0.02</b>	<b>0.06</b>	<b>0.15</b>	<b>0.20</b>	<b>0.03</b>	<b>0.05</b>	<b>0.01</b>	<b>0.01</b>	<b>0.02</b>	<b>0.00</b>	<b>0.01</b>	<b>0.00</b>	<b>0.01</b>
BCR-2	31.80	207.58	15.34	648.71	24.53	51.67	6.64	28.33	6.31	1.90	6.52	1.16	7.06
BCR-2	31.96	206.64	15.22	644.93	24.39	51.80	6.58	27.99	6.30	1.90	6.57	1.15	7.08
BCR-2	32.25	199.04	15.20	651.88	25.08	52.92	6.76	28.66	6.48	1.93	6.56	1.14	7.12
avrg	32.00	204.42	15.25	648.51	24.67	52.13	6.66	28.32	6.36	1.91	6.55	1.15	7.09
stdev	0.23	4.68	0.07	3.48	0.36	0.68	0.09	0.34	0.10	0.02	0.03	0.01	0.03
<b>lab*</b>	<b>31.70</b>	<b>197.00</b>	<b>14.20</b>	<b>651.00</b>	<b>24.30</b>	<b>52.00</b>	<b>6.61</b>	<b>28.00</b>	<b>6.42</b>	<b>1.90</b>	<b>6.55</b>	<b>1.00</b>	<b>6.24</b>
BR-688	17.76	59.00	4.90	166.46	4.93	11.49	1.69	8.30	2.37	0.98	2.82	0.47	3.32
BR-688	17.34	57.70	4.45	159.82	4.82	11.43	1.60	7.47	2.21	0.91	2.83	0.51	3.21
BR-688	17.53	58.46	4.99	164.82	5.01	11.47	1.63	7.75	2.33	0.95	2.84	0.48	3.13
BR-688	17.99	62.43	4.87	163.84	5.05	11.85	1.65	8.02	2.39	0.95	2.91	0.56	3.71
BR-688	17.95	62.99	4.97	161.48	4.98	11.43	1.64	7.94	2.34	0.94	2.93	0.49	3.25
BR-688	18.18	58.75	3.07	161.69	4.84	11.52	1.71	8.07	2.31	0.96	2.93	0.49	3.18
BR-688	18.20	59.24	4.36	165.43	4.92	11.91	1.69	8.09	2.32	0.94	2.96	0.46	3.26
BR-688	17.79	58.13	4.61	167.35	4.92	11.99	1.70	7.85	2.44	0.98	2.86	0.49	3.38
BR-688	17.75	63.03	5.75	162.83	4.99	11.54	1.64	7.84	2.32	0.96	2.81	0.48	3.21
BR-688	18.03	64.58	5.87	168.79	5.03	11.71	1.69	8.21	2.47	0.97	2.87	0.47	3.20
avrg	17.85	60.43	4.78	164.25	4.95	11.63	1.67	7.95	2.35	0.95	2.88	0.49	3.29
stdev	0.27	2.53	0.78	2.85	0.08	0.21	0.04	0.24	0.07	0.02	0.05	0.03	0.17
<b>accptd</b>	<b>17.00</b>	<b>60.60</b>	<b>ND</b>	<b>200.00</b>	<b>5.30</b>	<b>13.30</b>	<b>ND</b>	<b>9.60</b>	<b>2.79</b>	<b>1.07</b>	<b>3.20</b>	<b>0.45</b>	<b>3.40</b>
MRG-1	11.79	116.25	26.81	49.35	9.11	25.95	3.64	17.12	4.18	1.35	4.02	0.52	2.75
MRG-1	11.50	114.45	24.06	52.11	8.75	25.63	3.61	17.42	4.21	1.36	4.11	0.55	2.90
MRG-1	11.36	110.80	22.33	47.40	8.59	24.87	3.58	17.27	4.43	1.34	4.20	0.54	2.85
MRG-1	11.33	111.75	25.74	48.40	8.53	24.56	3.52	17.30	4.19	1.39	4.03	0.54	2.83
MRG-1	11.32	114.91	24.54	48.84	8.76	25.55	3.66	17.89	4.48	1.39	4.04	0.64	3.37
MRG-1	11.44	118.15	24.75	47.54	8.69	24.61	3.59	17.25	4.35	1.34	4.05	0.53	2.93
MRG-1	11.49	111.33	23.23	47.57	8.57	24.76	3.65	16.98	4.42	1.38	3.96	0.54	2.79
MRG-1	11.63	112.67	32.56	48.56	9.00	27.27	3.75	17.84	4.41	1.44	3.91	0.54	2.91
MRG-1	11.56	111.69	24.37	48.63	8.87	26.14	3.73	17.97	4.32	1.38	4.16	0.55	2.82
MRG-1	11.64	117.31	28.24	48.75	8.87	25.25	3.71	17.84	4.44	1.40	4.00	0.55	2.89
MRG-1	11.52	120.44	28.50	48.65	8.69	24.94	3.67	17.79	4.49	1.40	3.99	0.54	2.86
avrg	11.51	114.52	25.92	48.71	8.77	25.41	3.65	17.52	4.36	1.38	4.04	0.55	2.90
stdev	0.14	3.20	2.94	1.29	0.18	0.82	0.07	0.36	0.12	0.03	0.09	0.03	0.17
<b>accptd</b>	<b>14.00</b>	<b>108.00</b>	<b>20.00</b>	<b>61.00</b>	<b>9.80</b>	<b>26.00</b>	<b>3.40</b>	<b>19.20</b>	<b>4.50</b>	<b>1.39</b>	<b>4.00</b>	<b>0.51</b>	<b>2.90</b>
<b>lab*</b>	<b>11.50</b>	<b>107.00</b>	<b>22.30</b>	<b>49.40</b>	<b>8.83</b>	<b>25.80</b>	<b>3.71</b>	<b>17.60</b>	<b>4.34</b>	<b>1.38</b>	<b>3.97</b>	<b>0.52</b>	<b>3.00</b>

## Appendix 5

### Analytical Techniques

#### U/Pb Geochronology

Abraded zircon fractions and unabraded baddeleyite fractions were washed in distilled  $\text{HNO}_3$ , doubly distilled  $\text{H}_2\text{O}$ , then distilled acetone, prior to weighing on a microbalance and loading in Krogh-type teflon dissolution bombs. In the case of very small fractions, or single grains, samples loaded onto weighing boats in distilled acetone with a pipet, under a microscope to ensure that the entire sample was transferred. The acetone was allowed to evaporate prior to transferring samples into the bombs. A mixed  $^{205}\text{Pb}/^{235}\text{U}$  tracer was added in proportion to sample weight, along with  $\sim 25$  drops of distilled  $\text{HF}$  and 1 drop of  $\text{HNO}_3$ ; then the bomb was sealed and placed in an oven at  $210^\circ\text{C}$  for 5 days. Ion exchange chemistry was carried out according to the procedure of Krogh (1973), with modified columns and reagent volumes scaled down to one-tenth of those reported in 1973. The purified U and Pb were collected in a clean beaker in a single drop of ultrapure  $\text{H}_3\text{PO}_4$ .

Lead and uranium were loaded together on outgassed single Re filaments with silica gel and dilute  $\text{H}_3\text{PO}_4$ . Mass spectrometry was carried out using a multicollector MAT 262. For larger fractions, Pb was measured in static mode with  $^{204}\text{Pb}$  measured in the secondary electron multiplier (SEM) on ion counting mode. For small fractions, Pb masses were measured by peak jumping on the ion counter with measurement times weighted according to the amounts of each mass present. The Faraday cups are calibrated several times a day with NBS 981 standard and the ion counter is calibrated against a Faraday cup by measuring a known ratio. Uranium was measured by double static faraday collection. A series of sets of data are measured in the temperature range of  $1400^\circ$  to  $1550^\circ\text{C}$  for Pb and  $1550^\circ$  to  $1640^\circ\text{C}$  for U, and the best sets are combined to produce a mean value for each ratio. The measured ratios are corrected for Pb and U fractionation

of 0.1 %/amu as determined from repeat measurements of NBS standards. The ratios are also corrected for laboratory procedural blanks (2-10 pg, Pb and 1 pg, U) and for any common Pb above laboratory blank by the two-stage model of Stacey and Kramers (1975) for the age of the sample. Ages are calculated using the decay constants recommended by Jaffey et al. (1971).

The uncertainties on the isotopic ratios and ages are calculated using an unpublished Royal Ontario Museum program and are reported at absolute two sigma. Sources of uncertainty considered include uncertainties on the isotopic ratio measurements by mass spectrometry, assigned 80% uncertainty on U and Pb fractionation, assigned 50% uncertainty on the amount of Pb and U blanks and a 4% uncertainty on the isotopic composition of the Pb used to subtract the common Pb present above the laboratory blank. The uncertainties are quadratically added to arrive at the final 2 sigma (absolute, i.e.,  $2 \times 1$  sigma) uncertainties that are reported. Discordia lines are calculated using the program of Davies (1982) with individual data points having these 2 sigma uncertainties, and uncertainties on the intercept age are reported at the 95% confidence interval.

Zircon and baddeleyite are hand-picked, to select only the best quality grains and to distinguish different crystal morphologies. The zircons were usually extensively abraded (Krogh 1982) to remove the outer surfaces, in an attempt to minimize or eliminate Pb loss.

#### **Inductively Coupled Plasma-Mass Spectrometer (ICP-MS) analytical Procedure** (summarized from Longerich et al. 1993)

Two hundred mg (0.2 g) of sample and 800 mg of  $\text{Na}_2\text{O}_2$  are mixed well and heated at 500 degrees C for 1.5 hours in Ni crucibles. After cooling for about 20 minutes, 10 ml of distilled  $\text{H}_2\text{O}$  are added a few drops at a time, until the reaction stops. The mixture is then placed into a centrifuge tube, distilled  $\text{H}_2\text{O}$  is added to make a total volume of 30 ml, and the sample is centrifuged for 15 minutes. The liquid is poured off, the residue is rinsed with 25 ml of distilled  $\text{H}_2\text{O}$ , and the sample is centrifuged again. This rinsing is repeated a third time.

The residue is then dissolved in 2.5 ml of 8N HNO<sub>3</sub> and 4 ml oxalic acid. Then 4 ml of a 0.113 M HF/0.453M boric acid solution is added and the sample is left to sit in the drying oven for several hours. The sample is then transferred to a clean tube and the solution is made up to 50 grams with distilled H<sub>2</sub>O. The sample is then diluted before final analysis. This is done by accurately weighing approximately 2 grams of sample solution and 8 grams of 0.2N HNO<sub>3</sub> into a labeled test tube. This solution is analysed in the ICP-MS.

The sample is analysed on a modified SCIEX ELAN model 250 ICP-MS, with an in house built Ni sampler and skimmer, and a Gilson 212B auto sampler. All concentration calculations are made off-line using commercial spread sheet programs. The nebulizer gas flow is adjusted using a solution containing 100ppb Cs, Bi and Th so that: 1) ThO<sup>+</sup>/Th<sup>+</sup> < 10% (UO<sup>+</sup>/U<sup>+</sup> < 6%); 2) sensitivity of Sc > 1000 cps/ppb; and 3) sensitivity of Bi > 500 cps/ppb. This provides the optimum operating conditions by maximizing sensitivity while minimizing polyatomic ion formation.

Up to 56 samples, including standards, blanks and duplicates can be analysed per run. Data are acquired in cycles of 12 samples (including 4 standards, 1 calibration blank and 7 samples), using the auto sampler. An internal standard of Rb, Cs, Tl and U is pumped in with the sample at a ratio of 1 part spike to 2 parts sample for a total flow rate of 1g/min. Data is acquired at each mass for 10 seconds using a dwell time of 50 ms.

All samples and standards are background corrected using the mean of all calibration blanks in that run. Corrections are applied for a variety of oxide interferences on certain analytes. Calibration is from 4 external standards for most elements, except Nb and Ta which are calibrated using Zr and Hf, respectively, as surrogates. Matrix corrections are made using a mass interpolated ratio of the intensity of the internal standards in the sample group and the previous standards.

## Appendix 6

### Thin Section Petrography

#### South Lake igneous complex

##### *Gabbro (SLIC)*

The layering in the layered gabbro is defined by variations in the proportion of plagioclase and what was originally clinopyroxene, and minor orthopyroxene. Plagioclase appears to be only a cumulate phase, whereas the clinopyroxene and orthopyroxene may also have had adcumulate growth. The plagioclase is completely saussuritized, clinopyroxene is rimmed and extensively replaced by hornblende, and what is interpreted to have been orthopyroxene is now completely altered to bastite. There is also minor interstitial oxide which is partially altered to fine-grained granular sphene. Green, fine-grained acicular to bladed euhedral/subhedral amphibole has locally grown at the expense of the ragged amphibole which replaces the clinopyroxene, and is probably a result of regional metamorphism. Because of all the alteration and recrystallization it is difficult to interpret primary igneous textures.

Massive gabbro and gabbro pegmatite also have a significant cumulate component which includes plagioclase, either or both clinopyroxene and orthopyroxene, and Fe-Ti oxides. Interstitial minerals include any of the phases Fe-Ti oxide, plagioclase, quartz or hornblende. Hornblende commonly rims and replaces augite (Plate 2.3a) and is strongly compositionally zoned. The replacement and overgrowth amphibole are typically in optical continuity (Plate A6-1a), and vary from euhedral to interstitial depending on the space available for growth. These textures show that the amphibole is a late magmatic phase, and suggest that these magmas were quite H<sub>2</sub>O-rich. The cumulate plagioclase grains are strongly saussuritized (Plate 2.3a) suggesting that they were originally quite calcic, but the interstitial plagioclase is relatively fresh and more sodic (This compositional variation was confirmed by qualitative electron microprobe

analyses). Enstatite is almost completely altered to bastite (Plate 2.3b) and Fe-Ti oxides may be partially altered to fine-grained, granular sphene. Textural relationships suggest that the clinopyroxene and orthopyroxene were crystallizing from the magma simultaneously, as small inclusions of clinopyroxene can be found in altered orthopyroxene grains (Plate 2.3b), and visa-versa.

#### *Mafic Sheeted Dykes*

The dark green dykes in the ophiolite are very distinct petrographically from the grey ones. Both phenocrysts and groundmass are completely altered to amphibole. The phenocrysts are locally replaced by fairly coarse-grained tabular crystals, but the rock is dominantly fine-grained acicular pale green to colourless tremolite-actinolite and hornblende finely intergrown (Plate A6-1b) (compositions verified by qualitative electron microprobe analyses). In one sample relict augite is preserved in the core of one phenocryst (Plate A6-1c). Scattered throughout the groundmass, and included within the phenocrysts are euhedral oxide grains (Plate A6-1b) which may be a result of recrystallization, but could also be primary. These grains have the composition of chrome-spinel (qualitative analysis on electron microprobe).

The aphanitic and speckled grey dykes have the same petrographic features, the latter having a slightly coarser grain size. They have a relict diabasic to subophitic texture (Plate A6-1d) comprised of plagioclase laths (35-45 modal%) surrounded by sub-hedral to anhedral tabular hornblende (45-55 modal %). This hornblende shows some zoning and is probably primary. It is variably recrystallized to fine-grained aggregates of diamond-shaped hornblende which is probably metamorphic. The plagioclase is totally sausseritized and trace amounts of oxide are partially or totally replaced by fine-grained granular sphene.

#### *Hornblende Diorite*

The mineralogy and paragenesis of the hornblende diorite is very similar to the grey dykes in the ophiolite, although it is coarser grained and may contain significant amounts of interstitial quartz (quartz hornblende diorite). The plagioclase (40-45 modal %) occurs as small subhedral to anhedral tabular grains

enclosed in large anhedral hornblende (40–45 modal %) crystals (Plate 2.3c). Quartz occurs only as late interstitial phase (5–15 modal %). Trace amounts of oxide are present and are partially altered to fine-grained granular sphene. The hornblende is locally recrystallized as in the ophiolitic dykes, and is also locally altered to chlorite. The oxide is typically associated with the chlorite alteration and probably formed as a result of it, since chlorite can not accommodate as much Ti as hornblende. This process may happen in the finer-grained dykes as well, but is more difficult to recognize.

### *Tonalite*

The tonalite is comprised of variable amounts of plagioclase, quartz (at least 50%) and chlorite (< 1%) (after hornblende). The plagioclase occurs as two distinct phases, firstly as aggregates of subhedral to euhedral, zoned tabular crystals with more Ca-rich cores and interstitial chlorite and quartz (Plate A6-2a), and secondly as more Na-rich anhedral grains in granophyric intergrowth with quartz (Plate A6-2b). Quartz occurs as large anhedral grains between the plagioclase-chlorite aggregates and is partially intergrown with them, and as granophyric intergrowths with the more Na-rich anhedral plagioclase. The patches of chlorite are intergrown with oxides in a similar way to the chlorite and oxide in the altered patches of hornblende in the diorite. Some samples contain exclusively one type of plagioclase or the other and some contain both. This variation is reflected in their chemical composition.

### *Late mafic to intermediate dykes*

The set of late mafic to intermediate dykes have a relict diabasic texture comprised of relatively fresh plagioclase laths in a groundmass of chlorite, clinopyroxene, epidote and quartz (Plate A6-2c). Plagioclase and clinopyroxene also occur as rare phenocrysts or glomerocrysts which may represent cognate xenoliths. These dykes also contain abundant small, subhedral to euhedral skeletal oxide grains. Plagioclase generally comprises greater than 60 modal % of the rock with variable amounts of clinopyroxene, chlorite and epidote. Oxides comprise 1–2 modal % and quartz may or may not be present.

## Wild Bight Group

### *Group 1, island arc tholeiites*

The island arc tholeiitic basalts comprise fine-grained microlites of plagioclase (25-40%) in a groundmass of very fine-grained epidote and chlorite/actinolite in variable proportions, but dominated by epidote. A trace amount of tiny subhedral oxide grains occur scattered throughout the groundmass. Some samples contain amygdules filled with epidote, chlorite, quartz and calcite. The texture in these rocks is very similar to those of the low-Ti tholeiitic basalts (Plate A6-4a), although the modal mineral proportions are slightly different.

### *Group 2, low-Ti island arc tholeiites*

The low-Ti island arc tholeiitic basalts comprise fine-grained plagioclase laths (20-30%) in a groundmass of chlorite and epidote in approximately equal proportions. A trace amount of tiny subhedral oxide grains occur scattered throughout the groundmass. The texture and mineralogy of these rocks are very similar to the Group 1 and 3 volcanics, although they seem to have more chlorite.

### *Group 3, LREE-depleted, low-Ti island arc tholeiites*

The LREE-depleted, low-Ti island arc tholeiitic basalts have somewhat more variable mineral proportions, but most contain 1-7% clinopyroxene phenocrysts and/or glomerocrysts, which range from 1-4mm in size, and some contain rare plagioclase phenocrysts. The clinopyroxene phenocrysts may show oscillatory concentric zoning (Plate A6-4b). The groundmass typically contains fine-grained plagioclase laths (20-30%) with interstitial chlorite and epidote, and some samples also contain abundant sub-ophitic to interstitial clinopyroxene (10-20%) (Plate A6-4c). There is very little, if any primary oxide in these rocks. Samples with more abundant clinopyroxene appear to be less altered.

### *Group 4, low CaO/Al<sub>2</sub>O<sub>3</sub>, low-Ti, island arc tholeiites*

The low CaO/Al<sub>2</sub>O<sub>3</sub>, low-Ti island arc tholeiitic basalts are petrographically very similar to the other low-Ti IATs and comprise a groundmass of plagioclase microlites or laths (25-40%) with interstitial fine-grained chlorite,

and minor epidote, and tiny disseminated subhedral oxide grains (1-3%). Less altered samples also have subhedral fine-grained clinopyroxene in the groundmass (up to 10%), and or as microphenocrysts. Tiny euhedral crystals of reddish brown mineral (probably chrome spinel) were recognized in one sample. There is also typically abundant secondary calcite in the groundmass (up to 15%).

*Group 5, low CaO/Al<sub>2</sub>O<sub>3</sub> boninites*

The low CaO/Al<sub>2</sub>O<sub>3</sub> boninites comprise a groundmass of fine-grained plagioclase laths (30-45%) with interstitial to sub-ophitic clinopyroxene (15-25%) and fine-grained interstitial chlorite (25-40%) and minor epidote (<8%) (Plate A6-4d). One sample also contains 2-5% plagioclase and clinopyroxene phenocrysts, and the other contains scattered phenocrysts interpreted to have originally been Mg-rich olivine. These phenocrysts are subhedral to euhedral, and are strongly altered to oxides around the margins and along fractures, and cleavage (Plate A6-4e). The mineral, which has been altered, is not the primary olivine, but is a colourless, low-birefringence mineral with amphibole cleavage, tentatively identified as Mg-rich cummingtonite. There is very little primary oxide in the boninites, but there is abundant secondary hematite (Plate A6-4e). In more altered samples there is more chlorite and less clinopyroxene in the groundmass. These boninites also have abundant secondary calcite in the groundmass (up to 15%).

*Group 6, Rhyolites*

The rhyolites are comprised of a very fine-grained quartzo-feldspathic groundmass and 10-20% quartz and plagioclase phenocrysts. The quartz phenocrysts are typically embayed and the plagioclase is completely saussuritized. There is also abundant finely disseminated secondary hematite throughout the matrix which gives these rocks a red or purple colour.

*Group 7 and 10, calc-alkaline basalts-andesites*

The calc-alkaline mafic to intermediate rocks are typically plagioclase porphyritic, with 2-10 mm phenocrysts comprising up to 20% (Plate A6-3a). Plagioclase phenocrysts typically have concentric oscillatory zoning which is both

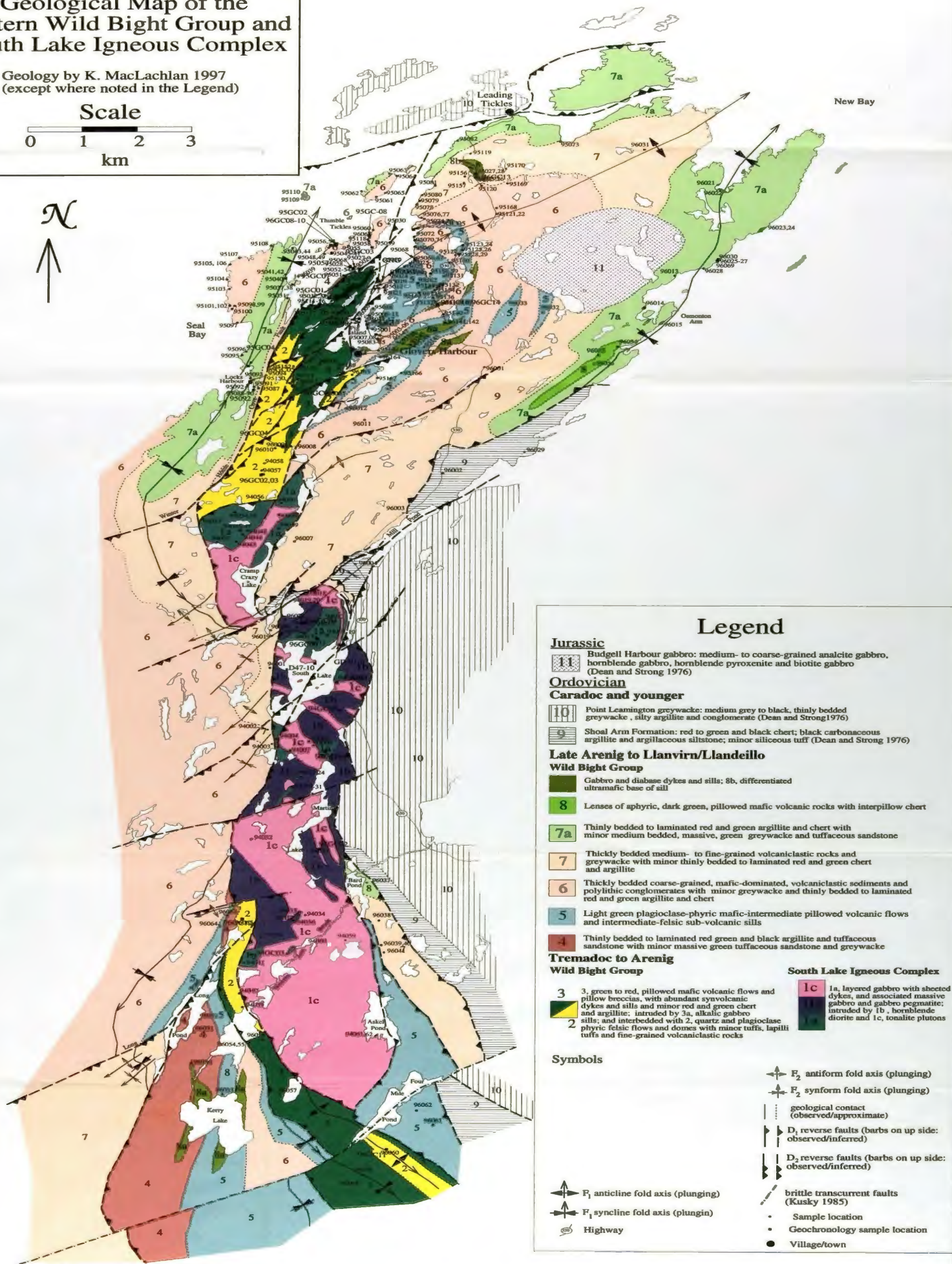
normal and reverse, and commonly have a sieve texture (Plate A6-3b). These rocks also contain rare, small clinopyroxene phenocrysts 1-2 mm in size (Plate A6-3b). The groundmass is comprised of fine-grained plagioclase laths with interstitial to subophitic clinopyroxene, and interstitial chlorite and epidote. The degree of alteration is quite variable, but the most altered samples do not have clinopyroxene, and the plagioclase is completely sericitized, whereas in less altered rocks the clinopyroxene is totally unaltered and the plagioclase is only speckled with sericite. However, in all samples the groundmass contains abundant epidote and chlorite. Other types of alteration include calcite, quartz, epidote and chlorite veinlets and amygdules.

*Groups, 8, 9 and 11 enriched tholeiitic to alkalic within plate basalts*

Most of the samples from these geochemical groups are intrusive rocks, and thus the textures are probably coarser-grained than the volcanic rocks, but the mineralogy is similar. Most of the dykes and sills have a fine- to medium grained sub-ophitic texture comprising plagioclase laths (40-50%) surrounded by oikocrysts of clinopyroxene (15-25%), with interstitial chlorite (15-25%) and minor epidote (< 5%) in some samples. These rocks also typically contain up to 5% subhedral skeletal oxide grains (1-4mm). These intrusive rocks commonly contain amygdules (probably shallow intrusions) with chlorite and calcite fillings. There are also some dykes/sills which are coarsely porphyritic, with large (4-15 mm) euhedral clinopyroxene and orthopyroxene (now totally altered to bastite), in a very fine-grained matrix which is completely altered to chlorite and epidote. One volcanic sample (96021), transitional between this Group and Group 10, is comprised of plagioclase laths (35-45%) with interstitial to subophitic clinopyroxene (15-25%) and fine-grained interstitial chlorite and epidote (Plate A6-3 c and d).

# Map A1 Geological Map of the Eastern Wild Bight Group and South Lake Igneous Complex

Geology by K. MacLachlan 1997  
(except where noted in the Legend)



## Legend

### Jurassic

**11** Budgell Harbour gabbro: medium- to coarse-grained analcite gabbro, hornblende gabbro, hornblende pyroxenite and biotite gabbro (Dean and Strong 1976)

### Ordovician

#### Caradoc and younger

**10** Point Leamington greywacke: medium grey to black, thinly bedded greywacke, silty argillite and conglomerate (Dean and Strong 1976)

**9** Shoal Arm Formation: red to green and black chert; black carbonaceous argillite and argillaceous siltstone; minor siliceous tuff (Dean and Strong 1976)

### Late Arenig to Llanvirn/Llandeillo

#### Wild Bight Group

**8** Gabbro and diabase dykes and sills; 8b, differentiated ultramafic base of sill

**7a** Lenses of aphyric, dark green, pillowed mafic volcanic rocks with interpillow chert

**7a** Thinly bedded to laminated red and green argillite and chert with minor medium bedded, massive, green greywacke and tuffaceous sandstone

**7** Thickly bedded medium- to fine-grained volcaniclastic rocks and greywacke with minor thinly bedded to laminated red and green chert and argillite

**6** Thickly bedded coarse-grained, mafic-dominated, volcaniclastic sediments and polyolithic conglomerates with minor greywacke and thinly bedded to laminated red and green argillite and chert

**5** Light green plagioclase-phyric mafic-intermediate pillowed volcanic flows and intermediate-felsic sub-volcanic sills

**4** Thinly bedded to laminated red green and black argillite and tuffaceous sandstone with minor massive green tuffaceous sandstone and greywacke

### Tremadoc to Arenig

#### Wild Bight Group

**3** 3, green to red, pillowed mafic volcanic flows and pillow breccias, with abundant synevolcanic dykes and sills and minor red and green chert and argillite; intruded by 3a, alkalic gabbro sills; and interbedded with 2, quartz and plagioclase phyric felsic flows and domes with minor tuffs, lapilli tuffs and fine-grained volcaniclastic rocks

**2** 2, green to red, pillowed mafic volcanic flows and pillow breccias, with abundant synevolcanic dykes and sills and minor red and green chert and argillite; intruded by 3a, alkalic gabbro sills; and interbedded with 2, quartz and plagioclase phyric felsic flows and domes with minor tuffs, lapilli tuffs and fine-grained volcaniclastic rocks

#### South Lake Igneous Complex

**1c** 1a, layered gabbro with sheeted dykes, and associated massive gabbro and gabbro pegmatite; intruded by 1b, hornblende diorite and 1c, tonalite plutons

### Symbols

F<sub>2</sub> antiform fold axis (plunging)

F<sub>2</sub> synform fold axis (plunging)

geological contact (observed/approximate)

D<sub>1</sub> reverse faults (barbs on up side: observed/inferred)

D<sub>2</sub> reverse faults (barbs on up side: observed/inferred)

brittle transcurrent faults (Kusky 1985)

Sample location

Geochronology sample location

Village/town

F<sub>1</sub> anticline fold axis (plunging)

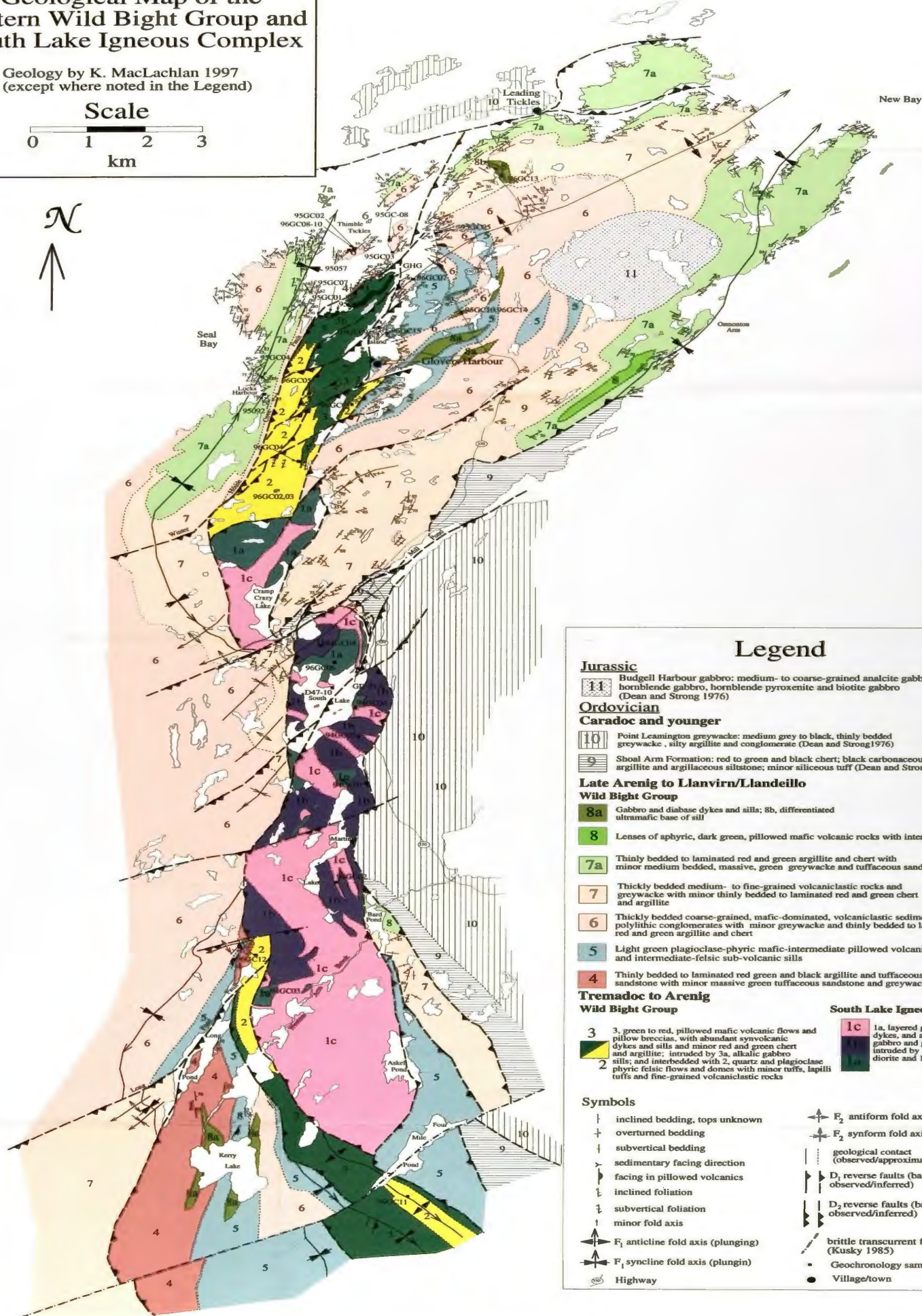
F<sub>1</sub> syncline fold axis (plunging)

Highway

# Map A1 Geological Map of the Eastern Wild Bight Group and South Lake Igneous Complex

Geology by K. MacLachlan 1997  
(except where noted in the Legend)

Scale



## Legend

### Jurassic

**11** Budgell Harbour gabbro: medium- to coarse-grained analcite gabbro, hornblende gabbro, hornblende pyroxenite and biotite gabbro (Dean and Strong 1976)

### Ordovician

#### Caradoc and younger

**10** Point Leamington greywacke: medium grey to black, thinly bedded greywacke, silty argillite and conglomerate (Dean and Strong 1976)

**9** Shoel Arm Formation: red to green and black chert; black carbonaceous argillite and argillaceous siltstone; minor siliceous tuff (Dean and Strong 1976)

#### Late Arenig to Llanvirn/Llandeillo Wild Bight Group

**8a** Gabbro and diabase dykes and sills; 8b, differentiated ultramafic base of sill

**8** Lenses of aphyric, dark green, pillowed mafic volcanic rocks with interpillow chert

**7a** Thinly bedded to laminated red and green argillite and chert with minor medium bedded, massive, green greywacke and tuffaceous sandstone

**7** Thickly bedded medium- to fine-grained volcaniclastic rocks and greywacke with minor thinly bedded to laminated red and green chert and argillite

**6** Thickly bedded coarse-grained, mafic-dominated, volcaniclastic sediments and polyolithic conglomerates with minor greywacke and thinly bedded to laminated red and green argillite and chert

**5** Light green plagioclase-phyric mafic-intermediate pillowed volcanic flows and intermediate-felsic sub-volcanic sills

**4** Thinly bedded to laminated red green and black argillite and tuffaceous sandstone with minor massive green tuffaceous sandstone and greywacke

#### Tremadoc to Arenig Wild Bight Group

**3** 3, green to red, pillowed mafic volcanic flows and pillow breccias, with abundant synvolcanic dykes and sills and minor red and green chert and argillite; intruded by 3a, alkalic gabbro sills; and interbedded with 2, quartz and plagioclase phyric felsic flows and domes with minor tuffs, lapilli tuffs and fine-grained volcaniclastic rocks

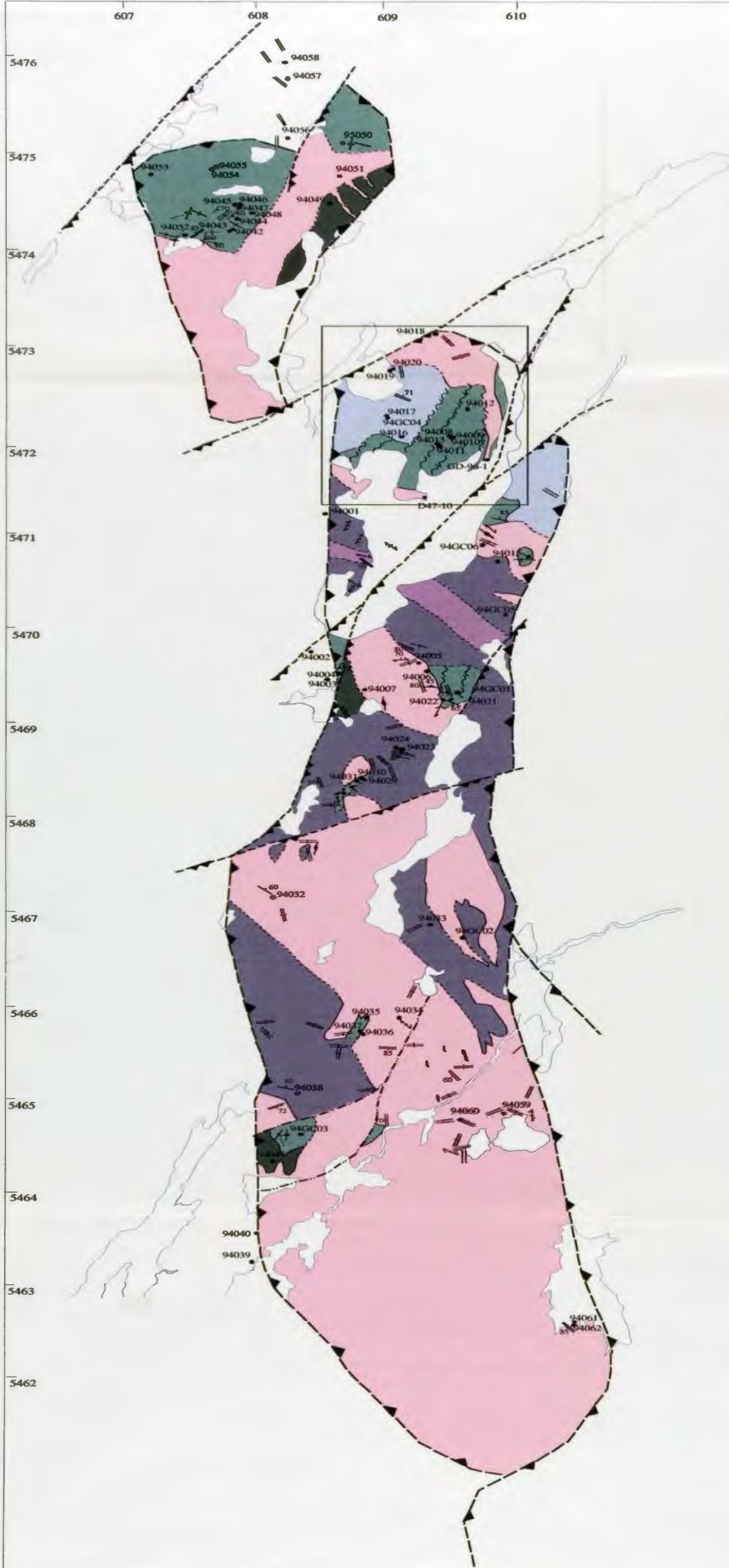
**2**

#### South Lake Igneous Complex

**1c** 1a, layered gabbro with sheeted dykes, and associated massive gabbro and gabbro pegmatite; intruded by 1b, hornblende diorite and 1c, tonalite plutons

### Symbols

- |   |   |
|---|---|
| inclined bedding, tops unknown                  | ↗ F <sub>2</sub> antiform fold axis (plunging)                        |
| + overturned bedding                            | ↖ F <sub>2</sub> synform fold axis (plunging)                         |
| subvertical bedding                             | geological contact (observed/approximate)                             |
| > sedimentary facing direction                  | ↗ D <sub>1</sub> reverse faults (barbs on up side: observed/inferred) |
| > facing in pillowed volcanics                  | ↖ D <sub>2</sub> reverse faults (barbs on up side: observed/inferred) |
| inclined foliation                              | brittle transcurrent faults (Kusky 1985)                              |
| subvertical foliation                           | • Geochronology sample location                                       |
| minor fold axis                                 | • Village/town  |
| ↗ F <sub>1</sub> anticline fold axis (plunging) |   |
| ↖ F <sub>1</sub> syncline fold axis (plunging)  |   |
| — Highway                                       |   |



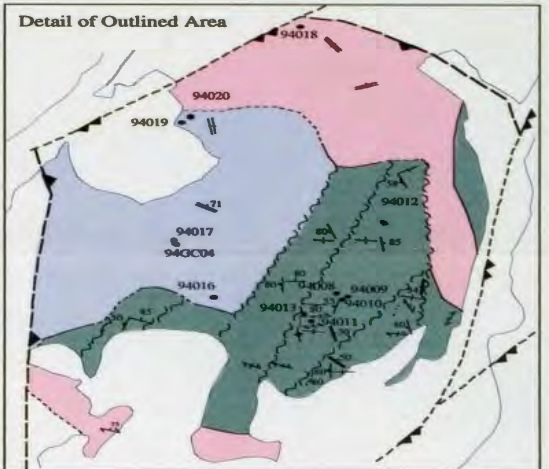
# **Map B** **Geological Map of** **The South Lake Igneous Complex** (Geology by K. MacLachlan 1997)

Scale  
 (~1:50,000)

0 1  
 km

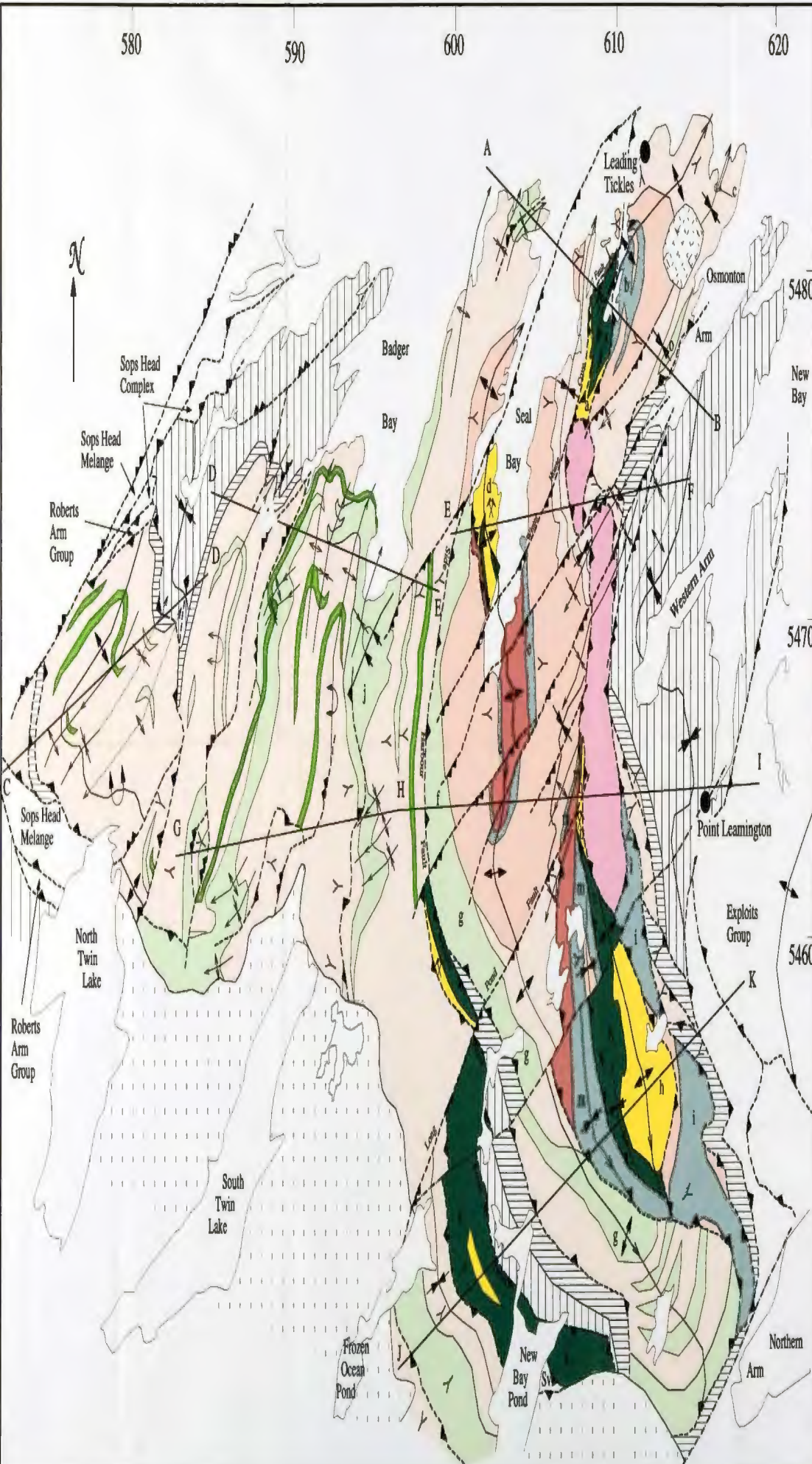
## **Legend**

- Tonalite
- Mixed hornblende diorite and tonalite
- Quartz hornblende diorite
- Hornblende diorite
- Massive gabbro
- Layered gabbro with sheeted dykes
- Regional D<sub>1</sub> reverse fault (barbs on up side)
- Regional D<sub>2</sub> reverse fault (barbs on up side)
- Faults/high-strain zones internal to the SLIC (major/minor)
- Faults in the layered gabbro complex
- Geological contact (observed/approximate)
- Late mafic-intermediate dykes (subvertical/dipping/dip unknown)
- Mafic dykes of sheeted dykes complex and dykes elsewhere which are not the late dyke set (subvertical/dipping/dip unknown)
- Layering in gabbro (subvertical/dipping)
- Foliation: cleavage, schistosity or flattening fabric (subvertical/dipping/dip unknown)
- Inclusion trains in tonalite (subvertical/dipping)
- Sample location



**Map C1**  
**Regional Compilation Map of the**  
**Wild Bight Group and adjacent rocks**  
(compiled by K. MacLachlan and B.H. O'Brien, 1997)

Scale  
0 5 10  
km



**Legend**

**Jurassic**

Badgell Harbour gabbro

**Siluro-Devonian**

Diorite and granite plutons

**Silurian**

Sy Batwood Group (terrestrial felsic volcanic rocks)

**Ordovician**

Caradocian and younger

10 Badger Group (marine greywacke, conglomerate and minor argillite, Williams 1993)

9 Seal Arm Formation (and biostratigraphic/lithostratigraphic equivalents: red to green and black shale and chert, carbonaceous black shale and minor siltstone) (Dean and Strong 1976)

**Late Arenig - Early Llanvirn**

**Wild Bight Group**

- 8 8, pillowed mafic volcanic and coarse-grained volcanoclastic rocks; f.a. gabbro and diabase sills and dykes
- 7 7, thinly bedded/laminated red, green and grey chert/argillite with minor fine to medium-grained volcanoclastic rocks
- 6 6, thickly bedded massive coarse-grained volcanoclastic rocks with minor argillite
- 5 5, light green, plagioclase phytic, pillowed mafic volcanic rocks and mafic to intermediate subvolcanic intrusions
- 4 4, thinly bedded to laminated red/green argillite/luciferous sandstone, minor massive green greywacke and black shale

**Tremadoc-Early Arenig**

**Wild Bight Group**

- 3 3, dark green to red pillowed mafic volcanic rocks interbedded with: 2, thickly bedded intermediate to felsic lapilli tuff/volcanoclastic rocks and quartzite and plagioclase-phyric rhyolite flows and domes
- 2 2

**South Lake Igneous Complex**

- 1 1 Layered gabbro/diorite dykes intruded by diorite and tonalite plutons

**Symbols**

- D<sub>1</sub> thrust faults (barbs on hangingwall side)
- D<sub>2</sub> thrust faults (barbs on hangingwall side)
- Late brittle transcurrent faults
- F fold axis, plunging (anticline; syncline)
- F fold axis, plunging (antiform; synform)
- Geological contact
- Sedimentary facing direction
- Pillow facing direction
- Volcanogenic massive nephelide showing/deposit

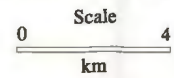
**Geographic Volcanic Units**

- a Glovers Harbour West
- b Glovers Harbour East
- c New Bay
- d Indian Cove
- e Seal Bay Bottom
- f Side Harbour
- g Big Lewis Lake
- h Nanny Bag Lake
- i Northern Arm
- j Badger Bay
- k New Bay Pond
- l Seal Bay Head
- m Kerry Lake
- n Long Pond
- o Osmonton Arm

Notes: Adjacent Ordovician rock groups that are not part of the Wild Bight Group (WBG) or that don't conformably overlie it are undivided and shown only by the group name. Geology for the western WBG is from O'Brien and MacDonald (1997) and O'Brien in prep. Geology for the eastern WBG is from this study. Geology of the Cambrian units on the southeast side of the WBG is from Williams and O'Brien 1994. Other sources used in producing this map include the compilation by Dean and Strong 1976, Swinden 1988, and Jenner and Swinden 1993. The coordinate system used is the UTM grid from 1:50,000 NTS maps.

# Map C2 Regional Structural Cross-Sections of the Wild Bight Group, South Lake Igneous Complex and adjacent rocks groups

(enlarged relative to Map C1)



## Legend

See Map C1 for stratigraphic units  
and section locations

- F<sub>1</sub> Folds (anticline/syncline)
- F<sub>2</sub> Folds (antiform/synform)
- D<sub>1</sub> Faults
- D<sub>2</sub> Faults
- Geological contact
- Regional stratigraphic facing direction

